Identification and Characterization of the ING1 and ING2 Tumor Suppressors During Thyroid Hormone-dependent Tadpole Metamorphosis

by

Mary Jeannette Wagner
B.Sc., University of Victoria, 1999

A Dissertation Submitted in Partial Fulfillment of the Requirements
for the Degree of

DOCTOR OF PHILOSOPHY

In the Department of Biochemistry and Microbiology

Identification and Characterization of the ING1 and ING2 Tumor Suppressors During Thyroid Hormone-dependent Tadpole Metamorphosis

by

Mary Jeannette Wagner

B.Sc., University of Victoria, 1999

Supervisory Committee:

Dr. Caren Helbing, (Department of Biochemistry and Microbiology)

Supervisor

Dr. Juan Ausió, (Department of Biochemistry and Microbiology)

Departmental Member

Dr. Paul Romaniuk, (Department of Biochemistry and Microbiology)

Departmental Member

Dr. Nancy Sherwood, (Department of Biology)

Outside Member

Supervisory Committee

Dr. Caren Helbing

Supervisor

Dr. Juan Ausió

Departmental Member

Dr. Paul Romaniuk

Departmental Member

Dr. Nancy Sherwood

Outside Member

ABSTRACT

The ING (INhibitor of Growth) tumor suppressor genes are conserved from yeast to humans and are implicated in several processes important to cell proliferation and apoptosis. ING proteins contain a plant homeodomain (PHD) finger that suggests these proteins may modulate transcription factor-mediated pathways. Little is known about the mechanism of action of INGs, especially in the context of normal development.

The ING family of proteins includes at least five different genes, *ING1-ING5*, with evidence for alternate promoter usage and splicing that generate multiple isoforms. To elucidate the role of ING in different tissues to modulate function, I used amphibian metamorphosis as a model system in which a single stimulus, thyroid hormone (TH), initiates apoptosis, proliferation, and remodeling in the tail, hindlimb, and brain, respectively. I discovered seven *ING1* and three *ING2* transcript variants in *Xenopus laevis* and investigated their expression patterns. High expression levels of most variants were found in adult brain, testis, and eye. During natural metamorphosis or precocious metamorphosis

induced by treating tadpoles with exogenous TH, *ING1* and *ING2* transcript variant levels were differentially regulated in a tissue-specific manner. Some variant levels increased with the induction of apoptosis of the tail, while levels of the same variants decreased upon induction of proliferation and differentiation in the hindlimb. Although levels of all *ING* variants were relatively high in whole brain, they did not change during metamorphosis or TH treatment. Given that ING has previously been shown to modulate apoptosis, it is likely that upregulation of specific isoforms may contribute to the tissue-specific TH-mediated response in the tail, and that downregulation facilitates proliferation of the hindlimb.

To further investigate the hypothesis that ING is regulated by TH, an analysis of *ING1* and *ING2* genomic sequences was carried out. Promoter sequences for each variant were determined and putative thyroid hormone response elements (TREs) located. To test whether thyroid hormone receptors associate with these elements, chromatin immunoprecipitations (ChIP) assays were done on tail homogenates from premetamorphic tadpoles treated with TH or vehicle control. Both thyroid hormone receptor α (TRα) and thyroid hormone receptor β (TRβ) differentially associate with *ING1* and *ING2* promoter regions. TR association increased significantly on promoters for *ING* variant transcripts that increase upon TH treatment, and decreased significantly on promoters for *ING* variant transcripts that decrease upon TH treatment. ChIPs also showed that ING associates with TH-regulated promoters including *TRβ*, *TH-Responsive Basic Leucine Zipper Transcription Factor (TH/bZIP)*, *ING1* and *ING2*. Furthermore, TR and ING were shown to co-immunoprecipitate with both purified proteins and using total tail homogenates from metamorphic tadpoles. The antibodies used for these experiments were made against *Xenopus* TRβ and ING2 and were characterized as part of this thesis. Bioinformatics revealed that TREs are present in promoters of ING genes for other species including human, mouse, and a related frog species, *Xenopus tropicalis*; therefore, it is likely that modulation by TH is a conserved mechanism of *ING* regulation.

These data suggest that there may be antagonistic regulation of *ING* transcript variants by TH that correlates with tissue fate. TRs associate with *ING* promoters, and ING is associated with TR-regulated promoters. Moreover, TR and ING proteins co-immunoprecipitate. It is therefore likely that TR and ING are co-regulators of gene expression during TH-dependent tadpole metamorphosis. This thesis contributes to the understanding of ING which is relevant to elucidating many disease states, as well as being critical in understanding the role of this tumor suppressor in the context of TH regulation and normal development.

TABLE OF CONTENTS

LIST OF TABLES

LIST OF FIGURES

ACKNOWLEDGEMENTS

Thanks to my supervisor, Dr. Caren Helbing. Thanks to Fang Zhang who provided cDNA for one set of experiments, and to Dominik Domanski, Karen Cheung and Mark Tessaro for their help purifying His-tagged proteins. Thanks to Rachel Skirrow, Dominik Domanski, Lan Ji and Drs. Mark Gunderson, Nik Veldhoen and Fang Zhang for helpful discussions. Special thanks to my husband, Rob Iuvale, for his support. This work was supported by a NSERC Canada Graduate Scholarship, PEO Scholar Award, University of Victoria Graduate Student Award, and Michael Smith Foundation for Health Research Award.

CHAPTER 1: INTRODUCTION

1.1 INHIBITOR OF GROWTH TUMOR SUPPRESSOR

Development of any multicellular organism involves a delicate balance between cell proliferation and apoptosis. Loss of normal cell cycle and apoptosis controls when damaged are hallmarks of cancer cells. When cells die inappropriately, disease states like Alzheimer's or muscular dystrophy may develop. This thesis examines a tumor suppressor protein called **IN**hibitor of **G**rowth (ING) that regulates the cell's decision to divide, differentiate, or die. Knowledge about the regulation of ING and its functions is relevant to understanding many disease states, as well as normal developmental processes.

ING was identified by subtractive hybridization of complementary DNAs (cDNAs) comparing normal and cancer cells combined with an *in vivo* selection assay to identify sense and antisense cDNA fragments able to promote neoplastic transformation [1]. ING protein, like the well-known tumor suppressor p53, can prevent the cell from making the transition to the DNA synthesis phase of the cell cycle during cellular stress such as DNA damage [42]. ING is also involved in cellular senescence [2-4], anchorage-dependent growth [5], chemosensitivity [5], angiogenesis [6], regulation of transcription, cell cycle progression, DNA repair, senescence, and apoptosis (reviewed in [7-9]). ING proteins contain a plant homeodomain (PHD) finger found in hundreds of proteins and that is associated with chromatin regulation [10, 11]. Numerous studies have established ING's ability to recruit both histone acetyltransferases (HATs) and histone deacetylases (HDACs) that remodel chromatin and affect gene transcription (reviewed in [9, 12, 13]). The involvement of ING in all these processes strongly suggests that these proteins may play a key role in modulating transcription factor-mediated pathways important to cell survival.

ING is rarely mutated; however, transcript expression is decreased for *ING1-4* in a variety of cancer cells resulting in ING's classification as a Type II

tumor suppressor (reviewed in [7, 8]). Currently, levels of ING5 in normal and cancer cells are unknown. The growing list of cancers and cancer cell lines with abnormalities in ING includes skin, colon, head, neck, breast, ovary, stomach, mouth, esophagus, lymph nodes, white blood cells, lung, brain, bladder, and liver and illustrates the importance of ING in normal cell function (reviewed in [7, 8]).

ING is conserved throughout evolution with sequences reported for numerous species including human, mouse, fruit fly, nematode, and fission and budding yeast [14, 15]. The ING family includes at least five different genes localized to distinct chromosomes; *ING1*, *ING2*, *ING3*, *ING4*, and *ING5* (Figure 1.1) [9, 15]. An additional *ING1* homolog that maps to the X chromosome, *INGX*, has been identified in humans, but no corresponding protein has been isolated [15].

This thesis will focus on ING1 and ING2 that I have isolated from *Xenopus laevis* during my graduate studies [15-17]. ING was known to be involved in apoptosis of abnormal cells, but no studies have investigated ING in normal development. My novel approach focuses on ING in a developmental model that is thyroid hormone-dependent and provides valuable new insight into ING regulation and function.

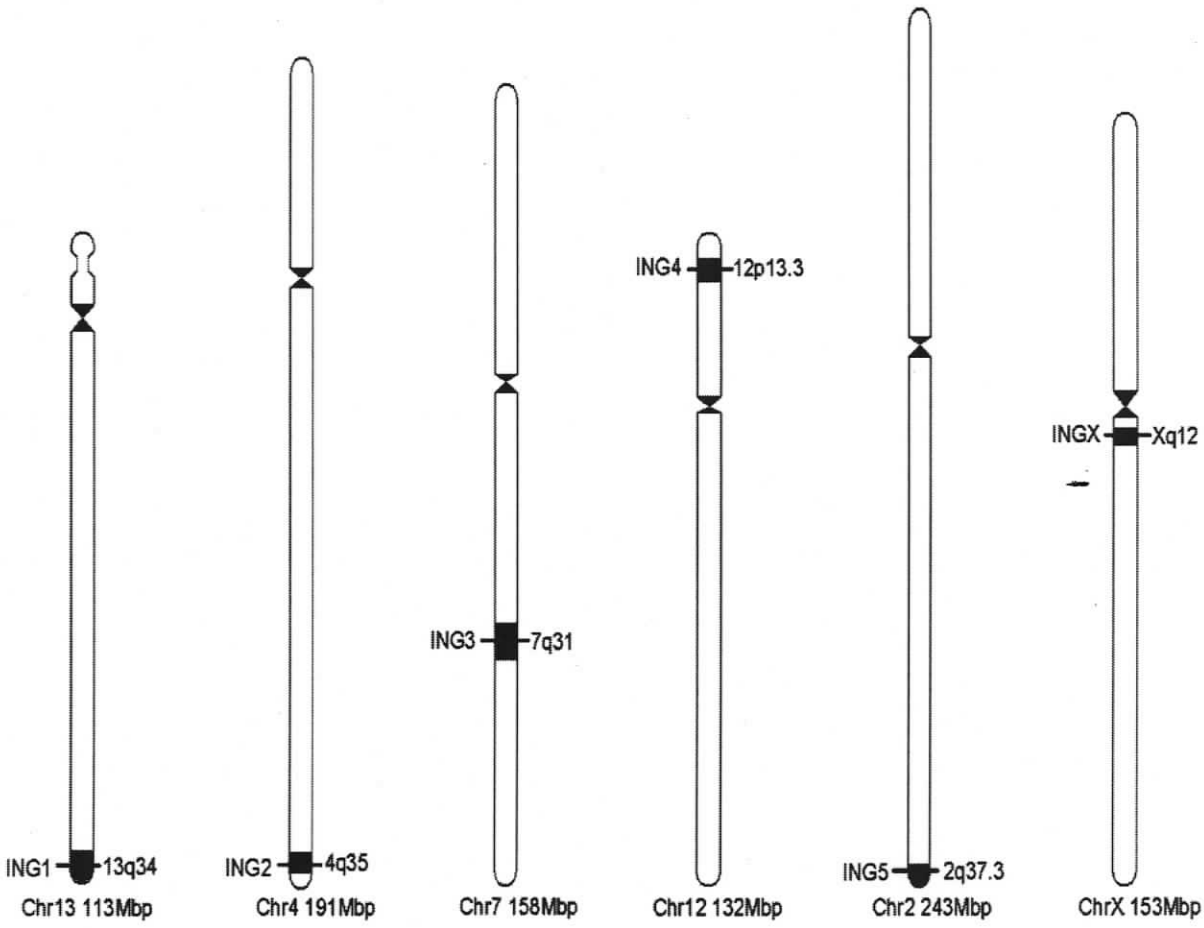

Figure 1.1. The five genes in the ING family.

The chromosomal localization of the *ING* genes in *Homo sapiens* is shown. Chromosome number and the approximate chromosomal length (in Mega base pairs (Mbp)) are indicated. The distance to telomeres is estimated to be ~4000 kb for *ING1*, ~6600 kb for *ING2*, ~38400 kb for *ING3*, ~6630 kb for *ING4*, and ~440 kb for *ING5*. *INGX* is located 11000 kb from the centromere of chromosome X. The centromeric regions are indicated as constrictions. This figure was modified from He et al., 2005.

1.2 ING STRUCTURE

1.2.1 ING Genes and Transcripts

The structure of the human *ING1* gene, shown in Figure 1.2, has been most thoroughly studied and consists of three different exon 1 sequences (1a, 1b, and 1c) that are alternatively spliced to a common exon 2 [14, 15]. The resulting known transcripts include *ING1a*, *b*, *c* and *d* and one predicted transcript is reported, *altING1c* ([15] and Genbank accession number NM198218). Similarly to human *ING1*, the genomic structure of mouse *ING1* includes alternative exons 1a, 1b, and 1c that are spliced to a common exon 2 giving rise to three transcripts where *ING1a* and *c* are homologous to human *ING1b* and mouse *ING1b* has a longer N-terminus similar to human *ING1a* [18]. *ING2* in human shares a similar two exon structure as *ING1*, but splice variants in human and mouse *ING2* have not been discovered [19]. ING1 proteins $p47^{ING1a}$, $p33^{ING1b}$, and $p24^{ING1c}$ are generated from transcripts *ING1a*, *b* and *c*, respectively. Putative proteins $p24^{altING1c}$ and $p27^{ING1d}$ are generated from transcripts *altING1c* and *ING1d*.

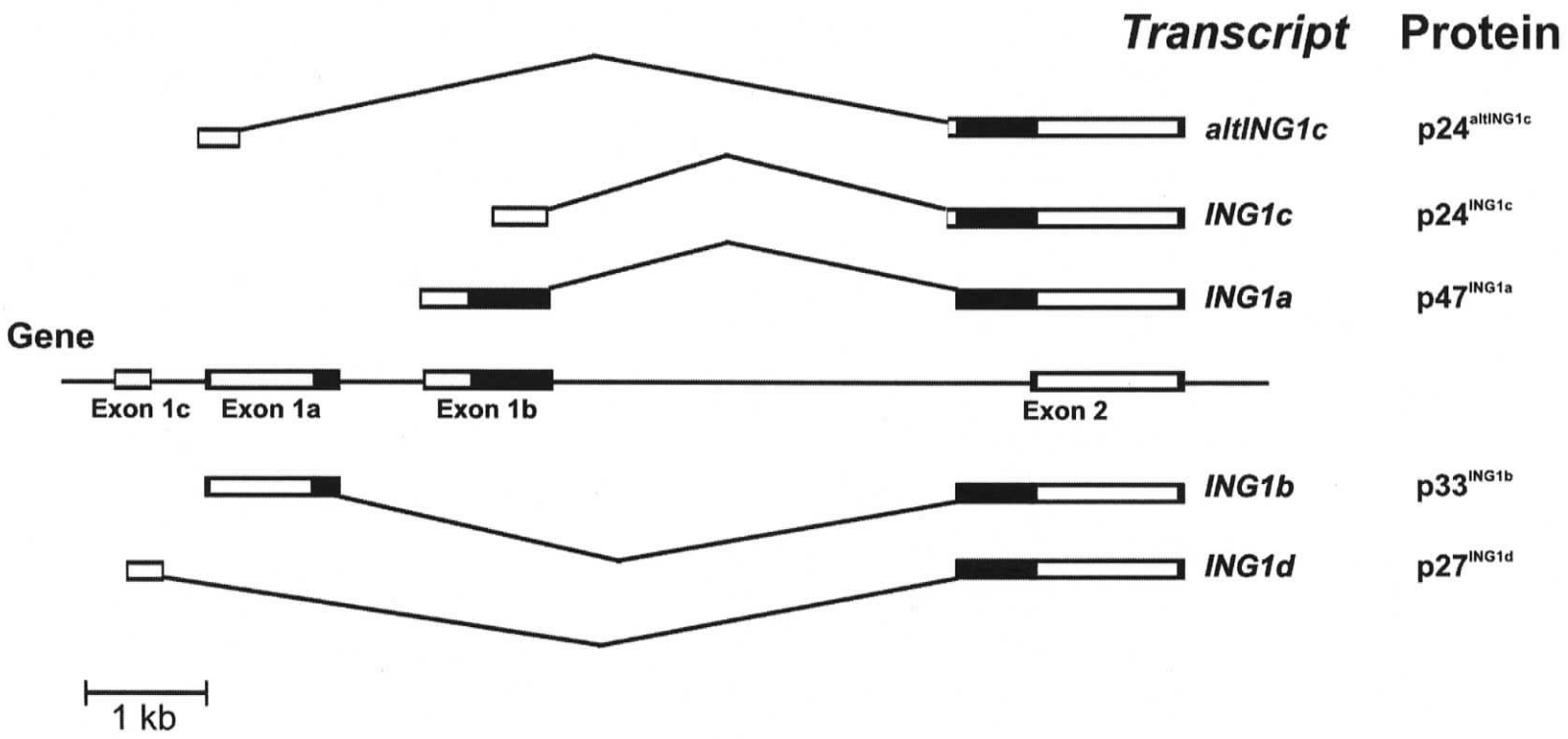

Figure 1.2. The *ING1* gene and its products.

Structure of the human *ING1* gene is shown along with the putative transcript and protein products. *ING1* exons are boxed (dark boxes represent coding regions). Known alternative (*ING1a*, *b* and *c*) and predicted (*altING1c* and *ING1d*) transcripts of the *ING1* gene are shown. One of three upstream exons is alternatively spliced onto a conserved exon 2 to encode the proteins $p27^{ING1d}$, $p33^{ING1b}$, and $p47^{ING1a}$. The smallest isoforms, $p24^{altING1c}$ and $p24^{ING1c}$, are generated by internal initiation within exon 2. This figure was modified from Gong et al., 2005.

Little is known about the genomic structure of other ING family members other than genome database information that reveals *ING3* consists of 12 exons (Genbank NM_019071), *ING4* consists of 8 exons (Genbank NM_016162.2) and *ING5* consists of 9 exons (Genbank NM_032329.4).

A systematic characterization of protein expression for different ING isoforms is lacking and no study of ING5 expression has been carried out to date; however, transcript expression data for *ING1-ING4* is available. Northern blots with a probe to a common region showed that *ING1* messenger RNA (mRNA) is found ubiquitously expressed in various human tissues [19]. Northern analysis of specific *ING1* variants showed that *ING1b* is the major form that is differentially expressed in normal tissues, while *ING1c* is also widely expressed but at lower levels than *ING1b* [20]. To date, several tissues examined express little if any *ING1a* [20]. Protein studies for products of these transcripts will be discussed in the following sections. In the published literature, the *ING1d* transcript has only been detected in one study in normal testis tissue, and no protein product has been identified [21]. However, there is evidence that this transcript as well as *ING1a* are more widely expressed than initially thought (Helbing *et al.*, unpublished data). Murine *ING1* homologs, *p31ING1* and *p37ING1*, are also ubiquitously expressed in adult tissues and during all stages of embryonic development [18]. ING2 is found in most fetal and adult human tissues [22] with particularly high levels in testis but low levels in lung, kidney and spleen [19]. *ING3* mRNA expression levels were found to be ubiquitous in normal human tissues as well, but with high levels in spleen and low levels in lung and brain [23]. *ING4* is also expressed in multiple human tissues with the highest expression in testis [6]. Three *Saccharomyces cerevisae* (Yng1, Yng2 and Pho23) and two *Schizosaccharomyces pombe* (Png1 and Png2) proteins are expressed in yeast and were found to contain high homology to human $p33^{ING1b}$ [24]. A yeast ortholog of $p47^{ING3}$, designated Yng2p, has also been identified [25]. Of the 60 ING-related sequences identified in a bioinformatics study based on their sequence similarity, most of the *ING* homologs remain uncharacterized [15].

Despite indications of tissue-specific regulation of *ING* variants and their known dysregulation in cancer cells, little is known about *ING* promoters and their regulation. Luciferase reporter assays show activity for alternative promoter regions for human *ING1a*, *b*, and *c* [26]. Promoter regions contain putative GC box, GATA box, TATA box and CCAAT box sequences [26]. In mouse, transcription initiation and termination sites were precisely determined for *ING1* homologs [18]. Bioinformatics analysis of mouse *ING1* promoter regions identified a putative TATA box and CCAAT box upstream of *ING1b*. While *ING1a* and *c* lack these features, they contain GC-rich and Sp1-binding sites typical of TATA-less promoters [18]. Transcription factor binding sites in *ING* promoters that could contribute to tissue-specific expression have not been identified.

1.2.2 ING Protein Structure

The mammalian ING proteins have several conserved domains shown in Figure 1.3. The ~55 amino acid (aa) potential chromatin regulation (PCR) domain may link ING proteins to HAT and HDAC complexes and is conserved in all five ING family members [15]. The first 125 aa of $p33^{ING1b}$ that includes this PCR domain are necessary for interaction with Sin3A-associated protein, 30kDa (SAP30), a member of mSin3/HDAC complexes [27]. This domain is conserved in ING2, and may have a similar function as ING2 has been found in similar complexes containing Sin3, HDAC1 and SAP30 [28]. A nuclear localization sequence (NLS) of ~50 aa is critical for ING's localization to the nucleus and is conserved in all ING family members. Within the NLS region, are three nucleolar translocation sequences (NTS; RRQR, KEKK, and KKKK) that in the case of ING1 are known to target the protein to nucleoli when cells are subjected to cellular stresses such as ultraviolet (UV)-induced DNA damage [29]. All three sequences are identical in ING2 and may have a similar function, but are not conserved in ING3-5. A phosphorylation-dependent interacting domain (PDIM)

with the 14-3-3-binding consensus sequence RSXpSXP is also present in both ING1 and ING2. In the case of $p33^{ING1b}$, phosphorylation-dependent binding to 14-3-3 protein was shown experimentally [30]. A PHD finger domain of ~45 aa is conserved for all the ING family members, and is discussed in more detail below. A peptide interacting motif (PIM) domain of ~15 aa enriched in acidic, basic, and aromatic residues is conserved in ING1 and ING2. PIM binds a defined subset of peptides [14] and, along with the PHD region binds to phosphatidylinositol monophosphates [31]. The unique N terminal region of $p33^{ING1b}$ contains a functional proliferating cell nuclear antigen (PCNA)-interacting protein (PIP) domain that upon UV damage causes association of the two proteins and regulates the induction of apoptosis [32]. The N terminal regions of ING2-5 contain a putative leucine zipper-like (LZL) domain that could indicate an ability to bind other leucine zipper-containing proteins [15].

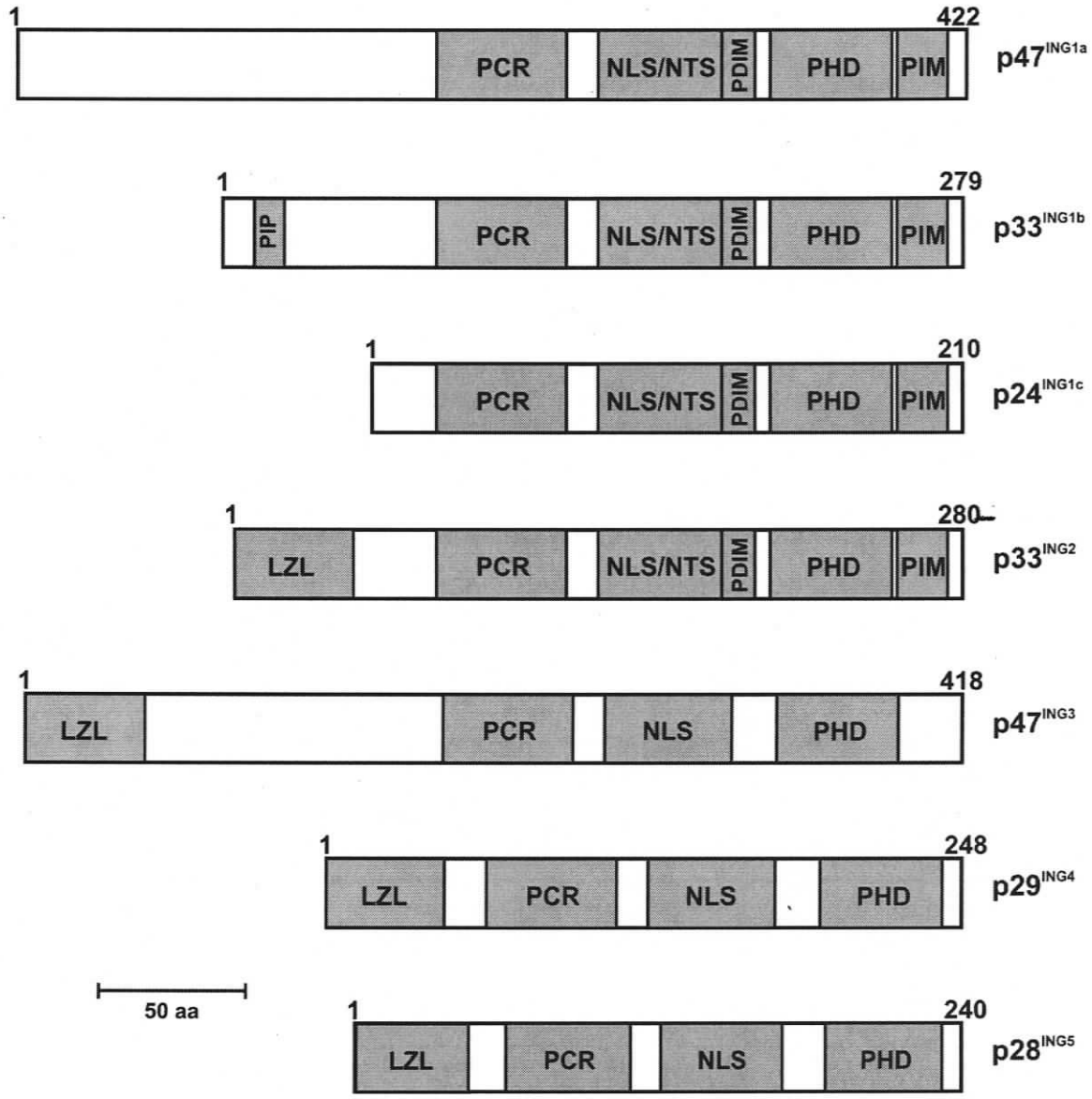

Figure 1.3. ING protein structures.

Features of mammalian ING proteins are shown including: a potential chromatin regulation domain (PCR); a nuclear localization sequence (NLS) that contains 3 nucleolar translocation sequences (NTS); a phosphorylation-dependent interacting domain (PDIM); a PHD finger (PHD); a peptide interacting motif (PIM) domain; a PCNA-interacting protein domain (PIP); and a leucine zipper-like domain (LZL). The first and last amino acid is numbered for each protein schematic. This figure was modified from He et al., 2005.

1.2.3 The PHD Finger of ING

The PHD finger discovered in plant homeodomain proteins is now known to be common to all eukaryotic genomes [11]. This zinc (Zn^{2+})-binding domain is found in over 400 eukaryotic proteins that are largely involved in transcriptional regulation [10, 11].

The PHD finger domain is ~60 aa (~45 aa in the case of the ING PHD fingers), characterized by specific spacing of 4 cysteine residues followed by a histidine and 3 additional cysteine residues (C4HC3) that bind 2 zinc ions [11]. There are additional hydrophobic residues that are highly conserved indicating an important role in stabilization of the structure. Several crystal structures have been solved that show the PHD domain uses an interleaved or cross-brace topology for the Zn^{2+}-coordinating residues where the first and third pair of coordinating residues bind one Zn^{2+} and pairs two and four bind the other Zn^{2+} in a three loop configuration [11]. This is similar to its closest relative, the RING finger which typically has a C3HC4 signature and also binds two zinc ions [11]. The PHD finger structure is conserved for ING2 that consists of three loops stabilized by two zinc-binding clusters and a small double-stranded anti-parallel β-sheet [33].

The PHD finger domain is generally associated with chromatin binding and protein-protein interactions in the nucleus [10, 11]. Recent studies have elucidated the crystal structure of the PHD finger of ING2 in association with histone H3 trimethylated at lysine 4 [33]. This binding is critical for transcriptional repression of the cell cycle regulator cyclin D [34]. The binding elements are conserved between ING family members and there is experimental evidence to support that all the ING family members can bind to trimethylated histone H3 *in vitro* [33, 34]. Earlier studies showed that upon DNA damage, ING2 binds to phosphoinositides in a manner that requires the PHD finger [31]. Phosphoinositides bound by the PHD finger include the rare phosphatidylinositol 5-phosphate (PtdIns(5)P) important in survival, growth, and proliferation signaling pathways [31]. The PHD finger of ING1 also binds phosphoinositides *in vitro*, but

in vivo studies are lacking [31]. The phosphoinositide and trimethylated histone H3 binding activities of the ING PHD finger are independent of each other [34]. Although mutation is less common than downregulation of ING expression in malignancies, mutations that have been identified are concentrated in the PHD finger region, suggesting the functions of the PHD finger are particularly critical [7].

1.3 ING FUNCTION

1.3.1 ING and Chromatin Remodeling

Studies with yeast homologs were the first to show ING's involvement in acetylation and continue to provide valuable insight into the role of ING family members in HAT and HDAC complexes, and their effects on nucleosome acetylation [24, 25, 35, 36]. It is now clear that Yng1 is a stable, stoichiometric component of the nucleosomal acetyl-transferase of histone H3 (NuA3) HAT complex and Yng2 is a stable stoichiometric component of the nucleosomal acetyl-transferase of histone H4 (NuA4) HAT complex (Table 1.1 [37, 38]). Both Yng1 and Yng2 facilitate the association and enzymatic activity of the HATs on chromatin. Pho23 is present within the reduced potassium dependency 3 (Rpd3) HDAC complex (Table 1.1 [25]).

Mammalian ING proteins from each gene in the ING family have been shown to associate with enzymes that remodel chromatin to alter gene expression. Some ING proteins associate with HATs that can increase gene expression, others with histone deacetylases HDACs that can decrease gene expression, or both (Table 1.1 and 1.2 and reviewed in [7, 9, 12, 30]). Differential association of ING isoforms with different proteins in HAT or HDAC complexes is observed. For example, the $p33^{ING1b}$ isoform of ING binds SAP30 in two distinct Sin3 transcriptional corepressor complexes containing active HDACs [27, 28]. One of the two complexes contains a corepressor brahma-related gene 1

(BRG1) and its subunits that are in involved in SWI/SNF-type ATP-dependent chromatin remodeling. The $p24^{ING1c}$ isoform does not associate with the complexes, suggesting it may have an alternate function [27]. $p33^{ING1b}$ associates with HAT complexes containing transformation/transcription domain-associated protein (TRRAP), cAMP-response element-binding protein (CBP), p300, and p300/CBP-associated factor (P/CAF) and increases the level of acetylation of histones H3 and H4 [39]. In contrast, the $p47^{ING1a}$ isoform binds HDAC1 and inhibits acetylation of these histones [39].

$P33^{ING2}$ was identified in HDAC complexes similar to those of $p33^{ING1b}$ using mass spectrometry of SAP30 immunoprecipitates [28]. Studies by Doyon *et al.* confirm the association of $P33^{ING2}$ with HDAC1/2 complexes and further characterize associations of HATs and HDACs for several other members of the ING family that include: ING3 association with Tip60/NuA4 HAT complexes [37]; ING4 association with histone acetyltransferase binding to ORC1 (HBO1) HAT complexes [12]; and ING5 association with both HBO1 HATs and monocytic leukemia zinc finger protein (MOZ)/MOZ-related factor (MORPH) HAT complexes [12]. It appears that ING proteins act as co-factors for distinct HAT and HDAC enzyme complexes, affecting chromatin conformation.

In a recent study, Goeman and colleagues identified two transcriptional silencing domains in $p33^{ING1b}$ whose function is not affected by p53, but is enhanced by rat sarcoma viral oncogene homolog (Ras). One of the domains is sensitive to the histone deacetylase inhibitor trichostatin A whereas the other is resistant, suggesting that $p33^{ING1b}$ confers gene silencing through both HDAC-dependent and HDAC-independent mechanisms [2].

Table 1.1. Protein complexes containing ING1 isoforms.

ING Isoform	Associated Proteins	Method	References
hp33^{ING1b}	RBP1, Sin3, ***HDAC1/2***, RbAp48, RbAp46, Sap30, Brg1, BAF155, p42, p35	AP-MS	[27, 28]
hp33^{ING1b}	TRRAP	IP	[39]
hp33^{ING1b}	p300/CBP, PCNA	IP	[39]
hp33^{ING1b}	P/CAF	IP	[39]
hp33^{ING1b}	***Sir2***	IP	[40]
hp33^{ING1b}	PCNA	IP	[32]
hp33^{ING1b}	GADD45	IP	[41]
hp33^{ING1b}	p53	IP	[42-44]
hp33^{ING1b}	14-3-3	GST, IP	[30]
hp33^{ING1b}	ERα	IP	[45]
hp33^{ING1b}	p14^{ARF}	IP	[46]
hp33^{ING1b}	p15^{PAF}	IP	[47]
hp47^{ING1a}	***HDAC1***	IP	[39]
mp37^{ING1b}	p53	IP	[18]
mING1	A1/Bfl-1	Y2H	[48]
yYng1	Sas3, Anc1/TAF30	IP, MS, AP	[38, 49]
yYng2	Tra1, Esa1, Epl1, Arp4, Act1, Eaf1, Eaf2, Eaf3, Eaf4, Eaf5, Eaf6, p53^{hr}	GST, AP Y2H, IP	[24, 25, 49, 50]
yPho23	***Rpd3***, Sap30, Sin3	AP	[25]

Histone acetyltransferases (HATs) are underlined and histone deacetylases (HDACs) are bold, italicized and underlined. Abbreviations: h, human; m, mouse; y, yeast; AP, affinity purification; MS, mass spectrometry; IP, immunoprecipitation; GST, glutathione-*S*-transferase pull-down assay; Y2H, yeast-two-hybrid; RBP1, retinoblastoma (Rb)-binding protein 1; RbAp48 and 46, Rb-associated proteins 48 and 46 kDa; SAP30, Sin3A-associated protein, 30kDa; BRG1, brahma-related gene 1; BAF155, barrier to autointegration factor 155; TRRAP, transformation/transcription domain-associated protein; CBP, cAMP-response element-binding protein; P/CAF, p300/CBP-associated factor; Sir2, sirtuin 2; PCNA, proliferating cell nuclear antigen; Gadd45, growth arrest and DNA-damage inducible gene 45; ER α, estrogen receptor α; p14^{ARF}, p14 alternative reading frame; p15^{PAF}, p15 PCNA-associated factor; BRMS1, breast cancer metastasis suppressor-1;Sas3, something about silencing 3; TAF30, TATA binding protein-Associated Factor 30 kDa subunit; Tra1, TRRAP-like 1; Epl1, enhancer of polycomb-like 1; Arp4, actin-related protein 4; Act1, actin 1; Eafs, Esa-1-associated factor; p53^{hr}, human recombinant p53; Rpd3, reduced potassium dependency 3.

Table 1.2. Protein complexes containing human ING2-5.

ING Isoform	Associated Proteins	Method	References
p33^{ING2}	Sin3, ***HDAC1/2***, RbAp48, RbAp46, Sap30	AP-MS	[28]
p33^{ING2}	RBP1, Sin3, ***HDAC1/2***, BRMS1, Brg1, Sap130, Sap30, RbAp48, RbAp46	AP-MS	[12]
p33^{ING2}	p300, p53	IP	[4]
p47^{ING3}	Tip60, EPC1	AP-MS	[37]
p29^{ING4}	Eaf6, HBO1, JADE1/2/3	AP-MS	[12]
p29^{ING4}	NFκB, p300, p53	IP	[51]
p28^{ING5}	Eaf6, HBO1, JADE1/2/3	AP-MS	[12]
p28^{ING5}	MOZ,MORF, BRPF1/2/3	AP-MS	[12]
p28^{ING5}	p300, p53	IP	[51]

Histone acetyltransferases (HATs) are underlined and histone deacetylases (HDACs) are bold, italicized and underlined. Abbreviations: AP, affinity purification; MS, mass spectrometry; IP, immunoprecipitation; RbAp48 and 46, Rb-associated proteins 48 and 46 kDa; SAP30 and 130, Sin3A-associated protein, 30kDa and 130 kDa; RBP1, retinoblastoma (Rb)-binding protein 1; BRMS1, breast cancer metastasis suppressor-1; Brg1, brahma-related gene 1; EPC, enhancer of polycomb homolog 1; Eafs, Esa-1-associated factor; HBO1, histone acetyltransferase binding to ORC1; JADE, gene for apoptosis and differentiation in epithelia; NFκB, nuclear factor kappaB; MOZ, monocytic leukemia zinc finger protein; MORF, MOZ-related factor; BRPF1/2/3 bromodomain- and PHD finger-containing.

1.3.2 ING Protein Interactions and Transcriptional Effects

In addition to interactions with HATs and HDACS that can affect transcription through chromatin remodeling, ING proteins bind to proteins critical to processes such as apoptosis, cell cycle regulation, and DNA repair (see Table 1.1 and 1.2) and regulate transcription of proteins involved in these processes.

Many studies link the action of ING to the transcription factor and DNA repair protein p53. For example, the enhancement of UV-induced apoptosis by p33^{ING1b} or p33^{ING2} requires the presence of p53 [52, 53]. Also, ING interacts with growth arrest and DNA-damage inducible gene 45 (GADD45) protein and

enhances p53-dependent repair of UV-damaged DNA [41]. Interactions between the PHD finger of ING2 and PtdIns(5)P regulate the ability of $p33^{ING2}$ to associate with chromatin and induce p53-mediated apoptosis in response to genotoxic stimuli [31].

Different ING isoforms may have antagonistic activities. Through interaction with p53, $p47^{ING1a}$ represses transcription of cyclin-dependent kinase inhibitor 1A, 21 kDa protein (*$p21^{CIP1}$*), whereas, $p33^{ING1b}$, $p47^{ING3}$, and $p33^{ING2}$ stimulate this promoter, and $p24^{ING1c}$ has no effect [40]. Through differential effects on $p21^{CIP1}$ protein levels, ING proteins have opposing effects on cell cycle arrest. The mouse homolog of human $p47^{ING1a}$, $p37^{ING1}$, also binds p53, inhibits accumulation of p53 protein and inhibits *$p21^{CIP1}$* transcription [18]. In contrast, the mouse homolog of $p33^{ING1b}$, $p31^{ING1}$, does not bind p53, but cooperates with p53 to enhance *$p21^{CIP1}$* transcription [18].

Interestingly, $p33^{ING1b}$ and $p33^{ING2}$ use different mechanisms to enhance p53 acetylation and increase its transcriptional activity. In both cases, induction of apoptosis and G1 phase cell cycle arrest occurs in a p53-dependent manner [22]. $p33^{ING1b}$ stimulates the transcriptional activity of p53 partly by inhibiting deacetylation by directly binding sirtuin 2 (Sir2) deacetylase and partly by inhibiting human murine double minute 2 (MDM2)-dependent degradation of p53 by competing with MDM2 for its p53 binding site [43]. $p33^{ING2}$ also enhances acetylation of p53 which in turn increases p53's transcriptional activation effects but *via* a different mechanism. $p33^{ING2}$ forms a complex with p53 and the HAT p300, and overexpression of $p33^{ING2}$ was associated with enhanced senescence in a p53-dependent manner [4]. In addition, both $p29^{ING4}$ and $p28^{ING5}$ physically interact with both p300 and p53 and enhance p53 acetylation *in vivo* [51]. $p47^{ING3}$ does not affect p53 acetylation, but does enhance transcription of *$p21^{CIP1}$* and *Bcl-2-associated X protein (bax)* in a p53-dependent manner [23].

The p14 alternative reading frame ($p14^{ARF}$) tumor suppressor protein plays a critical role in the activation of p53 in response to oncogenic stress. A recent study showed that the ability of $p33^{ING1b}$ to cause cell-cycle arrest and induction of $p21^{CIP1}$, or MDM2, is impaired in $p14^{ARF}$-deficient cells, and that $p33^{ING1b}$ and

$p14^{ARF}$ interact *in vivo* [46]. This provides yet another example of the complex interplay between p53 and ING in tumor suppressor pathways.

ING is also involved in apoptotic and DNA repair pathways that don't necessarily involve p53. Protein levels of $p33^{ING1b}$ increased during serum starvation-induced apoptosis in P19 mouse teratocarcinoma cells with inactive p53, and overexpression of $p33^{ING1b}$ promoted apoptosis while antisense expression protected against apoptosis in these cells [54]. Upon UV irradiation, $p33^{ING1b}$ causes cell cycle arrest and interacts with PCNA to promote DNA repair or induce apoptosis in cells preventing tumorigenesis depending upon the severity of DNA damage [32]. A recent study showed the ING/PCNA complexes also contain p15 PCNA-associated factor ($p15^{PAF}$) that competes for binding with the PCNA-inhibitor $p21^{CIP1}$ facilitating the DNA repair process [47]. The $p33^{ING2}$ PHD domain acts as a nuclear phosphoinositide receptor and this interaction regulates the ability of $p33^{ING2}$ to activate p53-dependent and p53-independent apoptosis [31]. Also, it was shown that $p33^{ING1b}$ has a subtle anti-proliferative effect even in the absence of p53, where the transcriptional activities of other members of the p53 family, p63α and p73α, are activated by $p33^{ING1b}$ [44]. Thus, although many tumor suppressor ING functions rely on p53, others do not.

Intriguingly, $p33^{ING1b}$ weakly associates with estrogen receptor α (ERα) and estrogen-induced transcription of genes by ERα was shown to be enhanced by $p33^{ING1b}$ in a dose dependent manner in transfected Cos-7 mammalian cells [55]. ING was originally cloned as a candidate tumor suppressor of human breast cancer and has diminished expression in breast cancer [1, 21, 56-58]. Taken together, this may indicate that ING's role in estrogen signaling is part of its tumor suppressor activity.

Specific genes have been identified as being affected by ING expression that further solidify ING as a tumor suppressor involved in numerous critical pathways. For example, $p33^{ING1b}$ protein binds DNA in an electrophoretic mobility shift assay (EMSA) at an AT-rich sequence that is also an hepatocyte nuclear factor 1 (HNF1) binding site in the promoter for α-fetoprotein (AFP) [40]. Aberrant expression of AFP is characteristic of hepatocellular carcinoma and

serves as a diagnostic tumor-specific marker [59]. $p33^{ING1b}$ represses AFP transcription by binding to the AT-motif and excluding HNF1 that is itself a positive regulator of AFP transcription. $p33^{ING1b}$ can also bind and inhibit the ability of Sir2 to deacetylate p53 protein, thereby repressing AFP by increasing the levels of active, acetylated p53 that is a negative regulator of AFP transcription [40]. All ING1 isoforms, as well as $p33^{ING2}$, were shown to repress the AFP promoter, even in the absence of p53 in the case of $p33^{ING1b}$ and $p33^{ING2}$ [60]. This involvement of ING in multiple AFP repression pathways may be a specific example of ING acting as a tumor suppressor in the liver.

Control of transcription of cell cycle regulators and apoptotic proteins by ING provide another mechanism of ING tumor suppressor action. $p33^{ING1b}$ enhances the expression of endogenous Bax and alters the mitochondrial membrane potential promoting apoptosis [52]. Overexpression of $p33^{ING2}$ significantly downregulates the expression of B-cell lymphoma protein 2 (Bcl-2) after UVB irradiation, and promotes apoptosis through the mitochondrial pathway, but also under non-stress conditions $p33^{ING2}$ upregulates Fas expression and activates caspase 8 promoting apoptosis through the death-receptor pathway [53]. Furthermore, overexpression of $p33^{ING1b}$ results in downregulation of the genes for the cell cycle regulator Cyclin B1 and proto-oncogene DEK, while upregulating tumor protein translationally controlled (TPT1) [60]. Also, levels of cell cycle inhibitor $p21^{CIP1}$ and proto-oncogene MDM2 were elevated in $p33^{ING1b}$-transfected cells [61]. $p33^{ING2}$, like $p33^{ING1b}$, can regulate the expression of genes involved in apoptosis such as *p21* ^{CIP1} and *bax* [22]. Thus, $p33^{ING1b}$ and $p33^{ING2}$ are clearly involved in multiple apoptotic pathways. In mouse, ING1 homologs also promote apoptosis and are inhibited by a direct interaction with the anti-apoptotic member of the Bcl-2 family, A1/Bfl-1 [48].

Although several differential effects have been observed, there appears to be substantial potential for ING1 isoforms and $p33^{ING2}$ to compensate for each other. A recent study showed that $p33^{ING2}$ is recruited to the *cyclin D* promoter via binding to histone H3 trimethylated at K4 [34]. All ING family members also bind histone H3 trimethylated at K4 *in vitro* [34]. It seems likely that over time the

other ING family members will be shown to regulate specific promoters *in vivo* as well. The binding of $p33^{ING1b}$ to 14-3-3 keeps ING sequestered in the cytoplasm preventing upregulation of $p21^{CIP1}$ [30]. Control of ING's cellular location ensures that the cell cycle is stopped only when DNA damage or other stimuli signal the relocalization of ING to the nucleus. The phosphorylation dependent interaction domain (PDIM) is conserved in all ING1 isoforms as well as in $p33^{ING2}$, and likely also plays a role in their localization [30]. Interestingly, a knockout mouse where all forms of ING1 were inactivated, did not have a severe phenotype, although stunted growth, and increased tendency toward developing lymphomas and increased sensitivity to DNA damage were observed [62]. It is likely that $p33^{ING2}$ or other ING family members are able to compensate for the loss of ING1.

Different ING family members with distinct, sometimes compensatory and sometimes antagonistic, cellular roles could be differentially regulated in the cell. The regulation of transcript expression of *ING1* and *ING2* in tissues with different cell fates is a major focus of this thesis.

1.5 MODEL OF ING MECHANISM

The mechanism of ING action in the context of cancer or DNA damage is beginning to come to light. Most studies have been done with human $p33^{ING1b}$, although recent studies with other ING family members have added important pieces to the puzzle. The role of ING in normal development, however, has not been characterized. A simplified model of ING action in a cell that undergoes DNA damage is shown in Figure 1.4. Initially, ING is localized in the cytoplasm where it is bound to the 14-3-3 protein [30]. Upon DNA damage, the PHD domain of ING binds to signaling phosphoinositides including PtdIns(5)P [31]. This targets ING to the nucleus where it can interact with proteins involved in different pathways including cell cycle regulators and DNA repair proteins, PCNA [32] and p53 [42-44]. ING can also interact with proteins that open chromatin conformation to enhance transcription including the HATS p300/CBP and P/CAF

[12, 39], and with proteins that condense chromatin to repress transcription including HDACs Sir2 [40] and HDAC1 and 2 [12, 27, 28]. Now in the nucleus, the PHD domain of ING is recruited to specific promoters with Histone H3 trimethylated at K4 [33]. Thus, ING is relocalized to the nucleus and tethered to specific promoter regions, while recruiting a variety of protein partners to affect transcription of genes involved in apoptosis such as *bax* [52, 53] and *MDM2* [61] and genes critical to cell cycle regulation such as $p21^{CIP1}$ [30, 40, 60], *cyclin B* [60], and *cyclin D* [34].

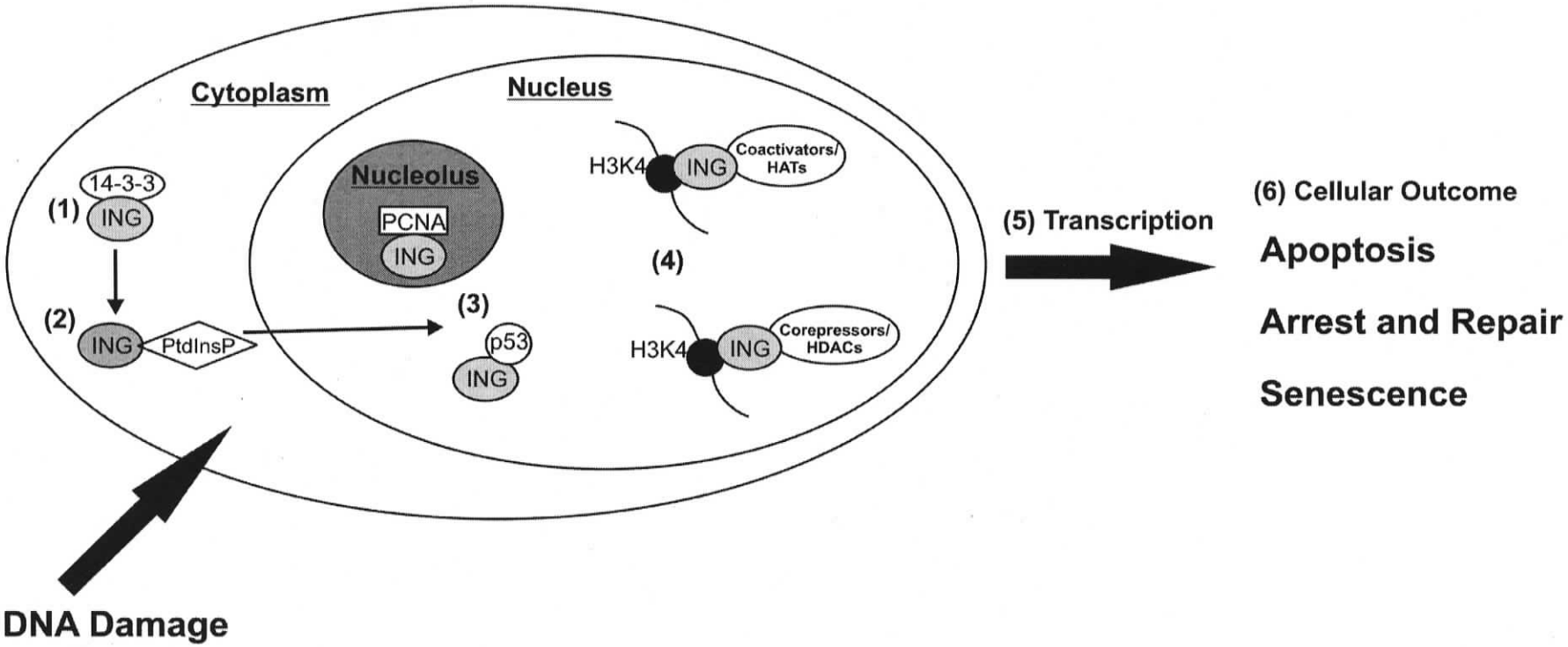

Figure 1.4. Model of ING's mechanism of action during DNA damage.

A generalized model of ING action is shown where initially ING is sequestered in the cytoplasm by interaction with 14-3-3 protein (1). Upon DNA damage, phosphoinositides (PtdInsP) bind to the PHD finger of ING (2) and target ING to the nucleus where it binds to DNA repair proteins such as p53 or to PCNA in the nucleolus (3). Once in the nucleus, ING is targeted to specific promoters by the PHD finger interaction with histone H3 trimethylated at lysine 4 (H3K4) along with coactivators (that may include p53) and HATs to enhance transcription or with corepressor and HDACs to repress transcription (4). Transcriptional effects (5) including both up and downregulation of genes leads to cellular outcomes (6) such as apoptosis, arrest and DNA repair, or senescence.

1.6 THYROID HORMONE AND THE TADPOLE MODEL

1.6.1 ING and the Tadpole Model

Most studies on ING focus on its tumor suppressor function in human and mouse, as well as its role in chromatin remodeling in yeast. However, at the onset of my graduate work, we knew that ING was widely expressed in normal tissues [19-21] and had anti-proliferative effects [1, 42], was involved in senescence [3] and promoted apoptosis [3, 42, 54, 63]. This suggested that a developmental model would be an important additional avenue of study.

Initially, Helbing and colleagues showed that ING protein expression correlated with apoptosis during tadpole tail regression in *Xenopus laevis* [16]. Analyses of premetamorphic *X. laevis* tadpole tissues showed a TH-induced accumulation of ING proteins in tail, whereas the levels in the leg were not affected. The TH-induced accumulation of ING was also observed in serum-free tail organ cultures and was prevented by inhibitors of tail apoptosis. Along with data presented in this thesis, this work presented the first link between ING expression and a hormonally regulated nuclear transcription factor-mediated apoptotic response opening up the possibility that ING family members may be involved in transducing the signal initiated by TH that determines cell fate. Subsequently, I have used TH-dependent tadpole metamorphosis as a model system to study ING in the context of normal development.

The remodeling of aquatic tadpoles into terrestrial juvenile frogs is totally dependent on TH. Amphibian postembryonic development and metamorphosis are divided into three phases: premetamorphosis, prometamorphosis, and metamorphic climax. The Nieuwkoop and Faber (NF) staging system is used throughout this manuscript [64]. Premetamorphosis (NF stages 45-54) is the interval of development that precedes thyroid gland function and is mainly a period of growth. At this stage, the tadpole is competent to respond to TH, but is functionally athyroid. Prometamorphosis (NF stages 55-59) begins with maturation of the thyroid gland and the low-level secretion of TH that initiates the

first metamorphic changes including limb growth. TH levels rise and peak dramatically at metamorphic climax (NF stages 60-64), which is characterized by the rapid, overt remodeling of the tadpole. 3,5,3',5'-tetraiodo-L-thyronine (T_4) reaches maximal levels at 7 nM at NF Stage 60-64 and 3,5,3'-triiodo-L-thyronine (T_3) reaches maximal levels at 8 nM at NF stage 62 [65]. TRs bind T_3 with a 5-10 fold higher affinity than T_4, with a K_d below 1 nM [66].

Figure 1.5 illustrates the progression of *X. laevis* development during metamorphosis as TH levels rise through prometamorphosis, peak during metamorphic climax, and decrease as tadpoles complete metamorphosis into froglets. Metamorphosis can be precociously induced in premetamorphic tadpoles by exposure to exogenous TH. In addition, metamorphosis can be inhibited and accelerated by a variety of agents [67].

In *X. laevis*, TRα appears during embryogenesis and is present throughout tadpole life [73]. TRβ is an early TH response gene with mRNA [68, 69] and protein [70] levels that follow the endogenous TH concentration [65, 71] and is elevated 50-100 times during TH-induced metamorphic climax [72]. *X. laevis* has 4 TR genes that produce receptors capable of binding TH: TRαA, TRαB, TRβA and TRβB where the TRβ genes each produce two alternatively spliced isoforms [73].

During metamorphosis, the tadpole tail regresses through apoptosis, while at the same time the legs proliferate, and the brain and other tissues undergo extensive remodeling in response to the same single stimulus of TH. This allows insights into the interplay between these diverse processes and makes this model ideal for this study.

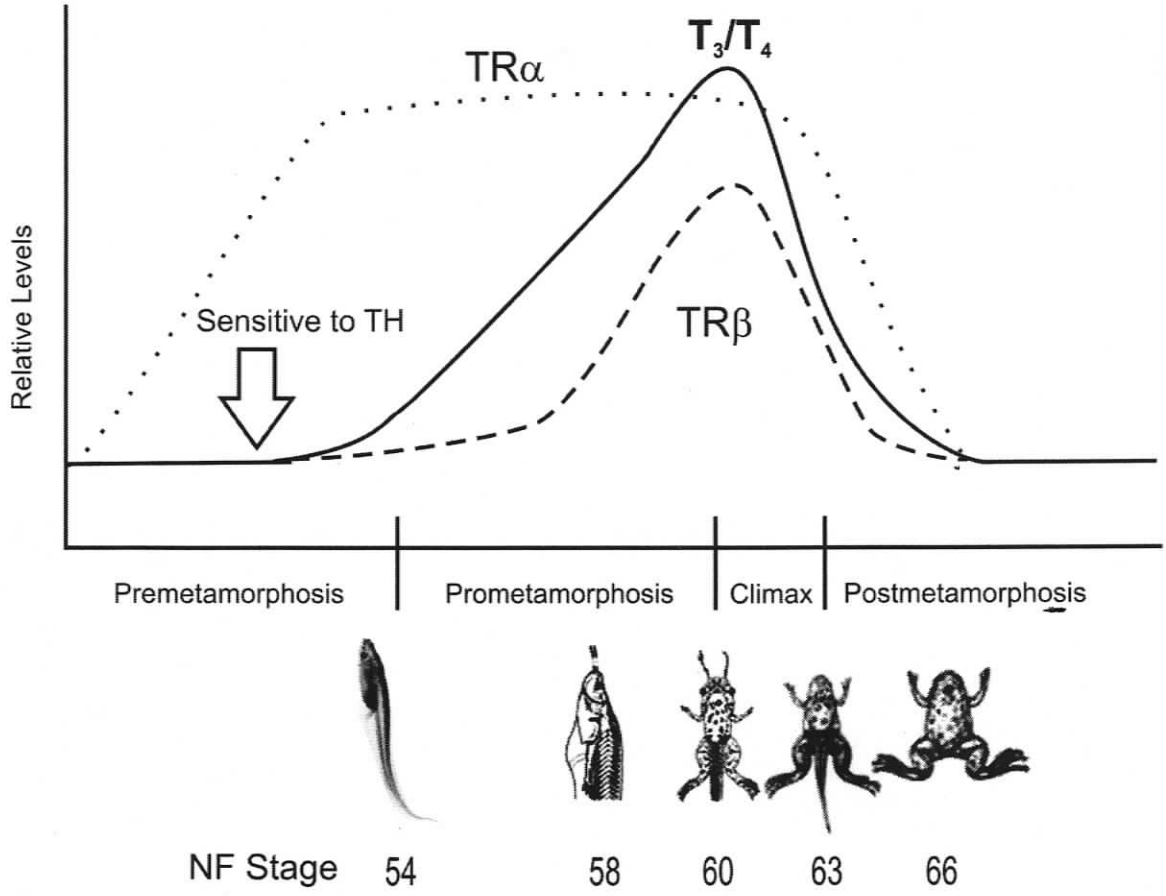

Figure 1.5. TH and the tadpole developmental model.

Shown is a schematic of *X. laevis* development through metamorphosis. Developmental stages are shown on the x-axis for premetamorphic NF stage 54, through prometamorphic NF stage 58, through metamorphic climax NF stages 60-63, through to the completion of metamorphosis NF stage 66. Relative levels of T_3/T_4 are represented by the solid line, TRα by the dotted line, and TRβ by the dashed line on the y-axis. Premetamorphic tadpoles are competent to respond to T_3 treatment which can be used to induce precocious metamorphosis. This figure was modified from Krain and Denver, 2004, and Furlow and Neff, 2006.

1.6.2 Thyroid Hormone Axis and Metabolism

Thyroid hormones have been implicated in controlling numerous and diverse processes such as growth, development, differentiation, apoptosis, and aspects of metabolism in nearly all tissues in a wide variety of organisms including amphibia, fish, most higher vertebrates and mammals [9, 72-74]. *X. laevis* metamorphosis depends on TH, and TRs are well characterized and are critical transcription factors in the process [9, 72-74]. The most widely studied mode of action of these hormones involves genomic effects *via* TH nuclear receptors that act as hormone-dependent transcription factors. However, there is increasing evidence of rapid non-genomic effects of TH which do not involve the TH receptors and gene transcription [75, 76]. Non-genomic effects can occur at the plasma membrane, at other subcellular organelles, as well as in the cytoskeleton and cytoplasm. Effects range from modulating ion channels, increasing glucose uptake, increasing actin polymerization, increasing oxygen uptake, increasing nucleotide translocation, increasing mRNA translation efficiency, and increasing or decreasing various enzyme activities or even causing their redistribution [75, 76].

Figure 1.6 shows the hypothalamus-pituitary-thyroid axis and the general steps in TH metabolism. Initially, thyrotropin releasing hormone (TRH) in mammals or corticotropin releasing factor (CRF) in amphibians from the hypothalamus acts on the anterior pituitary to release thyroid stimulating hormone (TSH) which then acts on the thyroid gland to cause TH synthesis [72]. Iodine is a key requirement for modifying the tyrosines of the thyroglobulin protein that make up TH. The majority of TH synthesized is T_4. Once released from the thyroid gland, THs provide negative feedback to the hypothalamus and anterior pituitary.

Carrier proteins that include thyroxine-binding globulin (TBG), serum albumin and thyroid binding pre-albumin (also known as transthyretin, TTR) keep levels of free TH in the serum very low and keep total T_3 and T_4 levels very stable [66]. TTR was identified as the major TH binding protein in the plasma of

metamorphosing tadpoles and in contrast to mammalian vertebrates, has higher affinity for T_3 than for T_4 [77].

Cellular uptake of lipophilic TH may involve passive diffusion; however, recent studies in *X. laevis* have demonstrated that the System L light chain amino acid transporter 1 (LAT1), and monocarboxylate transporter 8 (MCT8) mediate uptake of iodothyronines [78-80]. Also, in *Rana catesbeiana* tadpole red blood cells, the System T aromatic amino acid transporter mediates uptake of TH [81].

THs are bound by cytoplasmic TH binding proteins (CTHBP) that are multifunctional proteins that bind TH with affinities ranging from K_d of 1-100 nM [66]. One such protein representing the major binding activity of T_3 in the cytosol of *X. laevis* liver, is identical to aldehyde dehydrogenase class 1 (ALDH1) [82]. Another CTHBP, a *X. laevis* homolog of human M2 pyruvate kinase, binds TH as a monomer, whereas the tetrameric form of these proteins act as a pyruvate kinase [83]. High levels of this CTHBP mRNA were observed in the tail of premetamorphic tadpoles followed by dramatic repression with the onset of tail resorption, while in the hindlimb, the expression of this CTHBP is very low during morphogenesis [83].

T_4 is converted to the more active T_3 form by 5'-deiodinases that are regulated in a tissue-specific manner [66, 72, 73]. For example, Type II deiodinase (D2) is expressed at high levels in brain and hindlimb before metamorphosis allowing these tissues to respond to low levels of T_4 [73]. In contrast, in the tail that regresses late in metamorphosis when levels of TH are high, D2 rises dramatically at metamorphic climax [73]. T_3 enters the nucleus and binds TRs, most often as a heterodimer with retinoic X receptor (RXR) to elicit genomic TH effects. THs are inactivated by deiodinases and excreted in a tissue-specific manner [66, 73]. The deactivating type III deiodinase (D3) is expressed in the tail before metamorphosis and is induced by TH, followed by a decline at the onset of resorption, whereas, D3 expression is initially undetectable in the limb buds and rises modestly as the limbs complete morphogenesis [73].

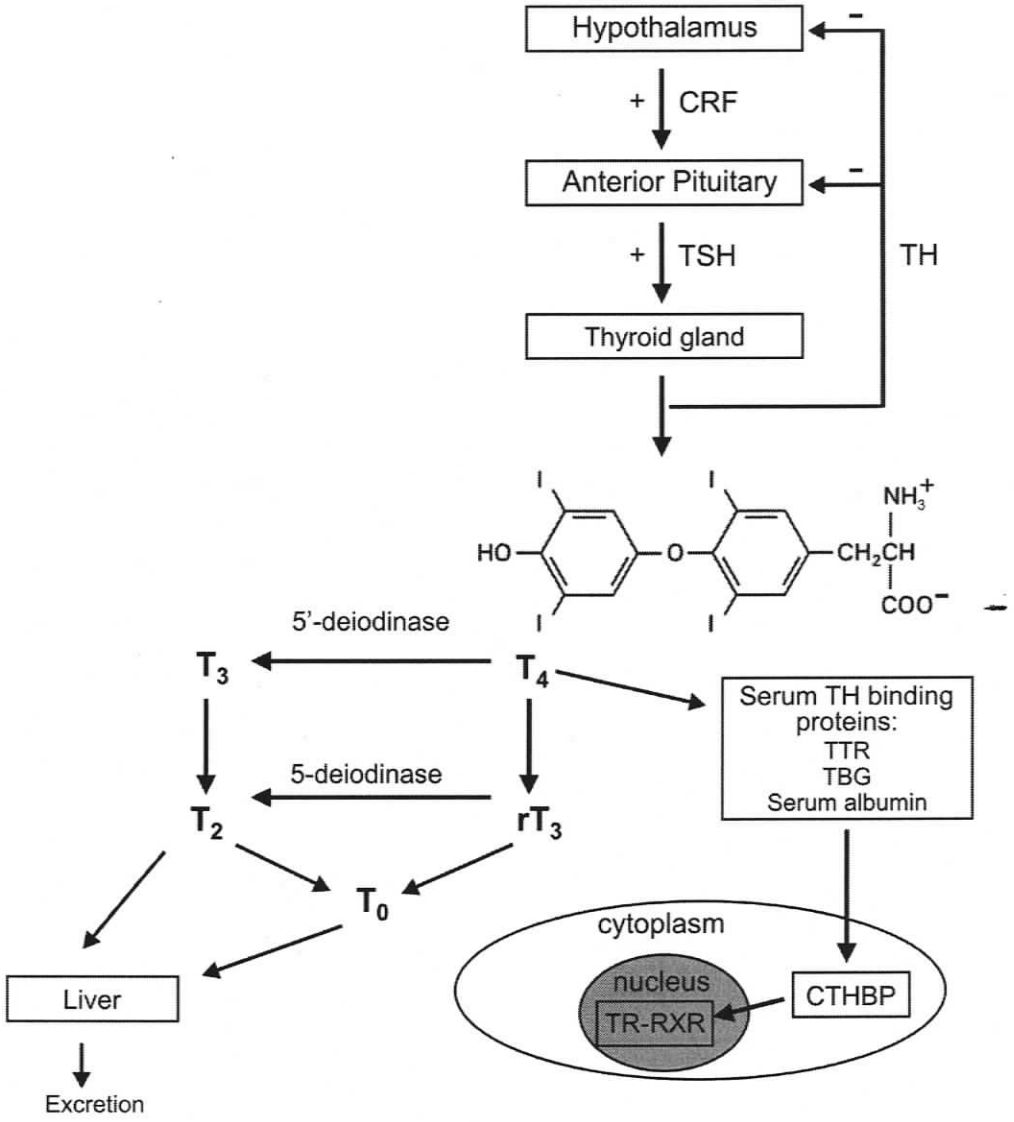

Figure 1.6. Thyroid hormone axis and metabolism.

A generalized pathway of the steps in thyroid hormone synthesis and metabolism are shown. CRF: corticotropin releasing factor; TSH: thyroid stimulating hormone; TH: thyroid hormones; (+): positive effect; (-): negative effect; CTHBP: cytoplasmic TH binding proteins; TTR: transthyretin; TBG: thyroxine-binding globulin; TR: thyroid hormone receptor; RXR: retinoic acid X receptor; T_4: 3,5,3',5'-tetraiodothyronine (thyroxine); T_3: 3,5,3'-triiodothyronine; rT_3: reverse-T_3;T_2: diiodothyronine; T_0: thyronine. Deiodinases are located within the cells of the thyroid gland and peripheral tissues. This figure is modified from Tata, 2006 and Greenspan and Gardner, 2004.

1.6.3 Thyroid hormone response elements

TRs bind to thyroid hormone response elements (TREs), which contain consensus hexamer half-site sequences AGGTCA with increased variation at 3 positions for lower affinity sites with consensus sequence (G/A)G(G/T)T(C/G)A. Positive TREs (pTREs) where T_3 induces transcriptional activation are the best characterized type of TRE. pTREs are most often bound by heterodimers of TRs with RXR, but TRs can bind as homodimers or monomers [72, 84, 85]. Negative TREs (nTREs) have been identified where T_3 induces repression of transcription. TRs bind nTREs as monomers to half sites [86, 87], or as homodimers [87, 88] or heterodimers with RXR [87, 89] to two half sites.

Most pTREs are located upstream of the promoter, but naturally occurring TREs have been identified in a variety of locations including the long terminal repeat of Moloney murine leukemia virus, the promoter and third intron of the rat growth hormone gene, and the intron of MDM2 [90]. There is considerable variation in the nucleotide sequences, number, spacing, and orientation of TRE half-sites. Among known natural TREs, direct repeats separated by 4 base pairs (bp) are most common [91]. Half sites are less commonly arranged as inverted palindromes separated by 6 bp or least commonly as palindromes with no spacing between half sites [92, 93]. An atypical site in the promoter of the enterocyte differentiation marker intestinal alkaline phosphatase (IAP) gene contains an everted repeat of two nonamers (TTGAACTCAgccTGAGGTTAC) separated by three nucleotides [94]. Still other arrangements of three or more TREs can be bound by multiple TRs such as in the rat growth hormone promoter [95].

Although less well characterized than pTREs, various types of nTRE sequences resembling TREs have been identified in a variety of locations including in the promoter (TSHβ and amyloid precursor protein), the first exon (c-Myc; cellular myelocytomatosis transcription factor), and the 3'-untranslated region (rat growth hormone and Clone 144) [86]. A novel nTRE sequence, TTTGGG, has been identified in the CD44 gene and the TSHβ gene [86].

1.6.4 Thyroid Hormone Receptor Action in Tadpole Metamorphosis

The general model of TR action during metamorphosis involves TRs binding DNA associated with corepressors and repressing gene expression in the absence of TH during premetamorphosis [72-74]. Corepressors such as silencing mediators of receptors of thyroid hormone (SMRT) and nuclear receptor co-repressor (NCoR) interact with the TR and RXR. SMRT and NCoR recruit the transcriptional repressor complex Sin3A and HDACs whose deacetylation function results in a more compact chromatin state and gene repression (Figure 1.7A). This model is complicated by the existence of nTREs, where transcription is active in the absence of T_3 and repressed in its presence [74, 92].

During metamorphosis, T_3 levels increase and binding to TRs generally activates transcription *via* recruitment of coactivators such as p160, steroid receptor coactivators (p160/SRCs), and thyroid hormone receptor (TR)-associated protein 220 (TRAP220), along with HATs that acetylate histones making chromatin more accessible for transcription [72-74] (Figure 1.7B). Similar to repression, the model is complicated by the fact that nTREs are repressed in the presence of T_3 [74, 92].

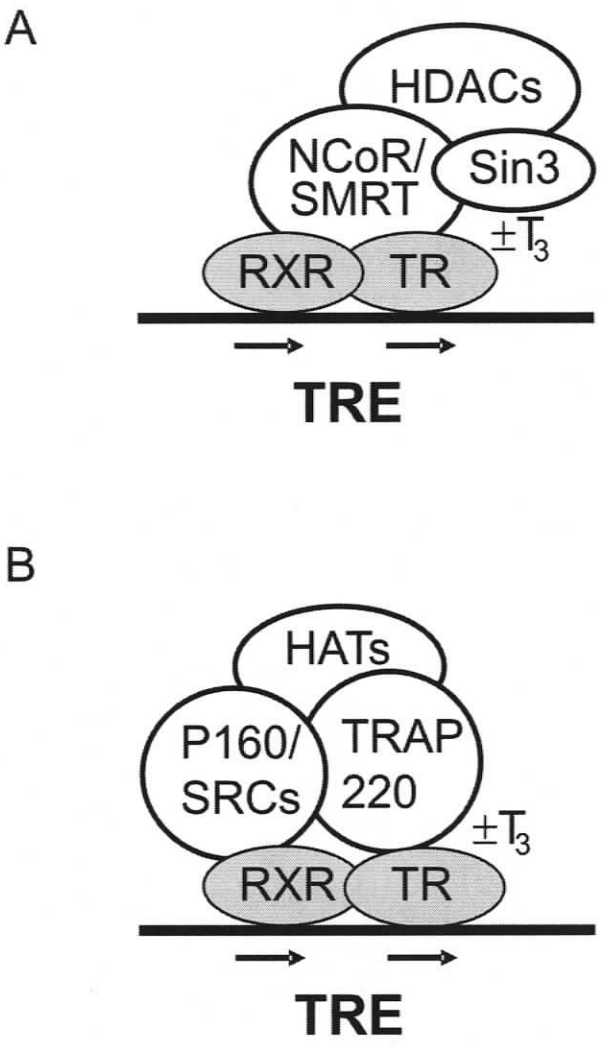

Figure 1.7. General model of TR action to repress and activate transcription.

(A) TRs bind TREs, most often as a heterodimer with RXR and repress transcription in the absence of T_3 ligand; however at nTREs, T_3 induces repression. This duality is represented by $\pm T_3$. Common corepressor NCoR, SMRT, and Sin3 along with HDACs that compact the DNA inhibiting transcription are shown. (B) Binding to TRs in the presence of T_3 generally activates transcription *via* recruitment of coactivators such as p160, SRCs, and TRAP220, along with HATs that acetylate histones making chromatin more accessible; however, at nTREs, transcription is active in the absence of T_3. This duality is represented by $\pm T_3$. This figure is modified from Yen, 2001 and Buchholz *et al.*, 2006.

TR complexes can directly affect the basal transcription machinery. During premetamorphosis, TR binds transcription factor IIB (TFIIB) inhibiting transcription of genes deleterious to growth, whereas during metamorphosis TR recruits TRAP220 that binds the RNA Polymerase II (RNA Pol II) complex activating transcription of genes required for metamorphosis [74, 91]. These transcriptional effects ultimately alter protein expression. New protein synthesis is required for metamorphosis [16, 96], but repression is also critical for proper development [74, 92].

1.6.5 Tissue-Specific Requirements of Tadpole Metamorphosis

The metamorphic program is quite different in different tissues. Tail undergoes complete regression *via* programmed cell death and activation of lytic enzymes (including collagenase, nucleases, phosphatases, and matrix metalloproteinases) and lysosome proliferation [72]. The morphological changes in brain include remodeling, axon guidance, axon growth, cell proliferation and death that requires the biochemical processes of cell division, apoptosis and new protein synthesis [72]. Limb bud involves *de novo* formation of bone, skin, muscle, and nerves through cell proliferation, differentiation and chondrogenesis [72].

Timing of tissue specific responses is critical to metamorphosis. An animal must complete the differentiation of the hind- and fore-limbs before the tail is lost, and the lungs must become fully functional before the gills are resorbed [73]. Thus, during natural metamorphosis, limbs grow when there are low levels of circulating TH (~NF stage 54) while the tail resorbs only after NF stage 60 once TH levels are maximal [66]. To achieve the tissue-specific developmental changes, numerous sets of genes are regulated by TH *via* TR transcriptional activity [72-74].

Analyses of tadpole tail during natural and precocious metamorphosis in the Helbing lab using a 420 cDNA array of known genes show that different

functional groups of genes are differentially regulated [97, 98]. Transcription factors gradually increase through metamorphosis with a transient decrease at NF stage 60, while structural proteins increase in premetamorphosis and then decrease during prometamorphosis to low levels during metamorphic climax [98]. Transcripts for proteins involved in metabolism, signaling and cell-growth control increase during prometamorphosis [98]. In comparison, during T_3-induced metamorphosis most functional groups, including transcripts for proteins involved in transcription, signal transduction, chromatin structure, hormone regulation, metabolism, cell growth control, apoptosis/degradation and structural proteins gradually increase up to 48 h, declining at 72 h [97].

Tissue specificity depends on TR isoforms and their cofactors being expressed in unique combinations and levels [73]. Other regulatory factors are likely involved, but are not well understood. Adult cell growth and differentiation required for limb development is characterized initially by high TRα and RXRα levels, along with high NCoR and SMRT levels and high type II deiodinase levels. Then corepressors are released for proliferation which is largely dependent on TRα. Coactivator recruitment required for differentiation may involve both TRα and TRβ. In contrast, the cell death and resorption of larval cells in tail is characterized by low TRα and RXRα, as well as low coactivator and corepressor levels. There is a high baseline of inducible type III deiodinase expression which declines at metamorphic climax. TRβ appears to be the most important TR for coactivator recruitment required for death and resorption of the tadpole tail.

Different TREs may direct specific coregulator assemblies. For example, T_3 regulates transcription of *rat sarcoendoplasmic reticulum calcium ATPase* in the heart through three differently configured pTREs [99]. Researchers found that one TRE recruits corepressor complexes containing NCoR and HDAC3 in the absence of T_3, and SRC1 containing coactivator complexes in the presence of T_3, while another TRE bound the same corepressor complexes without T_3 but showed only a weak association with SRC1 with T_3 [99]. In *X. laevis* tadpole tail, the coactivators SRC3 and p300 are present on the promoter of *TRβ* regardless

of T_3 status, whereas these coactivators are only present on *TH/bZIP* and the muscle-cell-specific *MyoD* promoters if T_3 is present, and are never present on the housekeeping gene, elongation factor 1a, and intestinal fatty acid binding protein promoters [100]. Although SRC3 was found to be dramatically upregulated during natural and T_3-induced *X. laevis* metamorphosis, p300 is expressed throughout postembryonic development [101] suggesting that both cofactor availability and promoter specificity are determinants in coregulator complex assemblies. Histone acetylation in transcriptional activation is also a variable requirement for regulation by TRs during amphibian development. In whole animal studies, changes in histone acetylation are not correlated with the expression of TH response genes, whereas, in the intestine and tail where TH response genes are dramatically up-regulated, TH treatment induces gene activation and histone H4 acetylation [102].

At nTREs, coregulators normally considered repressive may be activating and as with pTREs, coregulator requirements vary for different promoters. nTREs of the *Necdin* and *TSHβ* genes share coregulator requirements of RXR and NCoR/SMRT for full ligand-independent activation [89]. *Necdin* expression is influenced by deacetylase activity, suggesting that histone deacetylases and corepressors also function as activators of transcription, depending on the promoter context [89]. Another study showed that the corepressor SMRT can act as a strong coactivator while NCoR is a weak coactivator for TRα at a nTRE found in the *Rous sarcoma virus long terminal repeat* [88]. Different response elements appear to dictate whether a cofactor will function as a coactivator or a corepressor, likely due to conformational changes in the TRs that bind them.

At the novel nTRE of the *CD44* gene (a TTTGGG sequence shared by a nTRE in human *TSHβ*) NCoR enhances TR-mediated basal transactivation by a weak TR-DNA interaction in the absence of T_3, which is repressed by T_3 [86]. Furthermore, this study provides the first demonstration of a T_3-dependent negative regulation mechanism involving NCoR, GAGA-binding factor, and TRα [86]. With so many TH-regulated genes in different species that require tissue-

specific developmental regulation, there is much more to be learned about TREs and TR-mediated regulatory complexes.

1.6.6 Hormone Crosstalk in Metamorphosis

Although TH is an absolute requirement for metamorphosis and regulates key processes in all tissues, other hormones have been found to modulate this process. The molecular mechanisms include effects on peripheral TH metabolism and alterations in TR expression or function.

The role of amphibian prolactin (PRL) in metamorphosis is not clear, but PRL prevents both natural and TH-induced metamorphosis [66, 72]. Early studies indicated that PRL enhances larval growth and suppresses metamorphic changes [103-105]. PRL added at the same time as T_3 blocked both limb development and tail regression in organ culture [106]. PRL prevented the T_3-induced upregulation of TRα and TRβ mRNAs in premetamorphic *Xenopus* tadpoles and in organ cultures of tadpole tails [107]. Recently, Huang and Brown showed that overexpression of PRL in transgenic *Xenopus* resulted in an adult-shaped body with an unabsorbed tail, suggesting that the sensitivity to PRL is different for specific organs and tissues [108]. PRL receptor mRNA in the bullfrog tail, a tissue important to the larval stage, increased at the onset of climax and was maintained at a relatively high value at least until mid-climax while in the kidney, a tissue important to adult, PRL receptor mRNA gradually rose as metamorphosis progressed suggesting PRL has effects in development of larval and adult tissues [109].

Gonadal steroids such as testosterone and estradiol have been shown to inhibit amphibian metamorphosis [66]. The mechanisms are not well understood. Richards and Nace reported that sex steroid treatment inhibits larval development in *Rana pipiens* [110]. Gray and Janssens showed that testosterone and estradiol inhibited T_3-induced metamorphosis in premetamorphic *X. laevis* tadpoles [111]. They suggest that testosterone inhibits

the prometamorphic actions of bromocriptine, which stimulates metamorphosis by inhibiting production of the metamorphic inhibitor PRL [111]. Hayes and colleagues showed that estradiol and testosterone inhibit growth and development in *Bufo boreas* [112] and also that estradiol significantly inhibited tail resorption in *X. laevis,* but effects on hindlimb development were absent [113]. Based on their result that estradiol-treated animals that do not metamorphose completely lack a thyroid gland, whereas thiourea-treated animals have a hypertrophied thyroid gland, the researchers suggested that estradiol may act by inhibiting TSH, thus removing trophic stimulation by the pituitary [113]. In EMSAs, both TR and ER bound the TRE of the human glycoprotein hormone α subunit gene and estradiol inhibited T_3-mediated negative regulation of this gene, suggesting that ER and TR may compete for TRE binding [114]. Also, ER mutants that cannot bind DNA blocked T_3-mediated transcriptional activation possibly by competing for coactivator proteins [115]. Ovaries from anuran larvae are capable of producing estrogens, but estrogens have never been reported in tadpoles *in vivo* [113]. However, with mounting evidence of endocrine disrupting compounds (EDCs) in the environment with estrogenic and androgenic properties at concentrations that affect wildlife, the effects of these steroids on metamorphosis and development are highly relevant.

Glucorticoids may provide tadpoles with the ability to control the timing of metamorphosis dependent on environmental stresses [65]. For example, corticosterone increases in response to crowding and is likely responsible for the inhibition of growth and development when tadpoles are raised at high densities [113]. CRF stimulates adrenocorticotropin releasing hormone (ACTH) release from the pituitary in addition to causing the release of TSH. ACTH then causes the interrenal glands to produce glucocorticoids such as corticosterone and aldosterone [66, 72]. Glucocorticoids, as well as CRF and ACTH accelerate TH-induced metamorphosis, both in intact tadpoles and isolated tissues [105]. Like TH, corticosterone increases to a maximum at metamorphic climax [65] and antagonizes metamorphosis at low TH concentrations while accelerating metamorphosis at high TH concentrations [66]. A recent study showed that GR

mRNA was upregulated by exogenous T_3 in the tail but was downregulated in the brain of premetamorphic tadpoles and exogenous corticosterone upregulated TRβ mRNA in intestine [65]. Furthermore, a T_3-induced increase in TRα in *Rana catesbeiana* cultured red blood cells was completely abolished in the presence of either 34 nM corticosterone or 10 nM dexamethasone (a synthetic glucocorticoid) [116]. These results support the idea that tissue specific responses may be partly due to modulation by hormones in addition to TH.

The roles of these additional hormones are believed to coordinate metamorphosis in a tissue specific manner at different concentrations of TH and stages of development. The levels of each hormone and receptor and specific effects they have on other receptors are becoming better defined; however, the coregulatory complexes involved in gene regulation and other downstream events are still poorly understood.

1.6.7 Convergence of Thyroid Hormone Receptor and ING

A network of TR and ING inter-related effects suggest these proteins cooperate in cellular processes critical to cell fate. Both ING and TR are well-characterized for their involvement in chromatin remodeling and apoptosis. Although many studies are carried out with human proteins, the highly conserved counterparts in amphibians may act in the same manner. For example, TR, p53, and mitogen-activated protein kinase (MAPK) form a complex together in the nucleus resulting in the phosphorylation of p53 that decreased p53 transcriptional activity [117]. TRβ specifically inhibited p53-mediated induction of proapoptotic Bax and GADD45, involved in growth arrest and DNA-repair, but not the cell cycle inhibitor $p21^{CIP1}$ [118]. $p33^{ING1b}$ interacts with GADD45 [41], and both $p33^{ING1b}$ and $p33^{ING2}$ promote Bax-mediated apoptosis [52, 53]. Furthermore, through association with p53, $p47^{ING1a}$ represses transcription of the cyclin inhibitor $p21^{CIP1}$, whereas $p33^{ING1b}$, $p33^{ING2}$, and $p47^{ING3}$ promote $p21^{CIP1}$ transcription, and $p24^{ING1c}$ has no effect [40].

MDM2 protein binds p53 causing its degradation and transcription of the *MDM2* gene is enhanced by p53 in an autoregulatory loop. Although, MDM2 levels were elevated in $p33^{ING1b}$-transfected cells [61], ING binds and regulates p53 transcriptional effects in some instances by excluding binding of MDM2 and preventing p53 degradation [42-44]. TRα and TRβ bind the *MDM2* gene at the p53-response sequence, enhancing *MDM2* transcription in a TH-dependent manner [90]. TR transcriptional activity is antagonized by p53 binding to the DNA-binding domain of TRβ [119, 120]. The increase in MDM2 protein tips the balance towards p53 degradation and allows TRβ to increase transcriptional activity and at the same time causes decreased p53 transcriptional activity of other genes. Thus, there are many regulatory loops with protein-protein and protein-DNA interactions to provide tight control of transcription of genes likely important for processes critical for tadpole development including cell cycle control and apoptosis, but studies in this area are lacking.

ING has recently been found to associate with ERα and enhance transcription of a reporter construct [55]. Also, TRα and TRβ can potentiate estrogen-mediated transcription from a consensus estrogen response element (ERE)-driven reporter [121]. Furthermore, estrogen inhibits metamorphosis possibly by inhibiting TSH [113], and ER may compete with TR for TRE binding [114] or for coactivator proteins [115]. The relationship between ING and hormonal signaling pathways is largely unknown, but there is potential for crosstalk during metamorphosis.

1.7 RESEARCH HYPOTHESIS AND THESIS OUTLINE

Very little is understood about the regulation of ING transcripts. Changes in ING protein levels have dramatic consequences for regulation of cellular processes including DNA repair and apoptosis, and many cancers are known to have decreased mRNA and protein levels of the ING tumor suppressor. Early evidence suggested that ING protein expression was linked to TH-induced

apoptosis in *X. laevis* tadpole tail [16]. The ING family members present in frog, the nature of TH regulation of ING during development, and the role of ING in frog was not known. This thesis focuses on understanding the relationship between the ING1 and ING2 tumor suppressors and the control of TH-induced proliferation, remodeling, and particularly apoptosis in the *X. laevis* frog model system. Three hypotheses are addressed: 1) multiple variants of ING1 and ING2 exist in *X. laevis*; 2) ING1 and ING2 are regulated by thyroid hormone; and 3) ING is involved in TH-dependent gene expression. To investigate these hypotheses, I isolated *ING1* and *ING2* transcript sequences from *X. laevis*, and investigated their expression patterns in a variety of adult tissues, and during natural and T_3-induced metamorphosis in tadpole tails which are undergoing apoptosis, hindlimbs which are proliferating, and brains which are remodeling, discussed in Chapter 2. Novel antibodies specific to *X. laevis* ING and TR are characterized in Chapter 3, and they are used to test whether ING and TR proteins co-immunoprecipitate. In Chapters 3 and 4, I investigate ING's ability to associate with promoters of TH-regulated genes. In Chapter 4, the gene organization and sequence is analyzed for both *ING1* and *ING2*. Putative TREs were found and the association of TR with the promoters of *ING1* and *ING2* is discussed. These studies are critical in elucidating the regulation of ING by TH as well as beginning to understand ING's role in TH-induced tadpole metamorphosis. Because ING is so highly conserved from yeast to humans, there are larger implications for developmental systems in other organisms including mammals.

CHAPTER 2: MULTIPLE NOVEL TRANSCRIPT VARIANTS OF *ING1* AND *ING2* IN *XENOPUS LAEVIS* ARE DIFFERENTIALLY EXPRESSED AND THYROID HORMONE-RESPONSIVE

The majority of work presented in this chapter has been published in the following manuscript: Wagner, M.J., and Helbing, C.C. (2005). Multiple Variants of the ING1 and ING2 Tumor Suppressors are Differentially Expressed and Thyroid Hormone-responsive in *Xenopus laevis*. *General and Comparative Endocrinology*, Oct;144(1):38-50.

2.1 INTRODUCTION

My experiments had previously indicated that splice variants existed for *ING2* in *X. laevis* [16], but the sequences of these variants were unknown. In addition, we did not have any sequence information for *X. laevis ING1* at this time. Therefore, I used the Random Amplification of cDNA Ends (RACE) technique to isolate *ING1* and *ING2* variants. I examined expression of the variants and show they are differentially expressed in a variety of adult tissues.

We were the first to show that a hormone, in particular thyroid hormone, affects the expression patterns of *ING2* transcripts [16]. Protein work done by Dr. Helbing showed a TH-induced accumulation of ING proteins in tail that was observed in serum-free tail organ cultures as well [16]. This work provided the first link between ING expression and a TH-regulated apoptotic response.

To address the hypothesis that *ING* variants are regulated by TH, several transcript expression studies were carried out on T_3-treated *X. laevis* as well as with naturally developing tadpoles. I will show that *ING1* and *ING2* variants are

differentially expressed in tadpole brain, tail and hindlimb during natural and precocious metamorphosis. Intriguingly, *ING* transcript variants are significantly reduced in the hindlimb, a tissue that undergoes proliferation during metamorphosis, while many variants increase in the tail, a tissue that undergoes apoptosis. These data suggest that there may be antagonistic regulation of these variants by TH that correlates with the fate of these tissues.

2.2 MATERIALS AND METHODS

2.2.1 Experimental Animals

The care and treatment of animals used in this study were in accordance with the guidelines of the Animal Care Committee, University of Victoria. *Xenopus laevis* tadpoles Nieuwkoop and Faber (NF) stages 50-54, 58, 60, 62 and 63, and adult males [64] were purchased from Ward's Natural Science (St. Catharines, ON) and Xenopus I, Inc. (Dexter, MN) and maintained in polyethylene buckets at room temperature. Tadpoles were fed Seramicron daily (Rolf C. Hagen, Inc., Montreal, QC). Tadpoles were euthanized in 0.1% and adults in 1% tricaine methanesulfonate (MS-222; Syndel Laboratories, Vancouver, BC).

2.2.2 Isolation of RNA, Generation of cDNA Libraries, and 5'/3' RACE

Total RNA was isolated from various tissues using TRIzol (Invitrogen, Burlington, ON) following the manufacturer's instructions. Random Amplification of cDNA Ends (RACE)-ready cDNA libraries were made from poly(A)$^+$ mRNA isolated from *X. laevis* tadpole brain and tail using the Marathon cDNA amplification kit or from adult testis using the Smart RACE cDNA kit (BD Biosciences, Burlington, ON). The reactions used the universal primers supplied with the kit paired with the gene-specific primers for 5' RACE of x*ING1*

(5'-CCTGTTTTCATTGTTCCGCTGTCTCCTG and subsequently 5'-CAAGTTCTTGACTACGAATAAGAGCTCGCTGG) and for x*ING2* (5'-CCTGCCCCGGTAGTAACGTGCTAACTCTAC). For 3' RACE of x*ING1*, the gene-specific primer used was 5'-GTACAAGCAACAGCAGCAAAAACAACCAGG. Primer design was accomplished using Primer Premier software (Premier Biosoft International, Palo Alto, CA). Primers were used at 20 pmol in a 50 µl reaction containing 1x Advantage 2 DNA Polymerase Mix (BD Biosciences), 10 nmol deoxynucleotidylphosphates (dNTPs) (GIBCO Life Technologies, Montreal, PQ), and 1x Advantage 2 PCR Buffer (BD Biosciences). Touchdown PCR was performed on the RACE-ready libraries (94°C for 60 s; five cycles at 94°C for 30 s, and 70°C for 3 min; five cycles at 94°C for 30 s, 67°C for 30 s, and 72°C for 3 min; and 35 cycles at 94°C for 30 s, 65°C for 30 s and 72°C for 3 min, followed by 10 min at 72°C). The PCR products were cloned using the TOPO TA Cloning Kit Dual Promoter System with PCR II$^-$ TOPO vector and TOP10 cells (Invitrogen) as per the manufacturer's instructions. The putative positive clones were picked for creation of liquid stocks in Luria-Bertani (LB) broth containing 100 µg/mL ampicillin (Sigma-Aldrich, Oakville, ON). The stocks were used to inoculate 5 mL cultures of LB broth with 100 µg/mL ampicillin, which were grown overnight at 37°C with shaking. Plasmids were harvested with a Qiaprep Spin Miniprep kit (Qiagen, Mississauga, ON) and subsequently digested with restriction endonuclease *Eco*RI (New England Biolabs, Ipswich, MA). An 1% agarose gel was used to separate the inserts from plasmid vector, and positive clones were then sequenced. The DNA and derived amino acid sequences were aligned using ClustalW version 1.8 software (http://clustalw.genome.ad.jp). The sequences reported can be found in GenBank, accession numbers AY601659-AY601667.

2.2.3 *Sample Collection and Preparation of cDNA for 100 nM T_3 Study*

Premetamorphic (NF stage 54) *X. laevis* tadpoles were immersed in charcoal-filtered municipal water at 21±1°C to which 100 nM 3,5,3'-triiodothyronine (T_3; Sigma-Aldrich) was added dissolved in 400 μM sodium hydroxide (NaOH; EM Science, Gibbstown, NJ). Tadpoles were treated with T_3 and tissues were processed at 6, 12, 24, and 48 h time points. There were three groups of control animals to which an equal volume of NaOH was added. One group was processed at the beginning of the experiment (0 h control) and served as the control for the 6 and 12 h time points. Another control group was processed at 24 h, and the third group was processed at 48 h. The animals were not fed during the experiment. Tail, hindlimb and brain were dissected from individual animals (n=6 for 0 h control, n=7 for 6, 12, 24, and 48 h T_3 treatment, and n=8 for 24 and 48 h controls) and stored in RNA*later* (Ambion Inc., Austin, TX). For natural metamorphosis studies, tail, hindlimb, and brain were collected from 6 individual animals from each of NF stage 54, 58, 60, 62 and 63 and stored in RNA*later*. For determination of expression levels in adult tissues, samples were collected from individual males (n=3-4) and stored in RNA*later*. Two additional sample sets came from two separate pools of 3 males each.

Total RNA was isolated from various tissues using TRIzol reagent as described by the manufacturer (Invitrogen). Mechanical disruption of tissues utilized 700 μl TRIzol reagent (300 μl for NF stage 54 hindlimbs, 200 μl for tadpole brains), a 3 mm diameter tungsten-carbide bead, and safe-lock Eppendorf 1.5 mL microcentrifuge tubes in a Retsch MM301 Mixer Mill (Fisher Scientific Ltd, Ottawa, ON) at 20 Hz for six minutes. Mixing chambers were rotated 180 degrees halfway through the homogenization procedure. Glycogen (20 μg for tadpole brain; 40 μg for NF stage 54 hindlimb) was added prior to isopropanol precipitation to maximize RNA yield for these small tissues. Isolated RNA was subsequently resuspended in diethyl pyrocarbonate (DEPC)-treated RNase-free water and stored at -70°C.

One µg for tadpole and two µg for adult samples total RNA was annealed with 500 ng random hexamer oligonucleotide (Amersham Biosciences Inc., Montreal, QC) and cDNA was generated using Superscript II RNase H^- reverse transcriptase as described by the manufacturer (Invitrogen). The 20 µL reaction was incubated at 45°C for 2 h and diluted 10-fold for tadpole or 5-fold for adult samples. Analyses for variants *xING1b1-4*, *xING1b5*, *xING1c2*, and *xING2b* were done on undiluted cDNA.

2.2.4 Reverse Transcription- Polymerase Chain Reaction (RT-PCR) Analyses and Statistical Analyses for 100 nM T_3 Study

To determine the relative expression levels of *xING1* and *xING2* transcripts, RT-PCR analyses were performed. Primer design was accomplished using Primer Premier software (Premier Biosoft International), and primers were supplied by Alpha DNA (Montréal, QC). The primers used are shown in Table 2.1 and the primers amplifying exon 2 of *xING2* were reported previously [16]. RT-PCR was done on MX3000 and MX4000 thermocyclers (Stratagene, LaJolla, CA), but real-time quantitation was not possible for all primer sets due to primer dimer formation that confounded SYBRgreen detection. To maintain consistency and comparability between primer sets, we elected to evaluate relative variant expression levels using agarose gel-based semi-quantitative methods.

Agarose gels were prepared with OmniPur molecular grade agarose powder (EM Science) in 1X TAE buffer (40 mM Tris-acetic acid pH 8.0, 1 mM EDTA pH 8.0) containing 0.0015% ethidium bromide (Invitrogen). DNA samples were loaded in STOP buffer (7.0 M Urea, 50% sucrose, 50 mM EDTA, 0.1% bromophenol blue). DNA was visualized and photographed with an AlphaImager 2000 Documentation and Analysis System (Alpha Innotech Corporation, San Leandro, CA).

The PCR conditions for all ING primer sets were: 9 min at 95°C, 40 cycles of 30 s at 95°C, 30 s at the indicated annealing temperature (Table 2.1), and 35 s

at 72°C, except for the amplifications for *xING2 All Variants* which were stopped at 31 cycles, and for *xING2a* which were stopped at 34 cycles to ensure that products were in the linear range. TRβ transcript detection was done as follows: 9 min at 95°C, 26 cycles of 15 s at 95°C, 30 s at 55°C, and 45 s at 72°C [122]. Amplification of an invariant L8 ribosomal protein mRNA [16, 123] was also performed using the same conditions as for the ING primer sets but for 27 cycles. The L8 values were used to normalize the ING variant data. The amplified products were separated on 2% agarose gels, visualized by ethidium bromide staining. Densitometric analyses were performed using Northern Eclipse v5.0 (Empix Imaging Inc., Mississauga, ON). The identity of each amplicon was confirmed by sequencing and/or restriction enzyme digestion, and the primers were determined to have no detectable cross-reactivity in the PCR. To ensure comparability between gels, additional lanes were run on each gel containing the same amount of amplified DNA. The overall gel staining intensities were adjusted using these lanes. All samples of a given tadpole tissue were run together in the same PCR run for each primer set to ensure maximal comparability between stages and treatments. A similar approach was taken with adult tissue samples. Statistics were done on the L8 normalized densitometric values using pairwise comparisons using one way ANOVA with a Tukey posthoc test (SPSS Version 11.0, Chicago, IL) when the data were parametric. When the data were nonparametric, the Mann-Whitney U test was used.

Table 2.1. Primer sequences used for RT-PCR.

Primer	Sequence	Product size [bp] (primer pairs)	Specifi-city	Annealing Temp. (°C)
x1e2com	GCCTGGTCCTGTTCTCAAC			
x1e1b1-4	TCCTCGAACAGGCGCT	482 (x1e1b1-4/ x1e2com)	*xING1b1,2, 3 and 4*	54
xING1b5	CCTGCCGCCTTCTTTG	478 (x1e1b5/ x1e2com)	*xING1b5*	58
xING1c1	CTGAAGCTCACTCGGAGC	215 (x1e1c1/ x1e2com)	*xING1c1*	58
xING1c2	GAACGTCCCTTTATCGTAAC	298 (x1e1c2/ x1e2com)	*xING1c2*	54
xING1 sense	TGGTGGAGTTGGTTGAGAAC			-
xING1 antisense	CCTGGATCTTTTATTGCTGG	170 (xING1 sense/xING1 antisense)	*xING1*	54
xING2a sense	GAACTAGGTCAAGGAACGG			
xING2a antisense	GGAATCCAAGCGGGTC	243 (xING2a sense/xING2a antisense)	*xING2a*	54
xING2b sense	GGATTTCGCATCCACTT			
xING2b antisense	CACGCACTCCAGGTAC	648 (xING2b sense/xING2b antisense)	*xING2b*	58

2.2.5 Southern Blot Analysis of the xING2c Transcript Variant

Premetamorphic (NF stage 50-54) *X. laevis* tadpoles were immersed in dechlorinated tap water at ambient room temperature (approximately 22±1°C) to which 100 nM T_3 (Sigma-Aldrich) was added dissolved in dimethylsulfoxide (DMSO; ACP Chemicals Inc., St. Leonard, QC). Control animals had an equal volume of DMSO added to their water. The animals were not fed during the experiment. Hindlimb and tail was collected from 5 pooled animals at 0, 0.5, 2, 6, 12, 24, and 48 h after T_3 treatment. Brain samples were collected at 0 h (n=53

pooled animals) and 24 h (n=56) of 100 nM T_3 treatment in a separate experiment. For the natural metamorphosis sample set, animals were pooled from the following NF stages: stage 54 (n=5), stage 58 (n=21), stage 60 and 62 (n=8 each), and stage 63 (n=2). For determination of expression levels in adult tissues, samples were collected from 3 pooled males (except skin was from 1 male). Total RNA was isolated from various tissues using TRIzol (Invitrogen) following the manufacturer's instructions. Two µg total RNA was annealed with 500 ng random hexamer oligonucleotide (Amersham Biosciences) and cDNA was generated using Superscript II RNase H^- reverse transcriptase as described by the manufacturer (Invitrogen). The 20 µL reaction was incubated at 45°C for 2 hr and diluted 20-fold before use.

RT-PCR was carried out with primers spanning the *ING2* exon 1/2 boundary (forward primer 5'-GGGAGCTTAGAGTCTGAGC and reverse primer 5'-TTGGATGATTTTGATTTCTTCT) that were able to detect both a full length 635 bp *ING2* product that represents both the *xING2a* and *xING2b* variants (the forward primer being in the common region of exon 1), and the 350 bp *xING2c* deletion variant. The reactions were prepared with amounts of cDNA normalized by expression levels of L8 ribosomal protein transcript whose expression is not affected by T_3 treatment [123]. For amplification of control L8 ribosomal protein transcript, the sense primer (5'-CAGGGGACAGAGAAAAGGTG-3') and antisense primer (5'-ACGACGAGCAGCAATAAGAC-3') were used to generate a 700 bp amplicon. Primers were used at 20 pmol in a typical 50 µl reaction containing 1.5 units of *Thermus aquaticus* (*Taq*) DNA polymerase (Amersham Biosciences, Inc.), 10 nmol of dNTPs (GIBCO Life Technologies, Montreal, Canada), and 1.5 mM magnesium chloride ($MgCl_2$). The PCR reaction was: 5 min at 94°C, 30 cycles (L8) or 35 cycles (*xING2*) of 30 s at 94°C, 60 s at 54°C, and 60 s at 72°C. A final 10 min extension at 72°C was done. The amplified products were separated on 2% agarose gels and visualized by ethidium bromide staining. L8 samples were easily visible, but for detection of *xING2c*, a Southern blot was done by transferring the gel to Nytran Plus membrane (Mandel Scientific Co. Ltd., Mississauga, Ontario, Canada) using a VacuGene XL vacuum blotting

apparatus (Amersham Biosciences). The transfer was carried out as described in Protocol no. 1 supplied by the manufacturer, except that the membrane was UV cross-linked in a UV Stratalinker 2400 (Stratagene) immediately after transfer to immobilize the DNA. The membranes were hybridized overnight with a fragment of human *ING1* cDNA specific to the common exon 2 region, and bands were detected with CDP-Star reagent using AlkPhos Direct Kit reagents (Amersham Biosciences, Inc.).

2.2.6 Reverse Transcription- Polymerase Chain Reaction (RT-PCR) Analyses and Statistical Analyses for the 8 nM T_3 Study

In this study, NF stage 54 tadpoles were exposed to 8 nM T_3 for 24 or 48 h along with time-matched controls in a flow through system [124]. The cDNA was generously provided by Dr. Fang Zhang and its preparation is described in Aquatic Toxicology, 2006 [124]. I analyzed the expression of *ING1* and *ING2* variants by RT-PCR using the same methods as described in section 2.4. Analysis was done on 4 individuals with the following exceptions: in brain, n=3 for *xING1b5* and *xING2 All Variants* 24 and 48 h controls, for *xING1c1* 24 h control, and *xING2a* 48 h control; and in tail, n=3 for *xING1b4* 48 h T_3 treatment, and for *xING1b5* 24 h T_3 treatment.

2.3 RESULTS

2.3.1 Isolation of Novel X. laevis xING1 Transcript Variants

Isolation of *ING1* and investigation of its possible transcript variants from *X. laevis* was carried out using the 5' and 3' RACE technique. Figure 2.1 shows the transcript sequence variants for the first of two distinct *xING1* sequences. A schematic depiction of variants *xING1b1, 2, 3* and *4* shows how their unique 5'

ends of exon 1 are followed by shared sequence for exon 1 containing the start site, which is then spliced to a common form of exon 2 (exon 2A; Figure 2.1A). Variants *xING1b1, 2, 3* and *4* (isolated from brain, testis and tail) are very similar in their 5' untranslated regions, but the CLUSTALW alignment reveals they do have unique patterns of insertions and/or deletions and some unique sequence for *xING1b2* (Figure 2.1B). A schematic depiction of a second set of *xING1b* variants is shown in Figure 2.1C. *xING1b5* was isolated from brain and tail, whereas, *xING1c1* and *2* were isolated from testis. These variants have unique exon 1 sequences that are spliced to an exon 2 form (exon 2B) that they share in common with each other. This exon 2 is distinct from the exon 2 (exon2A) in *xING1b1, 2, 3,* and *4* with 28 bp differences in the 704 bp overlapping coding region and a high degree of sequence divergence in the 3' UTR. Variant *xING1b5* has a start site within its unique exon 1, while the other two variants do not have a start codon until well within exon 2B. In humans, there are 3 ING1 exon 1 sequences known: *ING1a, b*, and *c*. These are all different variants for exon 1 that are spliced to a common exon 2. In naming our transcripts, I aligned the sequences and chose the name for our frog variants based on whichever variant most closely aligned in human. For example, the 4 variants referred to as *xING1b1-4*, as well as the variant *1b5*, all aligned most closely with human *ING1b*. The two variants that do not have start codons until within exon 2 most closely resemble human *ING1c* which also does not have a start codon until exon 2. I did not isolate any sequences that aligned with human *ING1a*.

A

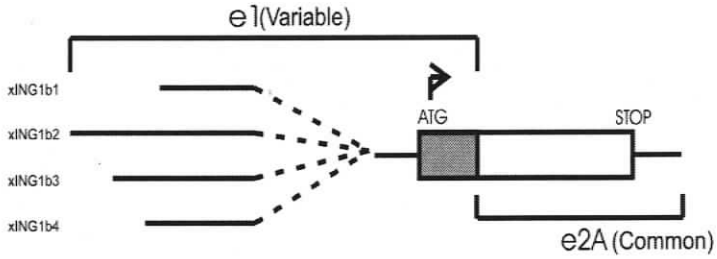

B

```
xING1b1     ----------------------------------------------------------------------------------------CTTCTTTTCCTTGTGCCACACAGCAGAAGCC
xING1b2     CTCCTTCAGCCCACTAGCAGTTCACTGGTAAACACCACAGAATGGCCCCCATTTGTTGTAACGCTTGATGAGGCAGGTGCTTCGCTGCACTTCTTTTCCTTGTGCCACACAGCAGAAGCC
xING1b3     ----------------------------------------------------------GAGATACACAGCCATTCAATCAGCT-GCTGCACTTCTTTTCCTTGTGCCACACAGCAGAAGCC
xING1b4     ----------------------------------------------------------CAGCCATTCAATCAGCT-GCTGCACTTTTTTTCCTTGTGCCACACAGCAGAAGCC
                                                                         *** **************************

xING1b1     CGCAGCTCCCTGCTCTCCCTCCTCACATGTCCATGCACCTCCGCGCCGGCAGCCTCATGCCAGGCTCACCCTGTCGCCTTTCCCTTCCTGGAACAGGCGCTTTTCTTTGTGTTTCCTCCC
xING1b2     T-------CCTGCTCTCCCTCCTCACATGTCCATGCACCTCCGCGCCGGCAGCCTCATGCCAGGCTCACCCTGTCGCCTTTCCCTTCCTCGAACAGGCGCTTTTCTTTGTGTTTCGTCCC
xING1b3     CGCAGCTCCCTGCTCTCCCTCCTCACATGTCCATGCACCTCCGCGCCGGCAGCCTCATGCCAGGCTCACCCTGTCGCCTTTCCCTTCCTCGAACAGGCGCTTTTCTTTGTGTTTCGTCCC
xING1b4     T-------CCTGCTCTCCCTCCTCACATGTCCATGC--------------AGCCTCATGCCAGGCTCACCCTGTCGCCTTTCCCTTCCTCGAACAGGCGCTTTTCTTTGTGTTTCGTCCC
            ***************************** ************************************ ********************** ****

xING1b1     CTGTGTGTTACTAGTCGGCGAGGAGACGA
xING1b2     CTGTGTGTTACTAGTCGGCGAGGAGACGA
xING1b3     CTGTGTGTTACTAGTCGGCGAGGAGACGT
xING1b4     CTGTGTGTTACTAGTCGGCGAGGAGACGA
            ****************************
```

Common region

```
TTTGTTGCAGGAGTGGGGTTGGCAAGTGCTTTGCAGAGGGGTAAGATCCTGGAGCAGACAGGAGCCAGTCGGTGTGTTAGTGCTGGAGACTGCGGCTGCACAAGATGCTGAGCCCGGCAAACGGAGAGCACATT
CACATGGTGAACTATGTGGTGGATTATCTGGACTCCATCGAGTCTCTGCCTTTCGACCTGCAAAGAAATGTCTCTCTCATGAGAGAAATCGACGCCAAATACCAAGGCATCCTAAAAGAATTGGATGAGTATTA
TGAAAAATTGAAGCGTGAATCTGATGCAATCCAAAAAAAGCGACTTTTGCAGTTTATCCAGCGAGCTCTTATTCGTAGTCAAGAACTTGGCGATGACAAAATCCAGATAGTGAGCCAAATGGTGGAGTTGGTTG
AGAACAAGACCAGGCAAATAGACAGCCATGTGGAACTGTTTGAGACTTGCCAGGATTTAAATGACAGTACAAGCAACAGCAGCAAAAACAACCAGGAAAAATCCAAAAATGAGGCCATTGCCCAGACTGAAAAG
ACCAGCAATAAAAGATCCAGGAGACAGCGGAACAATGAAAATAGGGAAAATTCAACGATCAACCATGACCACGATGACCTCACTTCAGGAACGCCCAAGGAAAAAAAGACAAAACCATCTAAGAAGAAAAAGAG
ATCCAAAGCCAAAGCTGAACGAGAGGCCTCCCCTGCTGATCTTCCAATCGATCCCAATGAACCCACATACTGTCTGTGCAATCAAGTTTCTTACGGAGAAATGATTGGCTGTGATAATGAAGAATGCCCCATCG
AGTGGTTTCACTTTTCTTGTGTTGGACTCAATCACAAACCAAAAGGAAAATGGTACTGTCCTGAATGTAGAGGAGAGAATGAGAAAACCATGGGGAAAGCACTTGAGAAATCTAAAAAAGAAAGGACATATAAC
AGGTAGTTCACAAAAAAAGACTGTATTTAGGAAAGGGAGTAAGGCAAAGAATTATATTTATTGTCCTTAGCACCTTGTGAAGGTTAAAGGATTGCAAATGGTATATTTTATTTTAAGGAAAGGGGCAACCCAT
TTCTGTGGACAGCAATAACATTACCCTTCTGTTGAAGAGCTCCCAGAAGGAAAGATTTCATGAGCCAAATTACCACAGTGGCCTGTAAGAGACATGCTCTCGGCCTTTATATATGGAAATAGTTCATACAACAA
CTGTGTGGCATGATGGGTTATATTAGAACTTTAAAAAACAAACATGCAAAGTACTGTGTCGTCCATTTATTTTACATATGTAGTGAGTTGGTATTAATATGCGTGTGTATGCCATAGCAAAAGGACTAACTGTT
TGTTGGGTTTTATTATCACTTGTCCTTTGTCATTTCATTATACTGTGGGTTTATGGAACTGATCTAGAACTGGAAAGAACAATGTTCTTTGTAAAATATAATGCTGGATAGTCCAACAGTGGAAGTAGCTTAAA
TATAAGAGGGTTGATATTAAACAGCAATGCCATGGTTACAATTTACATGGTAAACCTTTTATACTGAACACTGGTCTGTTATCCAGAAAAGGCCATTTTAAAATAATTGATTGAATTTTTTTATTGAACACACA
TTGGTTCACACAGATCAAGCTTTATACTGACTGGTAATGGGGAAGCAATCCTTCTTTGTATAAATGTACATTTTAAATGGAATTGCACTTGATGTATTATAACTGGAAATGCAGCCAAATGCCATGGTGTAACC
AATGTGCATTTTCTTCGGTATGTGTGAAGATTGTACAGCTGTGATAATGAAAATAAATGACAGATATATGAAAAAAAAAAAAAAAAAAAAAAAAAAAAAA
```

C

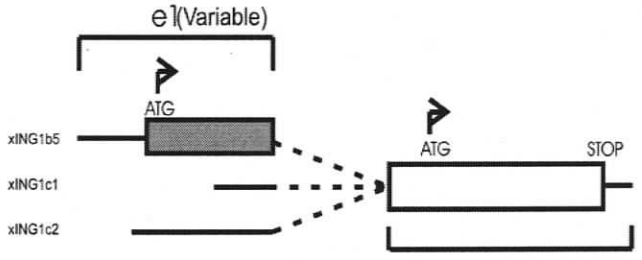

D

xING1b5

```
AGCAGAAGCCTCCTGCTCTCCCTCCTCACATGTCCATGCACCTCCGCGCCGGCAGCCTCATGCCAGGCTCACCCTGCCGCCTTCTTTGTGTTTCGTCCCCTGTGTGTTAGTAGTCGGCGAGGAGACGGTTGCA
TTTGTTCTAGGAGGGGGGTTGGCAAGTGCTTTGCAGAGGGGAAAGATCCTGGATCAGACAGGAGCCCGGCGGGGTGTTAGTGCTGGAGACTGCAGCCGCACAAGATGCTGAGCCCGGCAAACGGAGAGCACAT
TCACATGGTGAACTATGTAGAGGATTACCTGGACTCCATCGAGTCTCTGCCTTTCGACCTGCAAAGAAATGTCTCTCTCATGAGGGAGATCGACGCCAAATACCAAG
```

xING1c1

```
GACAGCAGCAGCGGCTGTTTGTTGAAAGCTGCGCACTGGCAGCCGGGCTGAAGCTCACTCGGAGCTCGACGTTTTATTCGTCTGT
```

xING1c2

```
GCCCCTTTAAAATCATTGGCTTCGGGTTTGGAAGGTCCCGGGCCGCGGCTGTCCTAGTCATTGGTTCTTTCCTTCAAATGAACGTCCCTTTATCGTAACGCCTCATGTTTCAGGTCCCACCTCTCAAAGATCA
TTTAAATGTGTCCGTCCGCCCTTCGGATTTTATTGGCTGTGGGAGTAGCCCGGCCAGCTCCATTCCG
```

Common exon 2B region

```
AAATCCTAAAAGAATTGGATGACTACTATGAAAAGTTCAAGCATGAATCTGATGCAGTCCAAAAAAAGCGTCTTTTGCAGTTCATCCAGCGAGCTCTTATTCGTAGTCAAGAACTTGGTGATGACAAAATCCA
GATAGTGAGCCAAATGGTGGAGTTGGTTGAGAACAGGACCAGGCAGGTAGACAGCCACGTGGAACTGTTTGAGACTTGCCAGGATTTGAATGACAGTACAAGCAACAGCAGCAAAAACAACCAGGAAAAATCC
AAAAATGAGGCCATTGTCCAGACTGAAAAGCCCAGCAATAAAAGATCCAGGAGACAGCGGAACAATGAAAACAGGGAAAATTCAACCATCAACCATGACCATGATGATCTCACTTCAGGAACGCCCAAGGAAA
AGAAGGCAAAACCATCGAAGAAGAAAAAGAGATCCAAAGCCAAAGCTGAACGAGAGGCCTCACCTGCTGATCTTCCAATCGATCCCAATGAACCCACATACTGTCTGTGCAATCAAGTTTCTTATGGTGAAAT
GATTGGCTGTGATAATGAAGAATGCCCCATTGAGTGGTTTCACTTTTCTTGTGTTGGACTCAATCACAAACCAAAAGGAAAATGGTACTGTCCTGAATGTAGAGGAGAGAATGAGAAAACCATGGGGAAAGCA
CTTGAGAAATCTAAAAAAGAAAGGACATATAACAGGTAGTTCACAGAAAAAGACTGTATTTGGGAAAGGAAGTGAGGCAAACAATTTATTTATTGTCCATAGCACCTTGTGAAGGTAAAAGGATTGCAAATG
GTATATTTCTTATTTTATGGAAAGGGCAACCCATTTCTGAGGCGAGCAATAACCTTACCCTTCTGTTGAACAGCTCCCACAAGGAAATCATTTCATGAGCCAAATGACCGCAGTGGCCTGTAAGATACATGC
TCTCGGCCTTTATATATGGGAATAGTTCATACAACAGCTGTGAGCCATGATGGGTTATATTAGAACTTTTAAACACAAACATGCAAAGCACTGTCATCCATTTATTTACATCTGTAGTGAGTTGTTAATAAT
ATGTATATGCCGTAGCACTTGTCCTTTGTCATTTCAGTATGCCACAGGTTTATGGAACTGAACTAGAACTGGAAAGTTCTAGTTTCCATTCATAGTTAGGACTGGTAAGAACCATGTTCTTTGTAAAATAGGA
TGGCGGATAGTCAAACAGTGGAAGTAGCATAAGAGGGTTTATATTAAATAGCAACACCATGGTTACAAGTTACATGGTAAACATTTTATACCGAAGTCTGGCCTGTTATCTGGAAAAGGCCATTTTAAAATAA
TTGATTGCATTTTTTTAATTGAACACACAGTGGTTTCACACAGATCAAGCTTTACATACTGACAGGTAATGGGGAAGCAATCCTAATTTGTATAAATGTACATTTTAAATGGAATTGCACTTGATGTATTAT
AACTGGAAATGCAGCCAAATGCCATTGTGTAACCAATGTGCATTTCCCTTGTGTATGTGTGAAGATTGTACAGCTGTGATAATGAAAATAAAAGACAGATCTATGGTAAAAATAAAAAAAAAAAAAAAAAAA
AAAAAAAAAAAAAAA
```

Figure 2.1. Transcript sequence variants for *xING1*.
(A) Schematic diagram for transcript variants *xING1b1*, *2, 3* and *4* with variable 5' ends of exon 1 (e1(Variable)) sequence followed by shared sequence for exon 1 containing the translation start site, which is then spliced to a common exon 2 (e2A(Common)). The start codon shared by all the variants is indicated with an arrow and the translation stop site (STOP) is indicated. (B) CLUSTALW alignment of the unique 5' ends of exon 1 for the *xING1b1*, *2*, *3* and *4* variants followed by the sequence they share. (C) Schematic diagram for variants *xING1b5*, *c1*, and *c2*. These variants have unique exon 1 (e1(Variable)) sequences spliced to a common exon 2 (e2B(Common)) that is distinct from the exon 2 of *xING1b1-4*. Start codons are indicated with an arrow. (D) The unique exon 1 sequences for the variants *xING1b5, c1*, and *c2* which do not align are shown followed by the common sequence for exon 2 of these variants. In part A and C, lengths of lines indicate relative sequence lengths. The open reading frame is boxed and exon 1 is shaded. In part B and D, the locations of primers used in RT-PCR are underlined (see Table 2.1 for details), start and stop codons are bold and underlined, and the first base of exon 2 is shaded in grey.

2.3.2 Isolation of Novel xING2 Transcript Variants

In my earlier work, I observed different patterns of *xING2* transcript levels when using primers specific to the common exon 2 compared to primers spanning exon 1 and 2 [16] that suggested that x*ING2* had multiple variants. To follow up on this work, I have identified three distinct *xING2* variants shown in Figure 2.2. Since no variants have yet been identified for this gene, we have elected to name ours, 2a, 2b and 2c, with the knowledge that these variants may or may not represent alternate exon 1 usage. They could also be from duplicated genes or a result of polymorphism. Figure 2.2A shows that the *xING2a* and *xING2b* transcripts have unique 5' ends followed by a common sequence in exon 1, which is then spliced to a common exon 2 (Figure 2.2B). The *xING2b*

sequence contains a putative start site further upstream than the putative start for *xING2a*. Another variant discovered, *xING2c*, has an in-frame deletion of 285 nucleotides that starts in exon 1 and continues into exon 2 (Figure 2.2B).

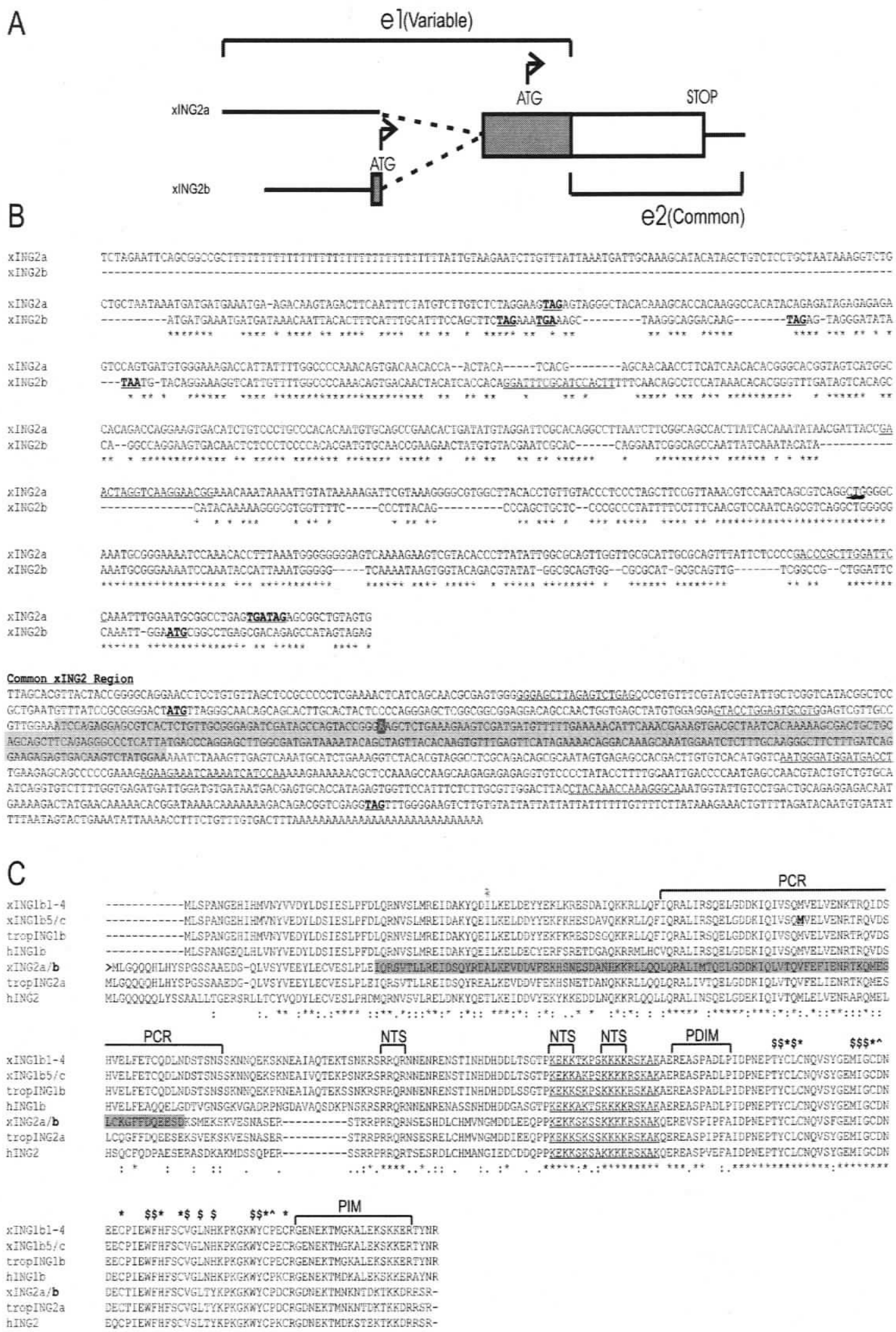
A
e1(Variable)
xING2a
xING2b
ATG
ATG
STOP
e2(Common)
B
Common xING2 Region
C
PCR
NTS
PDIM
PIM
xING1b1-4
xING1b5/c
tropING1b
hING1b
xING2a/b
tropING2a
hING2

Figure 2.2. Transcript sequence variants for *xING2* and protein sequence alignments.

(A) Schematic diagram for variants *xING2a* and *xING2b* with unique 5' ends of exon 1 (e1 (Variable)) sequence followed by shared sequence for exon 1 which is then spliced to a common form of exon 2 (e2(Common)). Lengths of lines indicate relative sequence lengths. The open reading frame is boxed and exon 1 is shaded. Start codons are indicated with an arrow. (B) CLUSTALW alignment of the unique 5' ends of exon 1 for the variants *xING2a* and *xING2b* is followed by common sequence. The locations of primers used in RT-PCR are underlined (see Table 2.1 for details); start and stop codons are bold and underlined; the region that is deleted in variant *xING2c* is shaded in light grey; and the first base of exon 2 is shaded in dark grey. (C) The derived protein sequences are compared using the CLUSTALW program. Variants of *X. laevis ING* cloned include xING1b1-4 (279 aa) which represents the four x*ING1* variants that use exon2A, xING1b5/c (279 aa) represents the three variants that use exon2B, and xING2a/b (278 aa) represents the shared amino acid sequence encoded by *xING2a* and *xING2b* transcripts (there are an additional 63 aa at the N-terminus for xING2b that are not shown but are indicated by a ">"). These sequences are compared to two human forms of *ING* [hING1b (279 aa) GenBank Accession Number AJ310392 and h*ING2* (280 aa) GenBank Accession Number AF053537] and two forms of *X. tropicalis* [trop*ING1* (279 aa) assembled from AASO434381.g1, AASO171898.b1, ZWK426176.b1, and UJS344469.y1 sequences from the Joint Genome Institute database and trop*ING2* (279 aa) assembled from UJS487311.x1, UJS250323.y1, and TKS219017.y1 sequences from the Joint Genome Institute database in addition to the sequence BX714794.1 *X. tropicalis* EST, clone TTpA016j24 5' from the Sanger Institute]. The putative ING1 and ING2 protein sequences contain a PHD finger motif common to a family of proteins known to be involved in chromatin remodeling. PHD finger consensus sequence zinc coordinating residues are indicated by "*", hydrophobic residues are indicated by "$", and other consensus residues are

indicated by "^". Note also that spacing of PHD finger residues conforms to the consensus sequence. The % symbol indicates the first amino acid of exon 2, the start codon for variants *xING1c1* and *xING1c2* is indicated in bold and underlined, the sequence that is deleted in-frame in the *xING2c* variant is indicated in light grey, and the conserved nuclear localization signal is underlined. Additional domains identified in human ING [15] that are conserved in amphibian ING1 and ING2 sequences are indicated with labeled brackets including: a potential chromatin regulation region (PCR); 3 nucleolar translocation sequences (NTS); a phosphorylation-dependent 14-3-3 interacting domain (PDIM); and a peptide interacting motif (PIM) domain. In the unique N terminal regions, $p33^{ING1b}$ has a proliferating cell nuclear antigen (PCNA)-interacting protein (PIP) domain, and $p33^{ING2}$ has a leucine zipper motif [15] that are also conserved in the amphibian counterparts.

2.3.3 Analysis of the Derived Protein Sequences from xING1 and xING2

The derived protein sequences are compared using the CLUSTALW program for *X. laevis, X. tropicalis* and human ING1 and ING2 (Figure 2.2C), and their percent identities with each other are shown in Table 2.2. The isoforms of *X. laevis* xING1b1-4 (279 amino acids (aa)) are represented together in the figure since all four variants are spliced to the same exon 2A and have an identical open reading frame (ORF) sequence. xING1b5/c represents three isoforms that are spliced to exon2B. The xING1b5/c sequences differ in their exon 1 sequences, and only xING1b5 has the initial start codon such that the derived protein sequence of 279 aa aligns with the full length human and *X. tropicalis* sequences. The other two variants, xING1c1 and 2, have their first methionine residue within exon 2 which is similar to the human $p24^{ING1c}$ variant [15]. This produces a putative protein of 21 kDa rather than the 33 kDa for the full length protein of the other forms of ING1 discovered in *Xenopus* so far. There are 9 aa differences between xING1b exon2A that splices with xING1b1-4 and exon 2B

that splices with xING1b5/c1-2. The variants for xING2a and b are identical for the derived protein sequence of 278 aa (32 kDa protein) shown in Figure 2.2C. However, xING2b has a putative upstream initiation site that results in a protein with an additional 63 aa resulting in a 341 aa sequence, giving a putative protein of ~38 kDa. The ING1 and 2 sequences from *X. laevis* are compared to two human sequences obtained from GenBank, hING1b (279 aa), and hING2 (280 aa). In addition, I assembled the putative transcripts for *X. tropicalis* ING1 (279 aa) and ING2 (279 aa) using the Joint Genome Institute (JGI) database for *X. tropicalis* and the *X. tropicalis* Expressed Sequence Tag (EST) library from the Sanger Institute (Appendices 3 and 4). The highly conserved C terminus of the ING proteins contain a PHD finger domain, common to a family of proteins known to be involved in chromatin remodeling [15]. Additional conserved domains in exon 2 of ING1 and ING2 include: a potential chromatin regulation region, 3 nucleolar translocation sequences, a phosphorylation-dependent 14-3-3 interacting domain, and a peptide interacting motif. A proliferating cell nuclear antigen (PCNA)-interacting protein (PIP) domain is conserved in the unique N terminal regions of all xING1b isoforms and is lacking in the xING1c1 and c2 isoforms. The unique N terminal regions of xING2a and 2b isoforms have a conserved leucine zipper motif which is only partially conserved in the xING2c isoform. The area shaded in grey in Figure 2.2C is that region that is deleted in the xING2c isoform which produces a putative protein of 183 aa (~21 kDa).

The boundary between exon 1 and 2 is conserved between the different species in the *ING1* and *ING2* genes. The boundary is known for the human genes, and the intron has been sequenced in our lab for *X. laevis ING2* (Appendix 2) and matches well with the assembled *X. tropicalis ING2* gene (Appendix 3). I also assembled the *X. tropicalis ING1* gene and found the exon/intron boundaries (Appendix 4). Since *X. tropicalis* shares such high sequence identity with *X. laevis* (95% for *xING1b1-4* and 97% for *xING1b5* variants, see Table 2.2), it seems highly likely that the x*ING1* boundary between exon 1 and 2 is in the position indicated in Figure 2.2C.

Table 2.2. Comparison of percent identities of ING proteins.

% Identity	xING1b5	tropING1	hING1b	xING2a	tropING2	hING2
xING1b1-4	96	95	80	53	55	55
xING1b5		97	82	55	56	56
tropING1			82	55	56	56
hING1b				53	55	55
xING2a					94	66
tropING2						70

2.3.4 Expression of ING Transcript Variants in Adult X. laevis Tissues

Different *ING* transcripts give rise to different proteins with different cellular functions (reviewed in [13-16, 125]). I investigated the expression patterns for the transcript variants of the *ING1* and *ING2* genes in multiple tissues to determine which ING forms are expressed in each tissue. Figure 2.3 shows the densitometric values obtained from RT-PCR products resolved on 2% agarose gels following their normalization to the L8 ribosomal protein transcript. A panel of *X. laevis* adult tissues was tested including the brain, muscle, testis, liver, skin and eye. Each primer set used for the specific variants (*xING1b1-5, xING1c1/2*, and *xING2a* and *b*) was compared to a primer set within exon 2 which represents all variants for *xING1* or *xING2*. Statistical significance is indicated relative to liver because it had the lowest expression of ING variants in most cases.

The expression patterns for all *xING1* variants (represented by primers that amplify the common exon 2 region of *xING1*) show that adult brain, testis, skin and eye have significantly higher expression levels than muscle or liver. The expression levels of specific variants show significantly higher expression levels in the brain for *xING1b1-4, 1b5*, and *1c2*. Substantially higher levels of *xING1b5*, *1c1*, and *1c2* are also evident in the testis. The eye has significantly higher levels of *xING1b1-4* and *xING1b5*. The expression patterns are similar for *xING2 All*

Variants and *xING2b* with high expression levels in testis, brain, eye and skin, whereas *xING2a* has elevated levels in brain, testis and eye.

In addition to comparing all tissues to the generally weakly expressing liver, each tissue was compared to each other tissue and is categorized as high, moderate or weakly expressing for each primer set. If one looks specifically at expression patterns for *xING1 All Variants*, tissues fall into three groups of high, moderate and weak expression. Brain and eye are significantly higher than all other tissues, while testis and skin are moderately expressing but significantly higher than muscle and liver which are weakly expressing. Expression of the *xING1b1-4* variants, reveals similar groupings but with less dramatic differences. Brain and eye are again significantly higher than all other tissues. However, in this case, testis and skin are moderately expressing, but not statistically higher than the lower expressing muscle and liver tissues. The *xING1b5* variant expression is significantly higher in brain compared to all other tissues, while eye is moderately expressing, but is significantly higher than testis, which is itself statistically higher than muscle, skin and liver that are all weakly expressing. Expression of the *xING1c1* variant is quite different. In this case, testis is the highest *ING* expressing tissue. Brain and eye are not statistically different from liver, but they are both statistically different from muscle which is a low expressing tissue similar to densitometric values for liver and skin for this variant. Furthermore, brain and eye are not statistically different from the highly expressing testis tissue, placing them in a moderate expression group. For the *xING1c2* variant, brain and testis are significantly higher than the other tissues. Although eye is not statistically significantly different from the liver, it is significantly higher than skin and muscle which are very similar in densitometric value to liver, placing eye tissue in a moderately expressing category.

A similar analysis was done for *xING2* variants. *xING2 All Variants* has expression patterns that fall into three groups. Brain, testis and eye are all highly expressing, skin is moderately expressing while muscle and liver are weakly expressing. Tissues expressing *xING2a* fall into three groups where brain and eye are significantly higher than muscle, liver and skin which are all weakly

expressing. Testis is not significantly different from either the high or weakly expressing tissues, placing this tissue in a moderate expression category. Finally, for the *xING2b* variant, the typically highly expressing brain and eye remain so, but for this variant skin is also highly expressing. Testis is significantly higher than liver, but is significantly lower than the high expressors. Muscle has a similar value to testis, but is not statistically significantly different from liver.

Taken together, these data show that *ING* expression is relatively high in brain, testis and eye, expression is relatively low in muscle and liver, and skin is quite variable depending on the variant.

Expression levels of *TRβ* transcript were also measured for each of these tissues and compared statistically. The eye, brain and skin are relatively highly expressing, compared to testis, muscle and liver. Eye has the highest expression, followed by brain, and then skin.

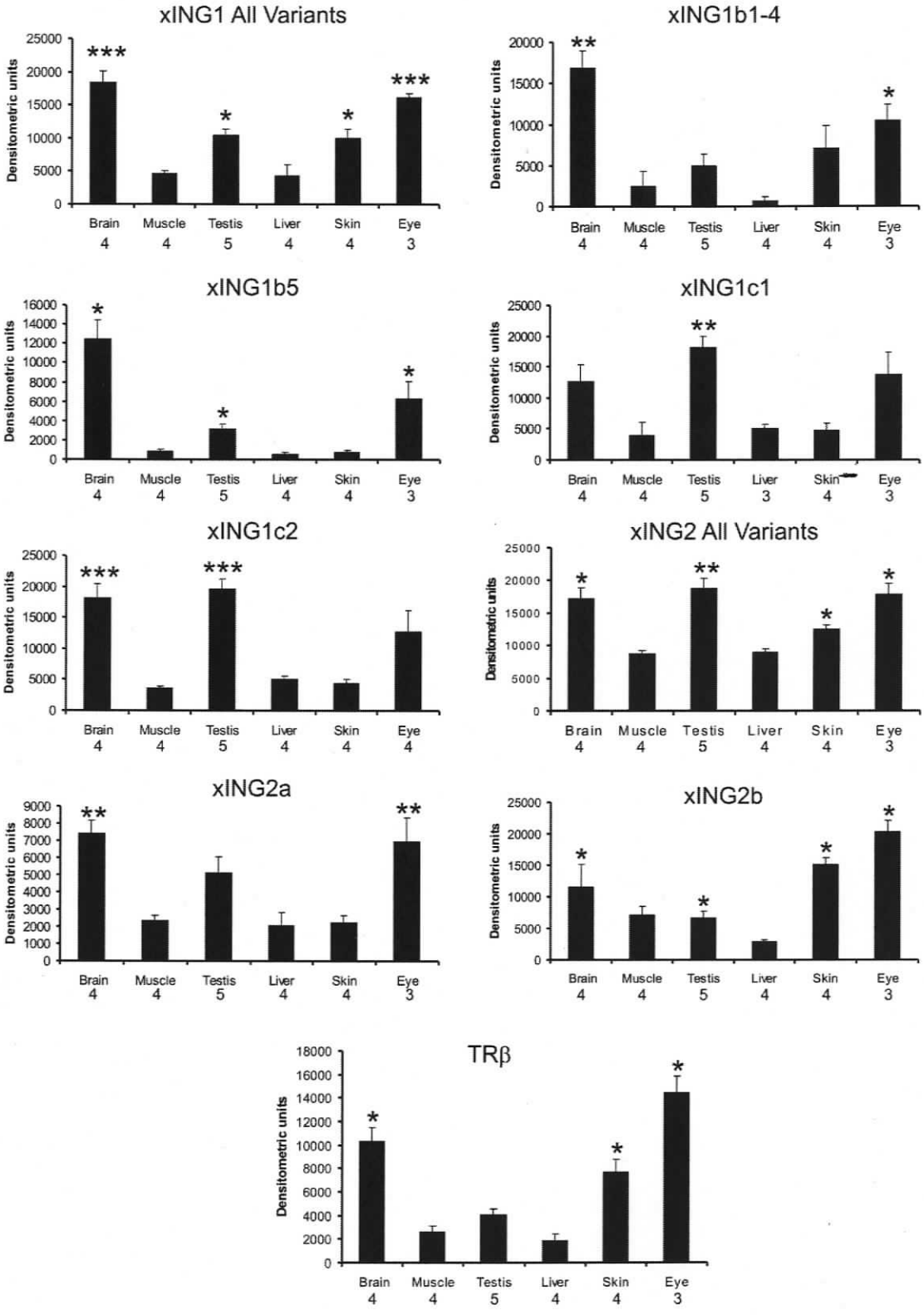
xING1 All Variants
Densitometric units
25000
20000
15000
10000
5000
0
***
*
*
***
Brain 4
Muscle 4
Testis 5
Liver 4
Skin 4
Eye 3
xING1b1-4
Densitometric units
20000
15000
10000
5000
0
**
*
Brain 4
Muscle 4
Testis 5
Liver 4
Skin 4
Eye 3
xING1b5
Densitometric units
16000
14000
12000
10000
8000
6000
4000
2000
0
*
*
*
Brain 4
Muscle 4
Testis 5
Liver 4
Skin 4
Eye 3
xING1c1
Densitometric units
25000
20000
15000
10000
5000
0
**
Brain 4
Muscle 4
Testis 5
Liver 3
Skin 4
Eye 3
xING1c2
Densitometric units
25000
20000
15000
10000
5000
0
***
***
Brain 4
Muscle 4
Testis 5
Liver 4
Skin 4
Eye 4
xING2 All Variants
Densitometric units
25000
20000
15000
10000
5000
0
*
**
*
*
Brain 4
Muscle 4
Testis 5
Liver 4
Skin 4
Eye 3
xING2a
Densitometric units
9000
8000
7000
6000
5000
4000
3000
2000
1000
0
**
**
Brain 4
Muscle 4
Testis 5
Liver 4
Skin 4
Eye 3
xING2b
Densitometric units
25000
20000
15000
10000
5000
0
*
*
*
*
Brain 4
Muscle 4
Testis 5
Liver 4
Skin 4
Eye 3
TRβ
Densitometric units
18000
16000
14000
12000
10000
8000
6000
4000
2000
0
*
*
*
Brain 4
Muscle 4
Testis 5
Liver 4
Skin 4
Eye 3

Figure 2.3. *ING* transcripts are differentially expressed in adult tissues. Shown are densitometry graphs for each variant based on values obtained from 2% agarose gels of RT-PCR products. Local background was subtracted and the band was normalized to a L8 ribosomal protein transcript. The specific variants are indicated and compared to a primer set designed to amplify a region within exon 2 of all variants of *xING1* or x*ING2* (xING1 All Variants and xING2 All Variants). The number of individuals used for statistical analysis is shown below each tissue listed (muscle and skin are from hindlimb). The error bars represent the standard error of the mean, and statistical significance relative to liver is indicated by * for $p \leq 0.05$, ** for $p \leq 0.01$, and *** for $p \leq 0.001$.

2.3.5 *Expression of ING Transcript Variants in Naturally Metamorphosing X. laevis Tadpole Tissues*

Frog tadpoles have a distinct postembryonic developmental phase that culminates in the complete metamorphosis of the tadpole into a juvenile frog. During metamorphosis, the tadpole tail regresses through apoptosis, while at the same time the hindlimbs proliferate and the brain and other tissues undergo extensive remodeling. Given that ING proteins have been implicated in the control of apoptosis and proliferation, I investigated the *ING1* and *ING2* transcript variant expression in these three tissues at different developmental stages.

Compared to premetamorphic NF stage 54, there is a striking decrease in all *xING1* and *xING2* variant transcript levels in the hindlimb at later stages (Figure 2.4). Concurrently, the levels of most of these transcripts increase in the tail and remain largely constant in the brain. *xING1c1* levels in the tail are an exception, resembling the hindlimb profile more closely than that of the other tail variants. In addition, the levels of *xING2 All Variants* show an initial decrease followed by an increase. *xING1c2* and *xING2b* are not detectable at any stage in the hindlimb or tail. However, these transcripts are present in the brain. *xING1c2* shows a transient significant increase at the beginning of metamorphic climax,

whereas *xING2b* levels do not change. I also examined the relative levels of *TRβ* transcript for each tissue which are known to be elevated during natural metamorphosis (for review see [66]). As expected, a significant induction of *TRβ* transcript is evident in all three tissues.

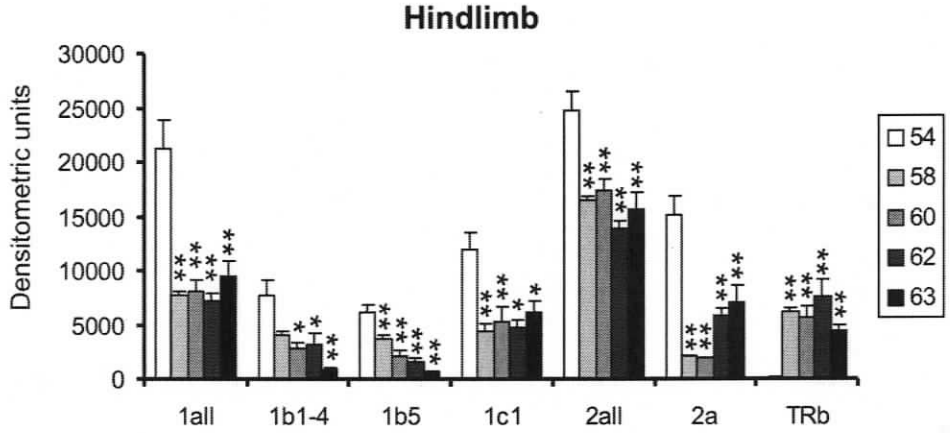
Hindlimb
Densitometric units
30000
25000
20000
15000
10000
5000
0
1all
1b1-4
1b5
1c1
2all
2a
TRb
54
58
60
62
63

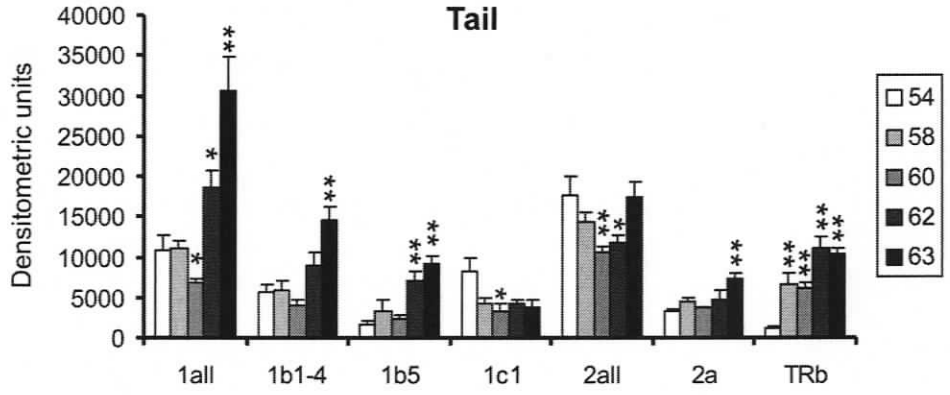
Tail
Densitometric units
40000
35000
30000
25000
20000
15000
10000
5000
0
1all
1b1-4
1b5
1c1
2all
2a
TRb
54
58
60
62
63

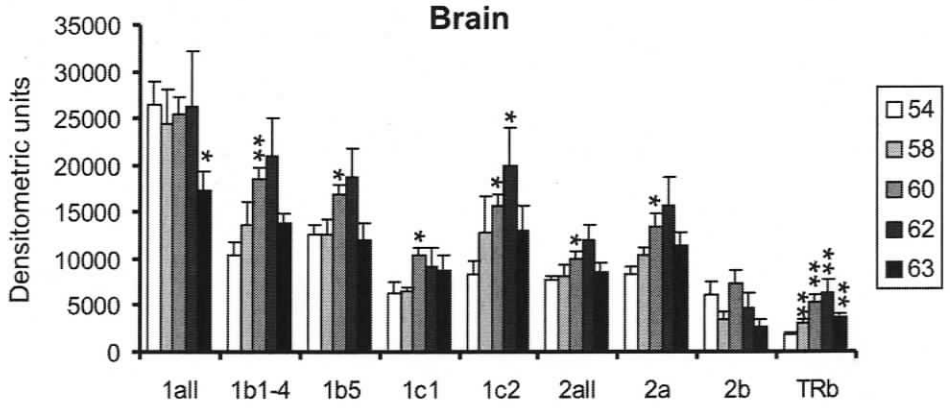
Brain
Densitometric units
35000
30000
25000
20000
15000
10000
5000
0
1all
1b1-4
1b5
1c1
1c2
2all
2a
2b
TRb
54
58
60
62
63

Figure 2.4. *ING* transcript levels are differentially affected in the tails and hindlimbs of naturally metamorphosing tadpoles.

ING transcript levels show differential changes in the tail and hindlimb of tadpoles undergoing natural metamorphosis from NF stages 54 to 63, but little change occurs in the brain. Shown are the densitometric values for each detectable *ING* variant, as well as *TRβ*, normalized to L8 ribosomal protein transcript. All bars with the exceptions listed below represent the mean of 5 individuals for brain and 6 individuals for tail and hindlimb. For tail samples, n= 5 for NF stage 54 animals for all primer sets tested. For *xING1c1*, n=5 for NF stages 58 and 60; and n=4 for NF stage 62. For hindlimb samples, n=5 for *xING2a* NF stage 54; and n=5 for *xING1c1* NF stage 62 and 63. The error bars represent the standard error of the mean, and statistical significance relative to NF stage 54 is indicated by * for $p \leq 0.05$ and ** for $p \leq 0.01$.

2.3.6 *Expression of ING Transcript Variants in 100 nM T_3-treated X. laevis Tadpole Tissues*

The remodeling of tadpoles into juvenile frogs is totally dependent on TH. Endogenous TH levels increase from virtually undetectable levels at NF stage 54 to maximal levels at around NF stage 60. After this point, the tissue-specific metamorphic genetic program is established and executed [66]. This process can be induced in premetamorphic tadpoles that lack TH by exposure to exogenous T_3. I treated NF stage 54 tadpoles with T_3 and analyzed the *xING1* and *xING2* transcript variant levels in the hindlimb, tail, and brain.

Figure 2.5 shows the fold changes in transcript variant levels relative to their matched controls. Both *xING1* and *xING2 All Variants* show a significant increase in the tail tissue with no change or a significant decrease, respectively, in the hindlimb. The brain tissue shows a transient decrease of *xING1* levels but no change in *xING2* levels. Examination of the specific variants reveals a dramatic contrast in initial responses to T_3 between the three tissues. The brain

remains essentially unchanged (with the exception of a significant, but modest and transient increase in *xING2a* at 12 h). All individual variants show a significant downregulation in the hindlimb, particularly at 6 h. *xING1b1-4* and *xING1b5* transcripts are reduced 3 to 8-fold relative to controls. This downregulation is followed by a shift to no change or an increase (2 to 5-fold relative to controls) at 24 and 48 h time points. In contrast, the tail shows an increase (2 to 4-fold) in these transcript variants and no change in *xING1c1*. The expression profile for *xING2a* in tail shows a rapid increase followed by a significant decrease which is in opposition to the expression pattern found in the hindlimb. Measurement of *TRβ* transcript levels show a rapid and dramatic induction of this transcript in all three tissues, verifying that all tissues had responded to hormone treatment.

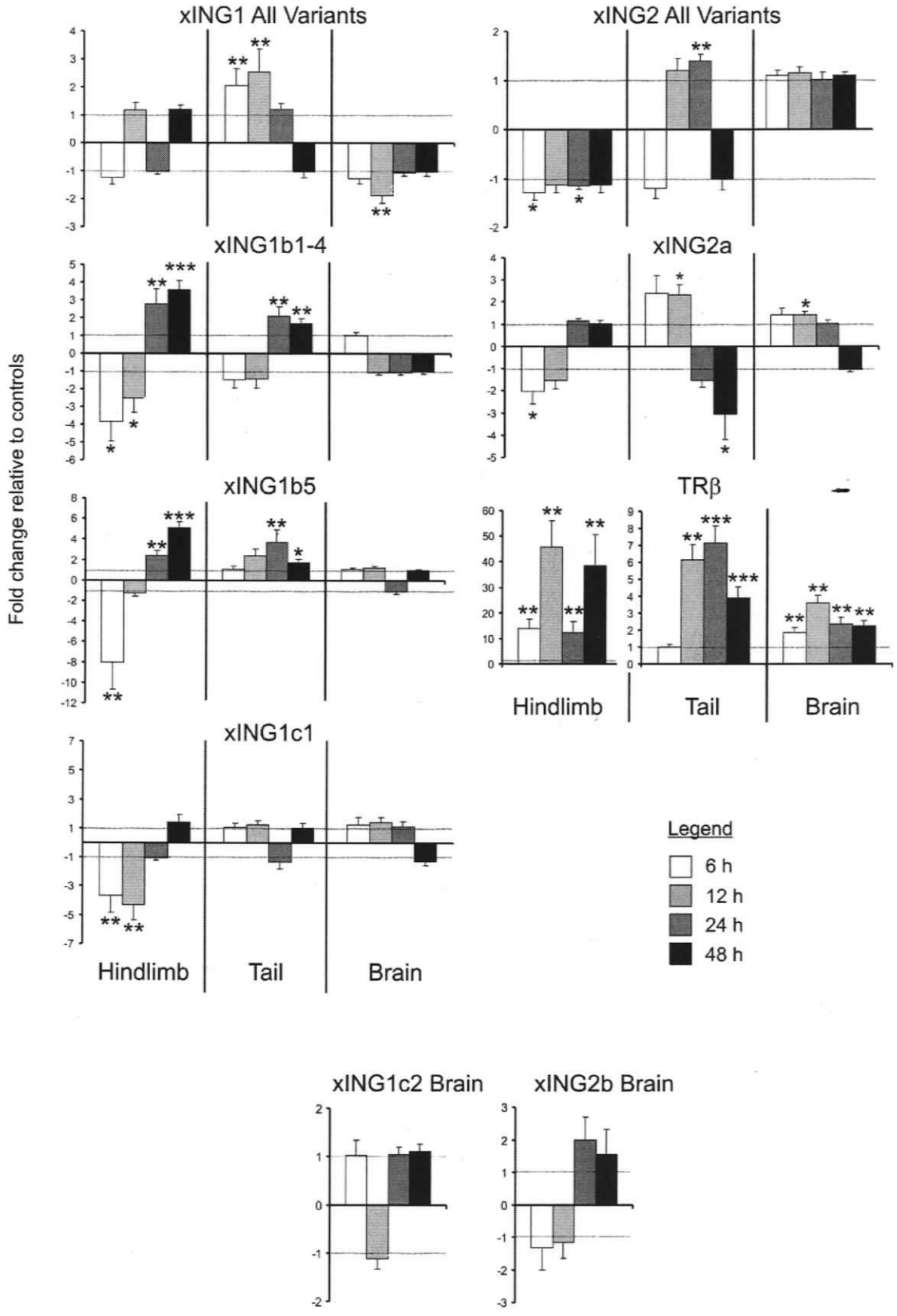
xING1 All Variants
xING2 All Variants
xING1b1-4
xING2a
xING1b5
TRβ
xING1c1
Fold change relative to controls
Hindlimb
Tail
Brain
Legend
6 h
12 h
24 h
48 h
xING1c2 Brain
xING2b Brain

Figure 2.5. *ING* transcript levels are differentially affected in the tails and hindlimbs of T_3-treated tadpoles.

Brains of T_3-treated tadpoles had high levels of ING transcripts including *xING1c2* and *xING2b* that were not detected in tail and hindlimb (data shown separately at the bottom of the figure), but are not greatly affected by T_3 treatment. Premetamorphic tadpoles (NF stage 54) were treated with 100 nM T_3 for up to 48 h. Shown are the fold change for the L8 normalized densitometric values for each *ING* variant or *TRβ* transcript relative to time-matched controls (0 h control was used for 6 and 12 h time points, and 24 h or 48 h matched controls were used for the 24 and 48 h T_3-treated time points, respectively). All bars with the exceptions listed below represent the mean of 5 individuals for brain and 7 individuals for tail and hindlimb. For the 24 and 48 h controls, n=8. For the tail, n=5 for the 0 h control; n=6 for *xING1c1* 12 h and 24 h T_3 treatments. For the hindlimb, n=6 for the 6 h and 12 h T_3 treatments and *xING2a* for the 0 h control; n=7 for *xING1c1* and *TRβ* for the 48 h control. The dotted lines indicate the regions that represent no change relative to the controls (between 1-fold up and 1-fold down). The error bars represent the standard error of the mean derived from the control and treatment densitometric values. Statistical significance of treatment relative to the matched control is indicated by * for $p \leq 0.05$, ** for $p \leq 0.01$, and *** for $p \leq 0.001$.

2.3.7 *Expression of xING2c Transcript Variant in Adult, TH-treated, and Naturally Metamorphosing X. laevis Tadpole Tissues*

Expression of the *xING2c* variant is lower than for other ING variants and was only detectable when a Southern blot was used (Figure 2.6). Nonetheless, in expression studies similar to those described above for adults, naturally metamorphosing tadpole hindlimb and tail, as well as 100 nM T_3-treated hindlimb, tail and brain, differential expression of this variant was observed. The upper band in the Southern blot represents at least both *xING2a* and *xING2b*

variants, as the primers were amplifying a region common to both, and may represent a variant that has not yet been identified. Similar to the adult tissues discussed previously, brain, testis and eye are relatively high in expression compared to muscle, liver and skin that are weakly expressing (Figure 2.6B). The lower band represents a novel variant, *xING2c* that has a deletion spanning both exon 1 and 2. No other expression data for this variant is available for a direct comparison. Although brain is still seen to have high levels, the other tissues are much weaker than the other *xING2* variants, except skin which is moderately expressing.

In tadpole brain, high levels of *xING2com* were observed, and *xING2c* was also detectable in this tissue but at much lower levels. Neither appears to change in response to TH (Figure 2.6C), similar to other data available for *ING2* in the brain.

In hindlimb, *xING2com* increased moderately at 48 h T_3 treatment compared to 0 h, but is much less than a large transient peak at 2 h (Figure 2.6D). In the sample set already discussed, *xING2a* was significantly decreased at 6 h, and data for *xING2 All Variants* showed a significant decrease at 6 and 24 h. This experiment cannot be directly compared as xING2com variants are measured together, but levels are undetectable at 6 and 12 h in reasonable agreement with the other *ING2* data. The *xING2c* variant also had a large transient peak, but at 0.5 h, and was undetectable at 6 h. Levels at 48 h of T_3 treatment were unchanged from 0 h where only weak expression was observed, but levels are considerably less than the high expression seen at 0.5 h. Naturally metamorphosing samples increased from virtually undetectable at prometamorphic NF stage 58 to moderate levels at a fairly late metamorphic climactic NF stage of 63 (Figure 2.6E). This upward trend matches what is observed in the previous experiment for *xING2a* for those stages, but if one compares to a premetamorphic state a downward trend would be anticipated in the hindlimb. However, the 0 h controls for this experiment do not represent only NF stage 54 animals as the sample set includes younger animals from NF stage 50-54. It is possible that if only NF stage 54 animals had been tested in the

Southern blot, a higher level of *xING2* variants would have been observed. The *xING2c* variant also increased from undetectable levels at NF stage 58, but only to weak levels (Figure 2.6E).

In tail, xING2com and *xING2c* increased substantially at 24 and 48 h T_3 treatment with a transient moderate increase at 0.5 and 2 h (Figure 2.6F). This large increase for all three variants is observed in naturally metamorphosing tadpoles as well, from undetectable levels at 0 h and NF stage 58 samples to very high levels during metamorphic climax NF stages 60-63 (Figure 2.6G). Results are similar to those obtained in Figures 2.4 and 2.5.

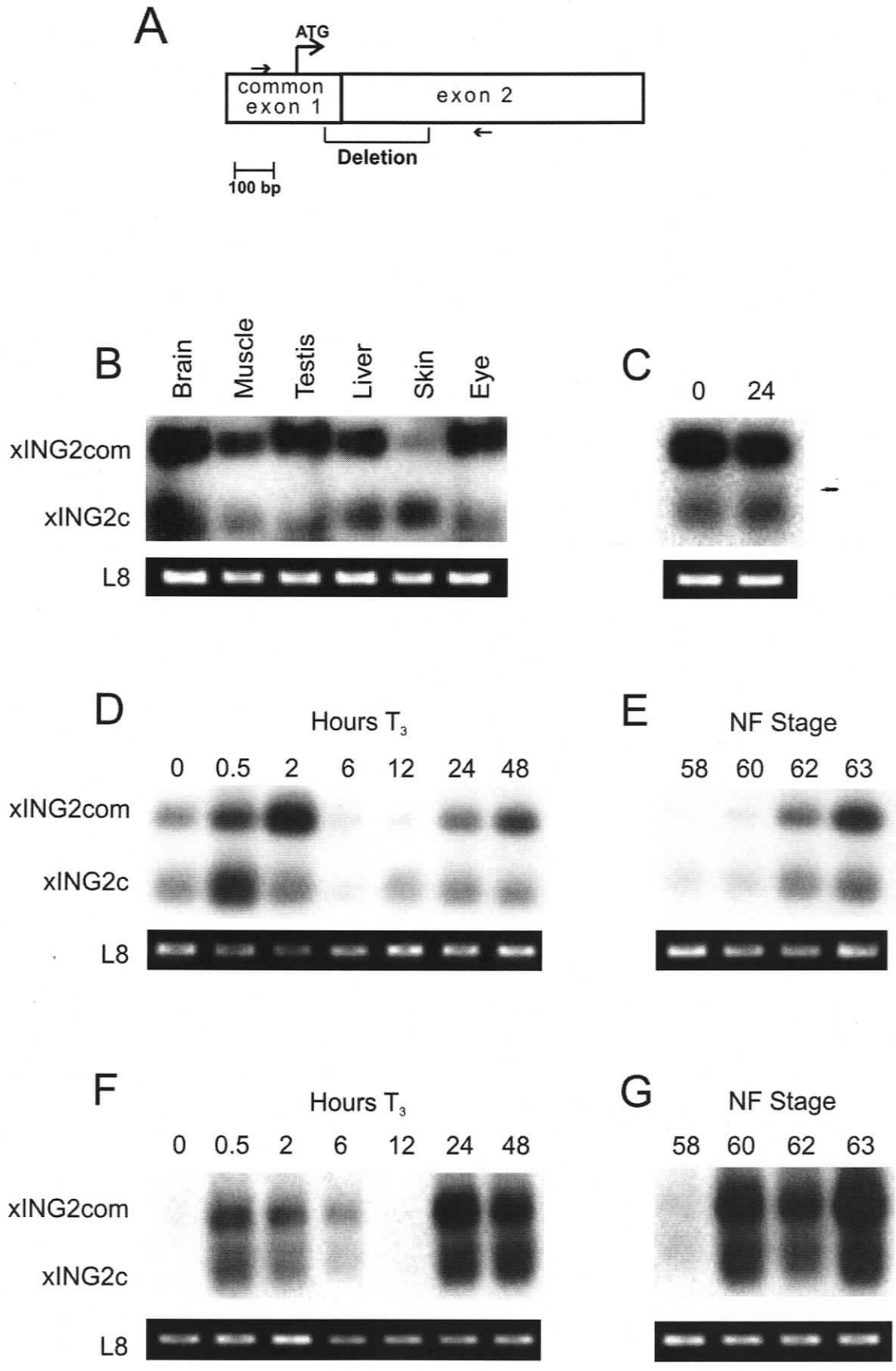
A
ATG
common exon 1
exon 2
Deletion
100 bp
B
Brain
Muscle
Testis
Liver
Skin
Eye
xING2com
xING2c
L8
C
0
24
D
Hours T_3
0
0.5
2
6
12
24
48
xING2com
xING2c
L8
E
NF Stage
58
60
62
63
F
Hours T_3
0
0.5
2
6
12
24
48
xING2com
xING2c
L8
G
NF Stage
58
60
62
63

Figure 2.6. Expression of *xING2c* varies in adult, T_3-treated tadpoles, and naturally metamorphosing tadpoles.

(A) Schematic showing the regions of *ING2* bound by the RT-PCR primers spanning the exon 1/2 boundary of *xING2.* The primers amplify a full length 635 bp *ING2* product that represents both the *xING2a* and *xING2b* variants and possibly an unknown variant with the forward primer being in the common region of exon 1. The primers also amplify a 350 bp *xING2c* variant where 285 bp of sequence is deleted. Panel B to G show Southern blots of RT-PCR products run on 2% agarose gels, and probed with a fragment of human *ING1* cDNA specific to the common exon 2 region. The L8 ribosomal protein transcript, which remains constant between tissues [123], is shown below each Southern blot and was used to normalize the *xING2* amplification products. Adult tissues were tested (Panel B) as well as premetamorphic tadpoles (Stage 50-54) treated with 100 nM T_3 for the times indicated (panel C, brain; panel D, hindlimb; and panel F, tail) or sampled during natural metamorphosis at stages according to Nieuwkoop and Faber (NF) as indicated (panel E, hindlimb and panel G, tail).

2.3.8 Expression of ING Transcript Variants in 8 nM T_3-treated X. laevis Tadpole Tissues

The previous T_3-induction experiments were done with 100 nM T_3, a supraphysiological concentration. Previous studies on gene expression with lower physiological concentrations have indicated that transcript levels are affected differently [124]. In order to determine that ING expression is affected at physiological concentrations (8 nM T_3), I examined *ING1* and *ING2* variant transcript levels for hindlimb, tail, and brain with RT-PCR using samples generated for another study [124]. This concentration represents the maximal T_3 levels attained during natural metamorphosis [65, 126].

Results for each tissue are shown in Figure 2.7. Individual variants in brain were not affected by T_3 treatment, as observed previously (Figure 2.4 and

2.5) except for *xING1c1* that transiently increased at 24 h, but it is no longer significantly elevated at 48 h. A significant decease was also observed for *xING2 All Variants* at 48 h. The variants *xING1c2* and *xING2b* were previously detected in brain, but this sample set was too dilute to allow detection of these weakly expressed transcripts. Levels of *xING1b1-4*, x*ING1b5* and *xING2a* variants decrease significantly in hindlimb and stay repressed through 48 h. In tail, *xING1 All Variants*, x*ING1b1-4* and *xING1b5*, but not *xING1c1* expression is significantly elevated in response to T_3. The *xING2 All Variants* data has a significant decrease at 48 h. Although the xING2a variant is increased significantly at 24 h, a significant decrease is observed at 48 h.

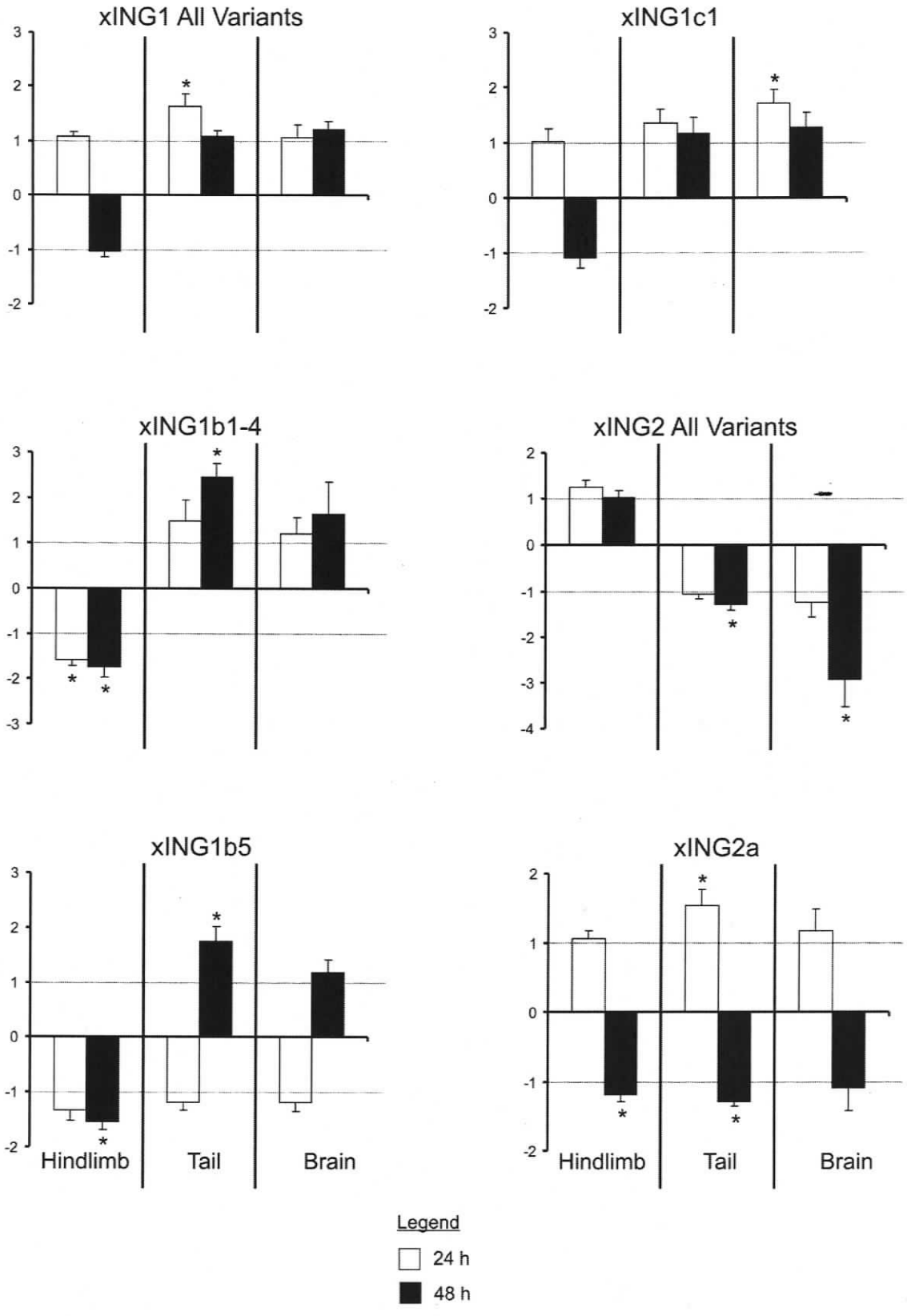
xING1 All Variants
xING1c1
xING1b1-4
xING2 All Variants
xING1b5
xING2a
Hindlimb
Tail
Brain
Hindlimb
Tail
Brain
Legend
24 h
48 h

Figure 2.7. *ING* transcript levels are differentially affected in the tails, hindlimbs and brains of tadpoles treated with 8 nM T_3.

RT-PCR analyses were done on premetamorphic tadpoles (NF stage 54) that were exposed to 8 nM T_3 for 24 or 48 h along with time-matched controls. Shown are the fold changes for the L8 normalized densitometric values for each *ING* variant transcript relative to the appropriate time-matched controls. Levels of specific *ING1* and *ING2* variants decrease in hindlimb, while increasing in the tail at certain time points. Brains of T_3-treated tadpoles show relatively constant expression for all except the *ING1c1* variant that transiently increases. All bars with the exceptions listed below represent the mean of 4 individuals. In brain, n=3 for *xING1b5* and *xING2 All Variants* 24 and 48 h controls, for *xING1c1* 24 h control, and *xING2a* 48 h control. In tail, n=3 for *xING1b4* 48 h T_3 treatment, and for *xING1b5* 24 h T_3 treatment. The dotted lines indicate the regions that represent no change relative to the controls (between 1-fold up and 1-fold down). The error bars represent the standard error of the mean derived from the control and treatment densitometric values. Statistical significance of treatment relative to the matched control is indicated by * for $p \leq 0.05$.

2.4 DISCUSSION

I showed previously that *ING2* transcripts are TH-responsive [16] and the data in this chapter concur with and substantially extend this finding. I have isolated several novel variants of two members of the ING family, *xING1* and *xING2,* in *X. laevis* and have compared their tissue specific expression patterns in adult and tadpole tissues. I also found that *xING1* and *2* variants are differentially expressed and inducible by T_3. These responses were similar during natural metamorphosis in a manner that reflects the known increase in endogenous TH levels [126, 65].

The transcripts provide evidence for multiple forms of exon 1 that combine with a common exon 2 for both *xING1* and *xING2*. This is in agreement with the

known structures for the human and mouse *ING* genes [26, 127]. Interestingly, I found two sets of *xING1* sequences that have several base pair substitutions that may reflect a gene duplication and evolutionary divergence over time. *X. laevis* has a pseudotetraploid genome and currently there is no evidence that the diploid *X. tropicalis* possesses two versions of *xING1*. To compare my work in *X. laevis* to the Joint Genome Institute Database for *X. tropicalis*, I assembled the *X. tropicalis* sequences for ING1 and ING2. I contributed this information along with my *X. laevis* derived protein sequences to a publication in which I am third author, He *et al.*, 2005. Several domains that were identified in human ING family members [15] are conserved in the sequence I isolated for *X. laevis* and the *X. tropicalis* sequence that I assembled and analyzed including: a potential chromatin regulation region; a nuclear localization sequence; a phosphorylation-dependent interacting domain that in the case of human $p33^{ING1b}$ binds to 14-3-3 protein [30], a PHD finger, and a peptide interacting motif (PIM) domain enriched in acidic, basic, and aromatic residues that binds a defined subset of peptides [14] and, along with the PHD region binds to phosphatidylinositol monophosphates [31]. Within the nuclear localization sequence, there are three nucleolar translocation sequences that for ING1 target the protein to nucleoli when cells are subjected to cellular stresses such as UV-induced DNA damage [29]. All three sequences are identical in ING2 and may have a similar function. In the unique N terminal regions, $p33^{ING1b}$ has a proliferating cell nuclear antigen (PCNA)-interacting protein (PIP) domain [32], and $p32^{ING2}$ has a leucine zipper [15]. Conservation of protein domains between human and amphibians suggests ING1 and ING2 function *via* similar mechanisms in both species.

It is difficult to do a direct comparison between the data presented here and that which is published on the relative expression levels of human and mouse isoforms because most of the studies that were done do not adequately differentiate between variants. There are no comprehensive studies that examine the relative expression of *ING2*, *ING1b,* and *ING1c*. However, the testis appears to have the greatest representation of ING isoforms expressed [18, 19, 21]. I found that, in addition to testis, the brain and eye also expressed

substantial levels of *xING1* and *xING2* transcript variants. Also, levels of *TRβ* are higher in brain, skin and eye, but not significantly higher in testis. The *xING2c* variant is expressed at extremely low levels as it was only detectable by RT-PCR followed by Southern blotting; however, it was expressed in a variety of adult tissues including brain, muscle, testis, liver, skin, and eye as well as in tadpole brain, hindlimb and tail.

Since ING belongs to a larger family of PHD-finger containing proteins that are important in chromatin remodeling and chromatin-mediated regulation of transcription [15], elevated levels of ING in testis may help in addressing specific requirements for chromatin packaging, remodeling and transcription control specific to spermatogenesis [128]. Indeed, Western blot analysis confirms that adult frog testis contains high levels of ING protein [16]. The high expression levels of *xING1* variants in adult brain and eye also suggest an important role of ING in these cells.

For a given variant, adult testis and brain contained transcript levels comparable to tadpole brain, whereas expression levels in the tadpole tail and hindlimb were generally an order of magnitude lower. Most variants were still detectable in tail and hindlimb; however, not *xING1c2* or *xING2b*, which were only reliably detected in the testis and brain in adult tissues as well as in the tadpole brain.

Thyroid hormones are essential for the induction of the diverse changes observed during tadpole metamorphosis. These changes include tail regression, hindlimb growth and brain remodeling that each involves changes in expression for a growing list of genes which now includes *ING*. Of particular note were the marked upregulation of *xING1b1-4* and *xING1b5* in the tail and the contrasting downregulation of these variants in the hindlimb during both natural metamorphosis and the TH-induced metamorphosis of premetamorphic tadpoles treated with 8 nM T_3.

In tadpole brain, few changes were observed, with no obvious up or downregulation trends. T_3 treatment had only transient effects at 6 h for *xING1 All Variants*, and *xING2a* at the 100 nM concentration, whereas, a significant

upregulation was observed at 24 h for the *xING1c* variant and a downregulation for *xING2 All Variants* at the 8 nM concentration. During natural metamorphosis, transient increases in expression were observed for all variants during metamorphic climax at NF stage 60 except *xING2b*, but all other stages were not statistically different from each other (except *xING1c2* at NF stage 62 was still increased as it was in stage 60, dropping again at stage 63). For most *ING* variants there may be a requirement such as expression of a cofactor, in addition to stimulation with T_3, in order for *ING* levels to be affected. In contrast to the brain, virtually all transcripts were T_3-responsive in the tail and hindlimb through to the later stages of natural metamorphosis or later time points examined in T_3-treated tadpoles. Maintenance of relatively constant levels of ING transcripts in tadpole brain during metamorphosis suggests that their encoded proteins may be essential for normal functioning of this tissue. Compared to other tissues, the presence of additional variants (*xING1c2* and *xING2b*) at high levels supports this idea.

Overall, the data for *xING1 All Variants* (common exon 2 primers) were represented well by the individual variants tested suggesting that I have examined the majority of the variants representing *xING1*. However, the concordance of the *xING2 All Variants* data with the three individual variants is relatively poor. The *xING2a* data differs substantially from the *xING2 All Variants* data, the *xING2b* variant was only detected in adult tissues and tadpole brain, not tadpole tail and hindlimb, and the *xING2c* variant was even more difficult to detect requiring a Southern blot. This suggests that there is at least one more variant of *xING2* that has yet to be discovered.

Comparison of the overall kinetics of natural to T_3-induced metamorphosis shows similarities in response for all three tissues. However, maintenance of the response differs particularly in the hindlimb in the 100 nM T_3 study. For example, *ING1* expression remains repressed during natural metamorphosis whereas this repression is transient during precocious metamorphosis. This may be due to a continued requirement for exposure to T_3 or absence of a cofactor expressed in older tadpoles. It also may reflect a desensitization of the hindlimb to the higher

than normal concentration of T_3 used in the 100 nM T_3 study, as the expression study I conducted on hindlimbs treated with 8 nM T_3 showed patterns that correspond more closely to the expression patterns observed during natural metamorphosis. Specifically, the variant x*ING1b1-4* and x*ING1b5* expression remains repressed up to 48 h in the 8 nM study. The data for *xING2a* in hindlimb also matches natural metamorphosis data more closely with 8 nM T_3 treatment where a significant decrease is observed at the end of the time course. In the tail, the decrease in *xING2 All Variants* during metamorphic climax is more closely represented at 8 nM T_3. This data further supports the hypothesis that *ING* gene expression is influenced by TH in a biologically relevant context.

Taken together, these data suggest that there may be antagonistic regulation of *xING* variants by T_3 that correlates with tissue fate. The nature of that regulation may involve tissue-specific factors. In the presence of T_3, elevated levels of ING may contribute to apoptosis and reduced levels may promote proliferation. The lack of response of *xING* to T_3 in the brain may reflect a constitutive requirement for the proteins encoded by these genes. However, since the brain undergoes extensive remodeling that includes proliferation, apoptosis and differentiation, it is possible that closer inspection of the response of different brain regions and cell types may disclose specific regulation that is not detectable by merely examining the entire brain.

Although the present study focuses upon TH-regulation of *ING* genes in frog tadpoles, it is highly likely that *ING* genes in other species, including mammals, are also under hormonal control. Bioinformatics analysis of 10,000 bp of genomic sequence upstream of *ING1* and ING2 genes identifies 7 putative TREs in human *ING1* sequence, 9 putative TREs in mouse *ING1* sequence, 3 putative TREs in human *ING2*, and 12 putative TREs in mouse *ING2*. In *X. tropicalis*, a sequence that aligns with the *xING1b1-5* variant of *X. laevis* was identified. In the 10,000 bp upstream of *X. tropicalis ING1b1-5*, 2 putative TREs were found. In the 1441 bp sequence that falls between the sequence that aligns with the *xING1b1-5* variant and that which aligns with the *xING1c* variant in *X. tropicalis*, 1 TRE is predicted. Upstream of *ING2* in *X. tropicalis,* 1 TRE is also

predicted. Experiments are needed in order to establish the functionality of the putative TREs in other species.

These studies have greatly increased the number of known *ING* transcripts, and have established that they are differentially expressed in different tissues and are TH-responsive. It will be important in the future to determine what proteins are expressed from these transcripts and how their regulation varies throughout TH-dependent development, as well as determining if putative TREs are functional in other species.

CHAPTER 3: ING PROTEIN ASSOCIATES WITH THYROID HORMONE RECEPTOR AND WITH PROMOTERS OF THYROID HORMONE RECEPTOR-REGULATED GENES

A portion of the work presented in this chapter is being prepared for publication: Caren C. Helbing, Mary J. Wagner, Jill Johnston, Rachel Heimeier, Lan Ji, Wei Ding, Leon Browder, Frank Jirik, Yun-Bo Shi (2006). Inhibitor of Growth ING1 and ING2 modulate thyroid hormone-dependent gene expression.

3.1 INTRODUCTION

ING family members form protein complexes that associate with DNA including critical regulators of chromatin structure, such as HATs and HDACs [7-9, 12] and bind directly to transcription factors including p53 [43] and NF-κB [6], as well as to the DNA-binding protein, PCNA [32]. TR is a transcription factor itself, and can also bind to p53 [90, 120] and to the HAT, p300 [129]. Numerous studies have implicated ING in facilitating apoptosis (reviewed in [7-9, 13]), a process that requires genomic actions of TR in the context of tadpole tail resorption (reviewed in [72-74]). This puts ING and TR in a similar cellular context.

Evidence is mounting that ING isoforms modulate cell function through altering gene expression. ING contains a PHD finger domain found in many chromatin-associated proteins [10, 11], and ING proteins from each gene in the ING family have been shown to associate with either HATs or HDACs, or both (reviewed in [7-9, 13]). ING1 protein binds DNA in an EMSA [40], and in a microarray study using antisense ING1 in mouse mammary epithelial cells

followed by overexpression studies of selected genes, ING1 can both up and downregulate gene expression [60]. TRs are transcription factors that also bind DNA and affect transcription in a TH-dependent way for numerous genes. I have shown that *ING* transcript expression is increased in the tadpole tail in both natural and T_3-induced metamorphosis [16, 17].

In this chapter, I discuss the creation of His-tagged constructs that were made for ING1, ING2, TRα, and TRβ for protein expression, and I characterize ING2-His and TRβ-His antibodies generated by Immuno-Precise Antibodies Ltd.. I show that purified TRβ-His and ING2-His proteins co-immunoprecipitate and that ING and TR proteins co-immunoprecipitate in tadpole tail homogenates. Considering ING's ability to associate with TR in the context of apoptosis of the tadpole tail, the question was asked whether ING associates with chromatin at well-known TH-regulated promoters. I demonstrate by ChIP assay that ING indeed binds to *TRβ* and *TH/bZIP* promoters that have known TREs and are also bound by TRα and TRβ. Taken together, data suggest that ING and TR could participate in the same regulatory complexes to alter gene expression.

3.2 MATERIALS AND METHODS

3.2.1 His-Tag Protein Purification and Antibody Production

To generate His-tagged proteins for expression and purification from bacteria, appropriate vectors were generated. PCR primers were designed using Primer Premier software (Premier Biosoft International) such that PCR products for the open reading frame of either *ING1*, *ING2*, *TRα*, or *TRβ* would have cut sites for NcoI and XhoI restriction enzymes on either end. The coding sequences are included in Appendix 5. In order to accommodate the NcoI restriction enzyme sites in *ING1* and *ING2* 1 bp was modified such that the first aa after the starting methionine is a valine rather than a leucine. To accommodate the XhoI site and allow for coding of 6 histidine residues at the C

terminal end of each protein, the stop codon was replaced with sequence coding for leucine and glutamate followed by 6 histidines. Primers were as follows: *ING1* forward primer 5'-CGACGCCATGGTGAGCCCGGCAA and reverse primer 5'-GCTACCTCGAGCCTGTTATATGTCCT; *ING2* forward primer 5'-CGACGCCATGGTAGGGCAACAGCAGCAC and reverse primer 5'-GGGTACCTCGAGCCTCGACCGTCTGTCTTT; *TRα* forward primer 5'-CGACGCCATGGACCAGAATCTAGCG and reverse primer 5'-GCTACCTCGAGAACTTCCTGGTCCTC; and *TRβ* forward primer 5'-CGACGCCATGGAAGGGTATATACCC and reverse primer 5'-GCTACCTCGAGGTCCTCAAACACTTCCAAG.

Primers were used at 20 pmol in a typical 50 µl reaction containing 1.5 units of *Thermus aquaticus* (*Taq*) DNA polymerase (Amersham Biosciences), 10 nmol of dNTPs (GIBCO Life Technologies), and 1.5 mM $MgCl_2$. PCR was done with adult testis cDNA described in section 2.2.3 as follows: 10 min 94°C denaturation, followed by 35 cycles of 94°C for 630 s, 55°C for 60 s and 72°C for 2 min, followed by 10 min at 72°C. PCR products were digested with NcoI and XhoI, gel-purified with the QIAEX II Gel Extraction Kit (Qiagen), and inserted into the pET21d$^+$ vector (Novagen, Madison, WI). The construct was verified by transfection into TOP10 cells (Invitrogen) and analysis of clones as described previously followed by sequencing. To expresses proteins with a His tag, chemically competent *Escherichia coli* BL21DE3 cells were transformed with each plasmid, and the His-tagged proteins purified as follows with the assistance of Mark Tessaro and Dominik Domanski (TRβ-His and ING2-His proteins) and Karen Cheung (TRα-His). Twenty mL cultures of LB-Ampicillin (Amp) broth (For 1 L: 10 g tryptone, 5 g yeast extract, 10 g sodium chloride (NaCl), pH 7.0 and 10 mL of 10 mg/mL filter sterilized ampicillin) were inoculated with bacterial stocks containing His-tag vectors with ING1, ING2, TRα, or TRβ inserts and grown overnight at 37°C with shaking at 240 rpm. The following day, 1 L of LB-Amp broth was inoculated with the 20 mL overnight culture and incubated at 37°C with shaking at 240 rpm until the OD_{600} reached ~0.6. At this point, 100 µL of the culture was removed and mixed with 20 µL of 6X SDS sodium dodecyl sulfate

(SDS) buffer (187.5 mM tris(hydroxymethyl)aminomethane hydrochloride (Tris-HCl), 6% SDS, 30% glycerol, 150 mM dithiothreitol (DTT), 0.03% bromophenol blue, pH 6.8), boiled at 95°C for 5 min and stored at -70°C for later SDS-Polyacrylamide gel electrophoresis (PAGE) analysis. Protein expression was induced by adding isopropyl-β-D-thiogalactopyranoside (IPTG) to a final concentration of 1 mM. In addition, 50 μM zinc sulfate ($ZnSO_4$) was added, and then the culture was incubated at 30°C for 2 h with shaking at 240 rpm. At the end of the 2 h incubation, 100 μL of the culture was removed, mixed with 20 μL of 6X SDS buffer, boiled at 95°C for 5 min and then stored at -70°C for later SDS-PAGE analysis. For the large culture, cells were centrifuged at 5000xg for 5 min at 4°C, and then the pellet was stored at -70°C.

Purification of the His-tagged protein was done with a column containing Talon metal affinity resin (Clontech, Palo Alto, CA). The column was prepared by first resuspending the Talon resin and transferring 2 mL to a centrifuge tube, and then centrifuging at 700xg for 2 min. The resin pellet was resuspended in 10 mL of extraction buffer (50 mM sodium phosphate ($NaH_2PO_4H_2O$), 300 mM NaCl, 5 mM imidazole, pH 7.0) and mixed briefly to pre-equilibrate the resin, then centrifuged at 700xg for 2 min. This step was repeated once. Next the frozen cell pellet was resuspended in 20 mL of extraction buffer on ice. The suspension was sonicated with an Ultrasonic Processor Model W-385 at 40% output (Heat Systems-Ultrasonics Inc, Farmingdale, NY) for 8 pulses of 15 s with 1 min on ice in between. The cell debris was centrifuged at 12000xg for 10 min at 4°C and the supernatant was saved. This supernatant was then added to the pre-equilibrated Talon resin and gently agitated at room temperature for 20 min on a platform shaker set at 90 rpm. This allowed the His-tagged proteins to bind the Talon resin. Next, the protein-resin mixture was centrifuged at 700xg for 5 min. The supernatant was discarded and the resin was washed twice with 20 mL extraction buffer by agitating the suspension at room temperature for 10 min on the platform shaker set at 90 rpm. Then, 1 mL extraction buffer was added to resuspend the protein-resin and the suspension was transferred to a 2 mL gravity-flow column. The resin was allowed to settle at 4°C for 10 min and then

the buffer was allowed to drain until it reached the top of the resin. The column was washed with 5 mL of extraction buffer. The His-tagged protein was eluted by adding 5 mL elution buffer (50 mM NaH_2PO_4, 300 mM NaCl, 150 mM imidazole, pH 7.0) without disturbing the resin, and then collecting 500 µL fractions.

The fractions and the samples of the uninduced and induced culture were quantified for total protein concentration using the Bio-Rad Protein Assay (Bio-Rad Laboratories, Mississauga, ON). Two µL of each fraction were analyzed by Coomassie-stained SDS-PAGE gels and 1 µL of each fraction was analyzed by Western blot (WB) as described below using an 1/1000 dilution of an anti-His (H-15) rabbit polyclonal immunoglobulin (Ig) G as the primary antibody (Santa Cruz Biotechnologies Inc., Santa Cruz, CA).

The xING2-His protein and the TRβ-His fractions were further purified by excision of the bands from an SDS-PAGE gel followed by destaining, electroelution, dialysis and lyophilization. The identity of these protein bands was verified by MALDI-TOF mass spectrometric analysis (experiments performed by Dominik Domanski). The purified xING2-His and TRβ-His proteins were used to generate antibodies by Immuno-Precise Antibodies Ltd..

3.2.2 Characterization of Antibodies by Immunoblotting

Purified His-tagged proteins boiled in SDS sample buffer were electrophoresed through 7-17% SDS –PAGE gradient gels made with a gradient maker (Hoeffer Scientific Instruments, San Francisco, CA) and Variable Flow Mini-pump (Control Company, Friendswood, TX). Gels were run using a Mini Vertical Slab Gel Apparatus (Bio-Rad) at 100 V for ~ 30 min for samples to pass through the 4% stacking gel, and then 150V for ~ 1 hour for the samples to separate well in the 7-17% gradient separating gel. Approximate protein sizes on the gels were determined by the addition of 5µl Precise Plus Protein Dual Color Standards on each gels (Bio-Rad).

The proteins were transferred to 0.2 µm nitrocellulose membrane (Bio-Rad) using a semi-dry transfer apparatus (2117 Multiphor II Electrophoresis Unit, LKB, Bromma, Sweden) with a current maintained at 0.8 mA/cm^2 for 1.5 h. Gels were placed on the nitrocellulose in a sandwich of Whatmann filter papers where the bottom 6 papers were soaked in Anode I Solution (0.30 M Tris, 20% MeOH), followed by 3 papers soaked in Anode II Solution (0.025 M Tris, 20% MeOH), and the top 9 papers were soaked in Cathode Solution (0.04M 6-amino-caproic acid, 20% MeOH).

Protein loading and transfer quality were verified by membrane staining with 0.1% Ponceau S (Sigma-Aldrich) in 5% acetic acid. Membranes were blocked with 5% nonfat milk in phosphate buffered saline (PBS; 0.2 M NaCl, 4.2 mM potassium chloride (KCl), 12.7 mM Na_2HPO_4, 2.3 mM KH_2PO_4) overnight at 4°C and then probed with primary antibody solutions.

In the case of anti-His WBs, an 1/1000 dilution of a His-probe (H-15) rabbit polyclonal IgG was used as the primary antibody (Santa Cruz Biotechnologies Inc.) diluted in 1% nonfat milk in PBS plus and 0.15% Tween 20 (PBST) for 1 h at room temperature with shaking.

In the case of the anti-ING and anti-TR WB screens, 5 µg of ING2-His or TRβ-His was loaded into a single preparative well and separated by SDS-PAGE, and then following transfer to nitrocellulose membrane, a Mini-protean II Multiscreen Apparatus (Bio-Rad) was utilized with 1/2 dilutions of tissue culture supernatants (600 µL volume per lane) in 1% nonfat milk PBST incubated overnight at 4°C. The positive ING2 mouse serum was taken from the same mouse used to create the mouse monoclonal anti-ING antibodies and was diluted 1/500. The negative control mouse monoclonal tissue culture supernatant anti-trout IgG or anti-herpes virus 6D9 antibodies were diluted 1/2. The same fusion strain and procedure that was used for the creation of anti-ING and anti-TR mouse monoclonals was used by Immuno-Precise Antibodies for creation of the negative controls. The positive control C191 anti-TR rabbit polyclonal was a gift from D. Brown, Carnegie Institute and was diluted 1/1000 [70].

When using the new anti-ING and anti-TR antibodies chosen from the screen in a standard WB, anti-ING 9H3 or anti-TR 9B2 mouse monoclonal tissue culture supernatants were each used at 1/10 dilution. In addition anti-TR mouse polyclonal serum taken from the same mouse that was used to create the monoclonal anti-TR antibody was used at 1/1000 dilution.

In the case of anti-ING rabbit polyclonal WBs, the antibody was provided as a gift from K. Riabowol, University of Calgary, and was used at 1/2000 dilution. This antibody was generated using a human GST-ING1 C-terminal end fusion protein which contains the highly conserved portion of ING [1].

After incubation with primary antibody, blots were washed for 6 x 10 min at room temperature in PBST with shaking. Then the blots were incubated with an IRDye 800CW conjugated anti-rabbit IgG secondary antibody with emission wavelength at 800 nm (Rockland Inc., Gilbertsville, PA) diluted 1/2000 in 1% nonfat milk/PBST for 1 h at room temperature with shaking. The blots were then washed with PBST for 5 x 10 min followed by 2 final washes with PBS for 2 x 5 min. Blots were scanned at 42 µm resolution with an Odyssey infrared imaging system (LI-COR Biosciences, Lincoln, NE).

In the case of the initial characterization of ING and TR mouse monoclonal antibodies by WB and immunoprecipitation (IP) screens as well as the anti-ING rabbit polyclonal IPs, blots were visualized with the enhanced chemiluminescence (ECL) method, as described by the manufacturer (Amersham). In these cases, secondary antibodies were either goat anti-rabbit or goat anti-mouse Horse Radish Peroxidase (HRP)-conjugated antibodies (Cedar Lane Laboratories Ltd., Hornby, ON) diluted 1/4000 in 1% nonfat milk/PBST and incubated for 30 minutes before exposure to Kodak Biomax x-ray film (Eastman Kodak Co., Rochester, NY).

3.2.3 Characterization of ING and TR Monoclonal Antibodies by Immunoprecipitation

Two µg of purified ING2-His were incubated with 200 µL of tissue culture supernatant from mouse monoclonal anti-ING antibodies or negative control anti-herpes virus 6D9 antibody or with 4 µL positive control anti-ING2 mouse serum taken from the same mouse that was injected with ING2-His to create the monoclonal antibodies. Two µg purified TRβ-His were incubated with anti-TR antibodies or negative control anti-trout antibody or with 2 µL positive control anti-TRβ mouse serum taken from the same mouse that was injected with TRβ-His to create the monoclonal antibodies. Protein-antibody complexes were incubated 20 min at room temperature while at the same time 30 µL protein G-sepharose beads (Amersham) per IP were incubated together with 10% by volume non-specific fetal bovine serum protein (HyClone, Logan, UT) for 20 min at room temperature in 1 mL IP buffer (50mM 4-(2-hydroxyethyl)-1-piperazineethanesulfonic acid (HEPES) pH 8.0, 150 mM NaCl, 2.5 mM O,O'-Bis(2-aminoethyl)ethyleneglycol-N,N,N',N'-tetraacetic acid (EGTA), 1 mM N,N'-1,2-ethanediylbis(N-(carboxymethyl)glycine)edetic acid (EDTA), and 0.1% Tween-20). The pre-blocked beads were then aliquoted to each IP tube such that final bead volume was 30 µL per IP and then each IP was made up to 1 mL final volume with IP buffer. The antibody-protein-bead mixtures were rotated at 4°C for 2 h. Then the beads were washed 3 times with 1 mL ice cold IP buffer by centrifugation at 3,000xg for 3 min at 4°C to pellet the beads each time. The proteins that bound to the beads were then eluted by boiling for 3 min in 20 µL 6x SDS buffer and then stored at -20°C until they were analyzed by immunoblotting as described above, using an 1/1000 dilution of a His-probe (H-15) rabbit polyclonal IgG as the primary antibody (Santa Cruz Biotechnologies Inc.).

3.2.4 Immunoprecipitations with Purified xING2-His and TRβ-His Proteins

To test if ING2 and TRβ co-immunoprecipitate, 1 µg purified xING2-His and TRβ-His proteins were incubated for 20 min at room temperature. Then 1 µL of anti-TR polyclonal mouse serum was added and the mixture incubated a further 20 min at room temperature. Also at this time, controls with ING2-His and TRβ-His alone were mixed with 1 µL of anti-TR polyclonal mouse serum and the mixture incubated for 20 min at room temperature. Then the protein-antibody complexes were mixed with 20 µL protein G-sepharose beads (Amersham) that were pre-incubated with 10% non-specific fetal bovine serum (HyClone) protein for 20 min room temperature in 1 mL IP buffer. The antibody-protein-bead mixtures were processed as described above.

3.2.5 Immunoprecipitations with Total Protein from Tadpole Tails

Tails from pools of 7 to 20 tadpoles during metamorphic climax, NF stage 60-62, were homogenized on ice using 2 pulses of 10 s each with a Heidolf DIAX600 Homogenizer (Heidolph Elektro GmbH & Co. KG, Kelheim, Germany) on setting 9500 min^{-1} in a buffer containing 25 mM HEPES (pH 7.0), 10 mM EDTA, 10 mM β-glycerophosphate, 0.1 mM sodium vanadate, 1 mM sodium fluoride, 1 mM dithiothreitol (DTT), 100 µM phenylmethylsulphonylfluoride (PMSF), 4 µg/mL aprotinin, 1 µg/mL leupeptin, 2 µg/mL antipain and 300 µg/mL benzamidine using a volume of 3 mL buffer per gram tissue based on [130]. Homogenates were centrifuged at 12,000xg for 10 min at 4°C and the collected supernatant was stored at -70°C. The homogenate concentration was determined using the Bio-Rad Protein Assay according to the manufacturer's instructions (Bio-Rad).

For IPs with tail tissue homogenates, 1 mg of total protein was diluted to a 500 µL volume in IP buffer with 10 µM $ZnSO_4$ added. Homogenates were precleared by rotation with 20 µL of protein G-sepharose beads (Amersham) for

30 minutes at 4°C. The mixture was centrifuged at 3,000xg for 3 min at 4°C to pellet the beads, and the precleared protein solution was transferred to a clean 1.5 mL tube and was incubated overnight with 5 μL of anti-TR polyclonal mouse serum. Control IPs without either protein or antibody were included. The following day, 20 μL of fresh beads were added to each IP. The antibody-bead-homogenate mixture was incubated for 6 hours at 4°C on an orbital shaker. Then the beads were washed and prepared for loading on SDS-PAGE gels as described above.

Immunoblotting was done as previously described using either anti-TR 9B2 or anti-ING 9H3 mouse monoclonal tissue culture supernatants for the primary antibody, each at 1/10 dilution. Each experiment was repeated three times with similar results. Binding specificity was determined by comparing WBs with unblocked anti-ING antibody to WBs with anti-ING antibody that was pre-incubated with either 5 μg of purified ING1-His or ING2-His. SDS-PAGE gradient gels (7-17%) were made in groups of 5 in a multicaster. This allowed for good reproducibility of sample running between gels, for example to compare blocked and unblocked blots. Large volume IP reactions were done in 1 tube and split in half for ING and TR WBs or in thirds for the blocking experiment so that eluted proteins from the IP were from the same reaction when loading the SDS-PAGE gels.

3.2.6 Characterization of an Anti-ING Rabbit Polyclonal Antibody by Immunoblotting and Immunoprecipitation

The anti-ING rabbit polyclonal that was utilized in ChIP assays was provided as a gift from K. Riabowol, University of Calgary. This antibody was generated using a human GST-ING1 C-terminal end fusion protein that contains the highly conserved portion of ING [1]. Immunoblots were done as described previously using the antibody at an 1/2000 dilution. Secondary antibody was

IRDye 800CW conjugated anti-rabbit IgG with emission wavelength at 800 nm, visualized with the Odyssey infrared imaging system.

The IP with ING2-His using this antibody was carried out as follows along with a negative control IP using an anti-herpes virus mouse monoclonal antibody (6D9). Ten μL anti-ING rabbit polyclonal was incubated overnight at 4°C with 20 μL protein G-sepharose beads. The following day, 2 μg purified ING2-His was added and IP Buffer up to 1 mL final volume. The antibody-bead-protein mixture was incubated for 3 h at 4°C on an orbital shaker. Then the beads were processed and immunoblotted as described above using an 1/1000 dilution of the anti-His rabbit polyclonal primary antibody, the 1/4000 goat anti-rabbit HRP-conjugated secondary antibody and visualized by the ECL/xray film method.

ING1-His was purified and tested in an IP as follows. One μg ING1-His was incubated with 5 μL anti-ING rabbit polyclonal or a negative control anti-herpes virus mouse monoclonal antibody (6D9) for 45 min at room temperature. Twenty μL beads per IP were pre-washed in IP buffer with the addition of 10 μM $ZnSO_4$. Twenty μL beads was then added to the antibody-protein mixtures and the volume made up to 1 mL in IP buffer with 10 μM $ZnSO_4$. This mixture was incubated for 2.5 h at 4°C on an orbital shaker. Then the beads were processed and immunoblotted as described above using both an 1/1000 dilution of the anti-His rabbit polyclonal primary antibody and an 1/10 dilution of anti-ING mouse monoclonal 9H3 primary antibody on the same blot. Two secondary antibodies were applied simultaneously at 1/2000 dilutions: an IRDye 700CW conjugated anti-mouse IgG with emission wavelength at 700 nm and an IRDye 800CW conjugated anti-rabbit IgG secondary antibody with emission wavelength at 800 nm. This blot was visualized with the Odyssey infrared imaging system at 700 and 800 nm as described previously.

3.2.7 Chromatin Immunoprecipiation (ChIP) Assays

Animals were obtained and cared for as described in Section 2.2.1. After being acclimatized to lab conditions at 21±1°C in polyethylene buckets, and having grown to the desired premetamorphic NF stages 52-54, *X. laevis* tadpoles were transferred to glass dishes with charcoal-filtered municipal water at 21±1°C with a density of ~5 tadpoles per liter. After 24 h during which time animals were not fed, either 10 nM T_3 (Sigma-Aldrich) dissolved in 400 μM NaOH (EM Science) was added to the water for treated tadpoles or an equal volume of 400 μM NaOH was added to control tadpoles. Animals were sacrificed after 48 h using 0.1% tricaine methanesulfonate (MS-222; Syndel Laboratories). Six independent sets of animals were tested and averaged for the TRβ promoter and β-actin promoter data, while 5 sets were averaged for the TH/bZIP promoter data where each pool contained cross-linked chromatin-protein complexes from 7-12 tails.

To obtain the chromatin-protein complexes, tadpole tails were placed in 1 mL nuclei extraction buffer (0.5 % Triton X-100, 10 mM Tris-HCl, pH 7.5, 3 mM calcium chloride ($CaCl_2$), 0.25 M sucrose, with a protease inhibitor tablet (Complete, Mini-EDTA-free, Roche, Laval, QC), 0.1 mM DTT, and 0.2 mM PMSF) in a dounce homogenizer on ice, and homogenized with 3x10 strokes using a Barnant Mixer setting 1.5, with cooling on ice for 1 min between each set. The homogenate was centrifuged at 2000xg at 4°C for 3 min, and the pellet was resuspended in 1 mL wash buffer (0.25 M sucrose, 10 mM Tris-HCl, pH 7.5, 3 mM $CaCl_2$, 1 mM PMSF, protease inhibitor tablet, 0.1 mM DTT, and 0.2 mM PMSF). The homogenate was centrifuged at 2000xg at 4°C for 3 min, and the pellet was resuspended in 720 μL wash buffer. The homogenate was then fixed in 1% formaldehyde (Anachemia, Lachine, QC) at room temperature for 20 min with mixing by inversion every 5 min, and then samples were flash frozen in liquid nitrogen and stored at -70°C.

The pellet was later thawed and resuspended in 1 mL SDS lysis buffer (1% SDS, 10 mM EDTA, 50 mM Tris-HCl, pH 8.1, 1 mM PMSF with protease

inhibitor tablet). This was incubated at room temperature for 15 min and then sonicated on ice to an average length of 600 to 800 bp using an Ultrasonic Converter Heyco PG7 probe and a Sonic Dismembrator Model 100 (Fisher Scientific Ltd, Ottawa, ON) on setting 1 with output power 4 Watts with 9 pulses of 15 s each, cooling 30 s on ice in between. The sonicates were then centrifuged at 16000xg for 10 min at 4°C, and the chromatin in the supernatant was frozen in aliquots at -70°C. The fragmentation of sonicates was verified visually by ethidium bromide stained agarose gel (data not shown).

For the ChIP, the DNA concentration was measured by OD_{260} (UV160U UV-Visible Recording Spectrophotometer, Shimadzu, Columbia, MD) and was adjusted to 100 ng/μL using SDS lysis buffer and then diluted to 10 ng/μL with ChIP dilution buffer (0.01% SDS, 1.1% Triton X-100, 1.2 mM EDTA, 16.7 mM Tris HCl, pH 8.1, 167 mM NaCl). Protein G-sepharose beads (Amersham) to be used in the ChIP and preclearing steps were prewashed in a buffer containing 0.5% Nonidet P40, 0.5% sodium deoxycholate, 1 mM EDTA, and 10 mM Tris-HCl, pH 8.0 for 5 min and then with TE buffer (10 mM Tris-HCl, pH 8.1, 1 mM EDTA pH 8.0) for 5 min both with rotation at 4°C. Beads were prepared for preclearing in a batch using the volume needed for a complete set of ChIPs (20 μL each for 5 test antibodies and the negative control + 10% for sample loss) mixed with an equal volume of 1 mg/mL calf thymus DNA (50% slurry). Samples were precleared in a batch using the volume needed for a complete set of ChIPs (400 μL each for 5 test antibodies and the negative control + 10% for sample loss). The samples and slurry of calf thymus DNA/beads were mixed and precleared for 30 min by rotating at 4°C.

Then samples were centrifuged at 350xg for 3 min and the OD_{260} of the supernatant was measured. Input samples were put aside and frozen at -70°C using a standardized amount of DNA (0.2 OD_{260} units per input sample for each independent animal pool). For the ChIP assays, the precleared sonicates were adjusted to a volume of 3 OD_{260} units per ChIP such that ~400 μL of each sample was added to tubes containing 5 μL of antibody (equivalent to 1 μg where known): either anti-TRα or anti-TRβ (gifts from D. Brown, Carnegie Institute,

(characterized by Eliceiri and Brown [70]); anti-acetylated histone H4 (Upstate Cell Signaling Solutions, Chicago, IL); anti-ING (gifts from K. Riabowol, University of Calgary); anti-RNA Polymerase II (RNA Pol II) antibodies (N-20; Santa Cruz Biotechnologies Inc.); or a negative control antibody specific to herpes virus (6D9; Immuno-Precise Antibodies Ltd, Victoria, BC) and incubated with rotation overnight at 4°C. At the same time, the beads to be used for the ChIP assay were prepared by mixing a fresh 50% slurry of calf thymus DNA/beads with the same volumes as in the preclear step made up to 900 µL with TE buffer and then adding 100 µL (10%) fetal bovine serum (HyClone) and incubating with rotation overnight at 4°C.

The following day, 100 µL blocked beads (non-specific DNA/non-specific protein/beads) were aliquoted into each separate antibody/protein-chromatin mixture and incubated with rotation for 1.5 h at 4°C. Then the beads were washed with 500 µl of ChIP buffer I (0.1% SDS, 1% Triton X-100, 2 mM EDTA, 50 mM HEPES, pH 7.5, 150 mM NaCl), ChIP buffer II (0.1% SDS, 1% Triton X-100, 2 mM EDTA, 50 mM HEPES, pH 7.5, 500 mM NaCl), ChIP buffer III (0.25 M lithium chloride, 0.5% Nonidet P40, 0.5% sodium deoxycholate, 1 mM EDTA, 10 mM Tris-HCl, pH 8.0), and washed twice with TE buffer in succession. After the last wash, 100 µL of elution buffer (0.5% SDS, 0.1 M sodium bicarbonate ($NaHCO_3$), 25 µg/mL Proteinase K (Roche)) was added to samples and thawed input controls and incubated for 1 h at room temperature, mixed, and then incubated at 65°C overnight. The ChIP DNA was purified using the Qiaquick PCR purification Kit (Qiagen) and eluted with 50 µL of EB buffer (Qiagen; 10 mM Tris-HCl, pH 8.5).

Analysis of ChIP DNA was done by PCR with primers specific for different promoter regions of interest along with control primers. Primer design was accomplished using Primer Premier software (Premier Biosoft International) and primers were supplied by Qiagen. The TRβ promoter region amplicon was 203 bp and contains a functional TRE [100, 131] that starts 5 bp before exon 1 and continues 11 bp into the exon. The primer sequences are published by Havis *et al.*, 2003 [100] (5'-GTAAGCTGCCTGTGTCTATA forward primer and

5'-GACAGTCAGAGGAACTG reverse primer) for ChIP assays (see Figure 3.7 for diagram). The TH/bZIP promoter region tested was 284 bp that is 47 bp upstream from exon 1 and contains two functional TREs [100, 131]. The primers are also from those published by Havis *et al.*, 2003 [100] (5'-TCTCCCTGTTGTGTATAATGG forward primer and 5'-CTCCCAACCCTACAGAGTTCA reverse primer) for ChIP assays (see Figure 3.7 for diagram). Primers specific for the *β-actin* gene were used as a negative control region for genomic DNA not associated with a promoter. The primers are published by Veldhoen *et al.*, 2002 (5'-TCACCACCACAGCCGAAAG forward primer and 5'-GGGCCAGACTCATCATACTCCT reverse primer) but were originally designed for amplification of *β-actin* mRNA of a 502 bp product in the open reading frame [98]. As the primers span exon 4 to 6 (according to GenBank sequence accession number M24770), they produce a genomic product of approximately 700 bp (determined empirically by agarose gel; data not shown).

PCR was done on a MX4000 thermocycler (Stratagene), but real-time quantitation was not possible due to primer dimer amplification with some of the primers that cannot be distinguished from products of interest using SYBRgreen detection. The PCR conditions for the primer sets were optimized to ensure the products were amplified in the linear range. Conditions for the TRβ promoter were: 9 min at 95°C and 40 cycles of 30 s at 95°C, 30 s at 60°C, and 30 s at 72°C. For the primer sets for TH/bZIP, the PCR conditions were: 9 min at 95°C and 37 cycles of 30 s at 95°C, 30 s at 60°C, and 30 s at 72°C. For the β-actin control, conditions were: 9 min at 95°C, and 34 cycles of 30 s at 95°C, 30 s at 62°C, and 30 s at 72°C. The PCR was done with 5 pmol primer (except TH/bZIP which was 2.5 pmol) in a 25 µl reaction with 10x reaction buffer (Invitrogen), 1.5 units of Platinum *Taq* DNA polymerase (Invitrogen), 10 nmol of dNTPs (GIBCO Life Technologies), and variable amounts of $MgCl_2$ (1.5 mM for TH/bZIP and β-Actin control, and 2 mM for TRβ).

The amplified products were separated on 2% agarose gels and visualized by ethidium bromide staining. To ensure comparability between gels, additional

lanes containing the same quantity of a standard PCR product was run on each gel. The overall gel staining intensities were adjusted using these lanes. For a given primer and sample set, all samples were run together in the same PCR run, and, whenever possible, also run on the same agarose gel.

Densitometric analyses were performed using Northern Eclipse v5.0 (Empix Imaging Inc.). Densitometric values were local background and negative antibody binding subtracted, and expressed as a fraction of the signal obtained from the input control for each sample set. Six independent sets of animals were tested and averaged for the *TRβ* promoter and *β-actin* control, while five sets were averaged for the *TH/bZIP* promoter data. Pairwise comparisons using one way ANOVA with a Tukey posthoc test (SPSS Version 11.0) were done when the data were parametric (TRβ protein on the *TRβ* promoter and RNA Pol II protein on the *TH/bZIP* promoter). When the data were nonparametric, the Mann-Whitney U test was used.

3.3 RESULTS

3.3.1 Characterization of ING and TR Antibodies

As no commercially available antibodies specific to *X. laevis* are available for ING and TR, we chose to generate our own through Immuno-Precise Antibodies Ltd.. We provided Immuno-Precise Antibodies with purified *X. laevis* ING2-His and TRβ-His (Figure 3.1A), and then I characterized the antibodies using ING1-His, ING2-His, TRα-His and TRβ-His purified proteins (Figure 3.1-3).

ING and TR antibodies were initially screened by WB (Figure 3.1B and C). Purified ING2-His running at 33 kDa with two additional bands at 17 and 20 kDa that may be proteolytic degradation products were recognized by anti-ING mouse monoclonal antibodies 9H3, 7H4, and 6B4. Purified TRβ-His running at 37 kDa was recognized by anti-TR mouse monoclonal antibodies 9B2, 9D2, and 1G12.

The ING and TR antibodies were then screened by IP (Figure 3.2). Panel A shows that mouse monoclonal antibodies 9H3, 7H4, and 6B4 are able to immunoprecipitate purified ING2-His seen by WB with an anti-His antibody. Panel B shows that mouse monoclonal antibodies 9B2, 9D2, and 1G12 are able to immunoprecipitate purified TRβ-His, again visualized with an anti-His WB.

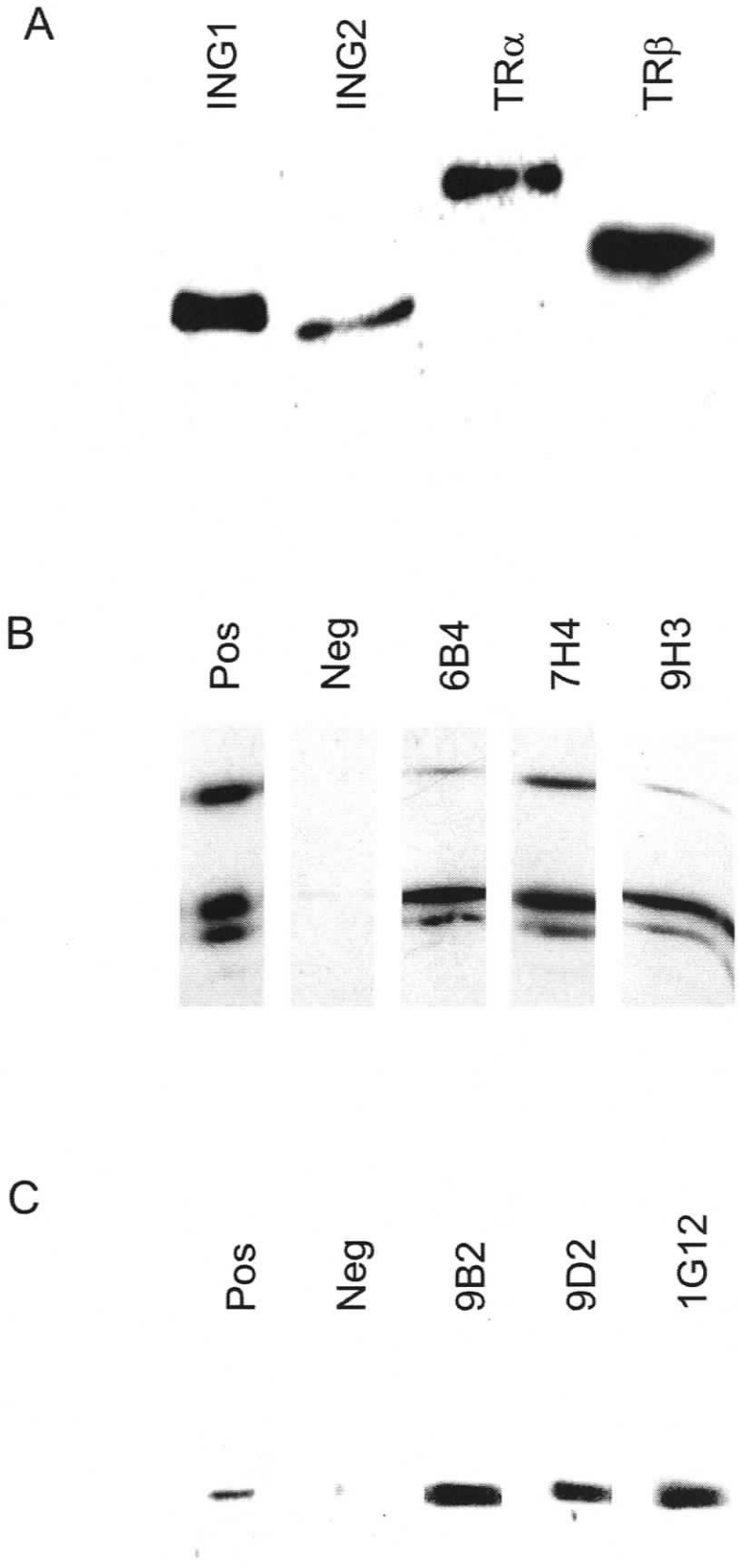
A
ING1
ING2
TRα
TRβ
B
Pos
Neg
6B4
7H4
9H3
C
Pos
Neg
9B2
9D2
1G12

Figure 3.1. Purification of His-tagged Proteins and Immunoblot Screen of ING and TR Antibodies.

(A) Samples of bacterially-expressed, Talon column-purified His-tagged proteins were separated by SDS-PAGE and immunoblotted with a commercial anti-His antibody (H-15, Santa Cruz Biotechnologies Inc.). One µg of each protein was loaded on the gel, except for 0.5 µg TRβ. The sizes of the proteins are as follows: TRα-His ~45 kDa, TRβ-His ~37 kDa, ING1-His ~33 kDa, and ING2-His ~32 kDa. (B) WB screen for anti-ING mouse monoclonal antibodies. Five µg of ING2-His was loaded into a single preparative well and separated by SDS-PAGE. The gel was transferred to nitrocellulose and probed with several primary antibodies including anti-ING mouse monoclonals 6B4, 7H4, and 9H3 along with a positive control anti-ING2 polyclonal mouse serum and a negative control anti-herpes virus (6D9) mouse monoclonal IgG on the same blot using a Mini-Protean II Multiscreen Apparatus. ING2-His runs at ~33 kDa with two additional bands at 17 and 20 kDa and is recognized by the positive control and test anti-ING antibodies shown. (C) WB screen for anti-TR mouse monoclonal antibodies. Five µg of TRβ-His was loaded into a single preparative well and separated by SDS-PAGE. The gel was transferred to nitrocellulose and probed with several primary antibodies including anti-TR mouse monoclonals 9B2, 9D2, and 1G12, along with a positive control C191 anti-TR rabbit polyclonal and a negative control anti-trout mouse monoclonal IgG on the same blot using a Mini-Protean II Multiscreen Apparatus. TRβ-His runs at ~37 kDa and is recognized by the positive control and the test anti-TR antibodies shown.

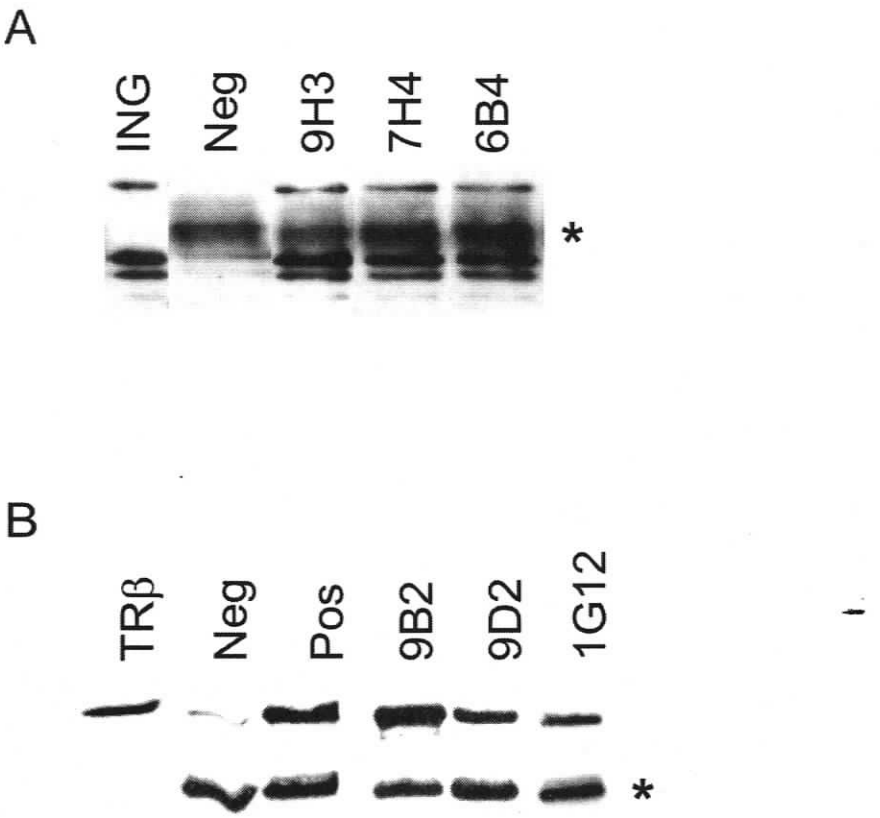

Figure 3.2. Screen Immunoprecipitations with ING and TR antibodies. (A) IP carried out with bacterially-expressed, Talon column-purified His-tagged *Xenopus laevis* ING2 protein and the mouse monoclonal antibodies 9H3, 7H4, and 6B4 that were directed against the ING2-His. A negative control (Neg) IP was done with supernatant from the fusion strain used to create the antibodies. (B) IP carried out with bacterially-expressed, Talon column-purified His-tagged *Xenopus laevis* TRβ protein and the mouse monoclonal antibodies 9B2, 9D2, and 1G12 that were directed against the TRβ-His. A negative control (Neg) IP was done with supernatant from trout IgG. A positive control (Pos) IP was performed with the ascites of a mouse immunized with *Xenopus laevis* TRβ. For both Panel A and B, a WB with an anti-His tag antibody followed the IP. Protein controls of the purified ING2-His (33 kDa with two additional bands at 17 and 20 kDa) and TRβ-His (37kDa) were included. A non-specific band is indicated by the asterix.

Following initial screening, anti-ING 9H3 and anti-TR 9B2 were chosen for further characterization (Figure 3.3). Their relative affinities and cross-reactivity to other His-tagged proteins were determined along with polyclonal TR mouse serum (taken from the mouse used for the creation of the TR monoclonal antibody). The polyclonal antibody was used in subsequent IP experiments while the anti-TR and anti-ING monoclonal antibodies were used in WBs. The anti-TR polyclonal antibody has a 5-fold greater signal for TRβ in WBs, but also recognizes TRα and does not cross react with ING1 or ING2. The anti-TR monoclonal (9B2) has a strong preference for TRβ, recognizing 200-fold higher amounts compared to TRα in WBs and does not cross react with ING1 or ING2. The anti-ING mouse monoclonal (9H3) recognizes both ING1 and ING2, with a 2 to 3-fold stronger signal for ING2 in WBs, and does not cross react with TRα or TRβ. A band at 35 kDa observed for ING1 may have been a result of differing acrylamide concentrations in the same gradient gel that caused resolution of two bands instead of only the expected 33 kDa band (Figure 3.3C). These experiments show that all three antibodies do not bind non-specifically to other His-tagged proteins. Thus the TRβ antibodies are specific for both TRβ and TRα, while the ING2 antibody is specific for both ING1 and ING2 with variable affinities.

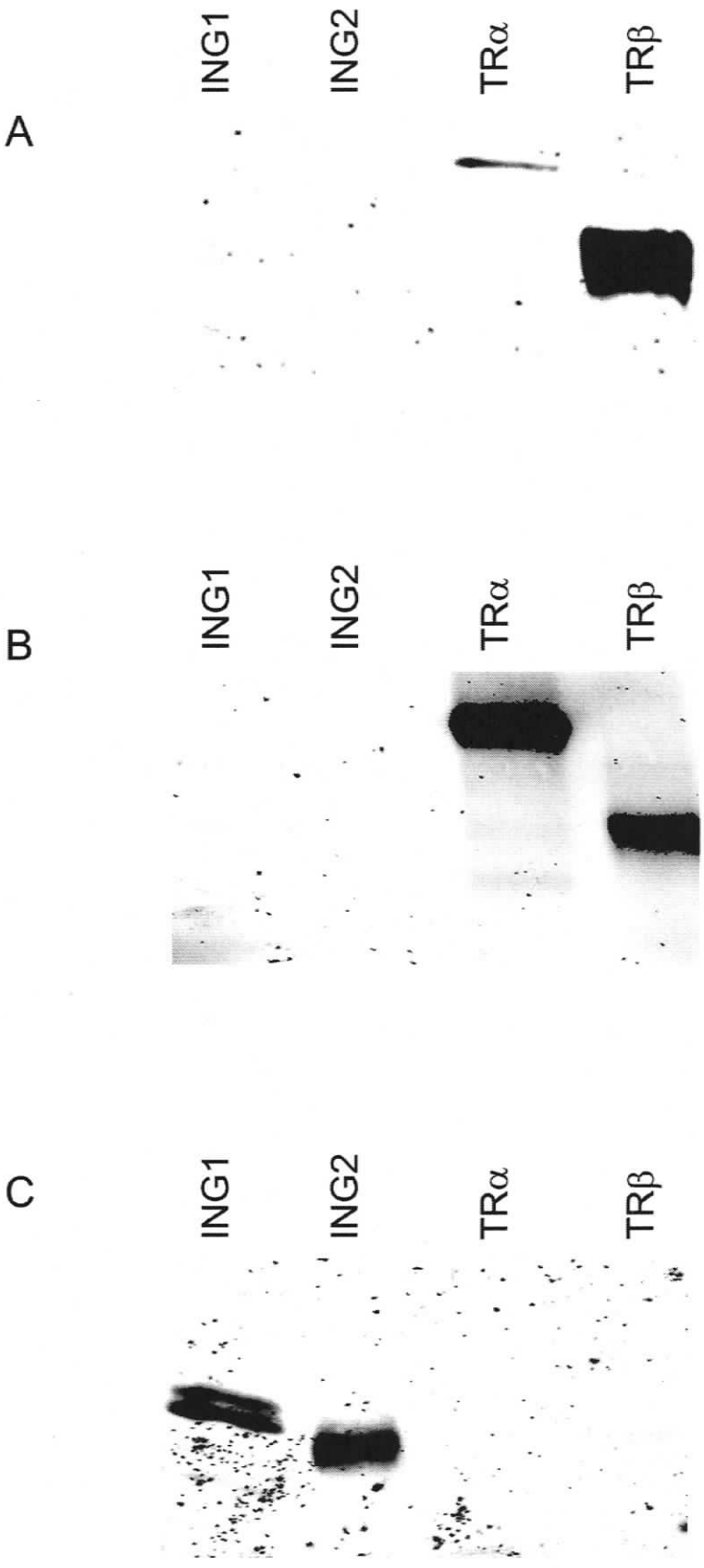
A
ING1
ING2
TRα
TRβ
B
ING1
ING2
TRα
TRβ
C
ING1
ING2
TRα
TRβ

Figure 3.3. Affinities and cross reactivity of TR and ING antibodies in immunoblots.

Antibodies were made against purified His-tagged ING2 and TRβ. To determine the specificity of these antibodies, samples of bacterially- expressed, Talon column-purified His-tagged proteins were separated by SDS-PAGE and immunoblotted with either a mouse polyclonal anti-TR antibody (Panel A), a mouse monoclonal anti-TR antibody (9B2) (Panel B), or a mouse monoclonal anti-ING antibody (9H3) (Panel C). The sizes of the proteins are as follows: TRα-His ~45 kDa, TRβ-His ~37 kDa, ING1-His doublet ~33 kDa and ~35 kDa, and ING2 ~32 kDa. In panel A, 0.5 μg protein was loaded except for 0.25 μg TRβ-His; in panel B, 1 μg protein was loaded except for 5 ng TRβ-His; in panel C, 1 μg protein was loaded except for 0.5 μg ING2-His. The TRβ antibodies recognize both TRβ and TRα with varying affinities, while the ING2 antibody recognizes both ING1 and ING2 also with varying affinity.

3.3.2 ING and Thyroid Hormone Receptor Co-immunoprecipitate

To examine whether ING and TR proteins could bind each other directly, purified ING2-His and TRβ-His proteins were immunoprecipitated with anti-TR polyclonal mouse serum followed by a WB with an anti-His antibody that recognizes both proteins. Results shown in Figure 3.4 indicate that ING2-His and TRβ-His co-immunoprecipitate. There was minimal background binding in controls including beads alone, beads with antibody, beads with TRβ-His, and beads with ING2-His. There was also no detectable non-specific binding of the anti-TR antibody to ING2-His protein, but the antibody was clearly able to pull down TRβ-His. In the reaction in which ING2-His and TRβ-His were co-incubated prior to IP with the anti-TR antibody, the anti-His antibody in the WB was able to detect TRβ-His strongly, but also ING2-His appeared to be co-immunoprecipitated. Thus, it is possible that ING2 and TRβ interact by directly binding to each other.

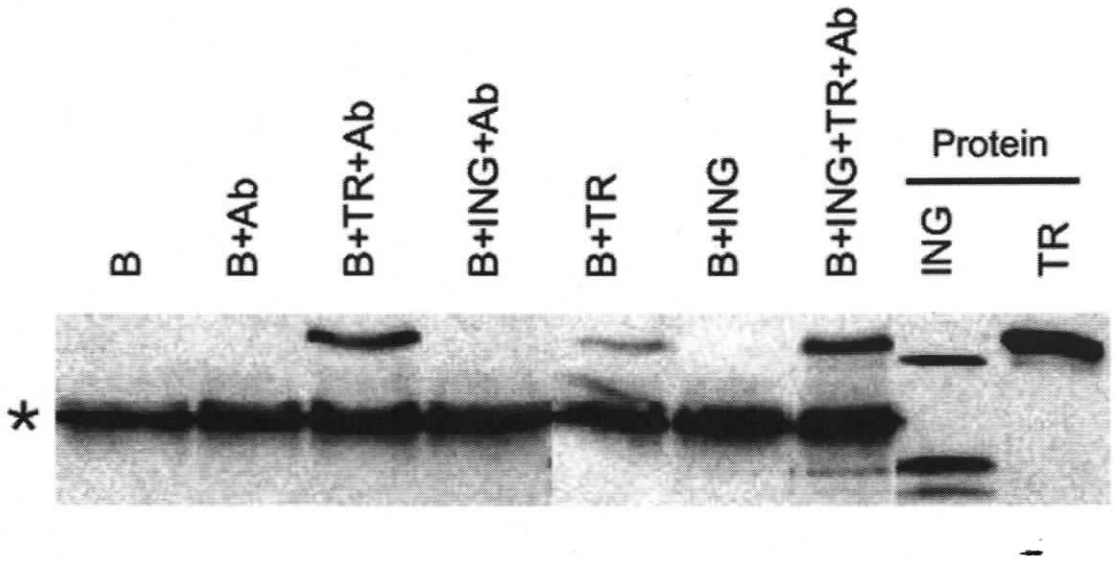

Figure 3.4. Purified ING and TR proteins co-immunoprecipitate.
Shown are IPs of bacterially-expressed, Talon column-purified His-tagged xING2 (1µg) and TRβ (1µg) proteins using a mouse polyclonal TRβ antibody. The IPs were run on SDS-PAGE gels and immunoblotted with an anti-His tag antibody to visualize both proteins. The xING2-His protein (ING; 1µg) is ~32 kDa and has two faster running bands at ~17 and 20 kDa. The TRβ-His protein (1µg) runs at ~37 kDa (TR). The components are indicated as follows: beads (B), TR-specific antibody (Ab). The asterisk indicates a non-specific band due to the beads.

To further investigate the interaction of ING and TR in a more biologically relevant context, IPs were carried out on homogenates of total protein from tadpole tails. Tadpoles undergoing metamorphic climax between NF stages 60-62 were tested, where levels of ING and TR are known to be high. The mouse monoclonal antibodies that were characterized above, made against *X. laevis* TRβ (9B2) and ING2 (9H3), were used in WBs following IPs with the same anti-TR polyclonal mouse serum as was used for the IPs with purified proteins. In Figure 3.5, a reproducible putative ING band is observed at ~33 kDa in the IP that co-migrates with a protein band recognized by the anti-ING monoclonal

antibody in a WB of total tail homogenate. This band is not seen in the negative control lanes which include beads incubated with protein alone or beads incubated with antibody alone. Similar results were obtained in six independent experiments. One large IP reaction was done with the anti-TR polyclonal antibody that was divided into three equal parts in order to run on three different gels all immunoblotted with the anti-ING monoclonal antibody. One of the gels was unblocked, one was blocked with 5 µg of ING1-His, and one was blocked with 5 µg of ING2-His. The 33 kDa band is greatly diminished in the blocked WBs. In these same IP complexes immunoblotted with an anti-TR monoclonal antibody, a putative TRα band was observed that co-migrated with the TRα-His protein at ~46 kDa (visible in the exposure of the WB shown in Figure 3.8B). In addition, a putative TRβ band was observed that co-migrated with TRβ-His protein at ~36 kDa (visible in a darker exposure of the same WB as shown in Figure 3.8B; data not shown). Similar results were observed in three independent experiments. Thus, using the same anti-TR antibody in IPs followed by either anti-ING or anti-TR antibodies in WBs, ING (Figure 3.8A) and TRα and TRβ (Figure 3.8B) were shown to co-immunoprecipitate in tadpole tails.

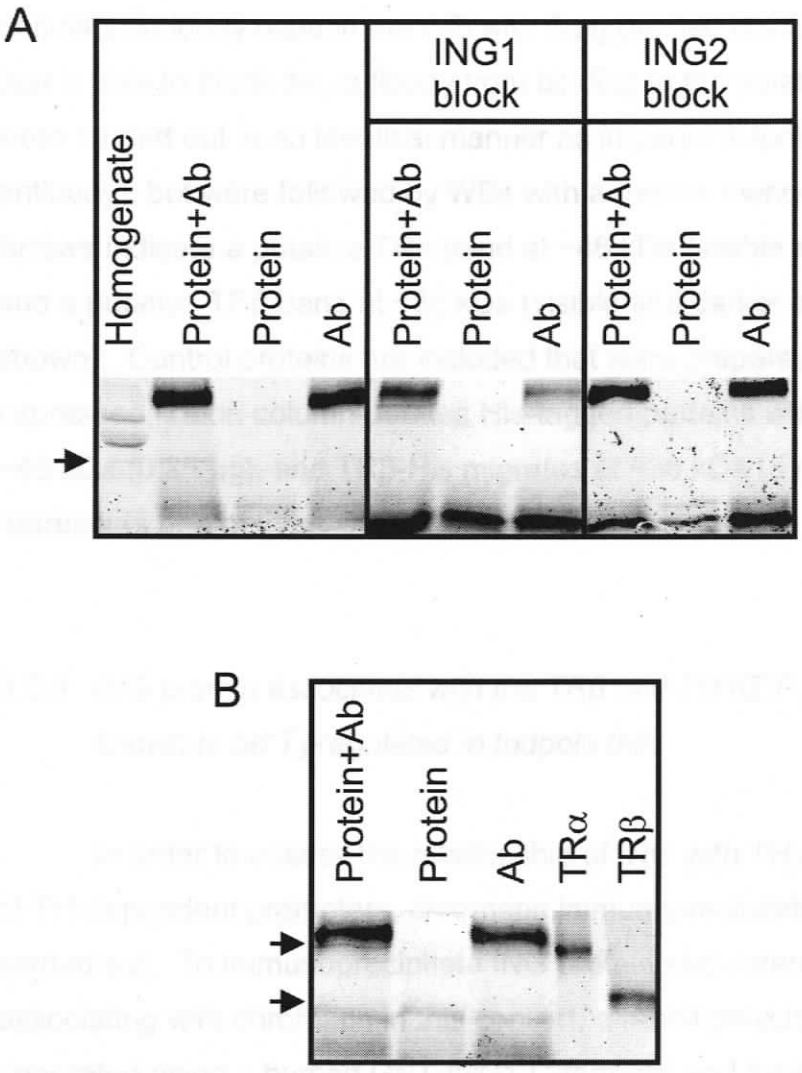

Figure 3.5. ING and TR co-immunoprecipitate in whole tail homogenates. (A) IPs were carried out with mouse polyclonal anti-TR antibody, followed by WBs with mouse monoclonal anti-ING antibody on *X. laevis* total tail homogenates from metamorphic NF stage 60-62 tadpoles. A highly reproducible putative ING band is seen at ~33 kDa in the IP (indicated by an arrow) that co-migrates with a protein band recognized by the anti-ING monoclonal antibody in the WB of total tail homogenate (30 µg). The gel shown represents one of six experiments with similar results. This band is not observed in the negative controls (beads incubated with protein alone (protein) or beads incubated with antibody alone (Ab)). This band is also not visible in samples that undergo an identical IP and WB procedure with the addition of a pre-incubation step of the

anti-ING antibody used in the WB with 5 µg purified His-tagged ING1 or ING2 that is able to block the antibody from binding to the putative ING band. (B) IPs were carried out in an identical manner as in panel A (polyclonal mouse anti-TR antibody), but were followed by WBs with a mouse monoclonal anti-TR antibody. Arrows indicate a putative TRα band at ~46 kDa (visible at the exposure shown) and a putative TRβ band at ~36 kDa (visible at a darker exposure; data not shown). Control proteins are included that were prepared from bacterially-expressed, Talon column-purified His-tagged proteins where TRα-His migrates at ~46 kDa (0.25 µg), and TRβ-His migrates at ~36 kDa (5 ng). The gel shown represents one of three experiments with similar results.

3.3.3 ING protein associates with the TRβ and TH/bZIP promoters that are known to be T_3-regulated in tadpole tails

In order to assess the relationship of ING with TH and TRs in the context of TH-dependent promoters, chromatin immunoprecipitations (ChIPs) were carried out. To immunoprecipitate ING protein and determine if it was capable of associating with chromatin in this context, a rabbit polyclonal antibody that was generated using a human GST-ING1 C-terminal end fusion protein was utilized (a gift from K. Riabowol). It was first important to test the specificity of this antibody in *X. laevis*. To that end, purified His-tagged proteins from *X. laevis* (Figure 3.1A) were tested in a WB probed with the anti-ING antibody (Figure 3.6A). The antibody has ~10-fold preference for ING1 over ING2, but recognized both proteins. His-tagged TRα and TRβ were not recognized under the conditions used. This antibody was also tested in IPs (Figure 3.6 B-D). With ING1-His, a band that co-migrated with ING1-His protein at ~33 kDa was observed in the anti-ING IP in an anti-His WB and an anti-ING WB that was not seen in the negative control. The second band observed at ~35 kDa in the anti-His WB is believed to be an artifact of different acrylamide concentrations in the gel. With ING2-His, a band was observed in the anti-ING IP that was not seen in

the negative control and co-migrates with ING2-His protein at ~32 kDa. Based on these results, I continued with ChIP assays using this antibody.

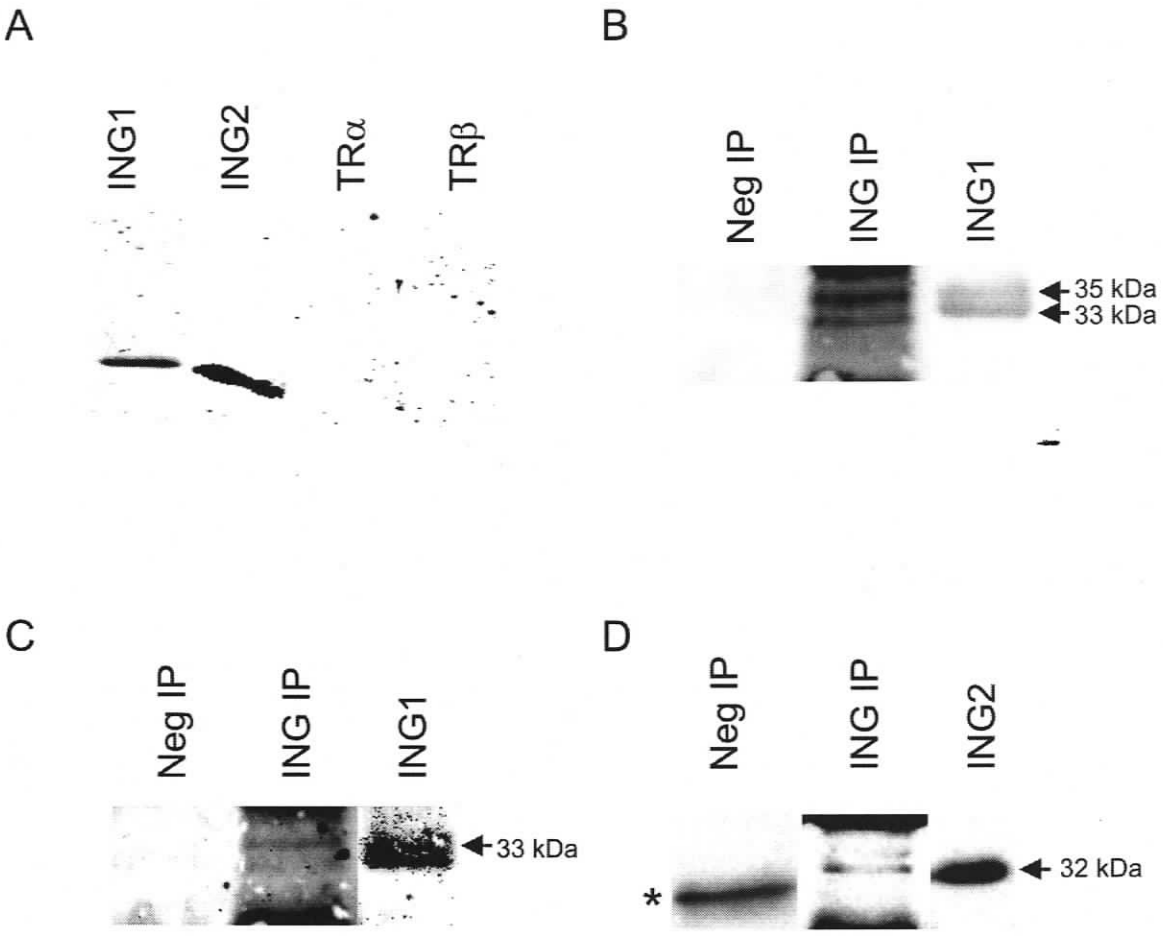

Figure 3.6. Characterization of the ING Polyclonal antibody used in chromatin immunoprecipitation assays.

(A) Samples of bacterially- expressed, Talon column- purified His-tagged proteins were separated by SDS-PAGE and immunoblotted with a rabbit polyclonal antibody specific for the common region of ING, generated using a human GST-ING1 C-terminal end fusion protein. One µg of each protein sample was loaded on the gel, except 0.1 µg ING1-His. The sizes of the proteins are as follows: TRα-His ~45 kDa, TRβ-His ~37 kDa, ING1-His ~33 kDa, and ING2-His ~32 kDa. In a WB, the anti-ING antibody has ~10-fold greater preference for ING1 compared to ING2, but does not recognize His-tagged TRα and TRβ.

Purified ING1-His was immunoprecipitated with the anti-ING rabbit polyclonal and immunoblotted with both an anti-His rabbit polyclonal (Panel B) and an anti-ING mouse monoclonal antibody (Panel C), visualized with an Odyssey infrared imaging system. Also shown is a protein control that shows ING1-His migrates as a doublet of ~33 and 35 kDa in the anti-His WB, and as ~33 kDa band in the anti-ING WB. (D) Purified ING2-His was immunoprecipitated with the anti-ING rabbit polyclonal and immunoblotted with an anti-His rabbit polyclonal, visualized by ECL. A protein control of ING2-His migrates at ~32 kDa. A non-specific band that may be associated with the beads is indicated by an asterix. For panel B-D, a negative control using anti-herpes virus mouse monoclonal antibody in the IP is also shown.

To establish in the ChIP assay that the tadpoles were responding to T_3 in an appropriate way, I examined the association of TRs with known TRE-containing promoter regions of two TH-responsive genes previously examined by others using ChIP assays, *TRβ* and *TH/bZIP* [100, 131]. Other laboratories have conducted ChIPs with antibodies that recognize both TRα and TRβ together or with antibodies specific to TRβ [100, 131]. I chose to study TRα and TRβ independently using antibodies that were previously characterized as specific for each isoform (gifts from D. Brown, Carnegie Institute [70]). To investigate the activation state of the chromatin, commercial antibodies were used for ChIPs with anti-acetylated histone H4, where a more open conformation of chromatin should be associated with a more highly acetylated histone H4. Also, the ability of RNA Pol II to bind to the promoters was studied with a ChIP using an anti-RNA Pol II antibody that recognizes the N-terminus of the RNA Polymerase II largest subunit (RPB1) of mouse origin in a phosphorylation-independent manner. This antibody does not differentiate between active and inactive RNA Pol II, but allows one to assess binding in general. Finally, a negative control antibody specific to herpes virus was used in a ChIP assay on the same chromatin-protein complexes as a test of ChIPs to ensure background binding was minimal.

Following the ChIP assays, analysis of purified DNA was done for promoter regions for known TH-responsive genes *TRβ* and *TH/bZIP*. Important features in the region of DNA tested in the ChIP assay are shown in Figure 3.7. The *TRβ* promoter region of 203 bp contains a functional TRE that starts 5 bp before exon 1 and continues 11 bp into the exon [100, 131]. This region also contains a putative TATA box located at position -88 to -94. The *TH/bZIP* promoter region of 284 bp is 47 bp upstream from exon 1 and contains two functional TREs [71, 100, 131]. A TATA box is located at position -31 to -25, but is outside the region tested in the ChIP assay.

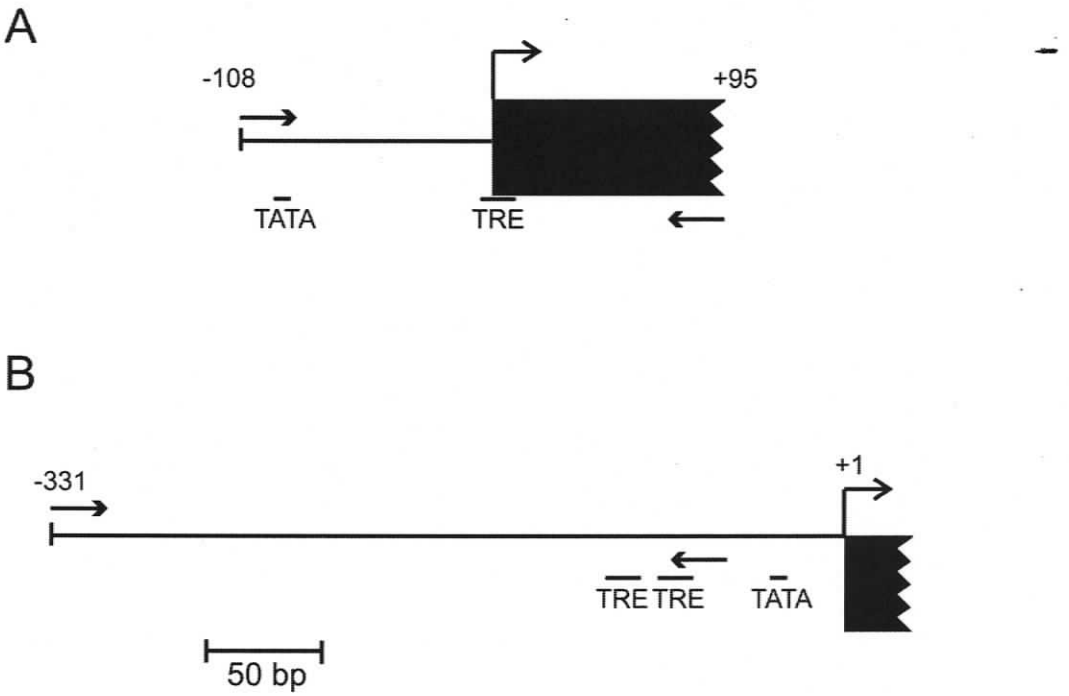

Figure 3.7. Schematic representation of the regions tested for *TRβ* and *TH/bZIP* ChIP assays.

(A) Diagram of the DNA regions of interest for the 203 bp PCR product of the primers used for ChIP for *TRβ* which includes part of the *TRβ* promoter and part of exon 1. A functional thyroid hormone response element (TRE) located at position -5 to +11, and a putative TATA box (TATA) located at position -88 to -94 are shown within the ChIP primer region. There is an additional putative TATA

box 11 bp upstream of the forward primer not shown. (B) Diagram of the DNA regions of interest for the 284 bp PCR product of the primers used for ChIP for *TH/bZIP* in the promoter as well as the contiguous sequence up to the transcription start site. Two functional TREs at positions -100 to -84 and -78 to -62 within the ChIP primer region are shown. A TATA box at position -31 to -25 is shown, but is outside the region tested in the ChIP assay. For both diagrams, the transcript start sites are indicated with a bent arrow, primers are indicated by straight arrows, and positions are relative to the transcript start site.

Figure 3.8 shows the averages of six and five independent ChIP assays on the *TRβ* and *TH/bZIP* promoters, respectively. Samples were normalized by first correcting for local background on the gel, then by subtracting the amount of background binding to the negative control antibody, and finally by dividing each sample by an input sample. The amount of chromatin for the input samples was a fraction of the total input for each ChIP assay based on an OD_{260} measurement done after the preclearing step of the ChIP protocol. The amount chosen allows for amplification in the PCR detection step to be in the linear range. The input sample was used for each set of the individual pools of animals tested allowing standardization between sample sets. A standardized amount of chromatin was also used for each ChIP assay and was based on the same OD_{260} measurement as was used for the input sample. Again, the amount chosen allowed for PCR detection to be in the linear range with the conditions employed.

TRβ and *TH/bZIP* genes are known to be TH-responsive, and ChIP assays showed that TRα and TRβ protein both increased significantly on both promoters in premetamorphic tadpoles treated with 10 nM T_3 for 48 hours. On the *TRβ* promoter, TRα and TRβ protein increased ~2-fold. On the *TH/bZIP* promoter, TRα protein increased by 4-fold, while TRβ protein increased over 2.5-fold. Although acetylated histone H4 levels did not change significantly with T_3 treatment compared to controls, there is clearly a presence of acetylated histone H4 (between 27 and 55% relative to input). Interestingly, RNA Pol II was

observed to bind to the promoters in the controls, and was significantly decreased on promoters in the T_3-treated tadpoles. On the *TRβ* promoter, levels decreased by nearly 5-fold and on the *TH/bZIP* promoter, levels decreased by 10-fold.

Primers specific for a non-promoter region of the *β-actin* gene were used to ensure that there was minimal non-specific binding to chromatin by proteins immunoprecipitated in the ChIP assays. Figure 3.8C shows that the binding was below detection limits on this region of DNA when PCR products were visualized on agarose gels for any of the ChIP assays. Only a positive signal with a product of 700 bp for a genomic *β-actin* product spanning from exon 4 to exon 6 was obtained for the precleared sonicate input sample which contains fragments representing all genomic DNA. Similar results were obtained for all six independent ChIP assays used in the study.

For the first time, native ING has been tested in a ChIP assay for its ability to bind to promoters. The binding of ING to these promoters does not appear to be T_3-responsive, but I found that ING protein associates with both the *TRβ* and *TH/bZIP* promoters at levels of ~ 20%, and ~30% relative to input, respectively, but not to the *β-actin* gene. This data suggests that ING is present in complexes that regulate gene expression in the context of TH and TRs.

A

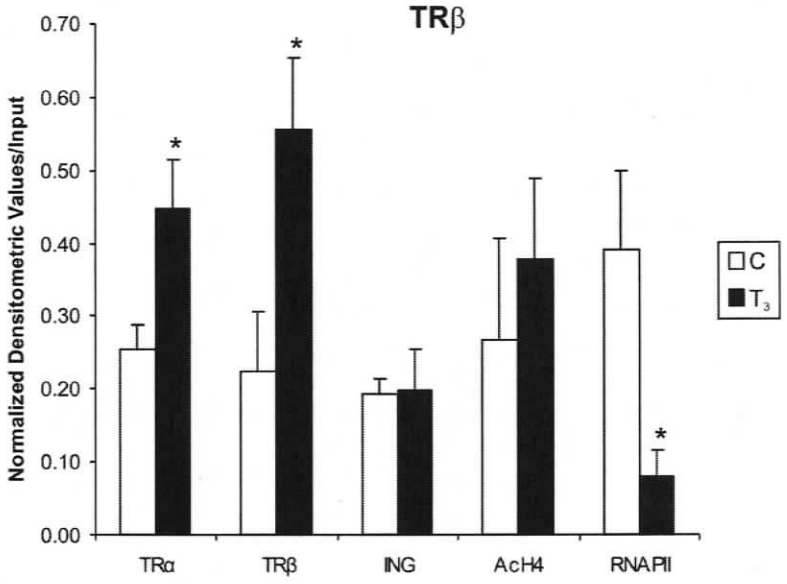
TRβ
Normalized Densitometric Values/Input
0.70
0.60
0.50
0.40
0.30
0.20
0.10
0.00
TRα
TRβ
ING
AcH4
RNAPII
C
T3

B

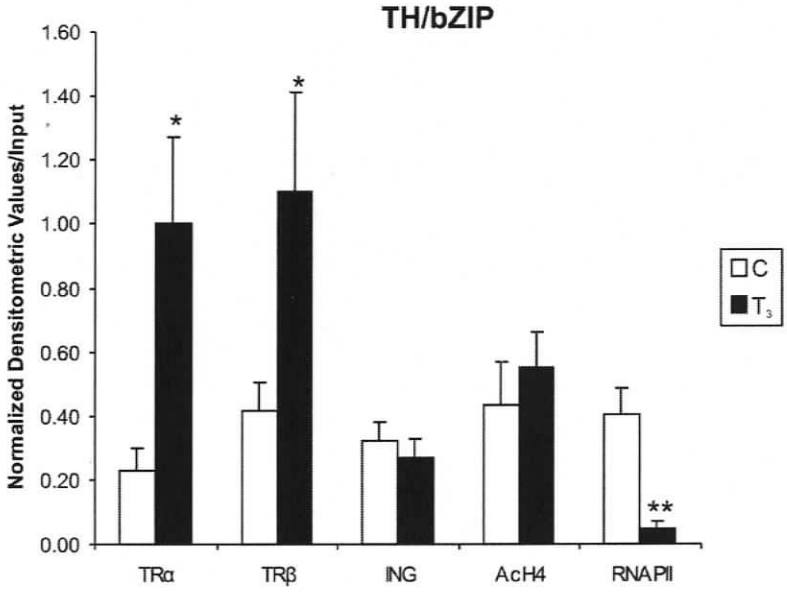
TH/bZIP
Normalized Densitometric Values/Input
1.60
1.40
1.20
1.00
0.80
0.60
0.40
0.20
0.00
TRα
TRβ
ING
AcH4
RNAPII
C
T3

C

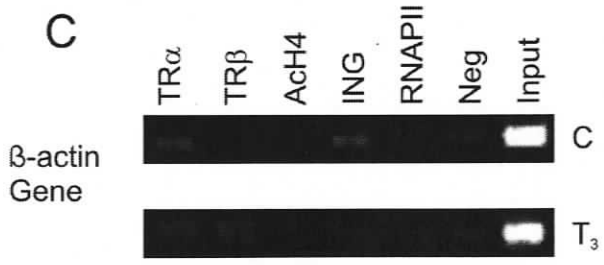
TRα
TRβ
AcH4
ING
RNAPII
Neg
Input
ß-actin Gene
C
T3

Figure 3.8. ING protein associates with the TRβ and TH/bZIP promoters that are known to be T_3-regulated in tadpole tails.

(A and B) Shown are densitometry graphs for each antibody tested by ChIP assay: TRα, TRβ, ING, acetylated histone H4 (AcH4), and RNA Polymerase II (RNAPII). Values were obtained from 2% agarose gels of PCR products for either the *TRβ* or the *TH/bZIP* promoter. Values were normalized by subtracting the local background of the gel, subtracting the background binding to the negative control antibody, and then dividing by the signal obtained from an input sample. The amount of chromatin used for the input sample was based on a fraction of the input for each set of ChIPs for an individual pool of animals tested. Where multiple PCR runs of the same pool were done, averages were taken prior to averaging across the sets. Chromatin-protein complexes were obtained from pools of 7-12 tails from tadpoles NF stage 52-54 that were either time-matched solvent controls (C) or treated with 10 nM T_3 for 48 hours (T_3). Six independent sets of animals were tested and averaged for the *TRβ* promoter while 5 sets were used for the *TH/bZIP* promoter. The error bars represent the standard error of the mean, and statistical significance for TH treatment relative to control is indicated by * for $p \leq 0.05$ and ** for $p \leq 0.01$. (C) Shown is a representative of six independent sets of results for PCR products using DNA purified from the same ChIP assays as in Panel A and B but using primers specific to a non-promoter region of the *β-actin* gene.

3.4 DISCUSSION

ING transcripts and protein increase in response to T_3 treatment in tadpole tails that are undergoing TH-dependent apoptosis [16, 17]. In this chapter, I establish that purified ING and TR proteins co-immunoprecipitate in experiments using novel antibodies that were made against *Xenopus laevis* ING2-His and TRβ-His, characterized herein. ING and TR also co-immunoprecipitate in total tail homogenates from tadpoles undergoing metamorphic climax. Furthermore,

through ChIP assays, I show that ING and TR are associated with the same promoter regions in a biologically relevant context of TH-responsive genes during T_3-induced apoptosis of the tadpole tail.

Screening by WB and IP showed that multiple mouse monoclonal antibodies generated by Immuno-Precise Antibodies recognize ING2-His or TRβ-His. The antibody with strongest binding in both types of experiments for each type of protein was chosen for further study. The 9B2 anti-TRβ monoclonal antibody is able to recognize both TR isoforms, but has a 200-fold greater affinity for TRβ. The 9H3 anti-ING2 antibody has a 2 to 3-fold preference for ING2 compared to ING1. Another antibody that proved useful in my studies was an anti-TR polyclonal mouse serum taken from the same mouse that was used to generate the anti-TRβ monoclonal antibody. This anti-TR polyclonal antibody has a 5-fold greater preference for TRβ, but also recognizes TRα. With these new tools available, it was possible to conduct IPs to determine if ING and TR interact.

ING2-His and TRβ-His were co-incubated prior to IP with an anti-TR antibody, and both proteins were detected with an anti-His antibody in a subsequent WB. This suggests the possibility that ING2 and TRβ proteins interact by directly binding to each other. In this artificial context particularly without TH present, it is risky to make any conclusions about the biological significance of the binding observed. Therefore, I investigated whether ING and TR could be co-immunoprecipitated in tadpole tails. We previously showed that ING protein levels are high in tadpole tails during metamorphic climax (NF stage 60-62) [16] coinciding with elevated TR levels [70] so tails from these stages were studied.

A putative ING band is observed at 33 kDa in a WB with an anti-ING antibody following an IP done with an anti-TR antibody. This band was blockable with both ING1 and ING2 proteins pre-incubated with the anti-ING WB antibody suggesting the band is ING-specific. The approximate size of both ING1 and ING2 are too similar (33 and 32 kDa, respectively) to allow differentiation between them with this method. Mass spectrometric identification of which ING

and TR isoforms as well as identification of possible other co-regulators involved would aid in understanding more specifically what mechanisms are being utilized by the cells; nevertheless, these results implicate ING and TR in regulatory complexes together.

Interestingly, Toyama *et al.*, 2003 showed that *in vitro* translated $p33^{ING1b}$ can weakly associate with ERα. Furthermore, in African green monkey kidney cells transfected with $p33^{ING1b}$, as expression levels increased, transcription of an ER-responsive reporter gene was enhanced [55]. These studies did not show protein interaction in a biological context and did not identify any specific target genes; however, the results suggest that ING may be involved in modulating hormone responsive genes on a wider scale beyond TH-induced tadpole tail regression.

Given that *ING* transcript expression is affected by TH, combined with the known role of ING in apoptosis, that ING protein expression correlates strongly with T_3-dependent apoptosis of the tadpole tail [16], and data presented herein that show ING and TR are found in the same immunocomplex, the stage is set for ING to play a role in chromatin-binding complexes in the context of TH-regulated genes. ChIP assays have been effectively utilized to investigate TH-regulated genes including *TRβ* and *TH/bZIP* [100, 131]. Therefore, I carried out ChIP assays using these same promoter regions and I show that ING associates with both of these promoters in regions that contain known TREs. ING protein associates with each promoter at ~20% and ~30% compared to total input, regardless of the presence of 10 nM T_3 for 48 hours. Also present on these promoter regions, were TRα and TRβ proteins. Both TRs increase significantly on both promoters during T_3 treatment, almost doubling for each TR on the *TRβ* promoter, and increasing 4-fold for TRα, and over 2.5-fold for TRβ on the *TH/bZIP* promoter. In the active complexes, both moderate levels of acetylated histone H4 (~40% of input), and a decrease of over 30% in RNA Pol II comparing treated to control samples was observed. It is well established that acetylation of histone H4 is associated with active chromatin regions. A decrease in RNA Pol II levels may be a result of less enzyme captured while it is actively transcribing or

that RNA Pol II is being recruited to a different region of DNA that contains the functional core promoter.

Using the ChIP method, it is not possible to determine whether ING is binding the chromatin directly or indirectly. Nevertheless, the results are consistent with the hypothesis that ING may regulate T_3-mediated gene expression and chromatin conformation, possibly though direct interaction of ING and chromatin or by participating in regulatory complexes.

The antibody used in our study is specific to the common region of ING, and recognizes both ING1 and ING2. It may also recognize other ING family members. It will be interesting to investigate these complexes further and determine which specific isoforms of ING may be present and whether they are recruiting other proteins to the complexes such as specific HATs, HDACs, or p53 that are known binding partners of both ING and TR. A complex picture is emerging where ING and TR could participate in the same complexes to regulate TR-regulated genes during apoptosis. The timing and type of response may be fine tuned by many other proteins such as p53, PCNA, HATS, and HDACs allowing exquisite control. My results open the door for further research into the possibility that ING variants may differentially associate with active chromatin in the context of normal development and modulate tissue-specific genetic programs, including the TH-dependent genetic programs leading to apoptosis or proliferation.

CHAPTER 4: THYROID HORMONE RECEPTORS AND ING PROTEINS ASSOCIATE WITH *ING1* AND *ING2* PROMOTERS

The work presented in this chapter is being prepared for publication:
Wagner, M.J., and Helbing, C.C. (2006). The *ING1* and *ING2* Tumor Suppressor Genes are Regulated by both Thyroid Hormone Receptor Alpha and Beta, and Auto-regulated by ING in *Xenopus laevis*, in preparation.

4.1 INTRODUCTION

Previous data suggested that there may be two or more genes for both *ING1* and *ING2*. The genome of *Xenopus laevis* was duplicated 30 million years ago, causing this organism to be psuedotetraploid [73], so it is plausible that duplicate genes could exist. I will show with Southern blot analysis that more than one *ING1* and *ING2* gene are present in the *X. laevis* genome.

The transcript sequence variants generated from *ING1* and *ING2* genes are differentially regulated by TH during natural and precocious metamorphosis [17]. From these experiments, it is unclear whether TRs directly bind to promoters of ING, or whether the response is indirect. The presence of putative TREs in human, mouse, and *Xenopus tropicalis* support the hypothesis that ING is regulated by TRs [17]; however, functional TREs can have considerable variability in sequence, spacing and number of elements compared to the consensus sequence [72, 86, 87, 89]. Therefore, ChIP assays using anti-TR antibodies were utilized to further investigate the regulation of ING genes in the context of T_3-induced apoptosis of the tadpole tail. First, it was necessary to isolate promoter sequence for *ING1* and *ING2* in *X. laevis* and analyze the sequence for putative TREs. ChIP analysis of promising regions in variants

xING1b, xING1c, xING2a and *xING2b* were compared. I will show that both TRα and TRβ bind *ING1* and *ING2* promoters with different relative occupancies. Furthermore, TRα and TRβ binding is differentially T_3-responsive on different promoters.

I was the first to show that ING protein could associate with promoters of T_3-regulated genes, discussed in Chapter 3. To further investigate the hypothesis that ING can associate with T_3-regulated promoters, the *ING1* and *ING2* genes themselves were tested. In this chapter, I will show that ING can associate differentially with regions in both *ING1* and *ING2* promoters. In the case of the *xING2b* variant, the association is shown to be affected by T_3 treatment. Experiments by Kataoka and colleagues show that ING competitively binds to an AT-rich sequence that is also an HNF1 binding site in the promoter for α-fetoprotein [40]. Sequences obtained were analyzed for this putative ING binding site.

The evidence herein that TR associates with ING promoters, and that ING associates with these same promoters, along with the previous evidence that ING and TR are found in the same immunoprecipitates raises the possibility that ING and TR act as co-regulators in the same complexes to regulate gene expression. With the presence of putative TREs in other species as diverse as amphibians and mammals, it may be that regulation of ING genes by TRs is a conserved mechanism.

4.2 MATERIALS AND METHODS

4.2.1 Genomic DNA Preparation

Nucleated blood cells were collected from an adult male *Xenopus laevis* with a syringe and 16 gauge needle and placed in a 1.5 mL microfuge tube containing 1 mL cold amphibian PBS (128 mM NaCl, 10 mM Na_2HPO_4, 10 mM NaH_2HPO_4) with 100 units/mL heparin (Sigma-Aldrich). Cells were washed twice

with 1 mL amphibian PBS/heparin with centrifuging at 16,000xg for 2 min at 4°C in between. The pellet was resuspended quickly on ice in 800 µL 1x cold resuspension buffer A (100 mM NaCl, 10 mM Tris-HCl, pH 8.0, 1 mM EDTA, pH 8.0). This was transferred to a 14 mL polypropylene tube and 3.2 mL digestion buffer B was added (100 mM NaCl, 10 mM Tris-HCl pH 8.0, 31 mM EDTA pH 8.0, 0.625% SDS with 100 µg proteinase K per mL (Roche) added immediately before use). This was gently shaken in a water bath (~100 revolutions/min) at 50°C for 18 h. Next, three phenol/chloroform extractions were done (25:24:1 Tris-saturated phenol: chloroform: isoamyl alcohol) using an equal volume of the solution (4 mL), and saving the aqueous layer each time. Then 1/10 volume (400 µL) 3 M sodium acetate pH 5.2 was mixed with the solution, and 3 volumes (12 mL) of 95% ethanol were added, causing a precipitate to form. This was stored at -20°C. At a later time, the DNA precipitate was spooled and transferred to a 14 mL polypropylene tube containing 5 mL 95% cold ethanol. This was centrifuged at 5,000xg for 10 min at 4°C. The pellet was washed with 70% ethanol and allowed to air dry. This pellet was gently resuspended in 4 mL TE buffer (10 mM Tris-HCl pH 8.0, 1 mM EDTA, pH 8.0) by shaking 3 h in a water bath (~100 revolutions/min) at room temperature. Next, 1 µg/mL of RNAse A (Qiagen) was added and the mixture was incubated for 1 h at 43°C in a shaking water bath. Then 0.1 mg/mL Proteinase K (Invitrogen) was added and the mixture was incubated overnight at 50°C in a shaking water bath (~100 revolutions/min). Phenol/chloroform extractions were repeated 5 times, and then 3 volumes (12 mL) of 95% ethanol was added and the DNA allowed to precipitate for 30 min at -20°C. The DNA was again spooled and transferred to a 14 mL polypropylene tube containing 5 mL 95% cold ethanol, centrifuged at 5,000xg for 10 min at 4°C, and the pellet was washed with 70% ethanol and allowed to air dry (~ 30 min). The pellet was gently resuspended in 2 mL TE buffer pH 8.0 by shaking at 60°C for 24 h. The OD_{260} was taken (UV160U UV-Visible Recording Spectrophotometer, Shimadzu) of the genomic DNA solution, and working aliquots were made by diluting in TE buffer pH 8.0 to 0.1 mg/mL. The quality of the DNA was assessed on a 0.8% ethidium bromide stained gel.

Undigested DNA was compared to an overnight digest at 37°C of 500 ng of genomic DNA with 15 units of DraI (Invitrogen) to ensure that the isolated DNA was intact, clean, and digestable. Agarose gels were prepared as described in Section 2.2.4.

4.2.2 Genomic Southern Blots

Twenty µg of genomic DNA was digested with either BamHI or PstI (New England Biolabs) in 250 µL reactions in a 1.5 mL microfuge tube overnight at 37°C. DNA was purified by adding an equal volume (250 µL) of Tris-saturated phenol and vortexing gently for 10 s. Tubes were centrifuged at 16,000xg for 1 min to separate the aqueous and organic phases. The aqueous upper layer was transferred to a fresh 1.5 mL microfuge tube, and an equal volume (250 µL) of chloroform was added, and the solution vortexed gently for 10 s. Tubes were again centrifuged at 16,000xg for 1 min to separate the aqueous and organic phases. The aqueous upper layer was transferred to a fresh 1.5 mL microfuge tube, and two volumes (500 µL) of ice cold 95% ethanol, and 1/10 volume (25 µL) 3 M sodium acetate pH 5.2 was added. The solution was vortexed gently for 10 s and centrifuged at 16,000xg for 10 min. The supernatant was decanted and the pellet washed in 100 µL of ice cold 80% ethanol. This was centrifuged at 16,000xg for 5 min. The supernatant was decanted and the pellet air dried. The pellet was then dissolved in 20 µL of TE buffer (10 mM Tris-HCl pH 8.0, 0.1 mM EDTA, pH 8.0) by vortexing gently for 10 s.

The full 20 µL of purified genomic DNA digest was separated on an 0.8% agarose gel (see section 2.2.4), and then transferred to Nytran Plus membrane, vacuum blotted and UV cross-linked as described in Chapter 2 Section 2.2.5. The membranes were hybridized overnight with probes listed below. Specific probes were used for the different exon 1 sequences of the different *ING1* and *ING2* variants as well as probes specific for exon 2 that represent all forms of *ING1* or *ING2*. Bands were detected with CDP-Star reagent using AlkPhos

Direct Kit reagents as described by the manufacturer (Amersham Biosciences, Inc.). To generate the probes, primers were used to amplify specific PCR products that were run on a 2% agarose gel. Primers were designed using Primer Premier software (Premier Biosoft International) and primers were supplied by Qiagen. The products were purified from the gel using the Qiaex II gel purification kit (Qiagen), and labeled for use in Southern blots with the AlkPhos Direct Kit reagents as described by the manufacturer (Amersham Biosciences, Inc.).

Primers, their sequences, and their product sizes are given in Table 4.1. Probes were designed to exon 2 of *ING1* or *ING2* that are able to detect all variants of each gene. For the *xING1b* variants, the sequences were too similar to design a specific probe for each, so one probe was used that detects *xING1b* variants *1* to *5*. Primers for this produced a 350 bp product for *xING1b5* and a 369 bp product for *xING1b1-4*. Specific probes were designed for *xING1c, xING1c2, xING2a,* and *xING2b* variants.

Table 4.1. Primers for Southern Blots.

Primer Name	Size (bp)	Sequence
***ING1* exon 2 forward**		5'-TGGTGGAGTTGGTTGAGAAC
***ING1* exon 2 reverse**	170	5'-CCTGGATCTTTTATTGCTGG
***xING1b1-5* forward**		5'-CCTCACATGTCCATGCACC
***xING1b1-5* reverse**	350 or 369	5'-CTTGGTATTTGGCGTCGATC
***xING1c1* forward**		5'-GCAGCAGCGGCTGTTTG
***xING1c1* reverse**	81	5'-ACAGACGAATAAAACGTCGAG
***xING1c2* forward**		5'-CATTGGCTTCGGGTTTGG
***xING1c2* reverse**	170	5'-GGCTACTCCCACAGCCAA
xING2 exon 2 forward		5'-AATGGGATGGATGACCT
xING2 exon 2 reverse	253	5'-TGCCCTTTGGTTTGTAG
xING2a forward		5'-GAACTAGGTCAAGGAACGG
xING2a reverse	243	5'-GGAATCCAAGCGGGTC

Primer Name	Size (bp)	Sequence
xING2b forward		5'-GAACTATGTGTACGAATCGCAC
xING2b reverse	96	5'-GAGCAGCTGGGCTGTAAGG

The sequence for the *xING1b5* variant has two PstI cut sites that result in an 848 bp product to which the probe can bind. One of the sites is within the probe region, so another downstream fragment of unknown size can also be detected by this probe. The *xING1b1-4* variants have a bp difference that results in no cut site. Therefore, this probe could bind to another fragment of unknown size. The sequence for exon 2 of *xING2* has two PstI cut sites that generate a fragment of 524 bp to which the probe for *xING2* exon 2 can bind. For the *xING2c* variant that has a deletion spanning exon 1 and 2, one of the cut sites is lost, so a larger fragment of unknown size can be detected by this probe. Other variants analyzed do not contain cut sites for either BamHI or PstI in the region of known sequence.

4.2.3 Genome Walking for ING1 and ING2 and Bioinformatic Analysis

The same preparation of genomic DNA that was used for Southern blots was also used for Genome Walking. Construction of genomic libraries and analysis by genomic PCR was done as per the manufacturer's instructions for the Universal GenomeWalker Kit (Clontech) with some modifications to the PCR protocol as noted. One M "GC melt" was added to the PCR reaction mix, and 5X GC Genomic PCR Reaction Buffer was used (Clontech). For the first round of PCR, a 1 min denaturation step at 94°C was done followed by 10 cycles of 94°C for 25 s, 70°C for 3 min and then followed by 40 cycles of 94°C for 25 s, 65°C for 3 min. For the second round of PCR, 1 µL of undiluted product from the first round of PCR was used. A 1 min denaturation step at 94°C was added followed by 5 cycles of 94°C for 25 s, 70°C for 3 min followed by 20 cycles of 94°C for 25 s, 65°C for 3 min. Adaptor-specific primers were supplied with the kit, whereas,

the gene-specific primers were designed using Primer Premier software (Premier Biosoft International) and primers were supplied by Operon (Huntsville, AL). Primers were designed to bind to known sequence close to the 5' end of each transcript sequence for each of the different exon 1 variants for *ING1* and ING2 as well as to the common region of *ING2*. The PCR products were cloned using the TOPO TA Cloning Kit Dual Promoter System with PCR II- TOPO vector and TOP10 cells (Invitrogen) as per the manufacturer's instructions. The putative positive clones were picked for creation of liquid stocks in LB broth containing 100 µg/mL ampicillin (Sigma-Aldrich). The stocks were used to inoculate 5 mL cultures of LB broth with 100 µg/mL ampicillin, which were grown overnight at 37°C with shaking. Plasmids were harvested with a Qiaprep Spin Miniprep kit (Qiagen) and subsequently digested with EcoRI (New England Biolabs). An 1% agarose gel was used to separate the inserts from plasmid vector, and positive clones were then sequenced in the DNA Sequencing Facility, Centre for Biomedical Research, University of Victoria. The DNA sequences were assembled using alignments with ClustalW version 1.8 software (http://clustalw.genome.ad.jp) and are included in Appendices 6 and 7. A second set of two primers was designed to obtain sequence upstream from the newly obtained genomic sequence. For the *xING1c2* variant, there was only one set of PCR done since the sequence obtained led into the known transcript sequence for *xING1c1*. For the *xING2* common region which is within the coding region of exon 1, there was only one set of PCR done since the goal was to determine if the sequence was contiguous with both the *xING2a* variant and the *xING2b* variant, as was the case. Primers for the two sets of Genome Walking experiments are given in Table 4.2 and 4.3.

Table 4.2. Original Primers for Genome Walking.

Primer Name	Sequence
***xING1b4* first round**	5'-CCACTCCTGCAACAAATCGTCTCCTC
***xING1b4* second round**	5'-TGTTCGAGGAAGGGAAAGGCGACAG
***xING1b5* first round**	5'-CCCTCCTAGAACAAATGCAACCGTC
***xING1b5* second round**	5'-GACGAAACACAAAGAAGGCGGCAGG

Primer Name	Sequence
***xING1c1* first round**	5'-AGACGAATAAAACGTCGAGCTCCGAG
***xING1c1* second round**	5'-CAGTGCGCAGCTTTCAACAAACAGC
***xING1c2* first round**	5'-ACTCCCACAGCCAATAAAATCCGAAG
***xING1c2* second round**	5'-GTTACGATAAAGGGACGTTCATTTGAAGG
***xING2* common first round**	5'-GGTACTCCTCCACATAGCTCACCAGTT
***xING2* common second round**	5'-CCTGCCCCGGTAGTAACGTGCTAACTCTAC
***xING2a* first round**	5'-CGTTCCTTGACCTAGTTCGGTAATCGT
***xING2a* second round**	5'-AGGTTGTTGCTCGTGATGTAGTTGGTG
***xING2b* first round**	5'-TCCTGGTGCGATTCGTACACATAGTTC
***xING2b* second round**	5'-CCTACTCTACTTGTCCTGCCTTAGCTTTC

Table 4.3. Second Set of Primers for Genome Walking.

Primer Name	Sequence
***xING1b4* first round**	5'-CCTTATTACCGTGTCGCATTCGCTAG
***xING1b4* second round**	5'-GACCTTTCATCCCCACATACGCTAC
***xING1b5* first round**	5'-TGTGGAGCGTCCAGTCAAGTAATAGAAC
***xING1b5* second round**	5'-CCTAAACCAGTAACACCAAGTTATCTTAACG
***xING1c1* first round**	5'-GGACAAGCTGTAGTTTACACGGGATATG
***xING1c1* second round**	5'-CACTGGTGCGTGTGTGTATGTGACAG
***xING2a* first round**	5'-GAGTTGACGGTCAATAAGCATGCCATC
***xING2a* second round**	5'-AAGTGGAGTAGGACCAGGCTTTAGG
***xING2b* first round**	5'-CATTTGGTCAGAAACGGAATGTCACAG
***xING2b* second round**	5'-CTAGGTAAGCACCACTGGGAGTTTTAGG

After sequence determination by Genome Walking, data mining of the Joint Genome Institute (JGI) database (http://genome.jgi-psf.org/Xentr4/Xentr4.home.html) which has the completely sequenced genome of the extremely closely related *Xenopus tropicalis* species was done to facilitate determining the organization of *X. laevis ING1* and *ING2* genes shown in

Figures 4.1 and 4.2. Predictions of putative TREs and other hormone response elements (HREs) as well as predictions for TATA box binding protein (TBP) and HNF1 binding sites were done using the Alibaba 2.1 software program with the TRANSFAC database version 7.0 (http://www.gene-regulation.com/pub/programs/alibaba2). Several regions of interest were analyzed for functionality by chromatin immunoprecipitations discussed in the next section.

4.2.4 Chromatin Immunoprecipitation (ChIP) Assays

Chromatin-protein complexes were obtained from pools of control and 48 hour 10 nM T_3-treated NF stage 52-54 tadpole tails, and ChIP assays were carried out as described in Chapter 3 Section 3.2.7 with animals cared for as described in Chapter 2 Section 2.2.1. Averages of 3 to 6 independent sets of animals were used in ChIP assays. Analysis of ChIP DNA was done by PCR with primers specific for different promoter regions of interest along with control primers. Primer design was accomplished using Primer Premier software (Premier Biosoft International), and primers were supplied by Qiagen. ChIP primer features are given in Table 4.4. Primers for three ChIP regions were created for analysis of *ING1* and three for *ING2*. Control primers for *β-actin* are described in Section 3.2.7.

Table 4.4. Primers for ChIP Assays.

Primer	Features (bp from transcript start)	Distance from Transcript Start (bp)	Size (bp)	Sequence
ING1b-1	TRE/GRE (1515); GRE/GRE (1239); TBPs (1049, 1090, 1121, 1239, 1335); HNF1 (1143) from *xING1b5* start	1374 to 999 from *xING1b5* start	375	forward: 5'-AGATAACTTGGTGTTACTGGT reverse: 5'-CAAATGCAGCTACAAGATTG
ING1b-2	TRE/RXR/TRE (702); TBPs (515, 623) from *xING1b5* start	786 to 459 from *xING1b5* start	327	forward: 5'-CTAGAACCCATTACCACTTTC reverse: 5'-GTTGCTATCAGTTCTGGAGG
ING1c	GREs (254, 186) from *xING1c1* start; TBP (43) from *xING1c2* start	301 from *xING1c1* to +1 from *xING1c2*	632	forward: 5'-TGGAGAGCTCTGCATTGTC reverse: 5'-CTACTTAAACTACGTTGACAAGG
ING2a	RevErbA (1493); GRE/GRE/GRE (1287) from *xING2a* start	1573 to 1021 from *xING2a* start	552	forward: 5'-GTAACTGTGCGAAGATTTCC reverse: 5'-TAAGCATGCCATCAATAGAG
ING2b-1	GRE (2087); TBPs (2331, 2042, 1959, 1905); HNF1 (2174, 1952) from *xING2b* start	1400 to 822 from *xING2b* start	583	forward: 5'-TATCTCAATGACAATGGTGC reverse: 5'-AGGAAGCAGAGTTTCTGTAAG
ING2b-2	GREs (1203, 1116); TRE/RXR (1013); HNF1 (1187) from *xING2b* start	2351 to 1768 from *xING2b* start	578	forward: 5'-TTGTATCAATTCTAACAACTGC reverse: 5'-GAGTCCTGAAATGAGTTTGC

PCR was done on a MX4000 thermocycler (Stratagene). The PCR conditions for the primer sets were chosen to ensure products were amplified in the linear range. Conditions for ING1b-1, ING2a, ING2b-1, and ING2b-2 were: 9 min at 95°C, and 40 cycles of 30 s at 95°C, 30 s at 60°C, and 30 s at 72°C. For the primer sets for ING1-2 and ING1c the PCR conditions were: 9 min at 95°C, and 37 cycles of 30 s at 95°C, 30 s at 60°C, and 30 s at 72°C. The PCR was done with 5 pmol primer (Table 4.4) in a 25 µl reaction with 10x reaction buffer (Invtrogen), 1.5 units of Platinum Taq DNA polymerase (Invitrogen), 10 nmol of dNTPs (GIBCO, Life Technologies), and variable amounts of $MgCl_2$ as indicated: ING1b-1, ING1c, and ING2b-1: 1.5 mM; ING1b-2 and ING2a: 2.5 mM; and ING2b-2: 3 mM.

Analysis of the products by densitometry of agarose gels and statistics on the normalized data is as described in Chapter 3, Section 3.2.7.

4.3 RESULTS

4.3.1 ING1 Genomic DNA Analysis

To investigate the possiblity that multiple *ING1* genes exist and that regulatory sequences contain TREs, Southern blotting and Genome Walking was carried out. The sequence obtained was analyzed for putative TREs and other hormone regulatory sequences using Alibaba 2.1 software. The genomic sequence obtained for *ING1* is included in Appendix 6. Figure 4.1 Panel A and B shows the organization of *ING1* genomic sequences with the locations of predicted HREs including TREs, reverse thyroid hormone receptor α (erythroblastic leukemia viral oncogene homolog; RevErbA), glucocorticoid response elements (GREs), RXR binding sites, and retinoic acid receptor (RAR) binding sites as well as predicted TBPs. The regions chosen for ChIP assays and probed in Southern blots along with PstI cut sites are also indicated on the schematic (Figure 4.1). ING binding sites were assessed as well. No similiarity

was found to the the AT-rich sequence that was identified as an ING binding site by Katoaka and colleagues [40] when compared with any of the *ING* variant genomic sequences using BLAST 2 Sequences software (http://www.ncbi.nlm.nih.gov/blast/bl2seq/wblast2.cgi). However, since ING competes with HNF1 for its binding site, I assessed the ING genomic sequences for HNF1 binding sites with Alibaba 2.1. A site in the ChIP regions for variant *xING1b5* is shown in Table 4.4 and on Figure 4.1. To support the genomic sequence analysis, Southern blots on digests of genomic DNA were done with probes specific to different variants of exon 1 and compared to results with probes specific to exon 2. Figure 4.1 Panels D to G show Southern blots of genomic DNA digested with either BamHI or PstI. Panel C shows that the genomic DNA preparation was of high quality, clean and intact (lane 1), as well as digestable (lane 2).

The variant of exon 1 referred to as *xING1b4* is spliced to a variant of exon 2 referred to as exon 2A (Figure 4.1A). The region upstream of the transcription start site contains two putative GRE half sites. Figure 4.2B shows the sequence for the variants *xING1b5, xING1c1*, and *xING1c2* that are known to splice with exon 2B based on transcript sequence. Based on Southern blot data with multiple banding patterns for *xING1c1* and *1c2*, it is possible that these variants also splice to exon 2A or another version of the *ING1* gene not yet discovered. The order of *xING1c1* and *1c2* is known from the sequence data, but *xING1b5* is presumed to be upstream based on alignments with the closely related species, *Xenopus tropicalis*, that is completely sequenced. The *ING1* introns were not sequenced in *Xenopus laevis*. In *X. tropicalis*, the first intron is between 825 and 1441 bp (little sequence homology was found for the *xING1c1* variant making this determination difficult), and the second is approximately 4370 bp.

The sequence upstream of the transcription start site for the *xING1b5* variant has several putative HREs including one RevErbA, six GREs, one RAR, three TREs, and one RXR shown in Table 4.5. Intriguingly, there are three clusters of elements that might each act as a functional unit. One grouping

includes a TRE 8 bp from a GRE in the following sequence: **TGACCg**TTATCCCA**TGTTCT** (the 6 bp consensus sequences are bold and underlined with mismatches to the consensus TRE (TGACCT) and to the consensus GRE (TGTTCT) in lower case). The second grouping includes a TRE followed directly by a direct repeat that is predicted to be an RXR that is in turn 1 bp from another palindromic TRE: **TGACCgTGACgT**C**AGGTCc** (the 6 bp consensus sequences are bold and underlined with mismatches to the consensus TRE (TGACCT), to the consensus RXR (TGACCT) and to the palindromic TRE (AGGTCA) in lower case). The third region contains a predicted half site GRE. Upon closer inspection of this region, 2 putative GREs are identified as a direct repeat with 11 bp between them: **gtTTCT**ATACAGTTTAT**TGTTCc** (the 6 bp consensus sequences are bold and underlined with mismatches to the consensus TGTTCT in lower case).
The sequence upstream of the transcription start site for the *xING1c1* variant has two putative GRE half sites. Scrutiny of the nearby sequence does not reveal any other putative HREs.

Table 4.5. Hormone Response Elements in ING1 ChIP Test Regions.

ChIP Region	Element Predicted	Alibaba 2.1 Consensus Sequence	ING Sequence
ING1b-1	TRE	wCrTGACCkn	tCaTGACCgt
ING1b-1	GRE	nTGTTCTrwy	aTGTTCTatt
ING1b-1	GRE	nCrsTTTsTr	aCagTTTcTa
ING1b-2	TRE	wCrTGACCkn	aCaTGACCgt
ING1b-2	RXR	TGAsrksArG	TGAcgtcAgG
ING1b-2	TRE	nwCAGGTCmy	gtCAGGTCct
ING1c	GRE	kkTACAwAsT	tgTACAtAcT
ING1c	GRE	AswnCAGyTT	ActaCAGcTT

Alibaba 2.1 was used with the TRANSFAC 7.0 database to identify putative hormone response elements. Symbols used in addition to A, C, G, or T are: W = A or T; S = C or G; R = A or G; Y = C or T; K = G or T; M = A or C; B = C, G, or T; D = A, G, or T; H = A, C, or T; V = A, C, or G; N = A, C, G, or T.

Southern blot data suggest there are multiple *ING1* genes. A probe that binds to exon 2 of *ING1* representing all the *ING1* variants bound to BamHI fragments at 1400 bp and 5300 bp (Figure 4.1D). This probe could not differentiate between exon 2A and exon 2B, so the appearance of two bands could represent binding of this probe to the two different exon 2 sequences with different restriction enzyme cut sites. The probe specific to exon 1 of *ING1* variants *xING1b1-5* bound to a BamHI fragment at ~12,000 bp as well as three smaller fragments at 7000, 5300, and 1400 bp (Figure 4.1E). This probe binds to sequences for variants *xING1b1-4* and *xING1b5*. Based on the transcript sequence data, *xING1b1-4* variants splice to exon 2A and *xING1b5* splices to exon 2B, and these variants could represent two or more genes. Since there are four bands observed, it is possible that multiple *ING1* genes exist. It is also possible that the BamHI digestion was not complete, but this is unlikely given the overnight digestion procedure. Fragments of 7000, 5300, and 1400 bp were bound by probes for both *xING1c1* and *xING1c2* in the BamHI digest (Figure 4.1F and G). Since there are no known cut sites for BamHI in the region to which the probe binds for either of the *xING1c* variants, the presence of three bands in each digest suggests the presence of multiple genes. From the genomic sequence analysis, it is clear these two variants are on a short contiguous region with only 247 bp between them, so it is likely that both probes bound to the same digested fragments.

Results from digestions with PstI also support the existence of multiple *ING1* genes. The probe for exon 2 of *ING1* bound to two fragments of 4700 and 5600 bp (Figure 4.1D) again, suggesting that exon 2A and 2B sequences are from different genes with different restriction cut sites. The fragment at 4700 bp was observed with the probes specific for each variant as well, suggesting that exon 1 variants and exon 2 are within approximately 4.7 kb (Figure 4.1 D-G). PstI fragments of ~8000 and 2000 bp were also observed with probes for each specific variant, suggesting these exon 1 fragments could be within 2000 bp of each other (Figure 4.1E-G). The presence of these three shared bands again suggest multiple forms of *ING1* that have different restriction sites. The

sequence for the *xING1b5* variant has one PstI cut site in the region that the probe binds and an upstream PstI cut site that would result in an 848 bp product to which the probe can bind. A band of this approximate size was observed as a weak fourth band in this digest. The *xING1b1-4* variants have a bp difference that results in no cut site in the probe region and there is no cut site in the region of upstream sequence that was obtained for that variant so this variant could be represented by any of the larger fragments observed.

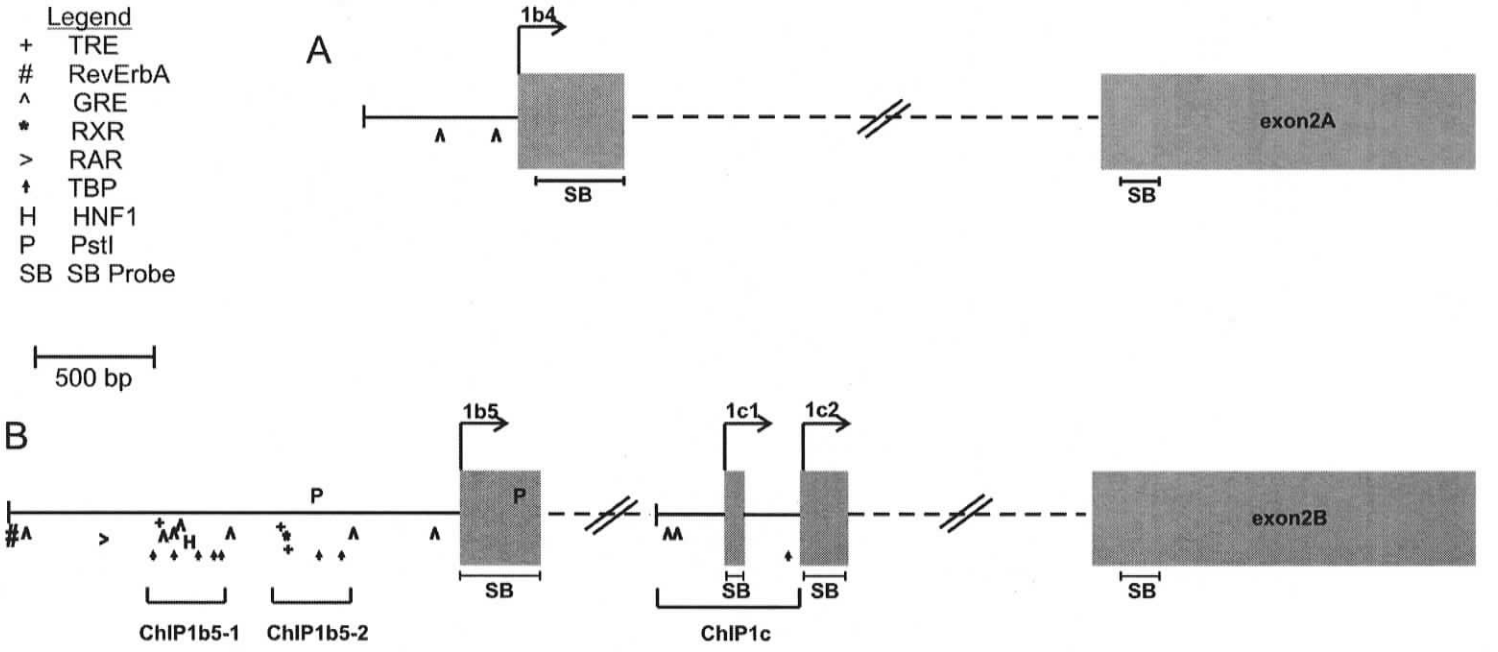
Legend
+ TRE
RevErbA
^ GRE
* RXR
> RAR
TBP
H HNF1
P PstI
SB SB Probe
A
1b4
exon2A
SB
SB
500 bp
B
1b5
1c1
1c2
P
P
exon2B
SB
SB
SB
SB
ChIP1b5-1
ChIP1b5-2
ChIP1c

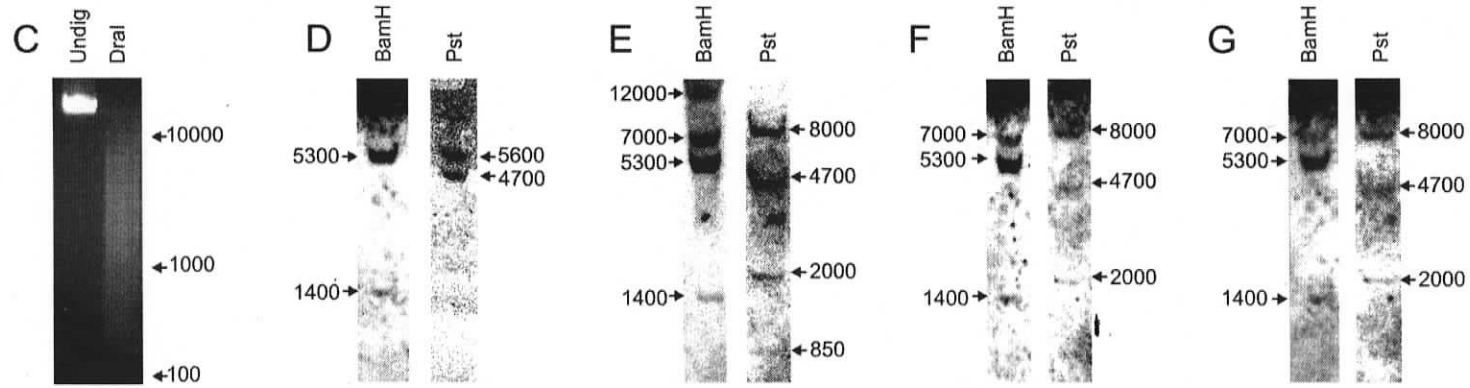
C
Undig
DraI
10000
1000
100
D
BamH
Pst
5300
1400
5600
4700
E
BamH
Pst
12000
7000
5300
1400
8000
4700
2000
850
F
BamH
Pst
7000
5300
1400
8000
4700
2000
G
BamH
Pst
7000
5300
1400
8000
4700
2000

Figure 4.1. Predicted binding sites and organization of multiple *ING1* genes.

Panel A shows the transcript variant *xING1b4* that splices to exon 2A. Panel B shows variants *xING1b5, xING1c1* and *xING1c2* that splice to exon 2B. Putative HREs, TBPs, and HNF1 sites predicted by Alibaba 2.1 are indicated by symbols given in the legend on the figure. Sequences are drawn to scale except where indicated by a dotted line with slash marks. Putative transcription start sites are indicated with a bent arrow. Exonic sequence is boxed and intronic or upstream sequences are indicated with a solid line where sequence is known and a dashed line where unknown, inferred from *X. tropicalis* sequence. In panel B, ChIP assay test regions are designated ChIP1b5-1, ChIP1b5-2 and ChIP1c. The quality of the genomic DNA from adult *X. laevis* used in Genome Walking and Southern blotting was assessed by comparing undigested and DraI digested DNA on a 0.8% agarose gel visualized by ethidium bromide staining (Panel C). Southern blots of genomic DNA digested with either BamHI or PstI show that *ING1* could be represented by multiple genes (Panel D-G). A probe that binds to exon 2 of *ING1* which is common to all the *ING1* variants (panel D), as well as probes specific to exon 1 of *ING1* variants including *xING1b1-5* (panel E), *xING1c1* (panel F), and *xING1c2* (panel G) were utilized. The binding sites for the Southern blot probes (SB) and PstI cut sites (P) are indicated on the genomic schematics in panels A and B. There are no BamHI sites in the known sequence. The same portion of the each blot is shown that represents between ~12,000 to 400 bp. Bands are indicated by arrows labeled with the approximate fragment size.

4.3.2 ING2 Genomic DNA Analysis

The same approach that was used to analyze the genomic sequence of ING1 was also used to analyze *ING2* including Genome Walking and Southern blots. *ING2* transcript variants also appear to come from different genes.

xING2a and *xING2b* transcripts have unique 5' ends followed by a common sequence in exon 1, which is then spliced to a common exon 2. Another variant transcript, referred to as *xING2c,* has a deletion that spans exon 1 and exon 2 in the open reading frame. A schematic summarizing the features of *ING2* genomic sequence including regions chosen for ChIP assays and probed in Southern blots is shown in Figure 4.2. The promoter sequence and the intronic sequence for *ING2* are included in Appendices 7 and 2 respectively.

The *xING2a* and *xING2b* variants share a common portion of sequence in exon 1 and splice to a common exon 2 (Figure 4.2A and B). The sequence upstream of the transcription start site for the *xING2a* variant has several putative HREs including one RevErbA, five GREs, one RAR, and two TREs shown in Table 4.6. Three direct repeats of a putative GRE are clustered together and may act as a functional unit with the sequence: **TGTTCT**CCC**TGTaCa**CTCTG**TcTTCT** (the 6 bp consensus sequences are bold and underlined with mismatches to the consensus GRE (TGTTCT) in lower case). In the middle element with two mismatches, it is equally valid to consider the reverse sequence AGAACA as the element. The sequence upstream of the transcription start site for the *xING2b* variant also has several putative HRE half sites including two RevErbAs, four GREs, one RXR, and one ERE (Table 4.6). On closer inspection, a TRE can be identified as a direct repeat 4 bp upstream of the predicted RXR with the sequence: **TGAACg**TCCC**TGAACT** (the 6 bp consensus sequences are bold and underlined with mismatches to the consensus (TGAACT) in lower case). HNF1 binding sites were again assessed by Alibaba 2.1. Sites in the ChIP regions for variant *xING2b* are shown in Table 4.4 and on Figure 4.2B.

Table 4.6. Hormone Response Elements in ING2 ChIP Test Regions.

ChIP Region	Element Predicted	Alibaba 2.1 Consensus Sequence	ING Sequence
ING2a	RevErbA	mnsykTGACC	ctcctTGACC
ING2a	GRE	nyTGTTCTsm	gtTGTTCTcc
ING2a	GRE	wmCAnTnTGT	taCAcTcTGT
ING2a	GRE	kGysTyCTGr	tGtcTtCTGa
ING2b-1	GRE	AGrACAywrk	AGaACActgg
ING2b-2	GRE	TskAwTkwCC	TctAaTttCC
ING2b-2	GRE	nyTGTTCTsm	ctTGTTCTcc
ING2b-2	RXR	CnsTGAmCys	CccTGAaCtc

Alibaba 2.1 was used with the TRANSFAC 7.0 database to identify putative hormone response elements. Symbols used in addition to A, C, G, or T are: W = A or T; S = C or G; R = A or G; Y = C or T; K = G or T; M = A or C; B = C, G, or T; D = A, G, or T; H = A, C, or T; V = A, C, or G; N = A, C, G, or T

ING2 genomic BamHI and PstI digests were analyzed by Southern blot (Figure 4.2C-E). A probe that binds to exon 2 of *ING2* that is common to all the *ING2* variants bound to two BamHI fragments at 7700 and 6000 bp, suggesting the presence of two *ING2* genes with different restriction cut sites. A fragment similar in size to the 7700 bp BamHI fragment bound by the exon 2 probe is not seen with probes for *xING2a* or *xING2b* and could represent the *xING2c* variant that has a deletion spanning exon 1 and 2 (refer to Figure 2.2) or an unknown variant. The known sequence for the common exon 2 of *xING2a* and *xING2b* has two PstI cut sites that generate a fragment of 524 bp to which the probe for *xING2* exon 2 can bind. In the *xING2c* deletion variant, one of the PstI sites is absent such that the exon 2 Southern blot probe would bind a larger fragment of unknown size. A fragment of ~520 bp was observed, and larger fragments at ~1000, 2000, 5100, and 9000 bp were also observed. This presents the possibility of even more than three *ING2* genes and may indicate that there are yet more *ING2* variants to discover. A second experiment shows that these bands are reproducible.

A probe specific to exon 1 of *ING2* for variant *xING2a*, bound to only a 6000 bp BamHI fragment, and a 9000 bp PstI fragment similar in size to fragments bound by the exon 2 probe. The probe for *xING2b* bound to a similarly sized 6000 bp BamHI fragment that may be bound by the exon 2 probe as well. In addition, the probe for *xING2b* bound to PstI fragments at 3200 and 2700 bp. This banding pattern supports the presence of two ING2 genes with sequence homology to the *xING2b* variant but that have different restriction cut sites.

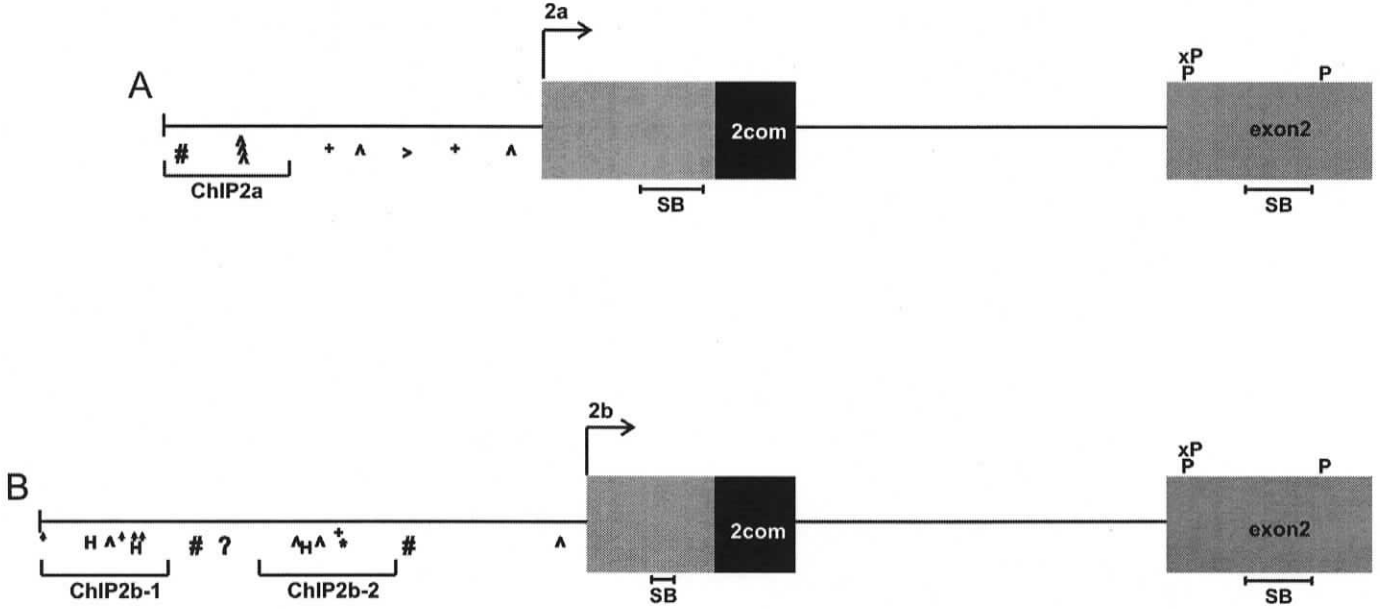

Legend

+	TRE
#	RevErbA
^	GRE
*	RXR
>	RAR
?	ERE
•	TBP
H	HNF1
P	PstI
SB	SB Probe
xP	missing PstI site for *xING2c* variant

500 bp

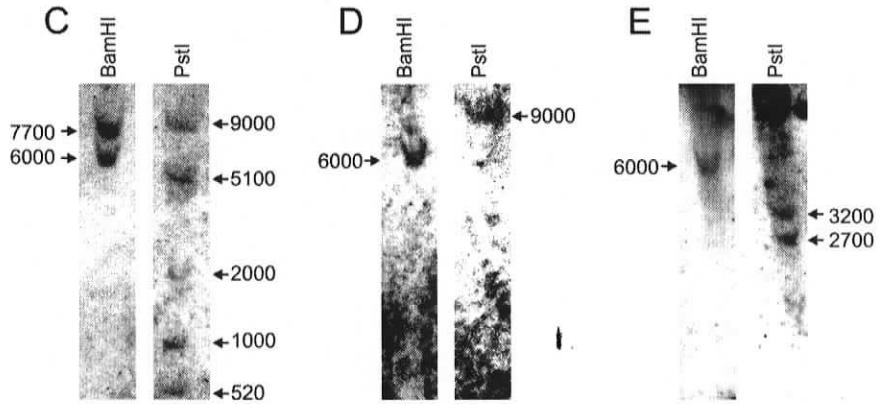

Figure 4.2. Predicted hormone response elements and organization of multiple *ING2* genes.

Panel A shows the variant *xING2a* and panel B shows the variant *xING2b*, both of which share a common portion of exon 1 sequence (2com) and a common exon 2. Putative HREs, TBPs, and HNF1 sites predicted by Alibaba 2.1 are indicated by symbols given in the legend on the figure. Sequences are drawn to scale; putative transcription start sites are indicated with a bent arrow; exonic sequence is boxed and intronic or upstream sequences are indicated with a solid line. ChIP assay test regions are designated ChIP2a (panel A) and ChIP2b-1 and ChIP2b-2 (panel B). Southern blots of genomic DNA from adult *X. laevis* digested with either BamHI or PstI show that *ING2* could be represented by multiple genes (Panel C-E). A probe that binds to exon 2 of *ING2* that is common to all the *ING2* variants (panel C), as well as probes specific to exon 1 of *ING2* variants *xING2a* (panel D) and *xING2b* (panel E) were utilized. The binding sites for the Southern blot probes (SB) and PstI cut sites (P) are indicated on the genomic schematics in panels A and B. The site where the *xING2c* variant is missing the PstI site found in the exon 2 sequence for *xING2a* and *xING2b* is denoted by "xP." There are no BamHI sites in the known sequence. The same portion of the each blot is shown that represents between ~12,000 to 500 bp. Bands are indicated by arrows labeled with the approximate fragment size.

4.3.3 Thyroid Hormone Receptor and ING Proteins Bind the ING1 Promoter

To assess if the putative response elements in the *ING1* promoter are bound by TRs, ChIP assays with antibodies for TRα and TRβ were done. I also tested ING's ability to bind to the *ING1* promoter, as I had already established that ING is associated with T_3-regulated promoters, *TRβ* and *TH/bZIP* (Chapter 2). Changes in protein association with *ING1* genomic DNA were investigated in the context of changing T_3 levels by comparing tails of control tadpoles to those

of tadpoles that were treated with 10 nM T_3 for 48 hours. To facilitate discussion in the next two sections, I will refer to levels of protein associated with a particular genomic DNA sequence as high if they are > 70% relative to input, moderate between 40-70%, low between 20-40% and very low if < 20%.

Two regions in the sequence upstream of the *xING1b5* variant were analyzed, ING1b-1 and ING1b-2 (Figure 4.3). ING1b-1 includes a predicted TRE in close proximity to a predicted GRE, plus another predicted GRE half site with a second putative GRE in close proximity, and five predicted TBPs. ING1b-2 includes a predicted TRE in close proximity to a predicted RXR and another TRE, as well as two predicted TBPs. TRα and TRβ display preferential binding for different regions of the DNA as well as differential changes in T_3-treated tadpoles. Levels of TRβ increased 8-fold to high levels upon T_3 treatment for the ING1b-1 region, while TRα remained fairly constant at moderate levels. Levels of TRα increased nearly 4-fold upon T_3 treatment to moderate levels in the ING1b-2 region, whereas TRβ remained constant at moderate levels. ING binds preferentially to specific DNA regions as well. ING had very little presence on the ING1b-1 DNA region. Although not T_3 responsive, levels of ING were moderate on the ING1b-2 region. Acetylation of histone H4 was moderate in the ING1b-2 region, and increased significantly upon T_3 treatment for the ING1b-1 region by 2-fold from low to moderate levels. RNA Pol II was not observed to bind the ING1b-1 region; however, levels of RNA Pol II were high in control tadpoles and decreased significantly upon T_3 treatment by ~2.5-fold on the ING1b-2 region.

The region upstream of the *xING1c1* transcript start site where two GRE half sites are predicted and the region upstream from *xING1c2* with a TBP site very close to the transcription start site was analyzed as a single unit. TRα increased ~15-fold from very low to moderate levels upon T_3 treatment. TRβ and ING binding were observed at moderate levels, while acetylated histone H4 and RNA Pol II were high.

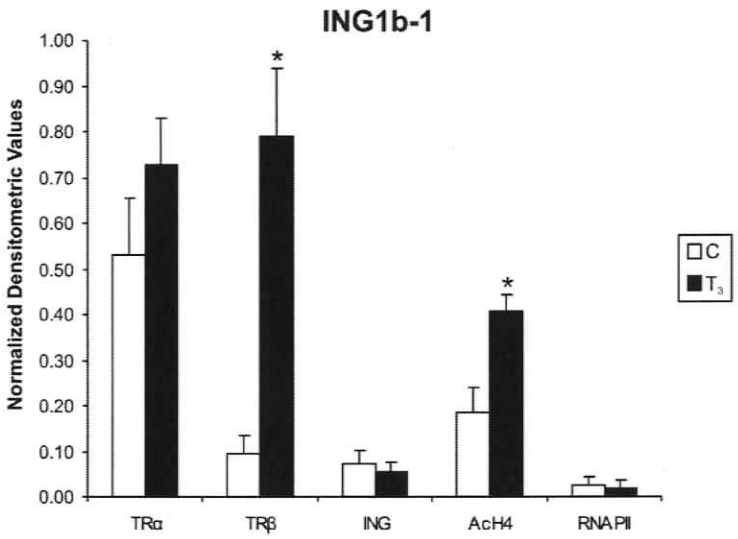
ING1b-1
Normalized Densitometric Values
1.00
0.90
0.80
0.70
0.60
0.50
0.40
0.30
0.20
0.10
0.00
*
*
C
T3
TRα
TRβ
ING
AcH4
RNAPII

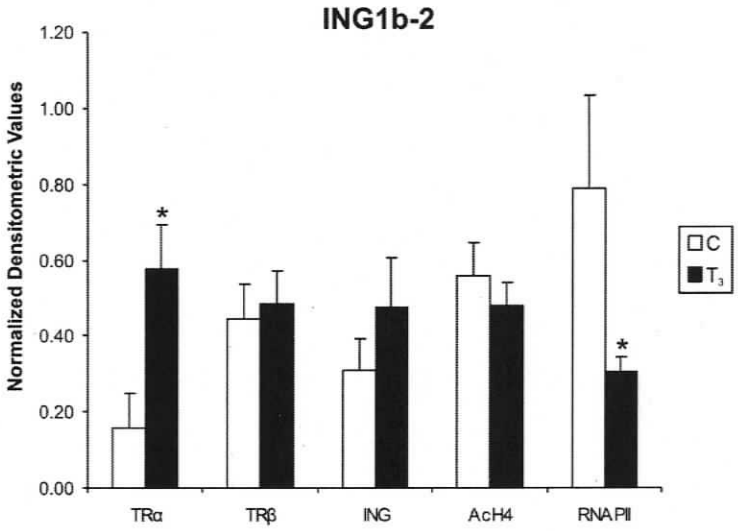
ING1b-2
Normalized Densitometric Values
1.20
1.00
0.80
0.60
0.40
0.20
0.00
*
*
C
T3
TRα
TRβ
ING
AcH4
RNAPII

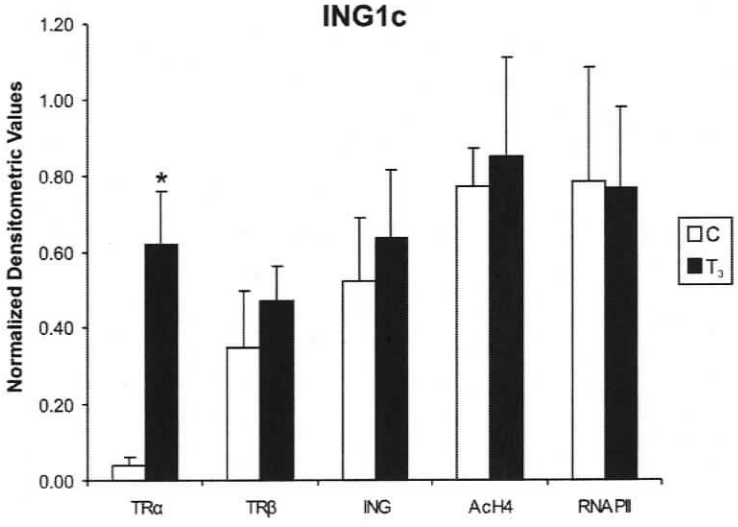
ING1c
Normalized Densitometric Values
1.20
1.00
0.80
0.60
0.40
0.20
0.00
*
C
T3
TRα
TRβ
ING
AcH4
RNAPII

Figure 4.3. TR and ING proteins differentially associate with *ING1* genomic DNA.

Shown are densitometry graphs for each antibody tested by ChIP assay: TRα, TRβ, ING, acetylated histone H4 (AcH4), and RNA Polymerase II (RNAPII). Values were obtained from 2% agarose gels of PCR products for genomic sequence regions in *ING1* designated as ING1b-1, ING1b-2 and ING1c (see Figure 4.1). Values were normalized by subtracting the local background of the gel, subtracting the background binding to the negative control antibody, and then dividing by the signal obtained from an input sample. The amount of chromatin used for the input sample was based on a fraction of the input for each set of ChIPs for an individual pool of animals tested. Where multiple PCR runs of the same pool were done, averages were taken prior to averaging across the sets. Chromatin-protein complexes were obtained from pools of 7-12 tails from tadpoles NF stage 52-54 that were either time-matched solvent controls (C) or treated with 10 nM T_3 for 48 hours (T_3). Three-six independent sets of animals were tested and averaged. Error bars represent the standard error of the mean, and statistical significance for T_3 treatment relative to control is indicated by * for $p \leq 0.05$ (AcH4: ANOVA; Mann-Whitney U test all others).

Figure 4.4 shows a schematic of the relative levels of different proteins and level of acetylation of histone H4 associated with the *ING1* ChIP regions. For the *xING1b5* transcript that is known to be activated by T_3 treatment, TRβ and acetylation levels increased on the ING1b-1 region with TRα already present, and TRα increased on the ING1b-2 region while RNA Pol II levels decreased with TRβ, ING and moderate levels of acetylated histone H4 already present (Figure 4.4A). For the *xING1c* transcript that is transcribed at relatively low but constant levels in naturally metamorphosing, as well as control and T_3-treated tadpoles, TRβ, ING, acetylated histone H4, and RNA Pol II are present in control tadpoles with TRα being recruited upon T_3 treatment (Figure 4.4B).

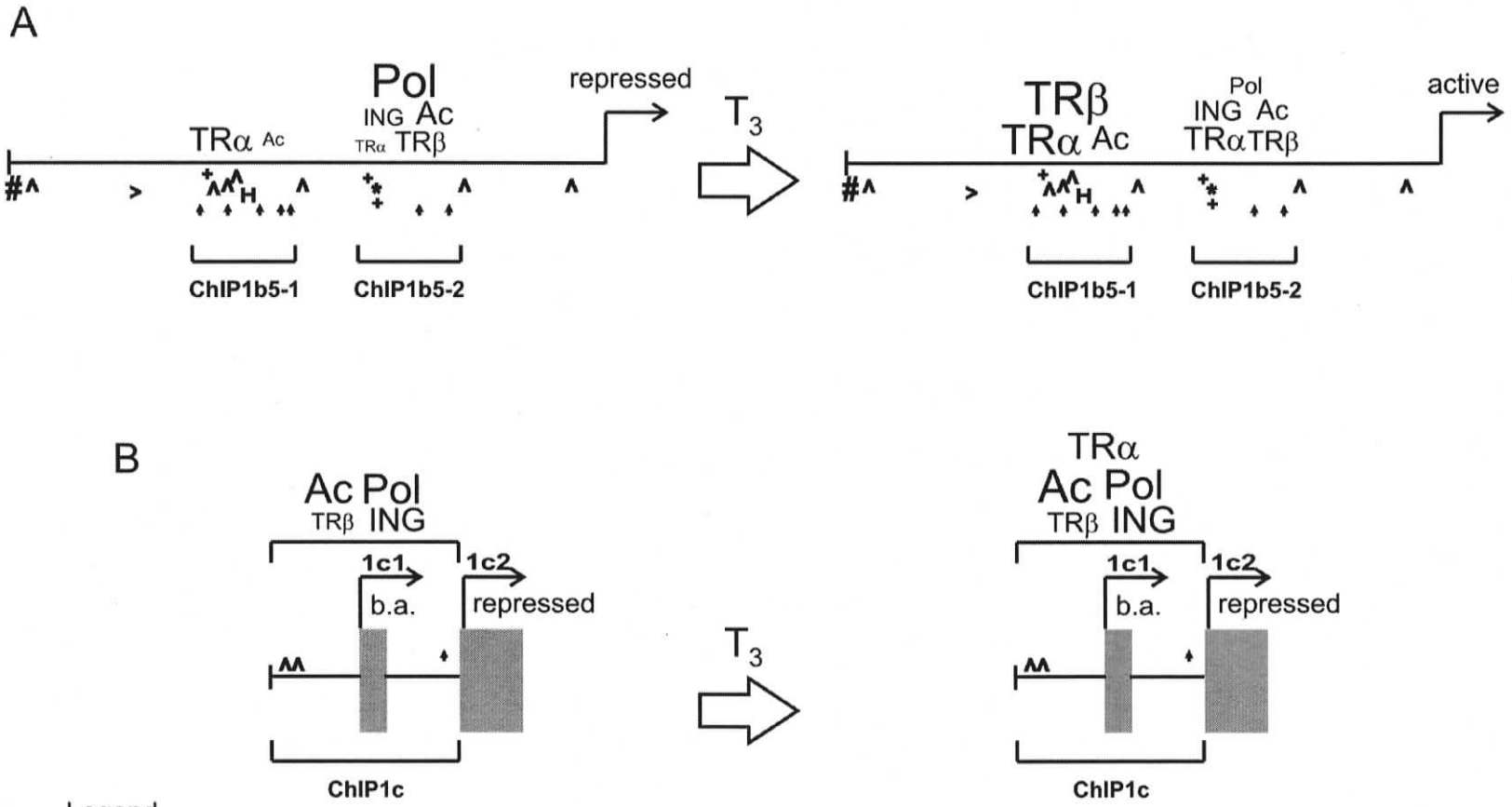
A
Pol
ING Ac
TRα TRβ
TRα Ac
repressed
T3
TRβ
TRα Ac
Pol
ING Ac
TRαTRβ
active
ChIP1b5-1
ChIP1b5-2
ChIP1b5-1
ChIP1b5-2
B
Ac Pol
TRβ ING
1c1
1c2
b.a.
repressed
ChIP1c
T3
TRα
Ac Pol
TRβ ING
1c1
1c2
b.a.
repressed
ChIP1c
Legend
+ TRE
RevErbA
^ GRE
* RXR
> RAR
TBP
H HNF1
b.a. basal activity
500 bp

Figure 4.4. Model of ING1 Promoter Regions.
ING1 genomic sequence described in Figure 4.1 is shown with TRα, TRβ, ING, and RNA Polymerase II (Pol) proteins that associate with the different promoter regions in ChIP assays shown (panel A, *xING1b5*; panel B *xING1c*) Different font sizes indicate relative levels (2 pt change for every 10% relative to input). It is not known which proteins of TRα, TRβ, ING, and RNA Pol II are bound to each other or to the DNA directly in these complexes. Histone H4 is part of the nucleosome and increased acetylation levels of histone H4 (Ac) are associated with a more open chromatin conformation. Features of the genomic DNA are given in the legend included on the figure.

4.3.4 Thyroid Hormone Receptor and ING Proteins Bind the ING2 Promoter

Putative regulatory regions of *ING2* genomic DNA were analyzed in a similar manner as for *ING1* and results of the ChIP assay analysis are shown in Figure 4.5. For analysis of *xING2a*, a ChIP region was tested that contains a predicted RevErbA half site and three predicted GREs in close proximity to each other. TRα levels increased 10-fold from very low to moderate levels upon T_3 treatment. Moderate TRβ levels were not affected by T_3. ING also was not affected by T_3 treatment, but was observed to associate with *ING* genomic DNA at moderate levels. Levels of acetylated histone H4 decreased significantly ~2-fold from high to moderate levels, while the amount of stationary RNA Pol II associated with the DNA increased 27-fold from virtually undetectable to moderate levels upon T_3 treatment.

For analysis of *xING2b* variants, two ChIP regions were tested. The region designated 2b-1 includes a predicted GRE half site and two TBPs. The region designated 2b-2 includes 2 predicted GREs and a predicted RXR site with a putative TRE 4 bp upstream. TRα levels were moderate for both regions and were not affected by T_3 treatment. TRβ levels remained constant at high moderate levels for the 2b-1 region, while increasing significantly for the 2b-2

region 8-fold from very low to moderate levels. The only DNA region for which ING binding was altered by T_3 treatment was 2b-1 where levels increased 2-fold from low to moderate levels. Concurrently, the lowest levels measured in this study of acetylated histone H4 were observed on this region. Also on this DNA region, RNA Pol II levels were seen to decrease 13-fold to very low levels upon T_3 treatment. ING protein associated with the 2b-2 region at moderate levels, but was not affected by T_3 treatment. Moderate levels of acetylated histone H4 and very low levels of RNA Pol II also did not change with T_3 treatment.

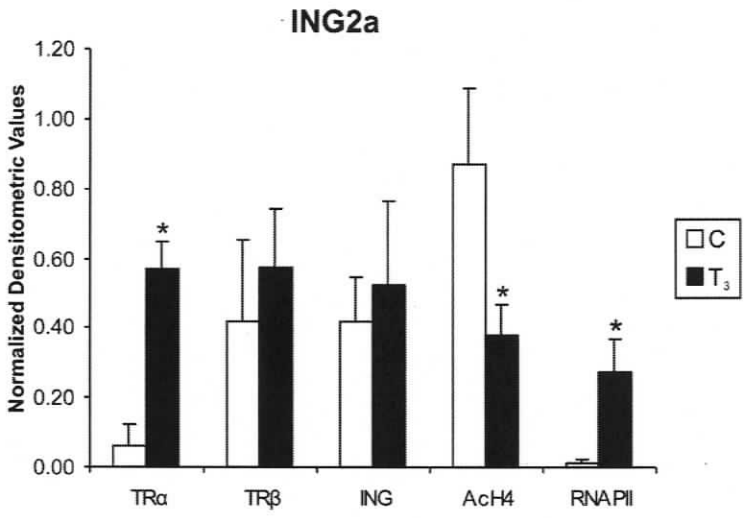
ING2a
Normalized Densitometric Values
1.20
1.00
0.80
0.60
0.40
0.20
0.00
*
*
*
TRα
TRβ
ING
AcH4
RNAPII
C
T3

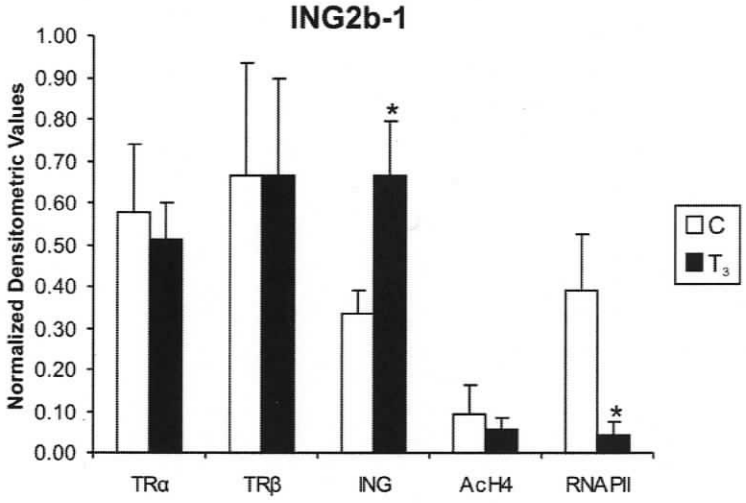
ING2b-1
Normalized Densitometric Values
1.00
0.90
0.80
0.70
0.60
0.50
0.40
0.30
0.20
0.10
0.00
*
*
TRα
TRβ
ING
AcH4
RNAPII
C
T3

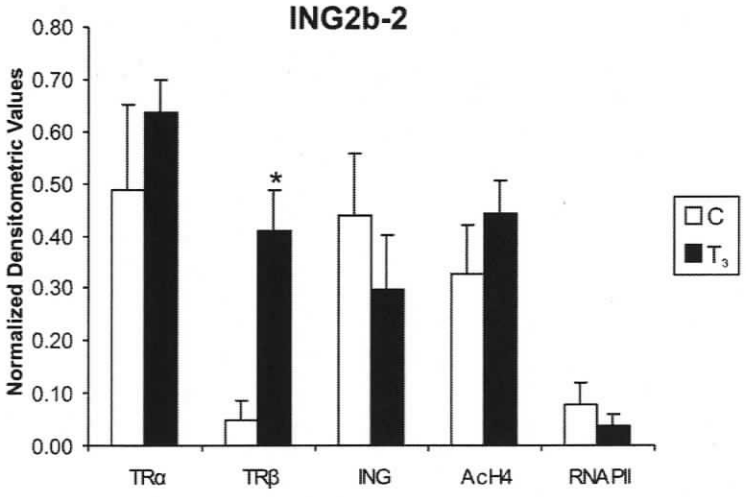
ING2b-2
Normalized Densitometric Values
0.80
0.70
0.60
0.50
0.40
0.30
0.20
0.10
0.00
*
TRα
TRβ
ING
AcH4
RNAPII
C
T3

Figure 4.5. TR and ING proteins differentially associate with *ING2* genomic DNA.

Shown are densitometry graphs for each antibody tested by ChIP assay: TRα, TRβ, ING, acetylated histone H4 (AcH4), RNA Polymerase II (RNAPII). Values were obtained from 2% agarose gels of PCR products for genomic sequence regions in *ING2* designated as ING2a, ING2b-1 and ING2b-2 (see Figure 4.2). Values were normalized by subtracting the local background of the gel, subtracting the background binding to the negative control antibody, and then dividing by the signal obtained from an input sample. The amount of chromatin used for the input sample was based on a fraction of the input for each set of ChIPs for an individual pool of animals tested. Where multiple PCR runs of the same pool were done, averages were taken prior to averaging across the sets. Chromatin-protein complexes were obtained from pools of 7-12 tails from tadpoles NF stage 52-54 that were either time-matched solvent controls (C) or treated with 10 nM T_3 for 48 hours (T_3). Three-six independent sets of animals were tested and averaged. The error bars represent the standard error of the mean, and statistical significance for T_3 treatment relative to control is indicated by * for $p \leq 0.05$. As the data was nonparametric, the Mann-Whitney U test was used.

Figure 4.6 shows a schematic of the relative levels of different proteins and level of acetylation of histone H4 associated with the *ING2* ChIP regions. The *xING2a* transcript is known to be active in control tadpoles and repressed by T_3 treatment. TRβ, ING and high levels of acetylation are initially present, and then TRα and RNA Pol II are recruited and acetylation of histone H4 is significantly reduced following T_3 treatment (Figure 4.6A). The *xING2b* transcript is known to be repressed in both T_3-treated and control tadpole tails. Initially, TRα, TRβ, ING and RNA Pol II are associated with the ING2b-1 region, but as ING levels increased upon T_3 treatment, RNA Pol II was displaced. Levels of acetylated histone H4 were virtually undetectable. On the nearby ING2b-2 ChIP

region, TRα and ING are initially present with low levels of acetylated histone H4. Following T_3 treatment, TRβ is recruited (Figure 4.6B).

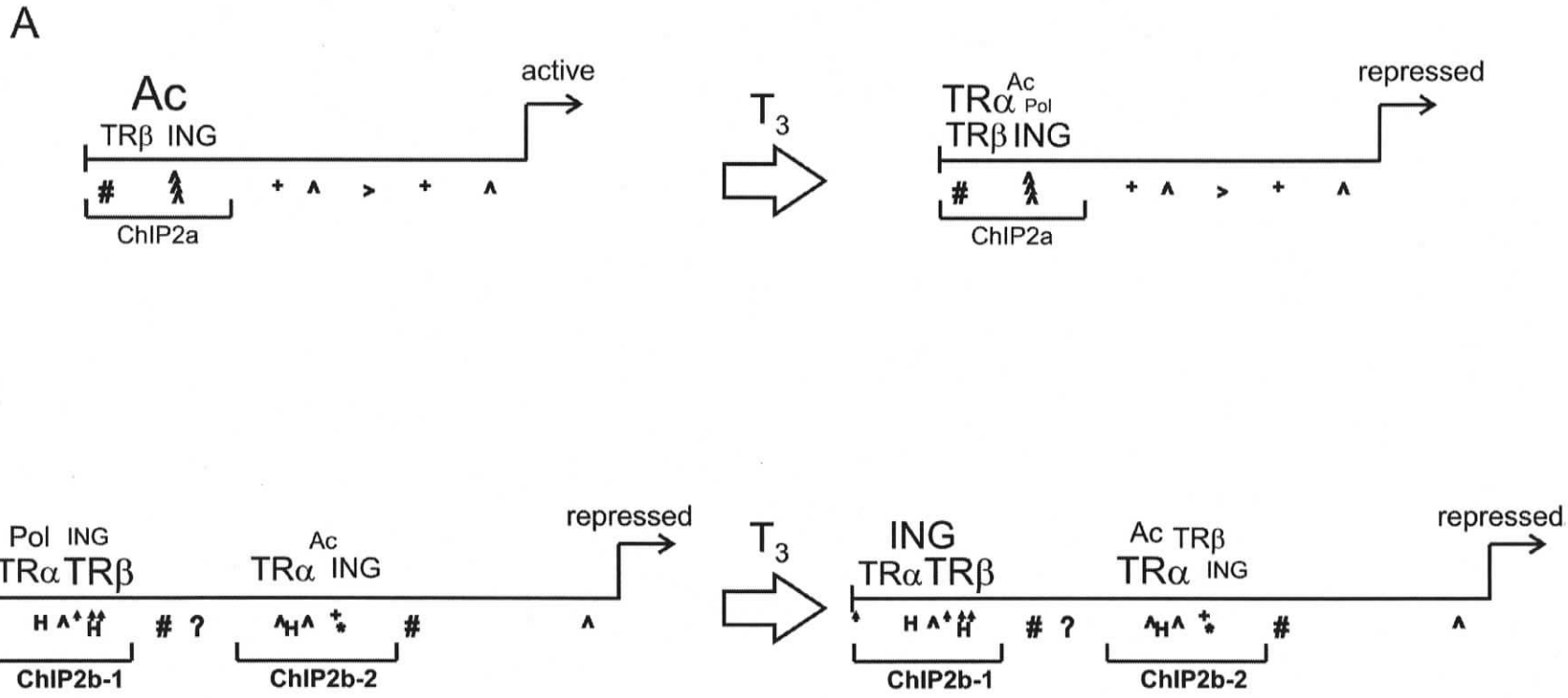
A
Ac
TRβ ING
active
ChIP2a
T3
Ac
TRα Pol
TRβ ING
repressed
ChIP2a
B
Pol ING
TRα TRβ
repressed
ChIP2b-1
Ac
TRα ING
ChIP2b-2
T3
ING
TRα TRβ
ChIP2b-1
Ac TRβ
TRα ING
repressed
ChIP2b-2
Legend
+ TRE
RevErbA
^ GRE
* RXR
> RAR
? ERE
TBP
H HNF1
500 bp

Figure 4.6. Model of ING2 Promoter Regions.

ING2 genomic sequence described in Figure 4.2 is shown with TRα, TRβ, ING, and RNA Polymerase II (Pol) proteins that associate with the different promoter regions in ChIP assays shown (panel A, *xING2a*; panel B *xING2b*). Different font sizes indicate relative levels (2 pt change for every 10% relative to input). It is not known which proteins of TRα, TRβ, ING, and RNA Pol II are bound to each other or to the DNA directly in these complexes. Histone H4 is part of the nucleosome and increased acetylation levels of histone H4 (Ac) are associated with a more open chromatin conformation. Features of the genomic DNA are given in the legend included on the figure.

4.4 DISCUSSION

I discovered several transcripts whose sequences suggested the existence of duplicate genes [17]. In this chapter, I present data that supports the existence of at least two genes for *ING1* and *ING2* in *X. laevis*. Expression of the *ING1* and *ING2* transcripts is affected by T_3 [17]. I present the analysis of genomic sequences for both genes that contain putative TREs and other HREs. Specific genomic regions were tested for functional association of TRs in ChIP assays. I show that both TRα and TRβ bind *ING1* and *ING2* promoters with different relative occupancies. Furthermore, TRα and TRβ binding is differentially T_3-responsive on different promoters.

ING associates with promoters of T_3-regulated *TRβ* and *TH/bZIP* genes (Helbing, Wagner *et al.*, in preparation). I show that ING can associate differentially with regions in both *ING1* and *ING2* promoters as well. Considering that ING and TR are present in the same immunocomplexes in the context of apoptosis of tadpole tails, it appears likely that ING and TR act in the same complexes that bind to promoters of T_3-regulated genes.

In Southern blots on digests of genomic DNA, patterns of 2 to 4 bands observed with each probe suggest the presence of at least duplicate genes for

ING1 that have different restriction enzyme digestion patterns. The exon 2 probe for *ING2* was able to bind two digestion fragments in one case, and five in the other. The banding pattern suggests that the *xING2c* variant is generated from a different gene than *xING2a* or *xING2b*. The additional PstI digest fragments bound by the exon 2 probe suggest that additional *ING2* variants exist that have not yet been discovered. The Southern blot data provide strong evidence for the existence of multiple *ING1* and *ING2* genes in *X. laevis*. A comparison of sequence data for *X. laevis* to *X. tropicalis*, human and mouse *ING1* and *ING2* shows that a similar gene structure is conserved in which variable exon 1 sequences are spliced to a common exon 2 [15]; however, multiple *ING1* and *ING2* genes may be unique to the psuedotetraploid *X. laevis*.

In amphibians, TR action on chromatin is characterized by repression of genes that inhibit growth in premetamorphosis by unliganded TR associated with corepressors and HDACs, followed by T_3-activation of genes required for metamorphosis at pTREs bound by TRs in association with coactivators and HATs [72, 73]. On regulatory regions for the *xING1b5* transcript which is known to increase in response to T_3, TRα and TRβ association increases significantly upon T_3 treatment along with increasing acetylation levels of histone H4 suggesting that chromatin is remodeled to an active state. Although direct binding of a protein to specific DNA sequences is not measured by the ChIP assay, the presence of predicted TREs in two test regions that strongly match the consensus sequence and the association of TRs with these regions suggest they contain classical pTREs. General transcription factors and RNA Pol II are recruited to enhancer elements early in gene activation with subsequent recruitment of RNA Pol II to the core promoter for activation of transcription [132]. Upstream of the *xING1b5* transcript in a presumed enhancer region, the amount of RNA Pol II decreases significantly in the T_3-activated state, perhaps indicating its recruitment to the core promoter for initiation of transcription.

TRs can also regulate gene expression through nTREs (reviewed in [74, 92]). At these response elements, T_3 induces TR-mediated repression. Shibusawa *et al*, 2003 showed that DNA binding is required for both positive and

negative gene regulation by TRs [133]. The *xING2a* transcript is known to decrease upon T_3 treatment, and in the ChIP region that contains three predicted GREs closely spaced, initially TRβ is present at moderate levels with high acetylation of histone H4 suggesting an active transcription region. Upon T_3 treatment, TRα is recruited, acetylation of histone H4 decreases and RNA Pol II increases significantly. This could indicate a repressive state of condensed chromatin where RNA Pol II is sequestered from the core promoter. Although TR binding is observed *in vivo* in this region, the DNA sequence involved is not known. It would be interesting to assess glucocorticoid receptor (GR) binding to the putative GREs as there is evidence to support crosstalk between TR and GR pathways in tadpole metamorphosis [65] and combinations of three GREs have been associated with repression [134].

To assess if ING associates with the same promoters as TRs for *ING* variants similar to the co-association of ING and TRs to promoters of *TRβ* and *TH/bZIP* (Chapter 3), ChIP assays were done with an anti-ING antibody. ING does associate with T_3-regulated promoters for both *ING1* and *ING2*. On *ING1* promoters, ING association is low on one promoter region for the *xING1b5* transcript but high for another site for the same transcript and also is high for another variant, *xING1c*, but is not affected by T_3 treatment. On *ING2* promoters, ING increases in response to T_3 treatment for one region upstream of the *xING2b* transcript, and binds all 3 *ING2* regions at moderate levels. ING may recruit HATS and HDACs to specific promoter regions as it associates with DNA upstream of both up and downregulated transcripts.

With ING protein observed on 7 of 8 ChIP regions tested for *TRβ, TH/bZIP*, *ING1* and *ING2* genes, it will be interesting to determine if ING binds the DNA directly or if cofactors such as TR are required. Experiments by Kataoka and colleagues show with nuclear extracts from Hepatocyte G2 cells that ING competitively binds to an AT-rich sequence that is also an HNF1 binding site in the promoter for AFP [40]. The researchers suggested the binding is indirect as they were unable to detect binding of *in vitro* transcribed/translated $p33^{ING1b}$ to the AT-rich motif; however it may be that posttranslational

modifications are required that were lacking in their system. Also, it is possible that other isoforms of ING may bind to DNA. Cofactors that bind DNA like p53 and TR or a histone modification such as trimethylation of histone H3 may also be required to target ING to DNA.

As an HNF1 binding site in the promoter of the AFP gene was shown to bind ING [40], I examined the regions tested in the ChIP assay for HNF1 sites and ING binding. For the ING1b-1 region that contains a predicted HNF1 site, no ING binding was observed. However, for the ING2b-1 region that contains two putative HNF1 binding sites, a significant increase in ING binding in response to T_3 was observed. In the ING2b-2 region that contains one HNF1 binding site, moderate levels of binding occurred. This putative ING binding sequence requires further analysis. Dissection of the promoter region with ChIP assays or EMSAs using short sequences is needed to determine if ING can bind a DNA sequence independently from the TRs and if there is a consensus binding motif for ING proteins.

The sequence upstream of *xING1c1* and *xING1c2* transcription start sites was also analyzed by ChIP assay as a single unit. There are two predicted GRE half sites upstream of *xING1c1* and a TBP 43 bp upstream of the putative *xING1c2* transcription start site. In contrast to other ChIP regions, this region likely contains the core promoter for both *xINGc1* and *xING1c2*. Thus, RNA Pol II may in part represent an active complex rather than a pre-initiation complex; however, the antibody used in the assay does not differentiate between active and inactive RNA Pol II. The only protein whose binding increased significantly upon T_3 treatment for this promoter region was TRα. TRβ and ING binding were observed at moderate levels, while acetylated histone H4 and RNA Pol II were high. This is in striking contrast to the patterns of protein binding observed for the promoter of *xING1b5*. This may relate to the observation that the *xING1c1* transcript was invariant with T_3 treatment and during natural metamorphosis and *xING1c2* was not detectable in tail (Chapter 2). Perhaps TRα is recruited to a nTRE that maintains the levels of *xING1c* variants in the face of large increases

in T_3 and TR levels during metamorphosis. Dissection of this ChIP region is needed to understand the regulation of each transcript variant individually.

Levels of the *xING2b* transcript were below detection limits in RT-PCR experiments in tadpole tail suggesting a repressed state in premetamorphosis as well as during TH-induced metamorphosis. Two regions were tested in ChIP assays. On the region farthest upstream from the transcription start site that contains a putative GRE half site, neither TRα nor TRβ change in response to T_3, but both TRs are present at moderately high levels. This is the only promoter region tested where ING levels increase in response to T_3. The levels of acetylated histone H4 are very low at this region suggesting the chromatin is compact and repressed. RNA Pol II levels decrease at this promoter region upon T_3 treatment, possibly indicating RNA Pol II is displaced further contributing to a repressed state. In the second *xING2b* ChIP region that contains two putative GRE half sites and a TRE/RXR site, TRβ increases significantly with T_3 treatment, while TRα levels remain high, ING and acetylated histone H4 levels are moderate and RNA Pol II is very low. Once again, it may be that a negative TRE is utilized, in this case by recruiting TRβ to the promoter to keep *xING2b* levels low during metamorphosis when T_3 and TR levels are high.

These results provide exciting new insight into the regulation of ING by TRs. The ability of ING to associate with T_3-regulated genes coupled with the observation that ING and TR proteins co-immunoprecipitate in tadpole tails places these two proteins in the same cellular context. Thus, ING and TR are intertwined in gene regulation during the process of apoptosis. For each ING promoter, it would be interesting to determine the minimal sequence required for the TRα and TRβ interaction by narrowing the regions tested in ChIP assays, or using short sequences in EMSAs. Putative TREs found in human, mouse, and *X. tropicalis ING1 and ING2* suggest that the link between ING and TR regulation of *ING* gene expression is conserved in a broader context.

CHAPTER 5. DISCUSSION

5.1 MULTIPLE ING TRANSCRIPTS ARE REGULATED BY TH

The isolation of several transcript variants with distinct tissue-specific expression profiles presents the possibility that ING is involved in specific pathways in different cell types. Certain transcripts including *xING1c2* and *xING2b* were only detectable in tadpole brain and in adult tissues suggesting they have a functional role in brain at an early stage, but are involved in several tissues in the adult life stage. Other variants were easily detectable in all tissues examined including tadpole hindlimb and tail, suggesting they have a role to play during development.

Western blots in a panel of adult tissues using an antibody directed against the highly conserved C-terminal end of human ING1 protein show that multiple ING protein products are expressed in frog. The antibody used is capable of recognizing both ING1 and ING2 proteins, and may recognize other ING family members as they share such a high degree of sequence homology in the C terminus. Most protein isoforms were observed in brain and testis that also have high levels of most transcript variants. Eye also has high ING transcript levels in adult frogs. ING levels for all ING variants are relatively high in tadpole brains, and may remain upregulated in the adult tissues of brain, testis and eye that are all derived from similar precursor cells of neural origin.

The exciting observation that *ING1b1-5* variants increase in the tail during both natural and T_3-induced metamorphosis, while this tissue is undergoing TH-dependent apoptosis, coupled with the observation that these same variants decrease in the hindlimb, a proliferating tissue, are in line with the current understanding of ING's involvement in apoptosis. The other *ING1* variant detectable in tail, *xING1c*, decreases significantly in hindlimb similarly to *xING1b1-5*, but also decreases modestly in tail (significant at NF stage 60). This

variant may be involved in different pathways compared to *xING1b1-5* that are not conducive to apoptosis.

Protein levels of ING in tail increase in both natural and T_3-induced metamorphosis, while levels in hindlimb appear to be unaffected [16]. It is not known which transcripts are represented by the proteins observed, but T_3-inducibility in the tail, supports the idea that ING levels are important in this tissue. My studies examined steady state levels of ING mRNA at specific time points. The stability of the mRNA was not tested; however, many genes governed by TH lack binding sites for TRs and are thought to be post-transcriptionally regulated by TH [135, 136]. Steroid hormones can also regulate protein expression by altering the stabilities of mRNAs [137, 138]. For example, in the pituitary, estrogen stabilizes thyroid hormone-releasing hormone receptor [139]. Although, I do show association of TRs on ING promoters in ChIP assays, there remains a possibility that TH has an effect on ING transcript stability as well that will ultimately affect protein levels. With so many potential proteins and cell-specific outcomes, future studies are needed to investigate the protein products of the transcripts in tadpole cells during different stages of TH-dependent development and in different tissues. It is also possible that some of the mRNA transcripts represent non-coding RNAs that may or may not be functional in the cell (reviewed in [140, 141]). For example, proteins encoded by the transcripts *altING1c* and *ING1d* are predicted but have not been isolated (He, Helbing *et al.* 2005 [15] and GenBank accession number NM198218). There is an additional ING1-like tumor suppressor protein in humans on chromosome X that encodes a putative 42 aa peptide with a calculated molecular mass of 5.0 kDa that contains only a partial PHD finger [15, 21]. Expression of this transcript was detected in all normal tissues tested (brain, colon, testis, kidney, liver, and breast) and in some breast and melanoma cancer cell lines using RT-PCR; however the protein has not been isolated [21].

There is generally good agreement for the data comparing individual transcript variants to the data from a primer set that amplifies all *ING1* variants, particularly during natural metamorphosis. Southern blot analysis supports the

existence of multiple *ING1* genes which may be regulated similarly as in the case of *xING1b1-4*, *xING1b5*, and *xING1c1* in the hindlimb but not necessarily, as may be the case for *xING1c1* in the tail. Data for all variants of *ING2* do not correlate well with the individual variants suggesting more variants exist that have yet to be identified. The Southern blot analysis supports this conclusion where digestion patterns are not explained by the variant sequences identified so far.

ING1 and *ING2* are early TH-response genes [16, 17] along with *TRα* and *TRβ* [96], placing ING in a potentially important role for the control of cell fate during TH-dependent metamorphosis. This work presents the first link between ING expression and a hormonally regulated nuclear transcription factor-mediated response. Because ING proteins associate with chromatin and TR protein, ING family members may be involved with the modulation of thyroid hormone receptor activity and may be a link to tissue-specificity of the TH-induced response. Conservation of putative TREs in other species may indicate that ING is regulated by TH in other species as well.

5.2 ING ASSOCIATES WITH TR PROTEIN

TR-mediated transcription is an integral part of the tadpole metamorphic program. The intriguing observation that ING can associate with TR in tails undergoing apoptosis during metamorphic climax not only suggests ING is involved in the metamorphic process, but provides a mechanism for this involvement. ING family members possess no known enzymatic activity. It is therefore likely that ING proteins act by facilitating specific protein-protein, possibly protein-DNA and even protein-phospholipid interactions.

ING may change the cofactor complement of TRE-associated complexes at specific promoters. ING co-immunoprecipitates with many proteins involved in DNA regulation including p53, NF-κB, and PCNA, as well as HAT and HDAC chromatin remodeling factors. TR itself binds DNA and to proteins that bind ING

such as the HAT, p300 and p53, but also associates with other coregulators such as NCoR and SMRT. It will be interesting to investigate further which proteins are involved in the ING/TR complexes under what conditions, particularly in response to changes in TH levels. Preliminary data suggests TR and ING interact in both stage 56-58 prometamorphic tadpoles and T_3-treated stage 54 premetamorphic tadpoles.

Specific isoforms of ING and TR may be involved in fine tuning the response. Results of the ChIP assays show that TRα and TRβ clearly bind preferentially to different ING promoter regions and are differentially affected by T_3 treatment. We know that ING also binds to ING promoters, but at this stage, we don't know what isoforms are involved. Since so many ING isoforms exist with the ability to bind different proteins and affect different pathways it seems likely that ING proteins would also associate with promoters differentially. Experiments using *in vitro* transcription of specific TR and ING isoforms, followed by immunoprecipitations or surface plasmon resonance to determine binding potential may be helpful in this regard. Care must be taken to ensure the proteins are properly posttranslationally modified. Currently, little is known about ING modifications and their effect on function and stability. However, it is clear that phosphorylation of a specific serine residue is critical for 14-3-3 binding to $p33^{ING1b}$ [30]. Identification of the components in naturally occurring complexes through mass spectrometry would be particularly informative.

The actions of ING and TR can oppose each other in some cases. For example, estrogen-induced expression of a reporter construct with an ER response element was attenuated by cotransfection of TRα in the presence of T_3 [142]. *In vitro* translated $p33^{ING1b}$ weakly associates with ERα, and transcription of an ER-responsive reporter gene was enhanced as $p33^{ING1b}$ expression levels increased [55]. In a second example, TR and p53 interact [117] and are antagonistic to each other's transcriptional activity [118-120], in addition to TR increasing p53 degradation by increasing MDM2 transcription [90]. $p33^{ING1b}$ [22], $p33^{ING2}$ [4], $p29^{ING4}$ and $p28^{ING5}$ [51] and p53 also interact, but ING prevents p53 degradation and enhances p53 transcriptional activity through promotion and

maintenance of p53 acetylation. Thus, ING and TR could oppose each other, and the balance of these two proteins such as both at high levels in tail, or TR high and ING low in hindlimb could contribute to cell fate.

Studies showed that ING2 interacts directly with TRβ using immunoprecipitations with purified proteins and using antibodies generated during my PhD. In tadpole tails of animals at metamorphic climax, immunoprecipitations show that ING and TR associate with each other, but it is not known if other proteins are required for the association. Coactivators of TRs and other nuclear receptors (NRs) often contain a leucine-rich motif with the consensus sequence LXXLL (reviewed in [143]). This motif is also known as the NR-interaction domain or NR box. Crystallographic and biochemical studies have revealed that the surface of a single LXXLL motif in an NR-coactivator (NCoA) directly contacts the ligand-activated AF2 domain of NRs [144-146]. Human ING2 has one such sequence, LQQLL, while in *X. laevis* and *X. tropicalis* the sequence is altered to LLQQL. Other coregulators that share this variation include NCoA-1 (LLEQL), NCoA-2 (LLDQL), CBP-interacting protein (pCIP) (LLDQL) and CPB (LQDLL), but these sequences have not specifically been shown to bind NRs [147]. Corepressor proteins, such as NCoR and SMRT, interact with unliganded TR using a nuclear-receptor-interaction domain with a core consensus motif: LXX I/H IXXX I/L designated a corepressor–nuclear-receptor (CoRNR) box [148]. In the same relative position as the LXXLL and LLXXL motif in ING2 in aligned sequences, amphibian ING1s have a sequence LXXFIXXXL. To test these putative NR box and CoRNR box sequences, ING could be mutated and binding to TR assessed.

Direct binding of ING and TR may not occur naturally, but association in the same complexes is likely given the two proteins association in immunoprecipitations and that they both associate with the same promoter regions for 4 different TH-regulated genes in ChIP assays: *TRβ*, *TH/bZIP*, *ING1* and *ING2*. Recent studies have uncovered an important role for multiple histone modifications involved in the transcriptional control by TR (reviewed in [92]). Along with other histone acetylations and phosphorylations associated with TR

transcriptional activity, Li and colleagues found that repression by unliganded TR is associated with a decrease in methylation of H3 lysine 4 (H3K4) and an increase in methylation of H3 lysine 9 (H3K9) while transcriptional activation by liganded TR is coupled with a decrease in both methylated H3K4 and H3K9 [149]. The researchers further showed that unliganded TR binds to and H3K9-specific methyltransferase[149]. Recent studies have shown that the PHD finger of all ING family members directly binds to trimethylated H3K4 *in vitro*, and that functional ING2 and methylated H3K4 are both requirements of repression of the cyclin D promoter *in vivo* [34]. The acetylation status of the histones plays a critical role in chromatin conformation important for transcription, but methylation of histones may be a critical feature for recruiting ING to specific promoters. The complexities of ING and TR participating in the same complexes to regulate TR-regulated genes during apoptosis at specific promoters will be discussed further in the next sections.

5.3 TRS ASSOCIATE WITH *ING1* AND *ING2* PROMOTERS

pTREs are most often bound by heterodimers of TRs with RXR [72], but TRs can bind as homodimers or monomers [84, 85]. nTREs are bound by TR monomers [86, 87], homodimers [87, 88] or heterodimers with RXR [87, 89]. *X. laevis* has 4 TR genes that produce receptors capable of binding TH: TRαA, TRαB, TRβA and TRβB where the TRβ genes each produce two alternatively spliced isoforms [73]. *X. laevis* has 3 RXR genes, α, β and γ, which are highly conserved with their mammalian counterparts [73]. I assessed the binding of TR proteins to ING promoters where the TRα antibody recognizes both TRαA and TRαB and the TRβ antibody recognizes three of the four TRβ isoforms (TRβA1, TRβA2, and TRβB1 but not TRβB2) [70]. Since TRβA1 is the major form of TRβ expressed in *X. laevis* [73], the antibody is presumably binding to all significant sources of TRβ. TRβ is highly induced in resorbing tissues such as tail, but

relatively low in most proliferating tissues [96]. In contrast, TRα is detectable in all cells tested but is particularly highly expressed in proliferating tissues such as limb buds, and specific areas of the brain [150, 151]. Although variable at different promoter regions, I observed significant binding of both TRα and TRβ on *ING1* and *ING2* promoters for both control and T_3-treated tadpole tails. The precise DNA sequences bound and whether receptor binding was as a monomer, a TR dimer with the same or different TR isoform or a heterodimer with RXR is not known. The levels of different isoforms of RXR are likely to have an effect as well as their expression varies throughout tadpole development in different tissues [73].

With so many receptor binding combinations, the outcomes can be quite diverse. Adding to this complexity, a typical TRE has the consensus sequence $AG_{G}/^{T}TCA$ but this sequence is shared with response elements for peroxisome proliferating antigen receptor (PPAR), vitamin D receptor (VDR), RXR, and RAR [91]. EREs also have the consensus sequence of AGGTCA and GREs have a similar consensus sequence AGAACA that is shared with response elements for mineralocorticoid receptor (MR), progesterone receptor (PR), and androgen receptor (AR) [91]. Some nuclear receptors adhere closely to their consensus sequences with conserved spacing between half sites. For example, ERs bind EREs as homodimers at inverted repeats separated by 4 bp; however, TRs are more promiscuous [91]. Given the similarity in consensus sequences combined with the fact that real sequences can vary from the consensus and that TRs bind direct repeats, inverted repeats, everted repeats, and palindromes of these sequences with different numbers of elements and spacing between elements, the ability to distinguish TR binding sites based on the half site consensus sequence is quite low. It has been estimated that only 2-35% of transcription factor binding sites actually match the consensus sequences [152]. Moreover, the *TRβ* and *TH/bZIP* promoters discussed in Chapter 2, known to be functionally associated with TRs shown in my own experiments and those of others [100, 131], do not contain sites predicted to be TREs. Specifically, the TRβ ChIP region contains a predicted ERE half site within the known functional TRE. The

TH/bZIP ChIP region contains a predicted GRE half site that is 50 bp upstream of the known functional TRE. The β-actin control region which was not bound by TRs has predicted half sites for ER, GR, and PR suggesting that the data is likely to represent specific TR binding at regulatory elements. The differential binding of TR isoforms to ING promoters and differential T_3 response also suggests that the binding is specific.

The concentrations of nuclear receptors and their ligands, as well as the nature of the HRE half-site sequence and flanking sequences together result in specific NR occupation of HREs in hormone-regulated genes that ultimately determines cellular outcome. As TH and TR levels increase dramatically during tadpole metamorphosis, HREs with otherwise very low affinity for TRs are activated or repressed by TRs bound to TH. Recent evidence supports this hypothesis where TRs bind to the *TH/bZIP* TRE with 4-fold lower affinity than to a *TRβ* TRE *in vitro* while in ChIP assays, the high affinity *TRβ* TRE site is occupied when TR levels are limiting during premetamorphosis, and the lower affinity *TH/bZIP* TRE sites are only occupied later when overall TR expression is higher during metamorphosis [131]. A recent study using a similar concentration of T_3 as in my study (8 nM compared to 10 nM) showed that at 48 h treatment TRα levels are elevated 2-fold in *X. laevis* tail [124]. In my studies, TRα was only present at low levels on one of the *xING1b5* promoter regions as well as *xING2a* and *xING1c* promoters in control tails, but was recruited upon T_3 treatment. This may indicate these test regions contain low affinity sites that require higher concentrations of TRα that are induced by T_3 or that a specific TR conformation or condition created by T_3 is required for binding. The same logic may explain the observation that TRβ was not present on one of the *xING1b* and one of the *xING2b* test regions in control tails, but was recruited upon T_3 treatment. In the same study as cited for TRα above, TRβ levels are elevated 5-fold in *X. laevis* tail at 48 h 8 nM T_3 treatment [124]. In my experiments, moderate levels of TRα on one of the *xING1b* and both of the *xING2b* test regions in both control and T_3-treated tails suggest these are moderate affinity sites for TRα. Similarly, moderate levels of TRβ on one of the *xING1b*, the *xING1c*, and one of the

xING2b test regions regardless of T_3 status indicates that these may be moderate affinity sites for TRβ.

Using Alibaba 2.1, I assessed ING sequences for TREs by comparing to the TRANSFAC 7.0 database that is largely based on studies of pTREs. There is recent evidence to suggest that a different sequence might allow TR binding specifically in the context of negative regulation. Kim *et al.*, 2005 studied the *CD44* gene that is negatively regulated by T_3 and showed TR binding in a ChIP assay. Further they showed by EMSA that the specific sequence bound by TRs is TTTGGG. This sequence is shared by a nTRE in human *TSHβ* and, in both genes when this novel nTRE sequence is mutated, there is a loss of TR binding and functional repression by T_3 [86]. I analyzed the genomic *ING* sequences that I isolated in *X. laevis* and found two such elements in the sequence upstream of *xING1b5*, but both were outside regions tested in the ChIP assay. Given that this transcript is upregulated in the tail in response to T_3, these may not be functional in that tissue. However promoters can have both pTREs and nTREs. For example, the rat growth hormone (GH) promoter contains a pTRE and a nTRE and partitioning of histone acetylases and deacetylases between the receptors and basal transcription factors is believed to be involved in regulation of the basal GH promoter by TRs [153]. Perhaps in the hindlimb where T_3 represses the *xING1b5* transcript these nTREs are utilized. Shibusawa *et al*, 2003 showed that DNA binding is required for both positive and negative gene regulation by TRs [133]. Therefore ChIP assays or EMSAs would be an appropriate method to study this further, comparing the specific sequences in tail and hindlimb.

The sequence upstream of the *xING1b4* transcript start site was not analyzed by ChIP assay. With the recommended stringency settings for the Alibaba 2.1 software, there were only 2 GRE half sites predicted in the 655 bp of genomic sequence that was obtained upstream of the putative transcript start site for this variant. Closer inspection of the sequence surrounding one of the predicted GREs at 361 bp from the putative transcript start site reveals an interesting pattern with 2 direct repeats and an inverted repeat of the sequence

TGTTTC (underlined in the following sequence) that surround the predicted GRE and that matches closely to the GRE consensus sequence TGTTCT (in bold and underlined with one bp mismatch in lower case):
TGTTTCTTAAGTGTTTCAAAC**TGcTCT**CCCTACTTTGT. A portion of this sequence containing the first two repeats is conserved in the *xING1b5* variant at a similar position from the putative transcript start (420 bp upstream). This sequence is not included in the ChIP regions tested. It would be interesting to investigate whether this element was hormone responsive. Whether this particular element is functional or not, considering that the transcript expression patterns for *xING1b1-4* and *xING1b5* were nearly identical in adult tissues and in naturally metamorphosing tadpoles and two concentrations of T_3 treatment in hindlimb, tail, and brain, it is likely that TREs exist in the *xING1b4* variant as well.

It was clear that expression of ING transcripts vary with TH in different tissues, but it was not known if TRs mediate these changes. Currently, ChIP assays done in the context of tadpole metamorphosis have analyzed binding of TRα and TRβ together or TRβ alone [100, 131]. I analyzed putative TREs found by bioinformatics analysis of *ING1* and *ING2* genomic sequence by ChIP assays using anti-TR antibodies specific to TRα or TRβ. I focused on the tadpole tail as a model tissue that undergoes extensive T_3-inducible apoptosis where ING levels are increased for *ING1b5*, decreased for *xING2a*, remain constant for *xING1c1*, and are very low for *xING1c2* and *xING2b* transcript variants. Also in support of this model, ING is well-characterized as a critical mediator of apoptosis in human (reviewed in [7-9, 13]) and mouse cells [48, 54], ING protein levels are high and T_3-inducible in the tail [16], and ING and TR proteins associate in immunocomplexes in tadpole tails (Helbing, Wagner *et al.*, in preparation).

In *xING1b5*, 2 TRE regions appear to be functional in that the two ChIP regions tested have specific TR binding patterns affected by T_3 treatment. For example, on the 1b-1 region levels of TRβ increased 8-fold upon T_3 treatment while TRα remains fairly constant. On the other hand, for the 1b-2 region, levels of TRα increased ~4-fold while TRβ remains constant. This is consistent with expression studies that show the transcript for *xING1b5* is upregulated in tadpole

tails during metamorphic climax with high levels of endogenous TH, and also increased in tails with 100 nM and 8 nM T_3 treatment. One possibility is that a TR monomer is initially bound to each TRE and a second TR is recruited forming a dimer that is activating.

There are two predicted GRE half sites upstream of *xING1c1* and a TBP 43 bp upstream of the putative *xING1c2* transcription start site the ChIP region designated ING1c. Close inspection of the 2 GRE half sites shows they do not agree with the consensus well and does not reveal any other obvious HRE patterns nearby. Nevertheless, TRβ binding was observed at moderate levels in both control and T_3-treated samples, and TRα binding increased ~15-fold upon T_3 treatment for this region. As the *xING1c1* transcript was invariant with T_3 treatment and during natural metamorphosis and *xING1c2* was not detectable, it is possible that TRα is recruited to a nTRE that maintains the levels of *xING1c* variants as T_3 and TR levels rise during metamorphosis.

On the ChIP region upstream of the *xING2a* transcript, initially TRβ was present at moderate levels. Upon T_3 treatment, TRα was recruited to moderate levels, a 10-fold increase, and TRβ remained unchanged. This region contains three direct repeats of a putative GRE that are clustered together and may act as a functional unit. Elements with three GREs have been shown to bind trimers of GR and be repressed [134]. It has also been shown that TRs can bind three tandem TREs and activate gene expression [95]. Since GREs and TREs are so similar in consensus sequence, more experimental evidence is necessary to investigate this further. Testing the DNA sequence containing only the 3 putative GREs in EMSAs for TR and GR binding individually and in competition with each other may reveal an HRE where crosstalk between NRs can occur.

There is also a RevErbA half site predicted in the ING2a ChIP region. The surrounding sequence does not contain any other obvious HREs; however the sequence TGACCA is only 1 bp different from the consensus palindrome TRE, TGACCT. Perhaps this sequence is bound by TRα and acts in a repressive manner. Other atypical TREs that were not recognized as putative HREs may

also be the true binding sites of TRα and TRβ, or the proteins may associate indirectly through a different transcription factor entirely.

I tested two regions upstream of the *xING2b* transcript start site in order to compare to each other and to ING1 ChIPs. I was initially most interested in the 2b-2 region with a predicted direct repeat of a TRE and an RXR site separated by 4 bp that strongly matches the consensus sequence in both half sites. I did not know how sensitive my technique would be, so this high affinity site was a logical starting point to test for a positive signal. The 2b-1 region has only one GRE half site that matches 100% with the consensus GRE so I thought perhaps this could be a control region that would not bind TRα and TRβ. I also wanted to assess the ability of my technique to differentiate between sites that were close to each other. The sonication procedure breaks the DNA into fragments of an average of 600 bp, but on an agarose gel of sonicates, DNA is visible as a smear ranging from 200 to 1,000 bp. These 2 ChIP regions are only 368 bp apart, so if the technique was too insensitive, I expected that the same binding patterns would be observed in each ChIP assay. The results showed several differences between the regions.

TRα and TRβ bound to the 2b-1 region at fairly high levels, while the 2b-2 region had similar binding of TRα but very low TRβ in the control that increased 8-fold upon T_3 treatment. The fact that the 2b-2 region had very low levels of TRβ in this specific promoter region illustrates that the ChIP assay can show differences between two closely spaced regions. Also, the fact that only the 2b-2 region had a T_3 response in TRβ suggests that this method can specifically detect changes in response to hormone even between close regions.

Analyzing these results in terms of the information available for the *xING2b* transcript is somewhat hindered by the fact that levels were so low, that they could not be detected in tail. However, this suggests the transcript is repressed in controls and T_3-treated tadpoles, as well as in naturally metamorphosing tadpoles. The 2b-1 region could be considered basally repressed while the 2b-2 region could be considered a standard nTRE where T_3 causes an increase in TRβ occupancy but is repressive rather than activating.

These elements may act together to keep *xING2b* transcript expression low in the tail. I was able to detect this transcript at fairly constant levels in the tadpole brain, albeit at low levels compared to the other *ING* variants. Transcript levels were easily detected in adult tissues with particularly high levels in brain, skin and especially eye. TRβ levels are also highest in these adult tissues. Perhaps the *xING2b* variant plays a larger role in adult frogs than in tadpoles and is under different regulatory control. Both the 2b-1 and 2b-2 ChIP regions are fairly large at 583 bp and 578 bp respectively, so further dissection of this region is needed to understand the regulation in this area in tadpoles and it would be interesting to compare to ChIP assays in adult frogs.

It has been suggested that TRα represses genes in the absence of T_3 [154, 155]. My data supports this idea as ING1b-1, ING2b-1 and ING2b-2 regions all have moderate TRα levels in control animals and the genes are repressed, whereas ING1c and ING2a regions from genes that are actively transcribed in controls have very low levels of associated TRα.

To date only 5 TREs have been characterized in *Xenopus laevis* and all are positive [74]. I have investigated 3 *ING1* and 3 *ING2* promoter regions that all exhibit some TRα and TRβ association. The T_3-induced repression of *xING2a* is the first example of a putative nTRE in this species.

As different tissues had unique T_3-dependent ING expression patterns, ChIPs in other tissues may reveal that the same TREs are differentially bound by TRα and TRβ or that different TREs are utilized. A promising starting place is with the ING1b ChIP regions as the *xING1b5* transcript is so clearly upregulated in tail, downregulated in hindlimb and highly expressed in brain. Focusing on even smaller DNA segments may also be helpful. Sections of the promoters could be analyzed for activity in reporter assays similar to studies by Gunduz *et al.* on human *ING1* [26].

It will be particularly important to compare to *ING* sequences from other species to look for conserved regulation sites that are likely to be biologically relevant. Comparison with mammalian and *X. tropicalis ING* genes reveals conservation in gene structure. Several TREs are predicted in human, mouse, *X.*

laevis, and X. tropicalis genomic *ING1* and *ING2* sequences. Modulation by TH may be a conserved mechanism of ING regulation.

5.4 ING ASSOCIATES WITH *ING1* AND *ING2* PROMOTERS

To differentially regulate genes, TR isoforms and coactivator requirements vary in different tissues [73]. The identification of specific coregulators at specific promoters and the identification of novel coregulators and TRE sequences in recent years suggests there is more to learn about TR regulatory complexes [88, 89, 99-101, 156]. My contribution of identifying ING as a potential player in these complexes by its association with chromatin at TH-regulated promoters makes an important link between TR complexes and a tumor suppressor's involvement in apoptosis in a critical developmental process in normal cells. Furthermore, ING's ability to affect so many cellular process including apoptosis, senescence, cell cycle progression, DNA repair, and angiogenesis (reviewed in [7-9]) is likely largely a result of ING interacting with a variety of protein partners that form complexes that bind DNA and regulate transcription. Through my work, we can now add TRs to the list of ING binding partners.

ING may be recruited to certain promoters by binding to TR that in turn binds to TREs, but the PHD finger of ING itself can bind to core histones at promoter regions. The PHD finger domain of all five ING family members binds to histone H3 peptide trimethylated at K4 *in vitro* [34]. ING2 was further characterized *in vivo* using ChIP assays where under conditions of DNA damage, ING protein was recruited to the cyclin D promoter, specifically *via* the recognition of trimethylated H3K4. On the same promoter, the damage response protein c-Myc along with HDAC1 were recruited and histone deacetylation was observed [34]. Trimethylation of histone H3 has been generally associated with transcriptional activation [157], so ING's ability to repress cyclin D is a novel finding. However, the outcome of the methylation may be determined by the protein that recognizes the modification and since different ING isoforms can

recruit HATS, HDACS, or both, it is possible that specific ING isoforms could bind trimethylated H3K4 at promoters and cause either activation or repression.

ING may also associate with DNA at AT-rich HNF1 binding sites directly or *via* a protein interacting partner [40]. In my ChIP assays, I showed the association of ING protein with promoter regions for *TRβ*, *TH/bZIP*, and *xING1b5* that are actively transcribed in response to T_3 in the tadpole tail. I also showed that ING associates with promoters of a gene transcribed at fairly constant levels (e.g. *xING1c*), a gene whose expression is decreased in response to T_3 (e.g. *xING2a*), and a gene that is not expressed in the tail (e.g. *xING2b*). The *xING2b* promoter regions contain three putative HNF1 binding sites, but further study is needed to determine if these sequences support ING binding. ING does not bind to all DNA, exemplified by the β-actin control region and the ING1b-1 ChIP region. It is not clear if ING binds DNA directly at HNF1 or other sites such as trimethylated H3K4; however, these results support the idea that ING can be involved in specific regulatory complexes for both upregulated and downregulated genes.

Regulation of transcription by ING and TR includes chromatin modification through recruitment of HATS and HDACs. Differences in acetylation levels of histone H4 were observed in ChIP assays, but no correlation was found with ING or TR levels. Although increases in acetylation of histone H4 have been observed at the *TRβ* and *TH/bZIP* promoters in previous ChIP experiments, the study used slightly older animals (NF stage 55) [100] compared to my study (NF stage 52-54). In another study that used younger animals (NF stage 47) no difference in acetylation between controls and T_3 treatment was observed [102]. Perhaps the older animals have a cofactor required for the increased acetylation lacking in the younger animals.

I observed moderate levels of acetylation that were significantly above background, but did not increase significantly with 48 hours of 10 nM T_3 treatment. In comparison to data published by others, strengths in my data include the greater sample size and the unbiased representation of all the data in a bar graph format with error bars that show the variability observed between

experiments. The data by Havis *et al.* with increasing acetylation is represented by a single gel that does not allow for analysis of variability [100]. In addition, several differences in my experimental protocol could contribute to variation in results including the age of animals studied, my use of calf thymus DNA as the non-specific DNA during preclearing and during the ChIP assay (other studies used salmon sperm DNA), and my visualization by ethidium bromide stained gels (other studies used autoradiography). It is evident that differences in protocol can greatly affect the results as illustrated by studies from the Shi lab [102, 131]. In experiments where autoradiography was used as the detection method, it was observed that TR levels on the *TRβ* promoter did not change in the presence of T_3 [102, 131]. This does not agree with my results. However, a study in the same lab using quantitative PCR was able to detect changes in TR levels on the *TRβ* promoter [131], similar to my observations. The acetylated histone H4 levels were not retested with quantitative PCR, but results may prove to be more similar to mine in the future.

My methodology was able to detect differences in acetylation levels at other promoter regions. For example, one region, ING2b-1, had very low levels of acetylated histone H4, while another region, ING1c, had very high levels. On the *xING2a*-specific promoter region for a transcript known to decrease with T_3 treatment, acetylated histone H4 decreased significantly by 2-fold. For the *xING1b*-specific promoter regions for a transcript known to increase with T_3 treatment, there are two ChIP regions tested, where only one has acetylated histone H4 increasing significantly by 2-fold compared to controls, while the other is moderately acetylated regardless of T_3 status. My experiments show steady state levels of promoter occupancy at a 48 h time point. It is possible that acetylation has already occurred to an extent that allows transcription factor binding at certain promoter regions that do not change with T_3 treatment (e.g. ING1b-2). Other regions may need further acetylation for increased transcription factor binding that is controlled by T_3 exemplified by the increased specific association of TRβ to the ING1b-1 region.

I have shown that ING transcript levels in the tail change in response to T_3 treatment. For example, the *ING1b5* variant increases and the *ING2a* variant decreases. Therefore, one might expect ING promoter occupancy to be affected by T_3 treatment. In my study, ING levels increased on the ING2b-1 ChIP region. Perhaps other promoter regions not tested have altered ING occupancy upon T_3 treatment as well. The antibody used in my studies recognizes the common C terminus of ING and is able to bind ING1 and ING2. This antibody does not differentiate between ING1 and ING2 isoforms and may recognize other ING family members as well. Homologs of human *ING3* and *ING5* genes have been identified in *X. tropicalis* through genome sequencing (GenBank NM_001008672 and NM_203536), and may also exist in *X. laevis*. Use of isoform-specific ING antibodies in ChIP assays may reveal a subset of genes that are regulated by a particular ING isoform where different INGs could bind and recruit different cofactors.

In control regions for 4 different genes, histone acetylation varies considerably. With ING present on all but the ING1b-1 region, it may be that specific ING isoforms can recruit HATs and HDACS to different promoter regions at different times. Differential control may be needed for timing and tissue-specific metamorphic changes. For example, tadpoles need time to develop strong limbs and functional lungs before the tail is apoptosed [72] and different genes are upregulated and downregulated at different stages of development [98]. Because the same ING can bind to both HATS and HDACs in some cases (e.g. human $p33^{ING1b}$), there could be rapid switching for tight control of expression at specific times in metamorphosis.

Although ING associates with specific promoters I tested, and ING is known to affect transcription of other genes, it is not known if ING affects gene expression of the particular genes I studied. Studies are currently underway with *ING1* and *ING2* transgenic tadpoles created in a collaboration with Browder and Jirik, University of Calgary. These studies will give further insight into ING function by examining effects of ING overexpression. In a quantitative PCR experiment, I observed enhanced transcript expression of *TRβ* in tails of T_3-

treated animals (10 nM T_3 for 48h) in ING2-His transgenics compared to control animals (Helbing and Shi, unpublished data). Furthermore, experiments were done in collaboration with the Shi lab where *X. laevis* oocytes were injected with a *TRβ* promoter-luciferase reporter DNA construct with a functional TRE element and co-injected with mRNA for TR and RXR. In the presence of T_3 (50 nM overnight), luciferase activity was induced. When oocytes were co-injected with either ING1-His or ING2-His mRNA, a dramatic enhancement of luciferase activity was observed in both cases (Helbing and Shi, unpublished data). This suggests that ING1 and ING2 can enhance TH-dependent transcript expression of *TRβ* and may prove to affect transcription of other TH-dependent genes as well. Future studies with mutant ING proteins or RNA interference assays that abolish function of ING followed by determination of *TRβ*, *TH/bZIP*, *ING1* and *ING2* transcript levels would provide further evidence to support a role for ING in regulating transcription of the genes I studies using ChIP assays.

5.5 ING AND TR-MEDIATED METAMORPHOSIS

ING binding to the promoters tested is independent of T_3 (except for ING2b-1). However, the promoters I investigated are differentially associated with TRs. On both the *TRβ* and *TH/bZIP* promoters, TRα and TRβ increase significantly on the same promoter region in response to T_3. On ING promoter regions, although TRα and TRβ associate with each region, in most cases they are individually upregulated in response to T_3 to varying degrees. As ING and TRs co-immunoprecipitate and associate with the same promoter regions, it is likely that they participate in the same complexes. Both ING and TR promoter binding levels are not correlated with a particular transcription state. Thus, they may be involved as both coactivators and corepressors, possibly due to the nature of a particular promoter containing either a pTRE or a nTRE.

Figure 5.1 shows a model of ING and TR acting in a repressive or activating manner at promoter regions. In a repressive state, at either a nTRE in the presence of T_3, or a pTRE in the absence of T_3, ING proteins associate with TR directly or indirectly and, along with TR, recruit corepressors and/or HDACs (Figure 5.1A). ING proteins may interact directly with the DNA, particularly at AT-rich HNF1 type binding sites or at histones such as trimethylated H3K4. Complexes may also contain unidentified tissue specific factors that keep target gene transcription repressed in certain tissues at particular developmental periods. Alternatively, in an activating state in the presence of T_3 at a pTRE or in the absence of T_3 at a nTRE, ING proteins may interact with TR, coactivators and/or HATs, tissue specific factors, modified core histones or directly with the DNA (Figure 5.1B).

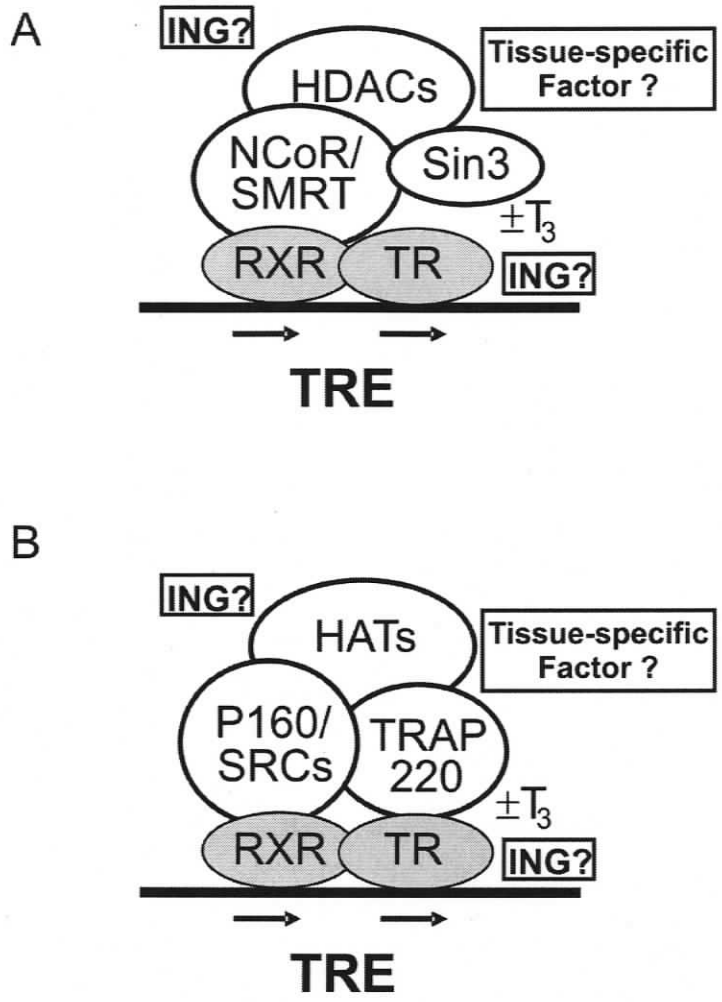

Figure 5.1. Model of ING and TR action to repress or activate transcription. (A) TRs bind TREs, most often as a heterodimer with RXR and repress transcription in the absence of T_3 ligand; however at nTREs, T_3 induces repression. This duality is represented by $\pm T_3$. Common corepressor NCoR, SMRT, and Sin3 along with HDACs that compact the DNA inhibiting transcription are shown. (B) Binding to TRs in the presence of T_3 generally activates transcription via recruitment of coactivators such as p160, SRCs, and TRAP220, along with HATs that acetyl ate histones making chromatin more accessible; however, at nTREs, transcription is active in the absence of T_3. This duality is represented by $\pm T_3$. It is not known but it is possible that ING binds to HDACs or HATs in association with TRs, or that ING binds DNA or other proteins in the complex (ING?). Additional tissue specific factors may be involved in the complexes (Tissue-specific factor?).

Specific target genes would be activated or repressed in a particular tissue depending on the metamorphic process relevant to that tissue. For example, target genes such as ING and TRβ involved in apoptosis of the tadpole tail are activated specifically in tail tissue, and genes that inhibit tissue-specific processes required for tail regression are repressed. ING and TR are both known to bind to the transcription factor p53 and the HAT p300 which may be involved in regulating a subset of promoters. In a cDNA array study of T_3-induced metamorphosis of *X. laevis* tail, PCNA increased 2-fold, while 14-3-3 decreased 2-fold [97]. Since ING is sequestered in the cytoplasm by binding to 14-3-3 [30], a decrease in this protein may facilitate ING relocalization to the nucleus. Furthermore, ING binds to PCNA and induces apoptosis [32], so an increase in PCNA may facilitate ING-PCNA-mediated apoptosis of the tadpole tail.

5.5 RNA POLYMERASE II IN ING/TR-MEDIATED TRANSCRIPTION

The relationship of ING and TR complexes with RNA Pol II is a complex one that depends on many factors including whether a particular promoter region contains the core promoter or if it is an enhancer or repressor region. Surrounding sequence and cofactors can direct unique transcription patterns for different promoters. Recent studies have shown that general transcription factors and RNA Pol II are recruited to enhancer elements early in gene activation. Thus, an important role of some enhancers is to function as centers for the assembly of the pre-initiation complex to regulate the timing of gene activation during development, differentiation and the cell cycle [132]. Subsequently, RNA Pol II is recruited to the core promoter for activation of transcription. Hormones have specifically been shown to act via this mechanism. Upon androgen treatment, the AR recruited some RNA Pol II to enhancer sequences initially, but over time following treatment, RNA Pol II decreased on

the enhancer region at the same time as RNA Pol II increased on the core promoter and transcription was activated [159]. Unliganded TRs are known to interact with the basal transcription machinery to facilitate repression, for example, TRs bind TFIIB repressing pre-initiation complex formation and TH reduces this interaction relieving the repression [160]. TRs also associate with corepressors such as NCoR and SMRT that interact with TFIIB and TBP associated factors (TAFs) [161, 162]. In the presence of TH, TRs dissociate from the corepressor and recruit coactivators such as TRAP220 that can bridge with the RNA Pol II complex facilitating transcription [143].

The decrease in RNA Pol II binding I observed in ChIP regions for *xING1b5, TRβ,* and *TH/bZIP* that are actively transcribed in response to T_3 could be a result of RNA Pol II being recruited away from an enhancer region to a core promoter to initiate transcription. For *xING2a* that is already actively being transcribed in control tadpoles, the opposite effect may contribute to repressing transcription. Upon T_3 treatment, an increase in RNA Pol II at an enhancer ChIP region that is between 1000 and 1500 bp from the putative transcription start site for *xING2a* may be repressive by sequestering RNA Pol II away from the core promoter.

A mechanism whereby RNA Pol II levels could decrease and indicate repression involves a specific repressor protein competing with RNA Pol II for binding at a specific promoter. This is seen for collagen transcription by Class II transactivator displacing RNA Pol II [163]. Perhaps for the ING2b-1 ChIP regulatory region (800 to 1400 bp from the putative *xING2b* transcription start site) where ING increases significantly while RNA Pol II decreases significantly upon T_3 treatment, ING may compete for binding with RNA Pol II, preventing a pre-initiation complex from forming.

In the ING1c ChIP region, the levels of RNA Pol II could be quite different given that this region begins at the -301 position relative to *xING1c1* transcription start site, encompasses the coding portion of the *xING1c* variant, and continues to the +1 position of the *xING1c2* transcript. Furthermore, a putative TBP is predicted 43 bp from the putative *xING1c2* transcription start site. The highest

levels of RNA Pol II observed in my study were measured at this promoter region for both control and T_3-treated tadpoles. The *xING1c1* transcript is actively transcribed in tails at low levels during natural metamorphosis and in both controls and T_3-treated tadpoles, while the *xING1c2* transcript was not detected. The antibody I used in the ChIP assays does not distinguish between active and inactive RNA Pol II complexes, but the high levels of RNA Pol II near the transcription start sites may indicate binding to a core promoter.

Further study is necessary to identify the true core promoter sequences for all the ING transcripts, and to establish if the RNA Pol II complex is active or inactive at each region. Regulation of RNA Pol II elongation rather than initiation can be the rate-limiting step in transcription [163-165]. Interaction with kinases or phosphatase modulates phosphorylation status of the C-terminal domain (CTD) of RNA Pol II and affects RNA Pol II promoter occupancy [163]. Conventional models suggest that pre-initiated Pol II would have a hypophosphorylated CTD, in contrast to the elongating Pol II, which would have a hyperphosphorylated CTD with either Ser-2 or Ser-5 phosphorylation [165]. To better understand the state of the complexes I studied, it would be interesting to look at the phosphorylation state of RNA Pol II and association of regulatory factors that initiate elongation.

RNA Pol II occupancy may also be regulated by nucleosome positioning and chromatin remodeling [34, 163, 166]. ING's involvement in chromatin remodeling through both HATs and HDACS may indicate ING is involved in RNA Pol II binding. Furthermore, ING binds to K4-trimethylated histone H3 and is associated with repression at the cyclin D promoter [34]. Interestingly, this histone modification is generally associated with transcriptional activation in yeast, whereas methylation of H3 at K9 is associated with repression [159, 166]. Other histone modifications may be discovered to affect ING and RNA Pol II binding. An additional connection between ING and RNA Pol II is through the DNA damage response where Rsp5 ubiquitin-protein ligase mediates DNA damage-induced degradation of the large subunit of RNA Pol II in yeast [167]. ING is involved in multiple DNA damage pathways that include p53, PCNA and

$p15^{PAF}$ protein interactions (Table 1.1) as well as transcriptional effects on apoptotic proteins Bax [52, 53] and MDM2 [61] and cell cycle regulators such as $p21^{CIP1}$ [30, 40, 60], cyclin B [60], and cyclin D [34].

5.6 ING AND TH PATHWAYS GONE AWRY

ING is a tumor suppressor with strong correlations of abnormal expression in a variety of cancers including skin, colon, head, neck, breast, ovary, stomach, mouth, esophagus, lymph nodes, white blood cells, lung, brain, bladder, and liver (reviewed in [7, 8]). All five ING family members are involved in apoptotic pathways that involve p53, another tumor suppressor frequently mutated in cancers [13]. The mechanism of one ING family member, ING4, is known to involve regulation of tumor angiogenesis through a physical interaction with NF-κB and subsequent downregulation of NF-kB-responsive genes involved in tumor vascularization [6]. Considering my data linking ING expression to TH and ING function to TR-mediated gene regulation in an apoptotic process, it is reasonable to consider that ING dysfunction may be involved in thyroid cancer as well. Thyroid cancers in particular have the highest estimated annual percentage increase in incidence amongst all cancer sites [168, 169]. In North America, about 7% of the population has thyroid disease making this the most common endocrine disorder [91]. Changes in TH levels due to endocrine disorders could affect ING expression thereby affecting cancer progression. In addition, THs target most cells of the body and may have general effects on oncogenesis in many cell types. Normal actions of TH are concentration and time dependent. Concurrent exposure to a carcinogen or endocrine disrupting compound (EDC) at a critical time could be an important factor in cancer progression.

The presence of TH is a prerequisite for neoplastic transformation in numerous cell culture and tumor model systems [170]. There are multiple mechanisms for TH involvement in oncogenesis including: regulation of gene products that are necessary for the initiation or maintenance of a neoplastic

state; alteration of TR isoform expression or function; or deregulation of normal TH-induced pathways that prevent transformation. The regulation of the tumor suppressor ING by TH and TR provides a means for each of these mechanisms. As TH affects ING expression and TRs bind differentially to different ING promoters, isoforms of ING expressed at a critical time co-incident with carcinogen or EDC exposure may lead to initiation of neoplastic transformation in a gain of function scenario. Similar deregulation of ING isoform expression could lead to a lack of tumor suppressor function causing oncogenesis. Also, as specific TR isoforms bind to ING promoters differentially, dysfunctional TRs that could include viral-ErbA that lacks the capacity to activate transcription and to interact with thyroid hormone [171] or cellular TR inaction or inappropriate action could lead to deregulation of ING expression or function that in turn could lead to cancer.

Cellular localization may also be a determinant in cancer progression. Mutations or rearrangements involving the MAPK pathway are known to be involved in transformation leading to thyroid cancer [169]. The phosphorylation state of ING is known to be critical for 14-3-3 binding and sequestering ING in the cytoplasm until DNA damage pathways are initiated [30]. It seems likely that other posttranslational modifications could regulate ING protein binding as ING has been found in so many different protein complexes (refer to Table 1.1). In the case of the ING-PCNA interaction, ING localization to the nucleolus could be affected. In the case of ING-TR interaction, targeting of ING to specific promoters could be affected. A number of PHD finger residues involved in trimethylated H3K4 binding, are found to be mutated in cancer cells, suggesting the vital role of this interaction that localizes ING to specific promoters such as the cell cycle regulator, cyclin D [33].

Disruptions in the MAPK or other pathways that lead to cancer or developmental abnormalities may involve ING, TR and p53. TR is phosphorylated by MAPK, inducing dissociation from the corepressors NCoR and SMRT and increasing TR transcriptional activity following binding of ligand [76]. Furthermore, TR/MAPK complexes are involved in an inactivating

phosphorylation of p53 [117]. Every member of the ING family is linked to p53-dependent pathways [8]. Estimated to be mutated on over 50% of cancers, p53 induces the expression of more than 50 proteins, including $p21^{CIP1}$, GADD45, MDM2, Bax, and PCNA which all mediate antiproliferative events *via* modulation of cell cycle progression, apoptosis, DNA repair, cell differentiation and senescence [172]. ING is also involved in upregulation of $p21^{CIP1}$, MDM2, and Bax and ING binds to GADD45 and PCNA facilitating DNA repair and apoptotic processes. TR is clearly an important mediator of apoptosis in tadpole tail regression, and it is possible that cell fate during metamorphosis may be controlled by a potential interplay between ING, p53, and TR. If any of these three proteins is dysfunctional, the regulation of cell death, differentiation, or proliferation could be lost leading to disease.

Alterations in chromatin structure by deregulation of HAT and HDAC activity contribute to the development of cancer and other diseases. For example, loss of acetylation of histone H4 is characteristic of cancer [173] and aberrant splicing or repression of tumor suppressor genes in cancer cells can result from deacetylation of nucleosomal histones within their promoters [174]. An important part of ING tumor suppressor function is to regulate transactivation of proteins involved in DNA repair and apoptosis by recruitment of specific HATs or HDACs. This is presumably critical to ING function in its role in tadpole development as well. Also, TRs properly recruiting HATs and HDACs to activate and repress genes is paramount to its function during metamorphosis.

ING may be one link between EDCs that disrupt TH and the potential for cancer to develop. Several compounds have been identified that disrupt the thyroid hormone axis. Because TH regulates ING expression, TRs bind ING protein and *ING* promoters, and ING appears to be involved in TH-mediated gene expression, dysregulation of TH or TR levels or actions has the potential to disrupt the tumor suppressor activities of ING. Polychlorinated biphenyls (PCBs) have been found to delay natural metamorphosis in *X. laevis* with differences observed for expression of specific genes including a neurotrophic factor and a neuro-hormone [175]. As ING levels are high in the brain, and may carry out

critical functions in that tissue, it would be interesting to see if ING expression is altered by PCB exposure. PCB disruption of the thyroid axis is not limited to *X. laevis*, with a correlation observed between PCB exposure and decreased serum/plasma T_4 levels, increased TSH, and increased T_4 excretion in a number of wildlife species, rats and humans [176-179]. Levels of contaminating brominated flame retardants such as tetrabromobisphenol A (TBBPA) or polybrominated diphenyl ethers (PBDEs) are on the rise [180]. TBBPA has been shown to compete with TH for human TRs, preventing T_3-induced transcription of a TRE-driven reporter gene and in *Ranid* amphibian species, TBBPA inhibited TH-induced tail shortening and limb development [181]. In the Pacific tree frog, *Pseudacris regilla*, TBBPA altered gene expression patterns including upregulation of TRα but not TRβ [182]. Similar to the effects of PCBs, PBDEs lower serum total T_4 concentrations, their metabolites bind the TH serum binding protein, transthyretin, and they have caused neuronal development problems in rat fetuses which led to behavioral abnormalities [183]. In the Helbing lab, studies in both *X. laevis* and *R. catesbeiana* tadpole tails showed that acetochlor accelerates TH-induced metamorphosis, and increased TRβ levels [122, 184].

The ability of additional hormones, besides TH, to modulate metamorphosis opens up the possibility that EDCs with estrogenic or other hormonal effects could affect metamorphosis [65, 72, 113]. Since ING associates with and enhances ERα transcription [40], further investigation of ING-ER-TR crosstalk could be particularly fruitful. Understanding the relationship between ING and other hormone-dependent tumor suppressors and EDCs is needed as human health and wildlife are increasingly threatened by the use of chemicals.

In the future, it will be useful to investigate the function of the different isoforms of ING protein in tadpole cells during different stages of TH-dependent development and in different tissues, in the presence of different environmental EDCs or other carcinogens as well as in dysregulated states that lead to cancer.

5.7 CONCLUSION

It is clear that ING family members are important in the regulation of critical cellular processes given their nuclear localization and association with key factors governing chromatin structure and transcriptional control. Using the *X. laevis* tadpole as a model system, I have made several novel findings. I show that there are multiple *ING1* and *ING2* transcript variants whose levels are differentially regulated by TH during apoptosis of the tail, proliferation of the limb, and remodeling of the brain. Furthermore, TRs bind to TREs in ING promoters in the tail in a T_3-regulated manner. My data provides the first evidence of hormonal regulation of ING, the first evidence of *ING2* splice variants for any species, and the first characterization of *ING1* and *ING2* in an amphibian. I also show that ING and TR proteins can interact and that ING is associated with the same promoter regions as TRα and TRβ for four different genes: *TRβ*, *TH/bZIP*, *ING1* and *ING2* in tadpole tail. This data provides the first evidence that ING may be directly involved in a hormone-mediated apoptotic process, and specifically that ING may be part of TR-regulatory complexes at specific promoters. Furthermore, this is the first evidence of ING autoregulation. It is not known which ING isoforms are involved. The combination of splice variants, multiple potential protein products and several related genes allows for considerable possibilities for ING to modulate cell fate as both agonists and antagonists in cellular processes. Deregulation of this critical TH-inducible pathway may be an important step in oncogenesis. There is a high degree of conservation in the thyroid hormone axis in vertebrates including humans where many developmental processes are dependent upon TH. Also, TREs in ING promoters are conserved in other species. Thus, these results have implications for other developmental systems. This thesis contributes to our understanding of the regulation and mechanism underlying the action of different isoforms of ING. These studies will give important insights into the relationship between TH regulation and ING tumor suppressor function during development.

Understanding these relationships is crucial to understanding regulation of apoptosis and proliferation that determines healthy and diseased states of a cell.

BIBLIOGRAPHY

1. Garkavtsev, I., et al., *Suppression of the novel growth inhibitor ING1 promotes neoplastic transformation.* Nature Genetics, 1996. **14**: p. 415-420.

2. Goeman, F., et al., *Growth inhibition by the tumor suppressor p33ING1 in immortalized and primary cells: involvement of two silencing domains and effect of Ras.* Molecular and Cellular Biology, 2005. **25**(1): p. 422-31.

3. Garkavtsev, I. and K. Riabowol, *Extension of the replicative life span of human diploid fibroblasts by inhibition of the p33ING1 candidate tumor suppressor.* Molecular and Cellular Biology, 1997. **17**(4): p. 2014-9.

4. Pedeux, R., et al., *ING2 regulates the onset of replicative senescence by induction of p300-dependent p53 acetylation.* Molecular and Cellular Biology, 2005. **25**(15): p. 6639-48.

5. Tallen, G., K. Riabowol, and J.E. Wolff, *Expression of p33ING1 mRNA and chemosensitivity in brain tumor cells.* Anticancer Research, 2003. **23**(2B): p. 1631-5.

6. Garkavtsev, I., et al., *The candidate tumour suppressor protein ING4 regulates brain tumour growth and angiogenesis.* Nature, 2004. **428**(6980): p. 328-32.

7. Campos, E.I., et al., *Biological functions of the ING family tumor suppressors.* Cellular and Molecular Life Sciences, 2004. **61**(19-20): p. 2597-613.

8. Gong, W., et al., *Function of the ING family of PHD proteins in cancer.* The International Journal of Biochemistry & Cell Biology, 2005. **37**(5): p. 1054-65.

9. Shi, X. and O. Gozani, *The fellowships of the INGs.* Journal of Cellular Biochemistry, 2005. **96**(6): p. 1127-36.

10. Aasland, R., T.J. Gibson, and A.F. Stewart, *The PHD finger: implications for chromatin-mediated transcriptional regulation.* Trends In Biochemical Sciences, 1995. **20**(2): p. 56-9.

11. Bienz, M., *The PHD finger, a nuclear protein-interaction domain.* Trends In Biochemical Sciences, 2006. **31**(1): p. 35-40.

12. Doyon, Y., et al., *ING tumor suppressor proteins are critical regulators of chromatin acetylation required for genome expression and perpetuation.* Molecular Cell, 2006. **21**(1): p. 51-64.

13. Russell, M., et al., *Grow-ING, Age-ING and Die-ING: ING proteins link cancer, senescence and apoptosis.* Experimental Cell Research, 2006. **312**(7): p. 951-61.

14. Feng, X., Y. Hara, and K. Riabowol, *Different HATS of the ING1 gene family.* Trends in Cell Biology, 2002. **12**(11): p. 532-8.

15. He, G.H., et al., *Phylogenetic analysis of the ING family of PHD finger proteins.* Molecular Biology and Evolution, 2005. **22**(1): p. 104-16.

16. Wagner, M.J., et al., *Expression of novel ING variants is regulated by thyroid hormone in the Xenopus laevis tadpole.* Journal of Biological Chemistry, 2001. **276**(December 14, 2001): p. 47013-47020.

17. Wagner, M.J. and C.C. Helbing, *Multiple variants of the ING1 and ING2 tumor suppressors are differentially expressed and thyroid hormone-responsive in Xenopus laevis.* General and Comparative Endocrinologyl, 2005. **144**(1): p. 38-50.

18. Zeremski, M., et al., *Structure and regulation of the mouse ing1 gene. Three alternative transcripts encode two phd finger proteins that have opposite effects on p53 function.* Journal of Biological Chemistry, 1999. **274**(45): p. 32172-32181.

19. Shimada, Y., et al., *Cloning of a novel gene (ING1L) homologous to ING1, a candidate tumor suppressor.* Cytogenetics and Cell Genetics, 1998. **83**: p. 232-235.

20. Saito, A., et al., *p24/ING1-ALT1 and p47/ING1-ALT2, distinct alternative transcripts of p33/ING1.* Journal of Human Genetics, 2000. **45**(3): p. 177-181.

21. Jager, D., et al., *Cancer-testis antigens and ING1 tumor suppressor gene product are breast cancer antigens: characterization of tissue-specific ING1 transcripts and a homologue gene.* Cancer Research, 1999. **59**(24): p. 6197-204.

22. Nagashima, M., et al., *DNA damage-inducible gene p33ING2 negatively regulates cell proliferation through acetylation of p53.* Proceedings of the National Academy of Sciences (USA), 2001. **98**(17): p. 9671-6.

23. Nagashima, M., et al., *A novel PHD-finger motif protein, p47ING3, modulates p53-mediated transcription, cell cycle control, and apoptosis.* Oncogene, 2003. **22**(3): p. 343-50.

24. Loewith, R., et al., *Three yeast proteins related to the human candidate tumor suppressor p33(ING1) are associated with histone acetyltransferase activities.* Molecular and Cellular Biology, 2000. **20**(11): p. 3807-3816.

25. Nourani, A., et al., *Role of an ING1 growth regulator in transcriptional activation and targeted histone acetylation by the NuA4 complex.* Molecular and Cellular Biology, 2001. **21**(22): p. 7629-40.

26. Gunduz, M., et al., *Genomic structure of the human ING1 gene and tumor-specific mutations detected in head and neck squamous cell carcinomas.* Cancer Research, 2000. **60**(12): p. 3143-3146.

27. Skowyra, D., et al., *Differential association of products of alternative transcripts of the candidate tumor suppressor ING1 with the mSin3/HDAC1 transcriptional corepressor complex.* Journal of Biological Chemistry, 2001. **276**: p. 8734-8739.

28. Kuzmichev, A., et al., *Role of the Sin3-histone deacetylase complex in growth regulation by the candidate tumor suppressor p33(ING1).* Molecular and Cellular Biology, 2002. **22**(3): p. 835-48.

29. Scott, M., et al., *UV induces nucleolar translocation of ING1 through two distinct nucleolar targeting sequences.* Nucleic Acids Research, 2001. **29**(10): p. 2052-2058.

30. Gong, W., et al., *Subcellular targeting of p33ING1b by phosphorylation-dependent 14-3-3 binding regulates p21WAF1 expression.* Molecular and Cellular Biology, 2006. **26**(8): p. 2947-54.

31. Gozani, O., et al., *The PHD finger of the chromatin-associated protein ING2 functions as a nuclear phosphoinositide receptor.* Cell, 2003. **114**(1): p. 99-111.

32. Scott, M., et al., *UV-induced binding of ING1 to PCNA regulates the induction of apoptosis.* Journal of Cell Science, 2001. **114**(Pt 19): p. 3455-62.

33. Pena, P.V., et al., *Molecular mechanism of histone H3K4me3 recognition by plant homeodomain of ING2.* Nature, 2006.

34. Shi, X., et al., *ING2 PHD domain links histone H3 lysine 4 methylation to active gene repression.* Nature, 2006.

35. Boudreault, A.A., et al., *Yeast enhancer of polycomb defines global Esa1-dependent acetylation of chromatin.* Genes and Development, 2003. **17**(11): p. 1415-28.

36. Selleck, W., et al., *The Saccharomyces cerevisiae Piccolo NuA4 histone acetyltransferase complex requires the Enhancer of Polycomb A domain and chromodomain to acetylate nucleosomes.* Molecular and Cellular Biology, 2005. **25**(13): p. 5535-42.

37. Doyon, Y., et al., *Structural and functional conservation of the NuA4 histone acetyltransferase complex from yeast to humans.* Molecular and Cellular Biology, 2004. **24**(5): p. 1884-96.

38. Howe, L., et al., *Yng1p modulates the activity of Sas3p as a component of the yeast NuA3 Hhistone acetyltransferase complex.* Molecular and Cellular Biology, 2002. **22**(14): p. 5047-53.

39. Vieyra, D., et al., *Human ING1 proteins differentially regulate histone acetylation.* Journal of Biological Chemistry, 2002. **277**(33): p. 29832-9.

40. Kataoka, H., et al., *ING1 represses transcription by direct DNA binding and through effects on p53.* Cancer Research, 2003. **63**(18): p. 5785-92.

41. Cheung, K.J., Jr., et al., *The tumor suppressor candidate p33(ING1) mediates repair of UV-damaged DNA.* Cancer Research, 2001. **61**(13): p. 4974-7.

42. Garkavtsev, I., et al., *The candidate tumour suppressor p33ING1 cooperates with p53 in cell growth control.* Nature, 1998. **391**(6664): p. 295-8.

43. Leung, K.M., et al., *The candidate tumor suppressor ING1b can stabilize p53 by disrupting the regulation of p53 by MDM2.* Cancer Research, 2002. **62**(17): p. 4890-3.

44. Tsang, F.C., et al., *ING1b decreases cell proliferation through p53-dependent and -independent mechanisms.* FEBS Letters, 2003. **553**(3): p. 277-85.

45. Toyama, T. and H. Iwase, *p33ING1b and estrogen receptor (ER) alpha.* Breast Cancer, 2004. **11**(1): p. 33-7.

46. Gonzalez, L., et al., *A functional link between the tumour suppressors ARF and p33ING1.* Oncogene, 2006.

47. Simpson, F., et al., *The PCNA-associated factor KIAA0101/p15(PAF) binds the potential tumor suppressor product p33ING1b.* Experimental Cell Research, 2006. **312**(1): p. 73-85.

48. Ha, S., et al., *Mouse ING1 homologue, a protein interacting with A1, enhances cell death and is inhibited by A1 in mammary epithelial cells.* Cancer Research, 2002. **62**(5): p. 1275-8.

49. Nourani, A., et al., *Opposite role of yeast ING family members in p53-dependent transcriptional activation.* Journal of Biological Chemistry, 2003. **278**(21): p. 19171-5.

50. Choy, J.S., et al., *Yng2p-dependent NuA4 histone H4 acetylation activity is required for mitotic and meiotic progression.* Journal of Biological Chemistry, 2001. **276**(47): p. 43653-62.

51. Shiseki, M., et al., *p29ING4 and p28ING5 bind to p53 and p300, and enhance p53 activity.* Cancer Research, 2003. **63**(10): p. 2373-8.

52. Cheung, K.J., Jr. and G. Li, *p33(ING1) enhances UVB-induced apoptosis in melanoma cells.* Experimental Cell Research, 2002. **279**(2): p. 291-8.

53. Chin, M.Y., K.C. Ng, and G. Li, *The novel tumor suppressor p33ING2 enhances UVB-induced apoptosis in human melanoma cells.* Experimental Cell Research, 2005. **304**(2): p. 531-43.

54. Helbing, C.C., et al., *A novel candidate tumor suppressor, ING1, is involved in the regulation of apoptosis.* Cancer Research, 1997. **57**: p. 1255-1258.

55. Toyama, T., et al., *p33(ING1b) stimulates the transcriptional activity of the estrogen receptor alpha via its activation function (AF) 2 domain.* Journal of Steroid Biochemistry and Molecular Biology, 2003. **87**(1): p. 57-63.

56. Tokunaga, E., et al., *Diminished expression of ING1 mRNA and the correlation with p53 expression in breast cancers.* Cancer Letters, 2000. **152**(1): p. 15-22.

57. Toyama, T., et al., *Suppression of ING1 expression in sporadic breast cancer.* Oncogene, 1999. **18**(37): p. 5187-5193.

58. Nouman, G.S., et al., *Downregulation of nuclear expression of the p33(ING1b) inhibitor of growth protein in invasive carcinoma of the breast.* Journal of Clinical Pathology, 2003. **56**(7): p. 507-11.

59. Caruso, M.L. and A.M. Valentini, *Overexpression of p53 in a large series of patients with hepatocellular carcinoma: a clinicopathological correlation.* Anticancer Research, 1999. **19**(5B): p. 3853-6.

60. Takahashi, M., et al., *Identification of the p33(ING1)-regulated genes that include cyclin B1 and proto-oncogene DEK by using cDNA microarray in a*

mouse mammary epithelial cell line NMuMG. Cancer Research, 2002. **62**(8): p. 2203-9.

61. Shimada, H., et al., *Facilitation of adenoviral wild-type p53-induced apoptotic cell death by overexpression of p33(ING1) in T.Tn human esophageal carcinoma cells.* Oncogene, 2002. **21**(8): p. 1208-16.

62. Kichina, J.V., et al., *Targeted disruption of the mouse ing1 locus results in reduced body size, hypersensitivity to radiation and elevated incidence of lymphomas.* Oncogene, 2006. **25**(6): p. 857-66.

63. Shinoura, N., et al., *Adenovirus-mediated transfer of p33ING1 with p53 drastically augments apoptosis in gliomas.* Cancer Research, 1999. **59**(21): p. 5521-8.

64. Nieuwkoop, P.D. and J. Faber, *Normal table of Xenopus laevis* 1956, Amsterdam: North Holland Publishing.

65. Krain, L.P. and R.J. Denver, *Developmental expression and hormonal regulation of glucocorticoid and thyroid hormone receptors during metamorphosis in Xenopus laevis.* The Journal of Endocrinology, 2004. **181**(1): p. 91-104.

66. Shi, Y.-B., *Amphibian Metamorphosis: From Morphology to Molecular Biology*. 1999, New York: John Wiley and Sons, Inc.

67. Tata, J.R., *Amphibian metamorphosis as a model for studying the developmental actions of thyroid hormone.* Annals of Endocrinology (Paris), 1998. **59**(6): p. 433-42.

68. Yaoita, Y. and D.D. Brown, *A correlation of thyroid hormone receptor gene expression with amphibian metamorphosis.* Genes and Development, 1990. **4**(11): p. 1917-24.

69. Kawahara, A., B.S. Baker, and J.R. Tata, *Developmental and regional expression of thyroid hormone receptor genes during Xenopus metamorphosis.* Development, 1991. **112**(4): p. 933-43.

70. Eliceiri, B.P. and D.D. Brown, *Quantitation of endogenous thyroid hormone receptors alpha and beta during embryogenesis and metamorphosis in Xenopus laevis.* Journal of Biological Chemistry, 1994. **269**(39): p. 24459-65.

71. Furlow, J.D. and D.D. Brown, *In vitro and in vivo analysis of the regulation of a transcription factor gene by thyroid hormone during Xenopus laevis metamorphosis.* Molecular Endocrinology, 1999. **13**(12): p. 2076-89.

72. Tata, J.R., *Amphibian metamorphosis as a model for the developmental actions of thyroid hormone.* Molecular and Cellular Endocrinology, 2006. **246**(1-2): p. 10-20.

73. Furlow, J.D. and E.S. Neff, *A developmental switch induced by thyroid hormone: Xenopus laevis metamorphosis.* Trends in Endocrinology and Metabolism, 2006. **17**(2): p. 40-7.

74. Buchholz, D.R., et al., *Molecular and developmental analyses of thyroid hormone receptor function in Xenopus laevis, the African clawed frog.* General and Comparative Endocrinology, 2006. **145**(1): p. 1-19.

75. Davis, P.J., F.B. Davis, and V. Cody, *Membrane receptors mediating thyroid hormone action.* Trends in Endocrinology and Metabolism, 2005. **16**(9): p. 429-35.

76. Bassett, J.H., C.B. Harvey, and G.R. Williams, *Mechanisms of thyroid hormone receptor-specific nuclear and extra nuclear actions.* Molecular and Cellular Endocrinology, 2003. **213**(1): p. 1-11.

77. Yamauchi, K., et al., *Purification and characterization of a 3,5,3'-L-triiodothyronine-specific binding protein from bullfrog tadpole plasma: a homolog of mammalian transthyretin.* Endocrinology, 1993. **132**(5): p. 2254-61.

78. Friesema, E.C., et al., *Thyroid hormone transport by the heterodimeric human system L amino acid transporter.* Endocrinology, 2001. **142**(10): p. 4339-48.

79. Friesema, E.C., et al., *Identification of monocarboxylate transporter 8 as a specific thyroid hormone transporter.* Journal of Biological Chemistry, 2003. **278**(41): p. 40128-35.

80. Ritchie, J.W., et al., *A role for thyroid hormone transporters in transcriptional regulation by thyroid hormone receptors.* Molecular Endocrinology, 2003. **17**(4): p. 653-61.

81. Shimada, N. and K. Yamauchi, *Characteristics of 3,5,3'-triiodothyronine (T3)-uptake system of tadpole red blood cells: effect of endocrine-disrupting chemicals on cellular T3 response.* The Journal of Endocrinology, 2004. **183**(3): p. 627-37.

82. Yamauchi, K., et al., *Xenopus cytosolic thyroid hormone-binding protein (xCTBP) is aldehyde dehydrogenase catalyzing the formation of retinoic acid.* Journal of Biological Chemistry, 1999. **274**(13): p. 8460-9.

83. Shi, Y.B., et al., *Tissue-dependent developmental expression of a cytosolic thyroid hormone protein gene in Xenopus: its role in the regulation of amphibian metamorphosis.* FEBS Letters, 1994. **355**(1): p. 61-4.

84. Katz, R.W. and R.J. Koenig, *Specificity and mechanism of thyroid hormone induction from an octamer response element.* Journal of Biological Chemistry, 1994. **269**(29): p. 18915-20.

85. Wu, Y., Y.Z. Yang, and R.J. Koenig, *Protein-protein interaction domains and the heterodimerization of thyroid hormone receptor variant alpha2 with retinoid X receptors.* Molecular Endocrinology, 1998. **12**(10): p. 1542-50.

86. Kim, S.W., et al., *A novel mechanism of thyroid hormone-dependent negative regulation by thyroid hormone receptor, nuclear receptor corepressor (NCoR), and GAGA-binding factor on the rat cD44 promoter.* Journal of Biological Chemistry, 2005. **280**(15): p. 14545-55.

87. Shen, X., et al., *Thyroid hormone regulation of prohormone convertase 1 (PC1): regional expression in rat brain and in vitro characterization of negative thyroid hormone response elements.* Journal of Molecular Endocrinology, 2004. **33**(1): p. 21-33.

88. Berghagen, H., et al., *Corepressor SMRT functions as a coactivator for thyroid hormone receptor T3Ralpha from a negative hormone response element.* Journal of Biological Chemistry, 2002. **277**(51): p. 49517-22.

89. Nygard, M., et al., *Thyroid hormone-mediated negative transcriptional regulation of Necdin expression.* Journal of Molecular Endocrinology, 2006. **36**(3): p. 517-30.

90. Qi, J.S., et al., *Regulation of the mdm2 oncogene by thyroid hormone receptor.* Molecular and Cellular Biology, 1999. **19**(1): p. 864-72.

91. Greenspan, F.S. and D.G. Gardner, *Basic and Clinical Endocrinology, 7th Edition*. 2004, New York: McGraw-Hill Companies.

92. Eckey, M., U. Moehren, and A. Baniahmad, *Gene silencing by the thyroid hormone receptor.* Molecular and Cellular Endocrinology, 2003. **213**(1): p. 13-22.

93. Yen, P.M., *Physiological and molecular basis of thyroid hormone action.* Physiological Reviews, 2001. **81**(3): p. 1097-142.

94. Malo, M.S., et al., *Thyroid hormone positively regulates the enterocyte differentiation marker intestinal alkaline phosphatase gene via an atypical response element.* Molecular Endocrinology, 2004. **18**(8): p. 1941-62.

95. Mengeling, B.J., F. Pan, and M.L. Privalsky, *Novel mode of deoxyribonucleic acid recognition by thyroid hormone receptors: thyroid hormone receptor beta-isoforms can bind as trimers to natural response elements comprised of reiterated half-sites.* Molecular Endocrinology, 2005. **19**(1): p. 35-51.

96. Wang, Z. and D.D. Brown, *Thyroid hormone-induced gene expression program for amphibian tail resorption.* Journal of Biological Chemistry, 1993. **268**(22): p. 16270-8.

97. Helbing, C.C., et al., *Expression profiles of novel thyroid hormone-responsive genes and proteins in the tail of Xenopus laevis tadpoles undergoing precocious metamorphosis.* Molecular Endocrinology, 2003. **17**(7): p. 1395-409.

98. Veldhoen, N., et al., *Distinctive gene profiles occur at key points during natural metamorphosis in the Xenopus laevis tadpole tail.* Developmental Dynamics, 2002. **225**(4): p. 457-68.

99. Gloss, B., et al., *Different configurations of specific thyroid hormone response elements mediate opposite effects of thyroid hormone and GC-1 on gene expression.* Endocrinology, 2005. **146**(11): p. 4926-33.

100. Havis, E., L.M. Sachs, and B.A. Demeneix, *Metamorphic T3-response genes have specific co-regulator requirements.* EMBO reports, 2003. **4**(9): p. 883-8.

101. Paul, B.D. and Y.B. Shi, *Distinct expression profiles of transcriptional coactivators for thyroid hormone receptors during Xenopus laevis metamorphosis.* Cell Research, 2003. **13**(6): p. 459-64.

102. Sachs, L.M. and Y.B. Shi, *Targeted chromatin binding and histone acetylation in vivo by thyroid hormone receptor during amphibian development.* Proceedings of the National Academy of Sciences (USA), 2000. **97**(24): p. 13138-43.

103. Dodd, M.H.I. and J.M. Dodd, *The biology of metamorphosis. In: Lofts, B. (Ed.), Physiology of Amphibia.* 1976, New York: Academic Press. 467–576.

104. Ensor, D.M., *Comparative Endocrinology of Prolactin*. 1978, London: Chapman & Hall.

105. Kikuyama, S., et al., *Aspects of amphibian metamorphosis: hormonal control.* International Review of Cytology, 1993. **145**: p. 105-48.

106. Tata, J.R., A. Kawahara, and B.S. Baker, *Prolactin inhibits both thyroid hormone-induced morphogenesis and cell death in cultured amphibian larval tissues.* Developmental Biology, 1991. **146**(1): p. 72-80.

107. Baker, B.S. and J.R. Tata, *Prolactin prevents the autoinduction of thyroid hormone receptor mRNAs during amphibian metamorphosis.* Developmental Biology, 1992. **149**(2): p. 463-7.

108. Huang, H. and D.D. Brown, *Prolactin is not a juvenile hormone in Xenopus laevis metamorphosis.* Proceedings of the National Academy of Sciences (USA), 2000. **97**(1): p. 195-9.

109. Hasunuma, I., K. Yamamoto, and S. Kikuyama, *Molecular cloning of bullfrog prolactin receptor cDNA: changes in prolactin receptor mRNA level during metamorphosis.* General and Comparative Endocrinology, 2004. **138**(3): p. 200-10.

110. Richards, C.M. and G.W. Nace, *Gynogenetic and hormonal sex reversal used in tests of the XX-XY hypothesis of sex determination in Rana pipiens.* Growth, 1978. **42**: p. 319-331.

111. Gray, K.M. and P.A. Janssens, *Gonadal hormones inhibit the induction of metamorphosis by thyroid hormones in Xenopus laevis tadpoles in vivo, but not in vitro.* General and Comparative Endocrinology, 1990. **77**(2): p. 202-11.

112. Hayes, T., R. Chan, and P. Licht, *Interactions of temperature and steroids on larval growth, development, and metamorphosis in a toad (Bufo boreas).* The Journal of Experimental Zoology, 1993. **266**(3): p. 206-15.

113. Hayes, T., *Steroids as Potential Modulators of Thyroid Hormone Activity in Anuran Metamorphosis.* American Zoologist, 1997. **37**: p. 185-194.

114. Yarwood, N.J., et al., *Estradiol modulates thyroid hormone regulation of the human glycoprotein hormone alpha subunit gene.* Journal of Biological Chemistry, 1993. **268**(29): p. 21984-9.

115. Yen, P.M., E.C. Wilcox, and W.W. Chin, *Steroid hormone receptors selectively affect transcriptional activation but not basal repression by thyroid hormone receptors.* Endocrinology, 1995. **136**(2): p. 440-5.

116. Schneider, M.J. and V.A. Galton, *Effect of glucocorticoids on thyroid hormone action in cultured red blood cells from Rana catesbeiana tadpoles.* Endocrinology, 1995. **136**(4): p. 1435-40.

117. Shih, A., et al., *Thyroid hormone promotes serine phosphorylation of p53 by mitogen-activated protein kinase.* Biochemistry, 2001. **40**(9): p. 2870-8.

118. Barrera-Hernandez, G., et al., *Thyroid hormone receptor is a negative regulator in p53-mediated signaling pathways.* DNA Cellular Biology, 1998. **17**(9): p. 743-50.

119. Bhat, M.K., et al., *Tumor suppressor p53 is a negative regulator in thyroid hormone receptor signaling pathways.* Journal of Biological Chemistry, 1997. **272**(46): p. 28989-93.

120. Yap, N., C.L. Yu, and S.Y. Cheng, *Modulation of the transcriptional activity of thyroid hormone receptors by the tumor suppressor p53.* Proceedings of the National Academy of Sciences (USA), 1996. **93**(9): p. 4273-7.

121. Zhao, X., et al., *Thyroid hormone can increase estrogen-mediated transcription from a consensus estrogen response element in neuroblastoma cells.* Proceedings of the National Academy of Sciences (USA), 2005. **102**(13): p. 4890-5.

122. Crump, D., et al., *Exposure to the herbicide acetochlor alters thyroid hormone-dependent gene expression and metamorphosis in Xenopus Laevis.* Environmental Health Perspectives, 2002. **110**(12): p. 1199-205.

123. Shi, Y.B. and V.C. Liang, *Cloning and characterization of the ribosomal protein L8 gene from Xenopus laevis.* Biochimica et Biophysica Acta, 1994. **1217**(2): p. 227-8.

124. Zhang, F., et al., *Evaluation of gene expression endpoints in the context of a Xenopus laevis metamorphosis-based bioassay to detect thyroid hormone disruptors.* Aquatic Toxicology, 2006. **76**(1): p. 24-36.

125. Cheung, K.J. and G. Li, ***The tumor suppressor ING1: structure and function.*** Experimental Cell Research, 2001. **268**: p. 1-6.

126. Leloup, I., M. Buscaglia, and A. de Luze, *[Modulation of T4 to T3 conversion. Comparative aspects (author's transl)].* Annals of Endocrinology (Paris), 1981. **42**(4-5): p. 454-60.

127. Zeremski, M., et al., *Localization of the candidate tumor suppressor gene ING1 to human chromosome 13q34.* Somatic Cell and Molecular Genetics, 1997. **23**(3): p. 233-236.

128. Sassone-Corsi, P., *Unique chromatin remodeling and transcriptional regulation in spermatogenesis.* Science, 2002. **296**(5576): p. 2176-8.

129. De Luca, A., et al., *p300/cAMP-response-element-binding-protein ('CREB')-binding protein (CBP) modulates co-operation between myocyte enhancer factor 2A (MEF2A) and thyroid hormone receptor-retinoid X receptor.* The Biochemical Journal, 2003. **369**(Pt 3): p. 477-84.

130. Minshull, J., et al., *A MAP kinase-dependent spindle assembly checkpoint in Xenopus egg extracts.* Cell, 1994. **79**(3): p. 475-86.

131. Buchholz, D.R., B.D. Paul, and Y.B. Shi, *Gene-specific changes in promoter occupancy by thyroid hormone receptor during frog metamorphosis. Implications for developmental gene regulation.* Journal of Biological Chemistry, 2005. **280**(50): p. 41222-8.

132. Szutorisz, H., N. Dillon, and L. Tora, *The role of enhancers as centres for general transcription factor recruitment.* Trends In Biochemical Sciences, 2005. **30**(11): p. 593-9.

133. Shibusawa, N., A.N. Hollenberg, and F.E. Wondisford, *Thyroid hormone receptor DNA binding is required for both positive and negative gene regulation.* Journal of Biological Chemistry, 2003. **278**(2): p. 732-8.

134. Latchman, D.S., *Transcription factors: bound to activate or repress.* Trends In Biochemical Sciences, 2001. **26**(4): p. 211-3.

135. Cuadrado, A., et al., *Neuronal HuD gene encoding a mRNA stability regulator is transcriptionally repressed by thyroid hormone.* Journal of Neurochemistry, 2003. **86**(3): p. 763-73.

136. Staton, J.M., A.M. Thomson, and P.J. Leedman, *Hormonal regulation of mRNA stability and RNA-protein interactions in the pituitary.* Journal of Molecular Endocrinology, 2000. **25**(1): p. 17-34.

137. Ing, N.H., *Steroid hormones regulate gene expression posttranscriptionally by altering the stabilities of messenger RNAs.* Biology of Reproduction, 2005. **72**(6): p. 1290-6.

138. Menon, K.M., et al., *Regulation of luteinizing hormone/human chorionic gonadotropin receptor expression: a perspective.* Biology of Reproduction, 2004. **70**(4): p. 861-6.

139. Kimura, N., et al., *Estradiol transcriptionally and posttranscriptionally up-regulates thyrotropin-releasing hormone receptor messenger ribonucleic acid in rat pituitary cells.* Endocrinology, 1994. **134**(1): p. 432-40.

140. O'Neill, M.J., *The influence of non-coding RNAs on allele-specific gene expression in mammals.* Hum Mol Genet, 2005. **14 Spec No 1**: p. R113-20.

141. Mattick, J.S. and I.V. Makunin, *Non-coding RNA.* Human Molecular Genetetics, 2006. **15 Spec No 1**: p. R17-29.

142. Zhu, Y.S., et al., *Estrogen and thyroid hormone interaction on regulation of gene expression.* Proceedings of the National Academy of Sciences (USA), 1996. **93**(22): p. 12587-92.

143. Belakavadi, M. and J.D. Fondell, *Role of the mediator complex in nuclear hormone receptor signaling.* Reviews of Physiology, Biochemistry and Pharmacology, 2006. **156**: p. 23-43.

144. Darimont, B.D., et al., *Structure and specificity of nuclear receptor-coactivator interactions.* Genes and Development, 1998. **12**(21): p. 3343-56.

145. Nolte, R.T., et al., *Ligand binding and co-activator assembly of the peroxisome proliferator-activated receptor-gamma.* Nature, 1998. **395**(6698): p. 137-43.

146. Shiau, A.K., et al., *The structural basis of estrogen receptor/coactivator recognition and the antagonism of this interaction by tamoxifen.* Cell, 1998. **95**(7): p. 927-37.

147. McInerney, E.M., et al., *Determinants of coactivator LXXLL motif specificity in nuclear receptor transcriptional activation.* Genes and Development, 1998. **12**(21): p. 3357-68.

148. Perissi, V. and M.G. Rosenfeld, *Controlling nuclear receptors: the circular logic of cofactor cycles.* Nature Reviews: Molecular Cell Biology, 2005. **6**(7): p. 542-54.

149. Li, J., et al., *Involvement of histone methylation and phosphorylation in regulation of transcription by thyroid hormone receptor.* Molecular and Cellular Biology, 2002. **22**(16): p. 5688-97.

150. Berry, D.L., et al., *The expression pattern of thyroid hormone response genes in remodeling tadpole tissues defines distinct growth and resorption gene expression programs.* Developmental Biology, 1998. **203**(1): p. 24-35.

151. Berry, D.L., R.A. Schwartzman, and D.D. Brown, *The expression pattern of thyroid hormone response genes in the tadpole tail identifies multiple resorption programs.* Developmental Biology, 1998. **203**(1): p. 12-23.

152. Euskirchen, G. and M. Snyder, *A plethora of sites.* Nature Genetics, 2004. **36**(4): p. 325-6.

153. Sanchez-Pacheco, A. and A. Aranda, *Binding of the thyroid hormone receptor to a negative element in the basal growth hormone promoter is associated with histone acetylation.* Journal of Biological Chemistry, 2003. **278**(41): p. 39383-91.

154. Oofusa, K., et al., *Expression of thyroid hormone receptor betaA gene assayed by transgenic Xenopus laevis carrying its promoter sequences.* Molecular and Cellular Endocrinology, 2001. **181**(1-2): p. 97-110.

155. Sachs, L.M., et al., *Nuclear receptor corepressor recruitment by unliganded thyroid hormone receptor in gene repression during Xenopus laevis development.* Molecular and Cellular Biology, 2002. **22**(24): p. 8527-38.

156. Sachs, L.M., et al., *Dual functions of thyroid hormone receptors during Xenopus development.* Comparative Biochemistry and Physiology Part B Biochemistry and Molecular Biology, 2000. **126**(2): p. 199-211.

157. Bannister, A.J. and T. Kouzarides, *Histone methylation: recognizing the methyl mark.* Methods in Enzymology, 2004. **376**: p. 269-88.

158. Paul, B.D., et al., *Coactivator recruitment is essential for liganded thyroid hormone receptor to initiate amphibian metamorphosis.* Molecular and Cellular Biology, 2005. **25**(13): p. 5712-24.

159. Kang, Z., O.A. Janne, and J.J. Palvimo, *Coregulator recruitment and histone modifications in transcriptional regulation by the androgen receptor.* Molecular Endocrinology, 2004. **18**(11): p. 2633-48.

160. Fondell, J.D., H. Ge, and R.G. Roeder, *Ligand induction of a transcriptionally active thyroid hormone receptor coactivator complex.* Proceedings of the National Academy of Sciences (USA), 1996. **93**(16): p. 8329-33.

161. Wong, C.W. and M.L. Privalsky, *Transcriptional repression by the SMRT-mSin3 corepressor: multiple interactions, multiple mechanisms, and a potential role for TFIIB.* Molecular and Cellular Biology, 1998. **18**(9): p. 5500-10.

162. Muscat, G.E., L.J. Burke, and M. Downes, *The corepressor N-CoR and its variants RIP13a and RIP13Delta1 directly interact with the basal transcription factors TFIIB, TAFII32 and TAFII70.* Nucleic Acids Research, 1998. **26**(12): p. 2899-907.

163. Xu, Y., et al., *Major histocompatibility class II transactivator (CIITA) mediates repression of collagen (COL1A2) transcription by interferon gamma (IFN-gamma).* Journal of Biological Chemistry, 2004. **279**(40): p. 41319-32.

164. Chan, A.Y., et al., *Influenza virus inhibits RNA polymerase II elongation.* Virology, 2006.

165. Cheng, C. and P.A. Sharp, *RNA polymerase II accumulation in the promoter-proximal region of the dihydrofolate reductase and gamma-actin genes.* Molecular and Cellular Biology, 2003. **23**(6): p. 1961-7.

166. Eissenberg, J.C. and A. Shilatifard, *Leaving a mark: the many footprints of the elongating RNA polymerase II.* Current Opinion in Genetics and Development, 2006. **16**(2): p. 184-90.

167. Beaudenon, S.L., et al., *Rsp5 ubiquitin-protein ligase mediates DNA damage-induced degradation of the large subunit of RNA polymerase II in Saccharomyces cerevisiae.* Molecular and Cellular Biology, 1999. **19**(10): p. 6972-9.

168. Weber, F. and C. Eng, *Gene-expression profiling in differentiated thyroid cancer--a viable strategy for the practice of genomic medicine?* Future oncology, 2005. **1**(4): p. 497-510.

169. Kondo, T., S. Ezzat, and S.L. Asa, *Pathogenetic mechanisms in thyroid follicular-cell neoplasia.* Nature Reviews: Cancer, 2006. **6**(4): p. 292-306.

170. Guernsey, D.L. and P.B. Fisher, *Thyroid hormone and neoplastic transformation.* Critical Reviews in Oncogenesis, 1990. **1**(4): p. 389-408.

171. Li, Q., et al., *Modification of Chromatin Structure by the Thyroid Hormone Receptor.* Trends in Endocrinology and Metabolism, 1999. **10**(4): p. 157-164.

172. el-Deiry, W.S., *Regulation of p53 downstream genes.* Seminars in Cancer Biology, 1998. **8**(5): p. 345-57.

173. Fraga, M.F. and M. Esteller, *Towards the human cancer epigenome: a first draft of histone modifications.* Cell Cycle, 2005. **4**(10): p. 1377-81.

174. Lund, A.H. and M. van Lohuizen, *Epigenetics and cancer.* Genes and Development, 2004. **18**(19): p. 2315-35.

175. Jelaso, A.M., et al., *Dietary exposure to Aroclor 1254 alters gene expression in Xenopus laevis frogs.* Environmental Research, 2005. **98**(1): p. 64-72.

176. Khan, M.A., et al., *The hypothalamo-pituitary-thyroid (HPT) axis: a target of nonpersistent ortho-substituted PCB congeners.* Toxicological Sciences, 2002. **65**(1): p. 52-61.

177. Wang, S.L., et al., *In utero exposure to dioxins and polychlorinated biphenyls and its relations to thyroid function and growth hormone in newborns.* Environmental Health Perspectives, 2005. **113**(11): p. 1645-50.

178. Kawano, M., et al., *Hydroxylated polychlorinated biphenyls (OH-PCBs): recent advances in wildlife contamination study.* Environmental Sciences, 2005. **12**(6): p. 315-24.

179. Tabuchi, M., et al., *PCB-Related Alteration of Thyroid Hormones and Thyroid Hormone Receptor Gene Expression in Free-Ranging Harbor Seals (Phoca vitulina).* Environmental Health Perspectives, 2006. **114**(7): p. 1024-1031.

180. Watanabe, I. and S. Sakai, *Environmental release and behavior of brominated flame retardants.* Environment International, 2003. **29**(6): p. 665-82.

181. Kitamura, S., et al., *Anti-thyroid hormonal activity of tetrabromobisphenol A, a flame retardant, and related compounds: Affinity to the mammalian thyroid hormone receptor, and effect on tadpole metamorphosis.* Life Sciences, 2005. **76**(14): p. 1589-601.

182. Veldhoen, N., et al., *Exposure to tetrabromobisphenol-A alters TH-associated gene expression and tadpole metamorphosis in the Pacific tree frog Pseudacris regilla.* Aquatic Toxicology, 2006. **78**(3): p. 292-302.

183. Legler, J. and A. Brouwer, *Are brominated flame retardants endocrine disruptors?* Environment International, 2003. **29**(6): p. 879-85.

184. Veldhoen, N. and C.C. Helbing, *Detection of environmental endocrine-disruptor effects on gene expression in live Rana catesbeiana tadpoles using a tail fin biopsy technique.* Environmental Toxicology and Chemistry, 2001. **20**(12): p. 2704-8.

APPENDIX I. ABBREVIATIONS

°C	Degree Celsius
µ	micro
µL	microlitre
aa	Amino Acid
ACTH	Adrenocorticotropin Releasing Hormone
AFP	α-Fetoprotein
ALDH1	Aldehyde Dehydrogenase Class 1
Amp	Ampicillin
AR	Androgen Receptor
Bax	Bcl-2-Associated X Protein
Bcl-2	B-Cell Lymphoma Protein 2
bp	Base Pair
BRG1	Brahma-Related Gene 1
$CaCl_2$	Calcium Chloride
cAMP	Cyclic Adenosine Monophosphate
CBP	CREB-binding protein
cDNA	Complementary Deoxyribonucleic Acid
ChIP	Chromatin Immunoprecipitation
CoRNR box	Corepressor-Nuclear-Receptor Box
CREB	cAMP-Response Element-Binding Protein

CRF	Corticotropin Releasing Factor
CTD	C-Terminal Domain
CTHBP	Cytoplasmic TH Binding Proteins
D2	Type II Deiodinase
D3	Type III Deiodinase
Da	Dalton
DEPC	Diethylpyrocarbonate
DMSO	Dimethylsulfoxide
DNA	Deoxyribonucleic Acid
dNTP	Deoxynucleotidetriphosphate
DTT	Dithiothreitol
E_2	17β-Estradiol
ECL	Enhanced Chemiluminescence
EDC	Endocrine Disrupting Compound
EDTA	N,N'-1,2-Ethanediylbis(N-(Carboxymethyl)Glycine)Edetic Acid
EGTA	O,O'-Bis(2-Aminoethyl)Ethyleneglycol-N,N,N',N'-Tetraacetic Acid
EMSA	Electrophoretic Mobility Shift Assay
ERE	Estrogen Response Elements
ERα	Estrogen Receptor Alpha
EtBr	Ethidium Bromide
EtOH	Ethanol

GH	Growth Hormone
GR	Glucocorticoid Receptor
GRE	Glucocorticoid Response Element
GST	Glutathione-S-Transferase
h	hour
H3K4	Histone H3 Lysine 4
HAT	Histone Acetyltransferase
HBO1	Histone Acetyltransferase Binding to ORC1
HDAC	Histone Deacetylase
HEPES	4-(2-Hydroxyethyl)-1-Piperazineethanesulfonic Acid
HNF1	Hepatocyte Nuclear Factor 1
HRE	Hormone Response Element
HRP	Horse Radish Peroxidase
IAP	Intestinal Alkaline Phosphatase
Ig	Immunoglobulin
ING	Inhibitor of Growth
IP	Immunoprecipitation
IPTG	Isopropyl-β-D-Thiogalactopyranoside
k	kilo
KCl	Potassium Chloride
K_d	Dissociation Constant

kDa	kiloDalton
LAT1	Light Chain Amino Acid Transporter 1
LB medium	Luria-Bertani Medium
LZL	Leucine Zipper-Like Domain
m	milli
M	molarity
MAPK	Mitogen-Activated Protein Kinase
MCT8	Monocarboxylate Transporter 8
MDM2	Murine Double Minute 2
mg	milligram
$MgCl_2$	Magnesium Chloride
min	minute
mL	millitre
mM	millimolar
MORPH	MOZ-related factor
MOZ	Monocytic Leukemia Zinc Finger Protein
MR	Mineralocorticoid Receptor
mRNA	Messenger RNA
NaCl	Sodium Chloride
$NaH_2PO_4H_2O$	Sodium Phosphate
$NaHCO_3$	Sodium Bicarbonate

NaOH	Sodium Hydroxide
NCoA	Nuclear Receptor Co-Activator
NCoR	Nuclear Receptor Co-Repressor
NF	Nieuwkoop and Faber
NF-κB	Nuclear Factor- κB
NLS	Nuclear Localization Signal
nm	nanometre
NR	Nuclear Receptor
nTRE	Negative TRE
NTS	Nucleolar Translocation Sequence
NuA4	Nucleosomal Acetyl-Transferase of Histone H4
ORF	Open Reading Frame
P/CAF	p300/CBP-Associated Factor
p160/SRCs	Steroid Receptor Co-Activators
$p21^{CIP1}$	cyclin-dependent kinase inhibitor 1A, 21 kDa protein
PAGE	Polyacrylamide Gel Electrophoresis
PBDE	Polybrominated Diphenyl Ether
PBS	Phosphate-Buffered Saline
PBST	PBS Tween 20
PCB	Polychlorinated Biphenyls
pCIP	CBP-Interacting Protein

PCNA	Proliferating Cell Nuclear Antigen
PCR	Polymerase Chain Reaction
PCR domain	Potential Chromatin Regulation Domain
PDIM	Phosphorylation-Dependent Interacting Motif
PHD finger	Plant Homeodomian Finger
PIM	Peptide Interacting Motif
PIP	PCNA-Interacting Protein
pmol	picomole
PMSF	Phenylmethylsulphonylfluoride
PPAR	Peroxisome Proliferating Antigen Receptor
PR	Progesterone Receptor
PRL	Prolactin
PtdIns(5)P	Phosphatidylinositol 5-Phosphate
pTRE	Positive TRE
QPCR	Quantitative PCR
RACE	Random Amplification of cDNA Ends
RAR	Retinoic Acid Receptor
Ras	Rat Sarcoma Viral Oncogene Homolog
RevErbA	Reverse Erythroblastic Leukemia Viral Oncogene Homolog; Reverse TRα
RNA	Ribonucleic Acid

RNA Pol II	RNA Polymerase II
rT_3	Reverse T_3
RT-PCR	Reverse Transcription - Polymerase Chain Reaction
RXR	Retinoid X Receptor
s	second
SAP30	Sin3A-Associated Protein, 30 kDa
SDS	Sodium Dodecyl Sulfate
SDS-PAGE	Sodium Dodecyl Sulfate-Polyacrylamide Gel Electrophoresis
Sir2	sirtuin 2
SMRT	Silencing Mediator of Retinoid and Thyroid Hormone Receptors
SRC	Steroid Receptor Coactivator
T_3	3,5,3'-Triiodothyronine
T_4	3,5,3',5'-tetraiodo-L-thyronine;Thyroxine
TAF	TBP Associated Factor
Taq	Thermus Aquaticus
TBBPA	Tetrabromobisphenol A
TBG	Thyroxine Binding Globulin
TBP	TATA Box Binding Protein
TFIIB	Transcription Factor IIB
TH	Thyroid Hormone
TH/bZIP	TH-Responsive Basic Leucine Zipper Transcription Factor

TPT1	Tumor Protein Translationally Controlled
TRAP220	TR-associated protein 220
TRAP	Thyroid Hormone Receptor Associated Protein
TRE	Thryoid Hormone Response Element
TRH	Thyrotropin Releasing Hormone
Tris-HCl	Tris(hydroxymethyl)aminomethane Hydrochloride
TRRAP	Transformation/Transcription Domain-Associated Protein
TR	Thyroid Hormone Receptor
TSH	Thyroid Stimulating Hormone
TTR	Transthyretin
UV	Ultraviolet
VDR	Vitamin D Receptor
WB	Western Blot
Zn^{2+}	Zinc
$ZnSO_4$	Zinc Sulfate

APPENDIX2. SEQUENCE OF *XENOPUS LAEVIS ING2* INTRON

GTGAGTTGTCTGTCAGTGTTGTGGGGGAGGGGCAATACCGTCGGTGTAGCT
ATAGGGCATCCACACTTCCCATCGCCCCTCCGTGAGACGATCCATCTGTGC
TCGTACATCAGACTGGCGCAGCGAGGGTTACTGCTTACTCGCGGTTATTTG
CCCCCCAAAGTCTACTCTCAGGGTTCCCCACACGTGGCGGGTGTCCCCCC
CTTCTGTAGCGATCTCACTCACGAGTGCACCTCACTGAACTCAACCCTACAC
GGAGTTCGGGGCTTATGGGAGCTGTAGTTGAGCAACAGTTGTGCATCGGTT
TGTCGTGTAGATTATATGCAAACACTTCTACCCAGTCACACAGGGAGAGCGT
CCCATTTACTTGCTAACACGCGGCCCTCCACATATTGAACAATTACAAATGA
ACAGGGAGGTTTACGTGGGATGCTGGGAGTTGTAGTTGTTTTTACTTGCGG
AGCATTAGCCTGCCCTGTGGGTGTATAGATGCTACTGTTACAGGCGAGCTG
GGAGTTTTGCGCTGTAATGTGTGGGGTTGGGGCTTATAGTGGCGCTGTCAA
TGATCACTGGGGGCAGGGCGGTGGCGTCATATCCGGGGCGGATACCCCTG
GCAAAGAAGGAAATCTGAAAAAGGTGCTGCTAAGGGGAGGGGTTTCTGTGC
ATAGATAGGTTTATAAGGCACATACGGGCTAGAGACTTCACTCTGTATTATT
TGCTATACTTCTCATGCAAAGGGTTATTGGGAGTTCTAGCTGCGCAAGTTTG
TCTGTCTATTGCACTAAGAAGTGACCCAACATTGAAATGGGCGGTGGCGGC
GAAACATAGGACAGGGAGGTTATAATGCGAGTGGCTAGTGGGCGGAACAA
GGAGGAGGTGGGGTTGATGCTAGTCACGTGGGAGGCGACACGGTGGGAG
AAGGGGGGGCTTGGCTAGATGGGAGGGGCGAGGCGCTATGGGCAGTGAC
TTAGACAGAGGGGTGGCACGCAGACTGGATAGAAAAAGAGGAGGAGGAGC
TACTGGTGTCGGCTTGAAGTGAGGCTTAGTGGGGAGGGGAGGGGAAGCTA
AAGTGGTTGGGGGTTGTGTTAAGGGACGCTAAATACAAGGAGTACGTTTAT
ATATTCCTTCTTGACATTTACCTGAATTCTAAAATCCTTGTACTTCTACTTTCT
CCCATATATTCATAATGATCGTCTGTAAGTGGCTTGTATCACCGTTGTACGG
CTTGGGGGCCATTCTCAGACCCTGCGCAACTGTTGCCCCTGACAACCAGTC
TATTTACCAAAGGCCTGTATTTACCAGCACATTATCATCTTTAACAATTCAGC
CAGAATGGAAATGCTTCTAGTTACTTCCTGATTATTTTGCTTCATCTGATAAC
AAGCTGCCTACACTGCCACAACTGAGATAGGGGGATGATTTGGTGCAATAG
TCTGCAAACGACTAAATCTGATCCCGTTGCTCAGCCTGTCAAGAGTACAGAC
CTAGCCTGCATTGGGTAATGCACATTTGCAGCTTAGCCTTTAATATAACTAA
ATAGTATGTTTTTTTTTTTTATTGTTTACAG

APPENDIX 3. *XENOPUS TROPICALIS ING2* ORF SEQUENCE ASSEMBLED

ATGTTAGGGCAACAACAGCAACACTTGCACTACTCCCCGGGGAGCTCGGC
GGCGGAGGACGGCCAGCTGGTGAGCTATGTGGAGGAGTACTTGGAGTGCG
TGGAGTCGTTGCCGTTGGAAATCCAGAGGAGCGTCACTTTGCTACGGGAGA
TCGATAGCCAGTACCGGG**A**AGCTCTAAAAGAAGTTGATGATGTTTTTGAAAA
ACATTCAAATGAAACTGATGCTAATCAGAAAAAGCGACTCTTGCAGCAGCTT
CAGAGAGCCCTCATTGTGACCCAGGAGCTTGGCGATGATAAAATACAGCTA
GTTACCCAAGTGTTTGAGTTGATAGAGAACAGGACGAAGCAAATGGAATCT
CTCTGCCAAGGCTTCTTTGATCAAGAAGAGAGTGAAAAGTCTGTGGAAAAAT
CTAAAGTTGAATCAAATGCATCTGAAAGGTCTACACGTAGACCTCGCAGGCA
GCGCAACAGCGAGAGCCGGGAGTTATGTCACATGGTCAATGGGATGGATG
ACATCGAAGAGCAGCCACCAAAAGAAAAGAAATCAAAGTCGTCCAAAAAGA
AAAAACGTTCCAAAGCCAAGCAAGAAAGAGAGGCATCCCCTATACCTTTTGC
AATTGACCCCAACGAGCCCACGTACTGTCTGTGCAATCAGGTGTCTTATGGT
GAGATGATAGGATGTGATAATGACGAGTGCACCATAGAGTGGTTCCATTTCT
CTTGTGTTGGACTTACCTACAAACCAAAGGGCAAATGGTATTGTCCTGACTG
CAGAGGAGACAATGAAAAGACTATGAACAAAAACACAGATAAAACAAAAAAG
GACAGACGGTCGAGGTAG

NOTE: START OF EXON 2 IS BOLD AND UNDERLINED

APPENDIX 4. *XENOPUS TROPICALIS ING1* ORF SEQUENCE ASSEMBLED

ATGCTGAGCCCGGCAAACGGAGAGCACATTCACATGGTCAACTATGTGGAG
GATTACCTAGACTCCATCGAGTCTCTGCCTTTTGATCTCCAAAGAAATGTAT
CTTTGATGAGGGAGATCGACGCCAAATACCAAG**A**AATCCTAAAAGAATTGG
ATGACTACTATGAAAAGTTTAAACGTGAATCGGATTCAGGCCAGAAAAAGCG
ACTTTTGCAATTTATCCAGCGAGCTCTTATTCGTAGTCAAGAACTCGGTGAT
GACAAAATCCAGATAGTAAGCCAAATGGTGGAGTTGGTTGAGAACAGGACA
AGGCAGGTAGACAGCCACGTGGAACTGTTTGAGACTTGCCAGGATTTAAAT
GACAGTACAAGCAACAGCAGCAAAAACAACCAGGAAAAACCCAAAAATGAG
GCCATTGCCCAGACCGAGAAGTCCAGCAATAAAAGATCAAGGAGACAGCG
GAACAATGAAAATAGAGAAAATTCAACCATCAACCATGACCACGATGACCTC
AGTTCAGGAACGCCCAAGGAAAAGAAGTCAAAACCATCAAAGAAGAAAAAG
AGGTCCAAAGCCAAAGCTGAACGAGAGGCCTCCCCTGCCGATCTTCCAATT
GATCCTAATGAACCCACATACTGTCTGTGCAATCAAGTTTCATATGGAGAAA
TGATTGGCTGTGATAATGAGGAATGCCCCATTGAGTGGTTTCACTTTTCTTG
TGTTGGACTAAATCATAAACCGAAAGGAAAATGGTACTGTCCTGAATGTAGA
GGAGAGAATGAAAAAACCATGGGAAAAGCACTTGAGAAGTCTAAAAAAGAA
AGGACATATAATAGGTAG

NOTE: START OF EXON 2 IS BOLD AND UNDERLINED

APPENDIX 5. ORFS OF HIS-TAGGED PROTEIN CONSTRUCTS

A) ING1 (287 aa)

```
  1 atggtgagcccggcaaacggagagcacattcacatggtgaactat
    M  V  S  P  A  N  G  E  H  I  H  M  V  N  Y
 46 gtagagggttacctggactccatcgagtctctgcctttcgacctg
    V  E  G  Y  L  D  S  I  E  S  L  P  F  D  L
 91 caaagaaatgtctctctcatgagggagatcgacgccaaataccaa
    Q  R  N  V  S  L  M  R  E  I  D  A  K  Y  Q
136 gaaatcctaaaagaattggatgactactatgaaaagttcaagcat
    E  I  L  K  E  L  D  D  Y  Y  E  K  F  K  H
181 gaatctgatgcagtccaaaaaaagcgtcttttgcagttcatccag
    E  S  D  A  V  Q  K  K  R  L  L  Q  F  I  Q
226 cgagctcttattcgtagtcaagaacttggtgatgacaaaatccag
    R  A  L  I  R  S  Q  E  L  G  D  D  K  I  Q
271 atagtgagccaaatggtggagttggttgagaacaggaccaggcag
    I  V  S  Q  M  V  E  L  V  E  N  R  T  R  Q
316 gtagacagccacgtggaactgtttgagacttgccaggatttgaat
    V  D  S  H  V  E  L  F  E  T  C  Q  D  L  N
361 gacagtacaagcaacagcagcaaaaacaaccaggaaaaatccaaa
    D  S  T  S  N  S  S  K  N  N  Q  E  K  S  K
406 aatgaggccattgtccagactgaaaagcccagcaataaaagatcc
    N  E  A  I  V  Q  T  E  K  P  S  N  K  R  S
451 aggagacagcggaacaatgaaaacagggaaaattcaaccatcaac
    R  R  Q  R  N  N  E  N  R  E  N  S  T  I  N
496 catgaccatgatgatctcacttcaggaacgcccaaggaaaagaag
    H  D  H  D  D  L  T  S  G  T  P  K  E  K  K
541 gcaaaaccatcgaagaagaaaaagagatccaaagccaaagctgaa
    A  K  P  S  K  K  K  K  R  S  K  A  K  A  E
586 cgagaggcctcacctgctgatcttccaatcgatcccaatgaaccc
    R  E  A  S  P  A  D  L  P  I  D  P  N  E  P
631 acatactgcctgtgcaatcaagtttcttatggtgaaatgattggc
    T  Y  C  L  C  N  Q  V  S  Y  G  E  M  I  G
676 tgtgataatgaagaatgccccattgagtggtttcacttttcttgt
    C  D  N  E  E  C  P  I  E  W  F  H  F  S  C
721 gttggactcaatcacaaaccaaaaggaaaatggtactgtcctgaa
    V  G  L  N  H  K  P  K  G  K  W  Y  C  P  E
766 tgtagaggagagaatgagaaaaccatggggaaagcacttgagaaa
    C  R  G  E  N  E  K  T  M  G  K  A  L  E  K
811 tctaaaaaagaaaggacatataacaggctcgagcaccaccaccac
    S  K  K  E  R  T  Y  N  R  L  E  H  H  H  H
856 caccactga 864
    H  H  *
```

B) ING2 (286 aa)

```
  1 atggtagggcaacagcagcacttgcactactccccagggagctcg
    M  V  G  Q  Q  Q  H  L  H  Y  S  P  G  S  S
 46 gcggcggaggacagccaactggtgagctatgtggaggagtacctg
    A  A  E  D  S  Q  L  V  S  Y  V  E  E  Y  L
 91 gagtgcgtggagtcgttgccgttggaaatccagaggagcgtcact
```

```
    E  C  V  E  S  L  P  L  E  I  Q  R  S  V  T
136 ctgttgcgggagatcgatagccagtaccgggaagctctgaaagaa
    L  L  R  E  I  D  S  Q  Y  R  E  A  L  K  E
181 gtcgatgatgtttttgaaaaacattcaaacgaaagtgacgctaat
    V  D  D  V  F  E  K  H  S  N  E  S  D  A  N
226 cacaaaaagcgactgctgcagcagcttcagagggccctcattatg
    H  K  K  R  L  L  Q  Q  L  Q  R  A  L  I  M
271 acccaggagcttggcgatgataaaatacagctagttacacaagtg
    T  Q  E  L  G  D  D  K  I  Q  L  V  T  Q  V
316 tttgagttcatagaaaacaggacaaagcaaatggaatctctttgc
    F  E  F  I  E  N  R  T  K  Q  M  E  S  L  C
361 aagggcttctttgatcaggaagagagtgacaagtctatggaaaaa
    K  G  F  F  D  Q  E  E  S  D  K  S  M  E  K
406 tctaaagttgagtcaaatgcatctgaaaggtctacacgtaggcct
    S  K  V  E  S  N  A  S  E  R  S  T  R  R  P
451 cgcagacagcgcaatagtgagagccacgacttgtgtcacatggtc
    R  R  Q  R  N  S  E  S  H  D  L  C  H  M  V
496 aatgggatggatgaccttgaagagcagcccccgaaagagaagaaa
    N  G  M  D  D  L  E  E  Q  P  P  K  E  K  K
541 tcaaaatcatccaaaaagaaaaaacgctccaaagccaagcaagag
    S  K  S  S  K  K  K  K  R  S  K  A  K  Q  E
586 agagaggtgtcccctatacctttgcaattgaccccaatgagcca
    R  E  V  S  P  I  P  F  A  I  D  P  N  E  P
631 acgtactgtctgtgcaatcaggtgtcttttggtgagatgattgga
    T  Y  C  L  C  N  Q  V  S  F  G  E  M  I  G
676 tgtgataatgacgagtgcaccatagagtggttccatttctcttgc
    C  D  N  D  E  C  T  I  E  W  F  H  F  S  C
721 gttggacttacctacaaaccaaagggcaaatggtattgtcctgac
    V  G  L  T  Y  K  P  K  G  K  W  Y  C  P  D
766 tgcagaggagacaatgaaaagactatgaacaaaaacacggataaa
    C  R  G  D  N  E  K  T  M  N  K  N  T  D  K
811 acaaaaaaagacagacggtcgaggctcgagcaccaccaccaccac
    T  K  K  D  R  R  S  R  L  E  H  H  H  H  H
856 cactga 861
    H  *
```

C) TRα (417 aa)

```
  1 atggaccagaatctcagcgggctggactgcttgtcagagccagat
    M  D  Q  N  L  S  G  L  D  C  L  S  E  P  D
 46 gaaaaaaggtggccggatgggaagcgaaaaagaaagaacagccaa
    E  K  R  W  P  D  G  K  R  K  R  K  N  S  Q
 91 tgtatgggaaaaagcggcatgtccggtgacagcttggtgtctctg
    C  M  G  K  S  G  M  S  G  D  S  L  V  S  L
136 ccctctgcagggtacatccccagctatctggacaaagatgagcca
    P  S  A  G  Y  I  P  S  Y  L  D  K  D  E  P
181 tgcgtggtgtgcagtgataaggccacggggtaccactaccgctgt
    C  V  V  C  S  D  K  A  T  G  Y  H  Y  R  C
226 atcacttgcgaggggtgtaagggtttctttcgccgcaccatccag
    I  T  C  E  G  C  K  G  F  F  R  R  T  I  Q
271 aagaacctgcacccctcctactcgtgcaagtacgatggctgctgc
    K  N  L  H  P  S  Y  S  C  K  Y  D  G  C  C
316 attatcgacaagatcacccgaaatcagtgccagctctgccgcttc
    I  I  D  K  I  T  R  N  Q  C  Q  L  C  R  F
361 aagaaatgcattgccgttggcatggcaatggatcttgtcctggat
```

```
    K  K  C  I  A  V  G  M  A  M  D  L  V  L  D
406 gatggcaagcgggtagccaagcgaaaactgattgaagagaatcga
    D  G  K  R  V  A  K  R  K  L  I  E  E  N  R
451 cagcggcggcggaaggaggagatgatcaagactctgcaacagcgt
    Q  R  R  R  K  E  E  M  I  K  T  L  Q  Q  R
496 cccgagccaagcagcgaggagtgggagttgattcgcattgtaaca
    P  E  P  S  S  E  E  W  E  L  I  R  I  V  T
541 gaagctcacaggagtaccaatgctcagggcagccactggaaacag
    E  A  H  R  S  T  N  A  Q  G  S  H  W  K  Q
586 cgtaggaagtttctgccggaagatatcgggcagtctcccatggct
    R  R  K  F  L  P  E  D  I  G  Q  S  P  M  A
631 tccatgccggatggggataaagttgacctggaagctttcagtgag
    S  M  P  D  G  D  K  V  D  L  E  A  F  S  E
676 ttcaccaagataatcaccccggcaattaccagagtggtggacttt
    F  T  K  I  I  T  P  A  I  T  R  V  V  D  F
721 gccaagaagctgcccatgttctctgagctgacttgtgaagaccag
    A  K  K  L  P  M  F  S  E  L  T  C  E  D  Q
766 atcatcctgttgaaaggatgttgtatggagatcatgtctctccgt
    I  I  L  L  K  G  C  C  M  E  I  M  S  L  R
811 gctgctgtacgctacgatccagacagcgagaccctaacgctgagc
    A  A  V  R  Y  D  P  D  S  E  T  L  T  L  S
856 ggagagatggctgtgaaacgggagcagcttaagaacggaggtctg
    G  E  M  A  V  K  R  E  Q  L  K  N  G  G  L
901 ggtgttgtctctgatgccatctttgacctcgggaggtcgcttgct
    G  V  V  S  D  A  I  F  D  L  G  R  S  L  A
946 gcgtttaaccttgacgatacggaagtggcgctgctgcaggctgtt
    A  F  N  L  D  D  T  E  V  A  L  L  Q  A  V
991 ttgctaatgtcatcagaccgaactggtttaatctgcacggacaag
    L  L  M  S  S  D  R  T  G  L  I  C  T  D  K
1036 atagagaaatgtcaagagacctaccttctcgcctttgaacactac
    I  E  K  C  Q  E  T  Y  L  L  A  F  E  H  Y
1081 atcaaccatcgcaaacacaacattccccacttctggcccaaactc
    I  N  H  R  K  H  N  I  P  H  F  W  P  K  L
1126 ctaatgaaggtgacggacctgcgcatgataggggcatgccatgcc
    L  M  K  V  T  D  L  R  M  I  G  A  C  H  A
1171 agccgctttctgcacatgaaggtcgagtgccccaccgagctcttt
    S  R  F  L  H  M  K  V  E  C  P  T  E  L  F
1216 ccaccgctcttccttgaggtctttgaggaccaggaagtt 1254
    P  P  L  F  L  E  V  F  E  D  Q  E  V
```

D) TRβ (377 aa)

```
   1 atggaagggtatatacccagctacttggataaagatgagctatgc
     M  E  G  Y  I  P  S  Y  L  D  K  D  E  L  C
  46 gtggtgtgtggagacaaggctacagggtatcattatagatgtatc
     V  V  C  G  D  K  A  T  G  Y  H  Y  R  C  I
  91 acctgcgagggctgcaagggctttttttagaagaactattcagaag
     T  C  E  G  C  K  G  F  F  R  R  T  I  Q  K
 136 aacctccacccaagctattcttgtaaatatgaaggaaaatgtgtt
     N  L  H  P  S  Y  S  C  K  Y  E  G  K  C  V
 181 atagacaaagtaacaagaaaccagtgccaagaatgtcgcttcaaa
     I  D  K  V  T  R  N  Q  C  Q  E  C  R  F  K
 226 aagtgcatcgctgttggaatggcaacagacttggttttggatgac
     K  C  I  A  V  G  M  A  T  D  L  V  L  D  D
 271 aacaaacgtttggcaaaaagaaagctcatagaagaaaacagagaa
```

```
    N  K  R  L  A  K  R  K  L  I  E  E  N  R  E
316 aaaagacggaaagatgagattcagaaatcacttgttcagaaacct
    K  R  R  K  D  E  I  Q  K  S  L  V  Q  K  P
361 gaacccacacaagaagaatgggagttgatacaagttgtcactgaa
    E  P  T  Q  E  E  W  E  L  I  Q  V  V  T  E
406 gcacatgtggccaccaacgcacagggaagccactggaaacagaaa
    A  H  V  A  T  N  A  Q  G  S  H  W  K  Q  K
451 agaaaatttttgccagaggacattggacaagctcccatagttaat
    R  K  F  L  P  E  D  I  G  Q  A  P  I  V  N
496 gcgcccgagggtggaaaagtggacttagaagccttcagccagttt
    A  P  E  G  G  K  V  D  L  E  A  F  S  Q  F
541 acaaaaataatcaccccagcaattacaagagttgttgattttgcc
    T  K  I  I  T  P  A  I  T  R  V  V  D  F  A
586 aaaaagctacctatgttttgtgagctgccatgtgaagaccagatc
    K  K  L  P  M  F  C  E  L  P  C  E  D  Q  I
631 atccttcttaaaggctgttgtatggagatcatgtcgctccgagca
    I  L  L  K  G  C  C  M  E  I  M  S  L  R  A
676 gcagtgcgttatgaccccgaaagtgaaactctaacgttaaatggt
    A  V  R  Y  D  P  E  S  E  T  L  T  L  N  G
721 gagatggcagtgacaaggggcagctaaaaaatggaggacttgga
    E  M  A  V  T  R  G  Q  L  K  N  G  G  L  G
766 gtggtttcagatgccatctttgacttaggggtatcgctttcttca
    V  V  S  D  A  I  F  D  L  G  V  S  L  S  S
811 ttcagtcttgatgataccgaagtcgccttgttgcaggctgtgctg
    F  S  L  D  D  T  E  V  A  L  L  Q  A  V  L
856 cttatgtcatcagatcggcctggtcttgctagcgtggagagaata
    L  M  S  S  D  R  P  G  L  A  S  V  E  R  I
901 gaaaagtgccaggaaggtttcctcttggcttttgaacactacatt
    E  K  C  Q  E  G  F  L  L  A  F  E  H  Y  I
946 aattacaggaaacataacattgcacacttttggccaaaactgctg
    N  Y  R  K  H  N  I  A  H  F  W  P  K  L  L
991 atgaaagtcaccgacctccgcatgattggagcgtgccacgccagc
    M  K  V  T  D  L  R  M  I  G  A  C  H  A  S
1036 cggttcctgcacatgaaggtggagtgccccactgaactgtttccc
    R  F  L  H  M  K  V  E  C  P  T  E  L  F  P
1081 ccactgttcttggaagtgtttgaggacctcgagcaccaccaccac
    P  L  F  L  E  V  F  E  D  L  E  H  H  H  H
1126 caccactga 1134
    H  H  *
```

APPENDIX 6. *ING1* GENOMIC SEQUENCES

A) *xING1b4*

CTGGCAGTAACAGCAGCGCTGTCAACGTGGTTAAAGGGACAGCACAGACG
TGGCTGAAGTATAGTAAGGGCACAATTGTCTCTATGTCTCACTGCAGCACTC
TGGCCTTGTTACACATTTAACGCCTGCACCATGAGCAGTATCGGTGTCCATG
ACAATCATTCCCTCTATATTAGTATGTAAATAGTGACGGCCGCACGTCGGAC
CTGCCTCTTTCCTCCAGAGGCGGAGCTTCTGTTGATAGCAACACAACTCTG
CGCACGCGCAATGCCAGCTATTTAAAGGGGAGGCGAATGTTTCTTAAGTGT
TTCAAACTGCTCTCCCTACTTTGTATGTAGCGTATGTGGGGATGAAAGGTCG
CATGGCCGCTCCGGGAGGCTAGCGAATGCGACACGGTAATAAGGGACAAA
TAGCAAAAAGAAGTGAGAGTGTGAAACGGTCGCCATTAGCAGCAGTGCCCA
CTGTAGCCAATCCTGCCATTATTATAGTGTGTCTCTGAGCCACCTCCATTCA
CTGCCAAACACCACTTCATCCTTCCTGCCCGCTGCTGCCACTACTGCTGCAT
TTCTACCCTCTGGCCCCCACCTTTTCCCCACCCCTTCACACACAAACACACC
CCACTACCTCCTTCTACTGTCTTCTTCCAGACTTGTCC

B) *xING1b5*

ATCGATTGGGGGGACCCTTGGCAGTCCCCACACATGGACAAATAAGATGCC
GAATCGGTCTAAAGGACCCATATCAGCAGCTTTAATCTGCCCATGTTTGGCC
ACCTTTACTCAGAGTTGGAGAGCTGAAAAGCAGGAAGTTGGGTTCTGTTCTA
TTCTGTTCGACATCTAATCACTCCAGCCTTTATACATTACATTTTTGGCTAAC
TATATTGAAAACATTTTTGAATTTTGCACAGTCTATCTATTTACCCAGTGTTTT
AATTTTACACTGAACTGTTCCTTTAATATATATGCTCACAATATTACCCCCAA
AGCTGTCTGAAGGAAAAGAAACAGACATTTGAATTGCAGATGGTTAAAAAAA
AAAAGCTTATGAGCTTTAGGTGATCCATGTGAAGCGGACTTTTGGTTCAGCA
CACAGAGGTATTCAAGCGGCCGTCACCTTTTCACATTCTGTTATGAAGCACT
TTGGAAGTCAGATTGAAGCTCAAAATTTAAAAAGAAAACCAAAGGGGAGAGT
AAGCCTGATTTATATAGAAGTTTGGGGGTAATTAAGTGTTAAGATAACTTGG
TGTTACTGGTTTAGGGGCAATGATCCTCTCCTTAAATAGAAGTCTCTCTCAT
GACCGTTATCCCATGTTCTATTACTTGACTGGACGCTCCACATTTTTCATCAG
CTCGTGAAACACCAAGGCAACAGTTTCTATACAGTTTATTGTTCCCAAGTTG
TCCATTACATTATTCTCCATTAAGGGAGACTTTCAGTGCATGGCAGAAAAGC
TAAGCGGTTTATGGTTAATGAATAGAATATTATTATAGCTGTGTCAGTATGTC
TTGCCTTTCATTTTTATCTTGCCATTGTTGCACCGTAATTGTGCGAGAGTAAC
GGTAAAAAAAAAAGCTCCAGCTCCAACAACAATCTTGTAGCTGCATTTGGGT
GTGTAAATATTGAATACAGTCTGCCGGACATGAATTCACTGTGATCCCCCCC
CACCCCACAGAAATTCAGAGGCAGTGATGCCTTCAATCATCCAACGACACA
ATGAACAGCCCCAGAACCTGAGGTAGAGGTTACAACCTGTACTAAACCTAC
AATACAAGTTGGCAACCCTGGGAATTTTGGTCCTGTCAAGAGTCGGCAGCC
ACCCACTAGAACCCATTACCACTTTCCCATGTTTGAATTTGCCGCTCACGGA
TAGGTAAGCCGCAGTGGAGCGGTCACATGGTAGGATCACATGACCGTGAC
GTCAGGTCCTTTCCTAGGATAGGAACTAGCCGCTACCCTTCTCTCACTGCA
GCCCCCTGGCGTTGTTATACTTTGATCAGAACGAATACACATGGGGCCACA

GCAATGCATTTCTCCCGCGGCGAGTCAGTGTCCATGAGATTCCTTCCCTCC
ACATTAACATTTGACGAGTACTATAAAGCGTGACGGGCCACAAGTTGAACAT
CCCTTCCTCCAGAACTGATAGCAACAGAACTCTGGCATGCGCTATTGAAAG
GGGGGGGGGTGAATGTTTCCCAAGTGTTTCAAACTGCTACTCGGCTTTTCC
ACGTTGTATGTCGCGTATGTGGGAATAAAAAGCTGCGTCGCCGCTCCGGGG
TTTAGTGAGTGGGAGCCGGTGAAAGGGACAAATAGGTAGTAGAGCGTCGAA
CAGTCGCCATTACCGGCAGTACGGTGCCCGCTAGTTCCACCCCAGTCCTGA
AATGATCCTGTGTCTGTAGTCAGTGCCAAACAACAATTCATCCCTCCTGCCC
GCTGCTACCACTATTGCTGCTGCCACTACTGCTGCATTTCTACCCTCCGGCC
CCCACCTTTTCCCCGCCCCTTCACACACAAACACACCCCACTACCTCCTTCC
CGACTTCTCCAGATAGACAGCCATTCAATCAGCTGCTGCACTTTTTTTTCCT
CTTCTTTTCACACAGTACAAC

C) *xING1c1*

CTGGAGAGCTCTGCATTGTCCTACATAAAGGCAGCCCTCTCTCTGTATGTAC
ATACTGTGTGCCTTATAACTGTCACATACACACACGCACCAGTGCTCAACAT
ATCCCGTGTAAACTACAGCTTGTCCTACACAAAGGGACGCGGCTTTGTTCAA
CCAGCTTTTCCCCGAATAATATTCACCTGTAACTTAAAACACCAAATGTTATG
GGGGCGGGGTACTGGGAGTTGTAGTGTCAATAACAACCGCAGGCTTCACG
TCCCCTTTCAGCCAACATTTTGGAGTGAAGCGACAAATGCGT

D) *xING1c2*

GTACGTGGTACCTTTATTCTTGCGAATAGTGTGTGAATGGGGAAGAAGTGG
ATAGTCGGATGAAGCGCTCACAGTAGCGTACGTTGTTACAGTATTATTCTTG
TGTTTAGCCGGACTATTTCCGTACTTATACCGAAAACAGGTGTAACTCCCAA
TCGTTTCCGTACAGCGCCAACCGCGCTTTAATCTAGCTGTACAACAAATTAC
TCTTTATATACGACGGGCCTTGTCAACGTAGTTTAAGTAGCCCC

APPENDIX 7. *ING2* GENOMIC SEQUENCES

A) *xING2a*

AAATAATATGTAACTGTGCGAAGATTTCCTTTGTGAAGAGTAACAAACGATCT
TCATGTTGCCAAAGCTCTCTTTACTCCATCCTTTTCCTCCTTGACCAATCATC
TGCATTTGACACGGTTGGCCTCTCACTCCTGGTGCAGATTCTGTATTCGCTT
GGCATCTGTAACCAGGCTGCATCTTGGCTCTCTTCTTACCTTTCTAACCGAA
CATCCACTGCCTCTTATGATAACAAAAACTCATCTCCAGTTCCACTTAATGTA
GGGGTGCCGCAAGGCTCTGTAATTGGTCCATTGTTGTTCTCCCTGTACACT
CTGTCTTCTGAAGATCGGTCATTTGGCTTTAATTATGATCTGTATGCTGATGA
TACCCAAAAATATTTATCCACCCCTTCATTAACAGCTGAAACTGAGGCTCAA
ATCTCCAACTGCCTCTTAGCTATCTCAATTTGGATGAATCAGAGCCACCTCA
AACTCAACCTAACAAAAACTGAACTAATAAACTTTCCCCTAAAGCCTGGTCC
TACTCCACTTTTTACTATCTCTATTGATGGCATGCTTATTGACCGTCAACTCA
GTACACTGTCTGGGGGGTAATCTTCGACCCCTCTCTCTCCTTCTCTGATCATA
TTAACACTACTGTCAAAACCTGTCACTTTTTCTTATGCAATATTGACAAAATC
CGTCCCTTCCTTTCACCTGCTACGGCCAAGACGCTCATGCATGCTCTCATCC
TATCCTGACTAGATTACTGTAACTTACTATGAACTGGCCTCCCTAACTCTCAT
CCCTCCCCTCCACAGTCTGTATTAAACACTGCTGCCAAAAATGATCCTCCTC
TCATCCAAAAGAGTACAGGCCCCTCCCCTGCTCAAGTCCTTATCATTGCTTC
CTATAAAACAAAGAATAATGTATAAACTCCTCCTCATAACTTTCAAAGCCCTT
AATTCCTCTGCACCTAACAACAACTCATCCCTTGTTTCTCTATATGTTCCTCC
CTGAAACCTCCGCTCCTCTCTGAGCAACCGCTTGGTTGTACCCCTCACTACT
ACTGCTGTTTCCAGTGCCAAACCTTTCTCTCTTGCGGCTCCTTATATTTGGA
ATGTCATTCCTGAATCTCTCCAGAGAGAATCCTCCTTCAATGTTTTTAAAACG
AAACTCAAAAACTACCTCTGGGAGCACCTGGATAACACTGGAACTGCCACTT
ATATGGCAGTGTCACACACTGTCACCTACATTGTTTTAATATCCCTCCAAATT
GTGTCCGTAAGTTACCCTCCCATTTAGACTGTAAGCCCCACTGTAGGGTCCT
CATTCCTTTTGTCTCCTTGACACCGAGCACTTAATCTGTATTTTTATCATATTT
ATGTCATTTGTATTTGTAATAATGCACTTATTGTTACTTAATAGCGCAGTGAG
CCCTTGTTTGTTACTACTAATTTGTTGTTTTGCTGTACAGTGCTTTGCCCTCA
AGGAGCGCTATACAAATAAAAATATACATACACACATCATGCCTTCAGATTG
TAAGCTCTTGAAAGGGACCTGTAATATATATATATGTTTTTCACTCAATGCTC
ATTTATA

B) *xING2b*

TATCTCAATGACAATGGTGCTATTTAGGTGCAATGGTGAGAATAACATAAGG
ATAAAACCTGCCACCTTCCCTAAAACTCCCAGTGGTGCTTACCTAGTTCTCT
CCTGTGACATTCCGTTTCTGACCAAATGGGATGCCAAGTCTCCCCATCTACA
AACTCCATAGCCAGGCAGATATAATGTTCCATAGAGAAAGAGGCGAATAATC
TAGTAAGGAAGTGGCAATTTTCCTTCTTTGCTAATAGCAGGATGCGTTGCTC
TCGGAGAACACTGGCAAAGAAATAACAACGACAGTTTCAATACAGGAGAAT

CATATACAGGACTAGTTCTACAACTGGGACTGGGGCAGAGCCTTTAATTGG
GAGACCCGTTTTTAAAATAACCCCCCCCCAATATATAATTTATTAACTCAAAG
TAATAGGTTTGTGGTTTTTAGTTCCATAGCTGTATAAAAGGGCCAGTAACATC
AAAAACATTTTTTTAAAAATTCGTCAGTACACAACGAAAAAAAACACCAACAC
AAATTAAACTTTAAAAAAGCAAAGTCTTTATTAAGAAATAACTTACAGAAACT
CTGCTTCCTGTCTTGTACAGAAACGGCAAAAGGGCGACCATCCATTGAGAG
GCACTTGATTTCTCCTCCCTGGCTCTCTGCTGCTGGATCTTTTAGCTGCCAC
ATTCTGTGCTTTCTGTAGTACAGCAGCACTTCCAGCATGAACTTTCTGCAGG
TCTGCGGTGCCTTGCCTTGCCTTACTGGTCCTTTAAGCACATACAGTACATT
ACTGCATTGGAACCTATCTTATATCCTCCTCAATCTTGAAGTTCCACTAGGTA
TTATTATAATGCTCAGGACAGCATCTCAGTAATCTAGGTATAGTACCTGAGA
AATGTTATAATTCGCCATATTAGTTGAAACATTTCTCAGAAGCATCTGTGGAA
TAGTAGCAACTATTGTATCAATTCTAACAACTGCCTTTAATGACAGTAAATTA
AAAAATCTATTTAAAAAATAAACCAGTTGAAAAAAAGTCTTCATTTCTTCATTT
CTAGTGAACTATCTGAAACCAACTGAACTGAAAAAGATTTGGAAGGTGAACA
ACCCCTTTAAGCGCTTATAGTACAACTGCACCTAGATGCACTGTTTACATTCT
AATTTCCAGTGCTTGCTGTTAATCTGGCTACTGTTCCTGCAGTTGCTGGTTC
CTCCAATACTGAGCTTGCATTATACCAACTCTCTTGTTCTCCTGAAATGCGTT
AAGGTGGGGAAAGTTTTGCAGAAAGTCTTGACCAGAGGATCTTGGTAGGTG
ATGTGGCAGGGCCACCAATGGAAATGAACGTCCCTGAACTCTTCATGTGAA
TAACACTGGCACACAAGCAGGAATCACTAATATGATGTAGCTTTGAAACAGG
CACTGTGTGATTGAACTGTTTCCTATGAAAAAAAGCCTGTTTGATGCATCCT
GAATAAGCAAAAGTGAAACTATACCACATAGTCACCAATTCTTTTCAGCAAA
CTCATTTCAGGACTCTATCTCTGTTTAACTGTGTCTGCAGAATTATTTCATAT
TACCATATACTGCATCATTTATTTGGACACAGAATGCAACTGAACTTTTTAGG
ACCTGTCCTCATATCCAGGAGGAGCAGGAGAATGTCTACTAATGACACTAAA
CTCATTAATGTAACTAAGCTTTGTATTTATTTTTAAGCAGCGTGATCCAATATA
TAAGTTTAACTTGATTATGTTGTTCTATTTGCTTGGAAAGTCAGATTACCAGG
CTACAAAGTGGGTACAGGCTCAGCAGCCTATCATAGAAGAGATGAACTATT
CAGCAGTGCAAACATTTCACTTTTTTTTTTCTTTAATGTTAAAGATGCAACAT
GAATCTTCCCAAACAGAATTATATATTACTAGTGTAAATTTACAATACATTACA
TTGTAATTGGTACAGCTTTTTAATGATAGGGTAAAATATAACTGGAGGATTGT
ATTTACTATTTAGGAGCATGTGCAAGATTTGGTGCCTAGAAGGTATGAAGCA
TATCAGGCTAAATTAGTCTGCAGTCTGCAATCCACATTTCTCACTTTTGCACA
TTAAAAAATGACTTTTAGAAATATGTAGCTGTGCAAGGATTTCCTTAATGATT
GGATGCATCCTGAATAATCAAAAAAGATAATACAATAACAAATCATTATTATT
TTCAACAACCTAATAAGCGTCAGTTGTTCCTCATGCCTTTAGATTGTAACATG
TTGAAAGGAGGGGCCTGTAATATGTACCTTTTCATCCTGACTCCTGTATATT
GATTTATTGTAATCAACTTCTTCTTCTTCGACTACTTCTTAAATG